Scratching the Surface: Characterizing the role of intracortical myelin in aging and Alzheimer's disease through quantitative relaxometry

By

Akshay Kohli

A dissertation submitted in partial fulfillment of

the requirements for the degree of

Doctor of Philosophy

(Neuroscience)

At the

UNIVERSITY OF WISCONSIN – MADISON

2022

Date of final oral examination: 07/22/2022

The dissertation is approved by the following members of the Final Oral Committee:

Barbara B. Bendlin, Professor, Geriatrics

M. Elizabeth Meyerand, Professor, Medical Physics, Biomedical Engineering, Radiology

Sterling C. Johnson, Professor, Geriatrics

Michael R. Koenigs, Professor, Psychiatry

Corinna Burger, Professor, Neurology

Table of Contents:

Acknowledgements

The formulation of this dissertation would not have been possible without the support of countless incredible individuals in my life. To my advisor, Dr. Barbara Bendlin, thank you for supporting me every step of the way. From the confidence you had in me at our very first meeting during my rotation, to the support in pursuing passions outside of research such as education and outreach, to the guidance in choosing a research topic and career advice, you have always been there to ensure my graduate school experience was as enriching as it could be. This dissertation is a product of your unrelenting mentorship and guidance. I truly appreciate all you have done for my educational and personal development.

To my parents, Anjli and Ashok, thank you for everything. You gave me an incredible childhood, one filled with love, laughter, kindness, and an emphasis on education that led me to pursuing this PhD. You encouraged my passion and interest in science and endlessly sought out resources to ensure I was in the best possible position for my future. You taught me to be grateful for what I've been given, and to give back to those that have less. The time, effort, and love that you both have put forth all these years is embedded into every word of this dissertation. Dad, your work with the space program was one of the biggest influences in me entering the scientific field. I have such incredible memories of all of the "take-your-kid-to-work" days and trips to the Kennedy Space Center in Florida. I am so privileged to have you both in my corner, always and forever. I love you both so much!

To my brother, Avneesh, you are my ultimate role model. You've shown me that hard work, kindness, loyalty, and dedication will bring success. I would not have made it to this point without your guidance and support. I am incredibly excited to be moving closer to you as I embark on my new journey into science consulting.

To my girlfriend, Rachel, you are an inspiration and have taught me so much about myself. From meeting during the interview weekend in Madison over 5 years ago, to me defending my dissertation, you have been my closest friend and always been by my side. You have helped me

grow intellectually, emotionally, and socially in ways I didn't know were possible. I have no doubt that the best part about coming to graduate school was that I got to meet you.

To the Puralewski family, thank you for opening your hearts and being my home away from home. There were many days that I wished I was with my family in LA, especially in the heat of the COVID-19 pandemic, but having a second family to laugh and unwind with on the weekends made this journey much more bearable. The table tennis tournaments, hikes, dinners, plays, trivia nights, board games, intense Five Crowns matches, and debates kept me lighthearted, energized, and motivated.

To the students and staff of the Wisconsin ADRC, this work could not have been done without you. From recruitment of participants and conducting study procedures, to quality-checking and managing data, all of these efforts made my work much easier to perform.

To the city of Madison and the University of Wisconsin, thank you for allowing me to have my graduate school experience here. I have loved Madison since I arrived here, and I'm sad to be leaving. From the long walks along the lakeshore path and hanging out with friends on State Street, to the unforgettable football games and the smiley cashiers at Metcalfe's, this city has become my home. I will always cherish my time in Madison and I hope I find my way back one day.

To John Williams, Hans Zimmer, Ramin Djiwadi, Klaus Badelt, Howard Shore, Michael Giacchino, Thomas Newman, Harry Gregson-Williams, Ludwig Goransson, and so many other brilliant composers, thank you for providing the soundtrack to my graduate education. The long days and nights of reading, hypothesizing, programming, designing, and writing were all enriched by the magical themes of my favorite movies and TV shows. I have the fondest memories of starting each day in the world of my choosing, whether that be with Frodo and Sam as I walked to lab, or with the Lannisters as I was paying my debts in MATLAB, or with Yoda as I was trying to understand why my results went against my hypotheses. If I consider my PhD to be one long movie, it had the best score thanks to these incredible musical geniuses.

Abstract

Demyelination within brain white matter is often observed in late life and is typically exacerbated in Alzheimer's disease (AD). Indeed, prior studies have linked reduced white matter myelin content with aging, cognitive impairment, genetic risk factors of AD, and biomarkers of AD pathology and neurodegeneration. Interestingly, observations of post-mortem brains inflicted with AD pathology have noted that the development of such pathology inversely mirrors cortical myelogenesis. However, few studies to date have investigated the trajectories of cortical myelin in late life, and studies assessing relationships with AD pathology have led to confounding results. Here, through the use of high fidelity quantitative relaxometry (R1) mapping, a metric sensitive to brain myelin content, this dissertation includes three specific aims that expand upon our understanding of the role of cortex-specific myelin in healthy and diseased aging. The first aim examines age-related relaxometry changes in the cortex, as well as associations with performance on cognitive tests and cortical alterations in individuals presenting with Alzheimer's clinical syndrome. The second aim assesses the effects of genetic risk factors including sex and apolipoprotein E genotype on cortical myelin. Finally, through the use of cerebrospinal fluid (CSF) biomarkers obtained via lumbar puncture in addition to imaging markers derived from amyloid and tau positron emission tomography (PET) imaging, the third aim identifies relationships between CSF biomarkers of AD pathology and neurodegeneration, as well as confirms the inverse spatial distributions of cortical myelin and AD pathology *in vivo*. Importantly, throughout this dissertation, all observations made within the cortex are reported in direct comparison to myelin content in adjacent white matter. This work adds to the growing body of literature aimed and elucidating the role of myelin in aging and AD-related pathogenesis and progression.

Chapter 1: Introduction

Aging, Alzheimer's Disease, and Dementia

Aging is a natural process that all living organisms undergo. While early development of the human brain typically leads to increased cognition that aid in one's ability to function in their environment, aging at the tail end of life characteristically follows the reverse pattern in many ways. Facets such as development of various pathologies, decreased microstructural integrity of brain tissue, and altered reliability of neuronal connectivity and communication are common in aging, and often lead the cognitive decline exhibited in older age[1–4]. Still, there are many elements to the aging phenomenon that are highly variable between individuals, and aspects of aging that continue to increase over time such as certain measures of intelligence[5,6].

The typically developing brain, especially in early life, is incredibly plastic and undergoes substantial growth. This post-gestational growth includes further differentiation of neurons and glia, increased synaptic pruning, and perhaps most pertinent to this dissertation, extensive myelination of axons. These developmental changes contribute to gross alterations in morphometry, including increased gyrification of the cortical surface, greater density in fiber tracts, and overall increases in regional volume. Although there exists variability across individuals, the brain typically continues to develop until 30 years of age, followed by a plateau between 30 and 50 years, with a subsequent decline until death. This slow decline in the late stages of life can be observed by progressive brain atrophy, characterized by cortical thinning, white matter degeneration, and ventricle enlargement. These changes occur in the absence of disease, but can be detrimentally exacerbated by genetic mutations, development of pathologies, poor cardiovascular health, and harmful interactions with the environment (for example, traumatic brain injury).

As individuals age, the propensity for developing diseases and disorders often increases. While this is not the case for some developmental and psychiatric disorders such as autism and schizophrenia, neurodegenerative disorders such as multiple sclerosis (MS), Parkinson's disease (PD), and Alzheimer's disease (AD) most often present later in life. In

addition, the brain does not function in isolation, and ailments to other systems in the body such as cardiovascular or respiratory distress can lead to damage and deterioration of the brain. As is discussed later in this introduction, aging is often a risk factor for developing disease. Common processes that the brain undergoes in daily function can lead to a buildup of toxic proteins or compounds, oxidative stress leading to neuronal damage, decreased blood flow leading to cell death, and other damaging phenomena.

Cognitive Aging

Human intelligence also appears to change across the lifespan. Often divided into two broad sub-domains, fluid and crystallized intelligence, fluid intelligence represents one's ability to solve abstract problems typically independent of prior experience and knowledge. In contrast, crystallized intelligence encompasses learned abilities and knowledge. Studies of intelligence and the aging brain have revealed that fluid intelligence typically peaks early in life (around age 20) and steadily declines with age, whereas crystallized intelligence peaks later in life and remains relatively stable, with gradual decline after the age of 65[5]. This has been observed in both healthy aging as well as individuals with neurological disorders. For example, a study of 494 cognitively unimpaired older adults between 60 and 84 years examined the effects of age and ß-amyloid plaque burden, a key pathological protein of Alzheimer's disease, on intelligence scores. Their mixed effects models found significant age-related decline in fluid intelligence, whereas crystallized intelligence remained relatively stable. In addition, the interaction between age and ß-amyloid deposition was significantly related to decreases in fluid, but not crystallized intelligence. Finally, declines in fluid intelligence were the largest indicator of progression from cognitively unimpaired to mild cognitive impairment[7].

Further studies have expanded upon our understanding of intelligence in aging through the use of neuroimaging-based analyses. A longitudinal study of 73 healthy older adults aged 49-83 examined changes in cortical thickness and regional volumes in relation to measures of

fluid and crystallized intelligence. Growth curve trajectories revealed significant decline in fluid intelligence and no change in crystallized intelligence, and steady decline in cortical thickness and regional volumes across a majority of extracted regions of interest (ROIs) (but not in motor or sensory cortices). Interestingly, the individuals with higher baseline fluid intelligence exhibited smaller reductions in cortical thickness and regional volumes, whereas individuals with higher baseline crystallized intelligence underwent greater reductions in cortical thickness and regional volumes[8]. It's possible that selective population biases, differences in initial brain sizes, and an individual subject's cognitive reserve could impact a study's ability to detect relationships in overall intelligence.

While cortical-based volumetric analyses have revealed fewer relationships with decline in fluid intelligence, a study of fMRI-guided white matter connectivity may explain why. 221 adults aged 20-80 underwent DTI and task-based fMRI (eliciting regional activation pertaining to facets of fluid and crystallized intelligence). Four distinct maps containing ROIs with significant activity related to specific cognitive domains. Tractography of the underlying white matter tracts corresponding to each of these ROI maps allowed researchers to determine how network interconnectedness may underpin fluid versus crystallized abilities. They found that vocabulary, a crystallized ability, was more localized and lateralized to proximal regions as compared to fluid abilities (reasoning and processing speed), which seemed to be distributed more widely across the brain[9]. Gray matter regions involved in tests of reasoning included dorsal and lateral frontal regions, precuneus, bilateral supramarginal gyri, superior and middle temporal gyri, and small portions of the right hippocampus, processing speed was distributed widely across the brain and included bilateral caudate, nucleus accumbens, thalamus, brain stem, bilateral anterior cingulate, bilateral superior portions of the lateral occipital cortices, the cuneus, and frontal regions (right precentral gyrus, middle frontal gyrus, bilateral orbital frontal cortices, and the insular cortices). In contrast, performance on tests of vocabulary was linked to more restricted regions, including left inferior frontal gyrus, precentral gyrus, superior and middle temporal gyri

and bilateral cerebellum. When examining patterns of white matter associations, processing speed —not surprisingly—was associated with the greatest number of white matter tracts with relationships distributed widely across the brain. In contrast, vocabulary was primarily associated with left superior longitudinal fasciculus/arcuate fasciculus. Given the significant age-related declines in white matter structural connectivity, it then perhaps not surprising that fluid intelligence tends to decline much more rapidly as opposed to crystallized abilities that don't rely on long-distance white matter connections. Still, there is an incredible amount of variation between individuals. Many factors including (but not limited to) education, diet/nutrition, and underlying physiology can play a substantial role in later life trajectories of fluid and crystallized intellectual abilities.

History, Risk Factors, Prevalence, and Pathological Hallmarks of Alzheimer's Disease

Alzheimer's disease (AD) is a progressive neurodegenerative disorder that primarily affects adults in mid-life to older age. First identified in 1906 by Alois Alzheimer, our understanding of AD etiology, pathogenesis, progression, and prognosis has grown substantially since then. AD is the leading cause of dementia, with an estimated 60-80% of all cases due to AD. However, it is not the only cause, with other potential pathologies such as Lewy bodies, Parkinson's, traumatic brain injury, cerebrovascular disease, among others also potentially leading to dementia. It is also the case that dementia due to AD can manifest alongside cognitive impairments from some of these other diseases or disorders. In fact, one study found that at autopsy, only 3% of 447 patients had AD pathology alone, with 82% having both AD pathology alongside another cause of dementia[10]. These numbers are staggering and highlight the continued need for sensitive measures of pathology and more defined diagnostic criteria.

There are a number of modifiable and non-modifiable risk factors for developing AD. Age is the strongest risk factor of AD. While increased age does not guarantee development of AD

dementia, the prevalence of AD is substantially higher in individuals above the age of 65, with nearly 33% of people over the age of 85 Alzheimer's dementia. It is important to note that age alone cannot cause dementia, just that the likelihood of developing AD dramatically increases. There are also genetic predispositions to developing AD. Apolipoprotein-E is a gene codes for the production of a protein involved in lipid transport. Studies have identified that allele variations in this gene, particularly those with the e4 allele, develop AD at much higher rates than those with the e3, and particularly the e2 variant[11,12]. Heterozygous e4 allele carriers develop AD at three times the rate of those with 2 copies of the e3 allele, and homozygous e4 carriers develop AD at up to 12 times the rate. Rare genetic mutations, such as those that impact the amyloid precursor protein (APP) and the presenilin-1 and presenilin-2 proteins, nearly guarantee one's propensity of developing AD if they live long enough. These individuals often develop symptoms earlier than those with sporadic AD.

Cardiovascular health is also a major risk factor for AD. Activities that negatively impact heart health, such as smoking, low aerobic activity, and a poor diet, can contribute to the development of dementia. As mentioned previously, the brain is not an isolated organ as it relies on nutrients from the rest of the body to function. Poor cerebral blood flow and/or blood that lacks proper nutrients or oxygenation risks damaging neurons, and can exacerbate the negative. As such, budding research suggests that modifiable lifestyle factors such as reducing smoking, eating a more balanced diet, reducing stress, getting adequate sleep, and exercising can all reduce the risk of developing AD.

A majority of AD diagnoses (~2/3rds) in the United States are in women. This is likely skewed by the fact that women, on average, live longer than men, and thus reach older ages where dementia is more likely to manifest. However, studies are still debating whether there are biological, cultural, and societal factors that influence the increased rate of AD diagnosis in women. One of the biological factors that may contribute to higher prevalence of AD in women compared to men is the presence of estrogen and other hormones[13,14], however, this is still

heavily debated. As such, it is important to investigate all possible neurological sex differences that could drive these higher rates.

Since the early 20th century, numerous developments have led to the differentiation of ways AD can manifest in humans. Early-onset AD (EOAD) consists of rare forms of the disease often driven by genetic predispositions for developing the underlying pathology that contributes to cognitive decline in AD. The most common form of AD is sporadic late-onset AD (LOAD) in which individuals develop clinical symptoms of the disease in late-life due to an unknown cause.

With regards to underlying etiology, the amyloid hypothesis is the most widely supported causative explanation for the pathogenesis of AD. Driven by abnormal cleavage of the amyloid precursor protein (APP), pathological isoforms of Aβ (specifically Aβ42) begin to accumulate within the extracellular space surrounding neurons. While in the early stages these proteins are considered to be largely non-toxic, plaque buildup leads to progressive oligomerization of soluble Aβ, leading to toxicity surrounding pre-and-post synaptic terminals. It is then believed, although not fully understood how, that these plaques trigger the hyperphosphorylation of tau protein within the axon. This leads to impaired transport of necessary proteins and eventual destabilization of the ion channel signaling within the synapse. Buildup of vesicles within the synaptic terminal, rich in APP and the enzymes involved in the cleavage of APP (including beta-secretase-1 and gamma-secretase), contributes to further accumulation of Aβ. This amyloid cascade hypothesis is widely supported through studies inherited forms of AD. One example is in individuals with down syndrome, who have three copies of chromosome 21, and thus, three copies of APP. These individuals exhibited heightened production of amyloid, leading to accelerated plaque accumulation, tangle development, and subsequent neurodegeneration early in life (~30-40 years old). Still, while the amyloid hypothesis is widely supported and is the target of numerous clinical trials testing pharmaceutical interventions, there are likely other mechanisms that contribute to the full cascade of pathologies exhibited in AD.

Diagnosis of AD and Dementia

Our understanding of dementia, as well as the different pathologies that lead to an individual's cognitive decline have improved drastically. Recent efforts to more accurately diagnose individuals along the Alzheimer's clinical syndromic spectrum have been proposed by the National Institutes of Aging and Alzheimer's Association (NIA-AA)[15]. The terms possible and probable AD refer to the potential clinical diagnoses that can be made; these typically rely on reports (made either by the patient or caregiver) of cognitive or behavioral symptoms that 1) impact the ability to function at work, hobbies, or other daily activities, 2) exhibit a decline from prior levels of functioning, 3) are not driven by delirium or psychiatric disorder, 4) impairments within 2 or more cognitive/behavioral domains (memory, reasoning, visuospatial, language, behavior/mood). Probable AD relies on gradual presentation of these symptoms in stereotypical patterns; either through amnestic presentation or with language, visuospatial, or executive dysfunction appearance. Possible AD depends on whether these symptoms present atypically, over an expedited period of time, or there is not enough medical history to determine speed of decline. Neuropsychological testing can be utilized as a measure of function, however, subjective reports from the patient and/or caregiver should be used as the primary measure.

Finally, as research continues to develop ways to measure the pathological hallmarks of AD, amyloid plaque burden and neurofibrillary tangles, diagnosis of possible or probable AD can now be supported by evidence of AD pathological processes. Through the use of cerebrospinal fluid (CSF) biomarkers, levels of Aβ42, total tau, and phosphorylated tau can be measured. Additionally, recent developments of PET radioligands allow for the *in vivo* measurement of brain amyloid plaque load and neurofibrillary tangle burden. While these tools may serve to increase the certainty that an individual's clinical symptoms are driven by AD pathology, it

should not be used for routine testing as more work is needed to validate and standardize the measures for use in clinical settings.

Biomarkers of AD pathology and the AT(N) Research Framework

Since the updates to these diagnostic guidelines, the NIA-AA formed a working group that has since established a new classification framework for AD researchers. Known as the AT(N) research framework, this classification scheme works by designating individuals along the Alzheimer's continuum according to presence of AD-specific pathology (amyloid (A) and tau (T)), in addition to the detection of neurodegeneration (N) markers. Within this framework, researchers determined that levels of aggregated Aβ could be measured through CSF Aβ42, Aβ42/40 ratio, or amyloid PET, neurofibrillary tangles could be identified through CSF phosphorylated tau or tau PET, and neurodegeneration could be assessed through structural MRI, glucose PET, or CSF total tau. According to this framework, an individual can be deemed positive or negative for each of these three categories.

In order for an individual to be classified along the Alzheimer's continuum, elevated levels of Aβ burden must be detected (A+). If an individual also has elevated tau (A+T+), as well as additional neurodegeneration (A+T+N+), they are designated as having Alzheimer's disease. Were they to present with amyloid only (A+T-N-) or with simultaneous neurodegeneration (A+T-N+), but not tau, they still exist on the Alzheimer's continuum, but are labeled as having Alzheimer's pathologic change or Alzheimer's and concomitant suspected non Alzheimer's pathologic change respectively. Finally, if an individual presents with elevated Tau and/or neurodegeneration in the absence of Aβ, they fall along the spectrum of non-AD pathologic change.

Neurodegeneration can be characterized in numerous ways. Overall brain size, hippocampal volume, and cortical thickness are common measures that can indicate the

amount of neurodegeneration that has occurred. In addition, CSF biomarkers including neurogranin, a measure of dendritic/synaptic loss, as well as neurofilament light chain and total tau proteins, measures of axonal degeneration. When an individual has undergone substantial neurodegeneration, elevated levels of these proteins are present in CSF. In AD, this increased degeneration is typically observed following the onset of amyloid and tau pathology, and most closely in temporal relation to cognitive impairment. While these CSF measures are sensitive to neuronal atrophy, they contain little information about the spatial distribution of this neurodegeneration. As such, it is important to continue developing novel neuroimaging approaches that can both detect this neurological change while providing specific regional information.

While the AT(N) research framework has enabled easy identification and classification of individuals along the AD spectrum, it is very much under continuous development. As our understanding of AD pathogenesis and progression increases, the need for further differentiation of AD or related disorders will grow. The addition of other markers, including vascular (V) and glial (G) categories have been posited. Although these are not specific to AD, they can help differentiate individuals who present with multi-etiology dementias, or help identify potential targets for therapeutic intervention. In this dissertation, a marker of myelin is assessed alongside characteristics and biomarkers of normal aging and AD pathology. While this work does not serve to standardize and validate a myelin (M) category, it adds to the growing literature into the relationships between myelin integrity and AD pathology, which can be used to better understand an individual's susceptibility of developing AD, as well as their progression along the AD pathological cascade.

Neuropsychological Testing to Assess Cognition

As described above, dementia is an umbrella term used to describe a set of symptoms one presents with. These symptoms typically manifest as cognitive impairments in executive

function, working memory, language, problem-solving, and other critical thinking skills. While Alzheimer's disease is just one potential cause of dementia, it is the most prevalent, accounting for nearly 80% of diagnosed cases. Cognitive impairments exhibited in dementia are typically self-reported, or reported by the family or caregivers of patients. These reports are crucial for accurate diagnosis, as well as tracking a patient's clinical progression of the disease.

While these subjective experiences are important to understand potential impairments to the patient's activities of daily life, objective measures are critical for 1) assessing and tracking which cognitive domains a patient may be most impacted by disease, 2) establishing novel criteria or cutoffs in diagnosis and/or disease staging, and 3) creating standardized measures that are comparable across a population. Cognitive screeners such as the Mini Mental State Exam (MMSE) or Montreal Cognitive Assessment (MoCA)[16] have been shown to have high sensitivity and specificity for measuring severity of dementia, however, the MoCA has demonstrated much higher reliability in detecting individuals in the preclinical and/or mild cognitive impairment stages as compared to the MMSE which often overlooks such subtleties[17]. Regardless, both of these cognitive screeners have strong utility in clinical settings, allowing for assessment of multiple cognitive domains in under 10 minutes, all while existing on point scales that are easily interpretable by clinicians and patients.

That being said, since the advent of these comprehensive tests, types of assessment methodology and medium of test delivery have evolved[18]. One such example is with the NIH Toolbox, a battery of cognitive, emotion, and motor tests first released in 2012 that is delivered using tablet devices such as an iPad. The NIH Toolbox cognition battery is comprised of the Dimensional Change Card Sort (DCCS) Test Age 12+, List Sorting Working Memory Test Age 7+, Pattern Comparison Processing Speed Test Age 7+, among others. Since its release, it been used to study cognition in healthy aging[19,20], associations with amyloid and tau pathology in prodromal AD and dementia[21,22], and even as outcome measures in clinical trials[23]. Cognitive

measures included in the NIH Toolbox have also been shown to correlate strongly with those assessed via the MoCA[24].

The DCCS test is a measure of executive function, and specifically cognitive flexibility, in which two stimuli are presented with different shapes and/or colors. A prompt is then displayed on the screen requesting the participant select their answer based on matching shape or color, followed by the test image in which the participant uses as the reference image. If the prompt is "shape", the participant should select one of the two stimuli that match the shape of the reference stimulus. If the prompt is "color", the participant should select the stimulus that matches the color of the reference stimulus. The test involves switching between shape and color, a task that individuals with cognitive impairment exhibit difficulty with. Both accuracy and reaction time are included in the overall score calculated by the toolbox.

The list sorting test provides an index of an individual's working memory, including storage and processing of information. The participant is presented with pictures and corresponding labels of foods or animals. They are then instructed to repeat back what they saw, either in the order in which they were presented, or in order from smallest to largest. In some trials, they may be instructed to repeat back the list in the order from smallest to largest for each category separately (food/animals). Accuracy on this task is a strong indicator of a participant's ability to actively maintain information in the short term, as well as interpret and process that information.

The pattern comparison processing speed test examines an individual's ability to compare two images and determine whether they are similar or different. During the task, a participant is presented with two images side-by-side. If they deem the images to be identical, they press "yes", otherwise, they press "no". The participant is instructed to perform this task as quickly as possible – higher neural processing speed is highly associated with better performance on this test[25,26].

Given the computerized nature of the NIH Toolbox, scores are easily exported and automatically standardized on a 100-point scale, with a deviation of 15 points above or below 100 indicating one standard deviation from the mean. The toolbox also outputs scores corrected for influential factors such as age. Within this dissertation, performance on these tests, including the DCCS test, the list sorting test, and pattern comparison test are related to neuroimaging-based tissue relaxometry metrics indexing cortical GM myelination in individuals across the Alzheimer's clinical spectrum; this is the first study to assess the impact of regional levels of cortex-specific myelin on performance across individual domains of cognition.

Myelination in Development, Aging, and AD

The following section discusses myelin in the context of aging and AD. The process of myelination in development, trajectories of brain myelination throughout the lifespan, and the role myelin plays in the aging process are reviewed. Additionally, the myelin theory of AD is introduced, including observations made through post-mortem staining and novel imaging techniques to assess myelin *in vivo*. Finally, cortex-specific myeloarchitecture is examined, as well as changes in cortical myelin in the aging process and the possible links with AD. This dissertation aims to expand on existing research investigating the role of myelin in aging and AD.

Composition, Development, and Role of Brain Myelin

The myelin sheath is a fatty substance that wraps and insulates axons, the "wires" that carry the electrical communication from the neuronal cell body to the axon terminal. Myelin serves a similar function to the rubber/plastic wrapping of an audio/video cable, which maintains conductance of the electrical impulse, increasing reliability and speed of signal conduction. Within the central nervous system (CNS), myelin is produced and maintained by supporting

cells known as oligodendrocytes, which get differentiated during development from oligodendrocyte precursor cells (OPC). While there may be subtle variations in the makeup of myelin depending on the its location and stage in development, its composition is primarily water, lipids (dense in cholesterol)[27], and proteins (myelin basic protein)[28]. Myelin has been found to be a very stable structure – in one study, scientists induced oligodendrocytic death in transgenic mice, but found that myelin remained intact for several weeks. The cholesterol bound within the lipid bilayers of the myelin sheath contribute to its stability[29]. Sheets of membrane that wrap neurons creating the myelin sheath are highly consistent,

Brain myelination in development until adulthood typically follows logarithmic trajectories, as has been measured through *in vitro* tissue staining[30], as well as MRI-based imaging studies in humans[31–34] and non-human primates[35,36]. While a majority of studies have focused on the abundance of myelin located within brain white matter, developments in both microscopy and MRI technologies have led to a large growth of scholarship into of observations of cortex-specific myelination, repair by oligodendrocytes, and OPC differentiation in both mouse models and humans *in vivo*. A study of axons of cortical pyramidal cells identified that distribution of myelin along these axons were inconsistent and highly diversified, with fluctuating lengths of segments with and without myelin on the same axon. Importantly, the more superficial layers exhibited more of this greater diversification[37]. These findings highlight that myelin may play a more complex role in the cortex as compared to white matter.

Building upon this work, researchers utilized longitudinal two-photon imaging *in vivo* to track myelin, oligodendrocytes, and OPCs in the mouse cerebral cortex. They imaged these components over the course of 50 days in young (2-4 months), middle-aged (10-14 months), and old (18-24 months) mice. The number of myelinating oligodendrocytes increased with age, even in the old mice population. However, a majority of new myelin produced and integrated onto axons was produced by newly differentiated oligodendrocytes as opposed to existing oligos[38]. These findings posit support that by increasing the amount of OPCs in the system

could increase new myelination and/or myelin repair, presenting a possible therapeutic mechanism for several diseases impact myelin. These researchers then went on to investigate how these newly differentiated oligodendrocytes went on to repair damaged cortical myelin. They found, also via two-photon microscopy, that these oligos preferentially remyelinated axons proximal to their location, and most interestingly, didn't solely repair damaged myelin, but also sheathed previously unmyelinated axons. These results indicate that the remyelinating process can significantly alter the composition of cortical circuitry[39].

The Myelin Model of AD

While the field has identified pathological Aβ42 plaque buildup and subsequent hyperphosphorylation of tau as the pathological hallmarks of the disease, there is still a debate about other contributing factors that increase an individual's susceptibility for developing such pathologies, allow for resilience to the cognitive impairments even in the presence of heightened neurotoxicity, and why progression of pathology occurs in certain stereotypical patterns. Seminar researchers in the AD field, Heiko and Eva Braak, authored numerous publications in the late 1980's and early 1990's characterizing the typical pathological spread of neuritic plaques driven by Aβ and neurofibrillary tangles caused by the hyperphosphorylation of tau[40–42]. They noted an obscure observation; that the typical progression of AD-related destruction of brain tissue followed the inverse pattern of cortical myelogenesis. As they described, tissue in the temporal and frontal cortices typically exhibit prolonged myelination into late life, whereas sensory/motor and visual cortices are the first to myelinate and peak much earlier in life. These observations agree with prior studies leveraging post-mortem tissue staining of myelin[43–47], as well as novel MRI-based neuroimaging techniques[34,48–60]. Importantly, they observed these typically late-myelinating regions are often the regions first impacted by toxic AD pathology.

Since these observations were made, much research has gone on to assess the role that myelin may play in the aging and AD pathological processes. Bartzokis et al. conducted numerous studies, both observational and experimental, assessing the trajectories of brain myelin in late life. They posited that AD pathology may result due to the breakdown of myelin due to normal aging[61], suggested that age-related demyelination could contribute to the cognitive symptoms exhibited in AD[32], and observed that regions with high Aβ deposition early in AD are regions that are typically late-myelinating[62]. Work by Bartzokis et al. focused on myelination in white matter, however, it paved the way for studies to be expanded into gray matter. As AD is often described as "as disease of the gray matter" due to the buildup of Aβ plaques and neurofibrillary tangles in cortical tissue, the natural evolution was to study myelin in cortical gray matter. Given the strong connection between the development and degeneration of brain myelin in the context of AD, it is imperative that studies further investigate these relationships in the large populations of older adults with and without Alzheimer's disease, as well as expand these examinations into the cortex.

How to Study Myelin *in vivo*

Human studies have leveraged a variety of MRI sequences to index myelin in the brain. Diffusion-based measures such as DTI, or more advanced models such as neurite orientation dispersion and density imaging (NODDI), enable the measurement of water diffusion within the brain. As such, DTI-derived metrics such as fractional anisotropy (FA) and mean diffusivity (MD) can serve as metrics of axonal (and potentially myelin) integrity. Additional work conducted recently has utilized NODDI metrics such as neurite density (NDI) and orientation dispersion (ODI) to assess changes in cortical microstructure in dementia as well as preclinical AD[63]. However, while these sequences have proved to be valuable tools to index tissue integrity, they are typically more sensitive to dendrites, neurites, and axons, than they are to myelin itself. One

imaging protocol that can utilized to assess myelin content is known as multi-component driven equilibrium single pulse observation of T1 & T2 (mcDESPOT)[64]. Through mcDESPOT, one can calculate the myelin-water fraction (MWF), a measure that estimates the amount of water trapped within the lipid bilayers of the myelin sheath. While mcDESPOT-derived MWF has shown a high degree of correlation with *ex vivo* assessment of myelin content and has been widely used to study myelin in aging[65] and disease[66,67], its application is limited due to the relatively low spatial resolution (~2-3mm voxel size). Given the cortex can be as thin as 1mm in some regions (sensory and motor cortices), this method has limited utility in assessing myelin in the cortex.

In the early 2010's, researchers defining processing guidelines for the Human Connectome Project developed a methodology of calculating the ratio of signal intensities between a T1-weighted and T2-weighted MRI scans (T1w/T2w ratio). Glasser and Van Essen observed that this ratio heavily correlated with brain myelin content, and while it could be used to examine white matter, decided to explore its utility in the cortex. Through cortical surface estimation within Freesurfer[68], they created "myelin maps" that represented the distribution of myelin throughout the cortex as indexed by this ratio[57,60]. Studies have since utilized this technique to explore age-related trajectories of myelin in the cortex[56,60], associations with cognition[55], and even relationships with AD pathology[69,70]. However, in the paper introducing this technique, Glasser and Van Essen warned, "The T1w/T2w ratio is a unitless quantity based on unitless raw intensity data… absolute myelin map values of a given region of cortex may differ according to the physical scanner or pulse sequence."

Glasser and Van Essen suggest the use of alternative MRI acquisition methods such as those that quantify T1 and T2 relaxometry as potential future directions. Indeed, tissue relaxometry, particularly of the longitudinal magnetization rate – R1 (=1/T1), has shown to be highly sensitive to brain myelination through both *ex* and *in vivo* measurement[52,58,71,72]. To date, indexing tissue relaxometry has had limited applicability due to the prohibitively long scan times

required to acquire the necessary information to calculate R1. mcDESPOT, as mentioned previously, does allow for the calculation of both R1 and R2 in short time, however, the resolution limits its applicability in studying the cortex. Recently, one novel sequence known as MPnRAGE[73,74] was developed that provides the necessary data and resolution to quantify R1 to a submillimeter scale. MPnRAGE is leveraged in this dissertation to explore R1 in a large population of adults in late-middle age. As R1 is a quantitative metric grounded in the physical properties of tissue relaxation, it has wide applications across the aging and Alzheimer's fields, with utility in creating better diagnostic criteria, elucidating mechanisms of AD pathogenesis, and revealing targets for potential treatment.

Specific Aims

Scientists continue to debate the etiology and prognosis of Alzheimer's disease (AD) with no preventative and limited efficacy among disease-altering treatments. While the impacts of amyloid beta (Aß) plaques and tau-driven neurofibrillary tangles (NFT) on brain atrophy and cognitive decline have been well studied, it remains unknown how the accumulation of these proteins within the cortex differentially target cortical and subcortical myelin in the progression of AD. Indeed, studies have linked widespread white matter (WM) demyelination to aging, AD pathology, and cognitive decline[32,61,62,67,75], however, the role of cortex-specific myelin in aging and the development and progression of AD is understudied. Early post-mortem observations made by Heiko and Eva Braak noted inverted patterns of cortical myelin in relation to AD-related neurodegeneration[76], however, this has yet to be shown *in vivo*. Novel quantitative MR methods have enabled the reliable and reproduceable quantification of tissue myelin in vivo through R1 mapping in addition to offering additional advantages over conventional T1-weighted (T1w) MRI such as greater signal contrast and diminished bias field inhomogeneities[77]. As early detection of AD in vivo remains a crucial goal of AD research, it is imperative we identify any possible alterations to tissue microstructure that may lead to a better understanding or sensitivity to AD development and progression. ***Therefore, the goal of this dissertation was to characterize the role of cortical myelin (as indexed by R1) in aging and AD through analysis of risk factors of AD, cognitive testing, structural neuroimaging, and cerebrospinal fluid (CSF) biomarkers.*** To achieve this characterization, this dissertation contains three aims:

Aim 1: Establish trajectories of late-life cortical and WM myelination in cognitively unimpaired older adults as well as individuals presenting with Alzheimer's clinical syndrome. While myelination of subcortical WM occurs early in life, human cortical GM shows protracted myelination at rates and quantities unlike that of any other species, particularly in the temporal and frontal cortices[43]. Attempts to model trajectories of myelin have primarily been limited to the study of subcortical white matter and are often within post-mortem analyses of brain

tissue, limiting the ability to determine changes in myelin content over time[78]. Studies have used MRI as a proxy for brain myelin through T1/T2 signal intensities, which have largely shown inverse quadratic or negative linear relationships with age throughout the brain[32,56,79,80]. However, it has yet to be seen in vivo how cortical and WM myelin are altered in late life in unimpaired older adults and those with an AD diagnosis. By employing quantitative R1 mapping, the known trajectories of myelination were extended to adults in late life and regional alterations in myelin in individuals with cognitive impairment were identified. Importantly, the objectives of this aim were replicated in an independent cohort. Finally, neuropsychological testing was used to determine the associations between regional cortical myelin and performance of individual cognitive domains (including executive function, working memory, and processing speed). ***We hypothesized that 1) older individuals would exhibit lower levels of global cortical myelin compared to younger individuals, 2) individuals with cognitive impairment would exhibit lower myelin content as compared to unimpaired participants, and 3) better performance within the three cognitive domains assessed would be positively associated with cortical and WM myelin, controlling for age effects.***

Aim 2: Determine associations between cortical and WM myelin, sex, and APOE genetic risk for AD. Apolipoprotein E (APOE) genotype has been well validated as a strong risk factor for the development of AD pathology, as carriers of an *ε4* allele experience higher rates of developing AD, while those with an *ε2* variant exhibiting reduced risk[11,12]. A major role of APOE is the transport of cholesterol throughout the brain[81], and given that the high cholesterol levels are essential for healthy myelination[27], there is likely a relationship between the pathologically-associated APOE genotype and integrity of global brain myelin. Indeed, studies have established that this genetic risk factor of AD is associated with degeneration of subcortical white matter microstructure[82,83], however, it is not yet known how cortical myelin is associated with this predictor. As R1 is particularly sensitive to the cholesterol that binds to myelin[59], we were well

positioned to assess the impact of APOE genotype on cortical and subcortical myelin content. Additional studies have shown that sex modifies the APOE-related risk of developing AD, with women demonstrating accelerated amyloid accumulation and age of disease onset[84]. While, sex-related differences in brain myelination have been noted in subcortical WM, particularly within the corpus collosum[85,86], these associations have yet to be made with intracortical myelin. Therefore, in this aim, we utilized the well characterized ADRC and WRAP cohorts to comprehensively assess relationships between APOE, sex, and cortical and WM myelination. ***We hypothesized that 1) older women would have lower levels of cortical myelin compared to older men, 2) carriers of the APOE ε4 allele would exhibit lower levels of cortical myelin compared to non-carriers, and 3) that this effect would be stronger in women.***

Aim 3: Assess relationships between cortical and WM myelin and biomarkers of AD pathology and neurodegeneration in individuals across the AD continuum. While early AD pathology and neurodegeneration markers associate with subcortical myelin changes[62,67,87–89], it is unclear whether these relationships hold true for intracortical myelin. Although prior research has shown broad associations between neuronal atrophy and the accumulation of amyloid plaques and neurofibrillary tangles, the selective vulnerability of brain regions and the spatial distribution of AD pathology is not fully understood. Given that myelination is nonuniform across the cortex, it seems plausible that areas with lower cortical myelin could be more vulnerable to neurologic disease and could explain the spatial distribution of early AD pathology. To date, no study has yet replicated the aforementioned observations made my Heiko and Eva Braak[76]. In this aim, 1) associations were identified between CSF biomarkers of AD pathology and neurodegeneration and cortical and WM myelin and 2) PET and MRI were employed to confirm the inverse spatial distributions between AD pathology and cortical myelin *in vivo*. ***We hypothesized that 1) CSF biomarkers of AD pathology and neurodegeneration would negatively associate with cortical and WM R1 and 2) in a participant with substantial AD***

pathology, we would be able to replicate the observations that cortical myelination inversely mirrors the spatial patterns of AD pathology in vivo.

Significance: Studying the role of cortical and WM myelination in healthy aging and cognitive impairment is crucial to understanding the timeline and pathogenesis of AD. Contextualizing their respective roles in the context of AD risk factors, AD pathology, and cognition could lead to the development of more reliable diagnostic criteria or targeted treatments.

Chapter 2: Establishing trajectories of late-life cortical and white matter myelination in cognitively unimpaired older adults as well as individuals with Alzheimer's clinical syndrome

Establishing trajectories of late-life cortical and white matter myelination in cognitively unimpaired older adults as well as individuals with Alzheimer's clinical syndrome

Prepared following guidelines for the journal Neuroimage

Authors: Akshay Kohli[1,2], Steven R Kecskemeti[3], Kao Lee Yang[1,2], Margo Heston[1], Rebecca L Koscik[1], Jennifer M Oh[1], Veena Nair[5], Vivek Prabhakaran[5], Shi-Jiang Li[6], Andrew L Alexander[3,4], Sterling C Johnson[1], Sanjay Asthana[1], Barbara B Bendlin[1]

Author Affiliations:

1) Wisconsin Alzheimer's Disease Research Center, UW-Madison SMPH, Madison, WI
2) Neuroscience Training Program, UW-Madison SMPH, Madison, WI
3) Waisman Laboratory for Brain Imaging and Behavior, Waisman Center, UW-Madison, Madison, WI
4) Department of Medical Physics, UW-Madison SMPH, Madison, WI
5) Department of Radiology, UW-Madison SMPH, Madison, WI
6) Geriatric Research Education and Clinical Center, William S. Middleton Memorial Veterans Hospital, Madison, WI
7) Department of Biophysics, Medical College of Wisconsin, Milwaukee, WI

ABSTRACT

Myelin plays a key role in maintaining optimal cognitive performance. Prior research studying myelin in humans has primarily focused on brain white matter, and studies of intracortical myelin have featured small cohorts and used less sensitive myelin measurements such as the T1w/T2w ratio. Here we studied intracortical and cortical-adjacent white matter myelin in a large cohort of older adults with and without cognitive impairment. We leveraged the novel MPnRAGE MRI sequence to estimate quantitative R1, a metric of tissue relaxometry highly sensitive to brain myelin. R1 metrics showed that intracortical myelin was higher in older age and among individuals with mild cognitive impairment (MCI) and dementia. In contrast, cortical-adjacent white matter R1 was lower with older age, MCI, and dementia. Importantly, these findings were replicated in an independent dataset. Finally, higher levels of cortical R1 were associated with worse performance on tests of executive function and working memory, but not processing speed, whereas higher WM R1 was associated with better processing speed. This work points to a differential role for myelin between cortical gray matter and white matter in aging. Future work will assess relationships between biomarkers of Alzheimer's disease (AD) and MPnRAGE-derived R1 to elucidate the role of intracortical myelin in AD pathogenesis and progression.

INTRODUCTION

Brain myelination is critical for efficient propagation of action potentials between neurons, allowing for healthy brain function. Although subcortical white matter (WM) contains most of the brain's myelin, intracortical axons are also substantially myelinated[47]. Postmortem observations from Braak et al. report that brain regions with high cortical myelin content appear to aggregate Alzheimer's disease (AD) pathology more slowly than regions with less myelination; however, this theory requires greater testing *in vivo*[41,42,76]. While substantial research has linked widespread subcortical WM degeneration to aging[90,91], cognitive decline[92,93], and AD pathology[67,82,88], the role of intracortical myelin in aging and cognitive impairment remains understudied.

A key limitation to studying cortical myelin *in vivo* has included measurement sensitivity. One estimation method calculates the ratio of an individual's T1-weighted (T1w) and T2-weighted (T2w) magnetic resonance imaging (MRI) scans; here, a higher ratio indicates greater myelin density[60]. This ratio has been applied to study cortical myelin in healthy aging[53,60,94], establishing a linear increase before 30 years of age, a plateau from 30-50 years, and a subsequent decline until death. Further, cortical T1w/T2w appears altered in multiple sclerosis[95] and Huntington's disease[96], suggesting a sensitivity to disease-related changes. However, the T1w/T2w ratio has yielded conflicting findings in AD studies of cortical myelin. Research has correlated higher T1w/T2w ratios in several cortical regions to AD diagnosis and worse cognitive performance[69], and has contrarily linked AD pathology to lower regional T1w/T2w ratios[70]. These incongruent findings may be attributed to variable T1w and T2w acquisition parameters, in addition to the variations in sensitivity to iron and macromolecules that exist between T1w and T2w sequences. These confounding results limit our ability to infer the role of cortical myelin in cognitive function in aging. Importantly, understanding this role may elucidate brain regions susceptible to cognitive change in late life, which may help identify potential targets for treatment or intervention in AD.

To overcome some of limitations of the T1w/T2w ratio, quantitative R1 (=1/T1) mapping can be utilized as a standardized metric of cortical myelination[51,52,97]. Studies have used quantitative R1 to probe myelination of the striate cortex[98] and the brainstem[99], as well as white matter maturation and degeneration[100]. Quantitative R1 mapping also improves upon existing imaging sequences sensitive to brain myelin, such as mcDESPOT[101], as we gain spatial resolution that allows us to probe intracortical myelin without contamination from CSF or subcortical WM[63].

Typical MRI sequences capable of R1 estimation have had limited applicability in clinical settings. These methods often rely on multiple T1w scans run sequentially, increasing time spent in the scanner which may be difficult for elderly participants and/or people with underlying health concerns. To address this, we employed a variant of the magnetization-prepared rapid acquisition gradient echo (MPRAGE)[102] T1w sequence called MPnRAGE with motion correction[73,74], which enables the acquisition of hundreds of differently contrasted T1w images during a single scan in under 10 minutes. This data-rich scan procedure allows for precise R1 estimation and results in a high-contrast T1w image. The sequence produces reliable estimates of R1 in cortical and subcortical regions when processed using Freesurfer and the FMRIB Software Library (FSL) segmentation algorithms[103]. MPnRAGE-derived R1 mapping has since been applied to study white matter development in rhesus macaques[36].

As cortical myelin's role in aging and cognition remains poorly defined, in this study we employed *in vivo* quantitative R1 mapping to 1) establish the relationship between cortical myelin and age in late life, 2) identify how cortical myelin varied in individuals living with and without cognitive impairment, and 3) assess the role of cortical and WM in performance on tests from the NIH toolbox cognitive battery. We hypothesized that 1) cortical myelin would show widespread parabolic decreases with increased age, 2) individuals with cognitive impairment due to AD would have lower cortical myelin than unimpaired individuals, and 3) higher cortical and WM myelin would be associated with better performance on individual tests of working

memory, executive function, and processing speed. This study is the first to employ MPnRAGE R1 mapping to investigate cortical and WM myelin in older adults with and without cognitive impairment.

METHODS

Participant Sample

For the primary study, data was included from 864 adults (mean age = 65.79 years, standard deviation [SD] = 8.08 years; 65% female) enrolled in the Wisconsin Alzheimer's Disease Research Center clinical core (ADRC) and the Wisconsin Registry for Alzheimer's Prevention (WRAP) studies (Table 1). 791 were cognitively unimpaired, 43 were diagnosed with mild cognitive impairment (MCI), and 30 were diagnosed with dementia. In replication analyses, data was derived from 157 adults (mean age = 69.70, SD = 8.31 years; 52.90% female) enrolled in the Alzheimer's Disease Connectome Project (ADCP) (Table 2). 79 were cognitively unimpaired, 49 were diagnosed with MCI, and 29 were dementia. Consensus conference of participant cognitive performance and functional ability were conducted to determine clinical diagnosis. Diagnosis of MCI or dementia were assigned based on National Institute on Aging-Alzheimer's Association (NIA-AA) criteria.[15,104]

Institutional approvals and consent

All protocols for the ADRC and WRAP studies were approved by the University of Wisconsin Health Science Institutional Review Board. All protocols for the ADCP study were approved by the Medical College of Wisconsin Institutional Review Board. Written informed consent was provided by all enrolled participants.

MRI acquisition and processing

Participants enrolled in ADRC or WRAP underwent MRI via a General Electric 3T Discovery MR750 scanner (Waukesha, WI) with a 32-channel receive-only head coil (Nova Medical, Wilmington, MA) or a General Electric 3T Signa Premier scanner using a 48-channel receive-only head coil at the University of Wisconsin. Participants enrolled in ADCP underwent MRI at UW-Madison via the aforementioned scanners, or at the Medical College of Wisconsin using a General Electric 3T Discovery MR750 scanner (Waukesha, WI) using a 32-channel head coil. T1w structural scans were acquired via MPnRAGE[73], a variation of the MPRAGE[102] sequence that allows for sampling over many time points, n, along the inversion recovery curve. Four MPnRAGE sequence variants were used over the course of the study; a group-wise breakdown of sequences and scanning parameters can be found in Supplemental Figures 1 & 2. T1w images were reconstructed with motion correction[74], 6 iterations of bias field correction and total variation denoising via Advanced Normalization Tools (ANTs)[105]. Quantitative T1 maps were constructed by estimating T1 in each voxel using previously published methods[74]. Quantitative R1 maps were then produced by calculating the reciprocal of the T1 maps using FSL[106]. As the R1 maps are inherently registered to the T1w composite images, no co-registration was required before further processing and analyses. All T1w images and R1 maps were visually inspected for quality assurance.

For each participant, T1w composite images were processed through the *recon-all* function in Freesurfer v6. Briefly, structural scans underwent gray matter (GM) and WM tissue segmentation; surface estimation was subsequently performed at the GM-WM boundary and at the pial surface. To extract cortical GM R1 values, R1 was sampled along the midpoint between the two surface meshes to create a central cortical R1 mesh for each participant. Resulting R1 surface meshes were inflated to Freesurfer template space and smoothed with a 10 mm full width-half maximum Gaussian kernel (in geodesic distance)[56]. Mean R1 was then extracted for each region of interest (ROI) using Desikan-Killiany parcellation [107]. Similarly, to extract cortical-

adjacent WM R1 values, average R1 was sampled using from each subject's *wmparc* file, which labels WM tissue with 5mm of the cortex, and parcellates the tissue using the closest cortical ROI in the Desikan atlas. This resulted in 34 independent ROIs for cortical GM R1 and 34 ROIs for cortical-adjacent WM R1. The *ggseg* package in R was used to visualize data for each ROI[108]. Cortical surface meshes and WM segmentations were visually inspected to ensure accurate tissue delineation. Full processing steps are depicted in Figure 1.

ComBat harmonization across MPnRAGE protocols

Because multiple MPnRAGE protocols were implemented across the ADRC and WRAP cohorts, data harmonization was required to pool these data for statistical analysis of R1. Harmonization was performed using ComBat, a tool originally developed for large gene sets[109] and subsequently adapted for neuroimaging data. Supported by an empirical Bayesian framework, ComBat is robust to outliers in small samples and pools information across features to shrink estimates, with the goal of removing batch variance while retaining biological variance. Prior implementations have successfully harmonized cortical thickness[110], diffusion tensor imaging[111], and functional connectivity metrics[112]. Additionally, Fortin et al. (2018) showed that ComBat's location and scale adjustment method outperforms models that treat image batch as a covariate[111]. In the present study, ComBat was independently applied to each regression model estimated for cortical GM R1 and cortical-adjacent WM R1. To minimize bias from extreme outliers, R1 values beyond 3 x interquartile range for each ROI were removed before harmonization was initiated. As consistent acquisition protocols were used throughout ADCP, no harmonization was performed within that dataset; however, R1 values beyond 3*IQR were removed for analysis for consistency with the ADRC/WRAP dataset.

Statistical analysis

Regional patterns of GM and WM R1 in unimpaired individuals

To assess regional variation in GM and WM myelin in normal aging, R1 was averaged across all 791 cognitively unimpaired participants for each of the 34 bilaterally averaged ROIs. A surface map of cortical GM R1 for a single subject and a population-averaged R1 map across the cortex and cortical-adjacent white matter can be seen in Figure 2.

Cross-sectional relationships between R1 and aging

To test the hypothesis that cortical GM and WM myelin decreases with increased age, multiple regression models were employed per ROI for both cortical GM and WM R1 (34 total models for each tissue). Participants included cognitively unimpaired individuals enrolled in the ADRC or WRAP studies who underwent an MPnRAGE scan (N = 791). As GM and WM myelin has previously shown parabolic relationships with age, both linear and quadratic age effects were tested. The outcome measure for each ROI's model was mean R1; predictors of interest included age at MRI visit and age^2, and sex was included as a covariate. Resulting FDR-corrected *p*-values (*q*-values) were deemed significant at 0.05; Benjamini-Hochberg FDR adjustment was performed per group of 34 tests for cortical GM and cortical-adjacent WM separately. This analysis was repeated with the ADCP dataset (N=79).

Group differences in R1 with cognitive impairment

To assess the extent to which cortical GM and WM myelin is altered with cognitive impairment, multiple linear regression models were employed per ROI for both cortical GM and WM R1 (34 total models for each tissue). Participants included individuals in the ADRC or WRAP studies who were cognitively unimpaired (N = 791), diagnosed with MCI (N = 43), or dementia (N = 30), and underwent an MPnRAGE scan. Due to the small number of participants

with MCI or dementia, these groups were pooled into an "impaired" category (N = 73) to test the effect of cognitive impairment. The outcome measure for each ROI's model was mean R1; covariates included age or age^2 and participant sex. Resulting FDR-corrected *p*-values (*q*-values) were deemed significant at 0.05; Benjamini-Hochberg FDR adjustment was performed per group of 34 tests for GM and WM separately. Post-hoc t-tests were then performed per ROI to detect differences in R1 between MCI and dementia participants; Bonferroni correction was applied to control for multiple comparisons. This analysis was repeated with the ADCP dataset (CU = 79, MCI = 49, Dementia = 29).

Associations between cortical GM and WM R1 and NIH Toolbox cognitive battery performance

To assess the role of cortical myelin in function of individual cognitive domains, as subset of the ADCP cohort (n = 143; Table 3) with MPnRAGE MRI also underwent testing via the NIH Toolbox Cognitive Battery. The NIH Toolbox has successfully been used to identify cognitive change in Alzheimer's disease[18,20,21]. Within this analysis, individual ROIs from the Desikan-Killiany atlas (as observed in Figure 1) were compiled into 5 bilateral composite ROIs indexing R1 in the posterior cingulate, anterior cingulate, frontal, parietal, and temporal cortices. Composite regions of interest are displayed in Figure 8. Uncorrected standard scores were computed by the NIH Toolbox for each measure of executive function (dimensional change card sort test; DCCS), working memory (list sorting test; LS), and processing speed (pattern comparison test; PC). Multiple linear regression models (5 ROIs * 3 Cognitive Tests) were employed for cortical GM and cortical-adjacent WM. Test scores were the dependent variable in each model, regional R1 was the predictor of interest, and age, sex, and years of education were covariates.

RESULTS

Regional variation in cortical GM and WM R1

Within-brain cortical R1 variation was observed within a single subject (Figure 2a) and in a population map averaged across the cognitively unimpaired participants (Figure 2b). The precentral, postcentral, cuneus, precuneus, entorhinal cortex, and transverse temporal ROIs exhibited the highest levels of R1 in the cortex. The inferior and middle temporal gyri, the inferior and superior frontal, rostral anterior cingulate, supramarginal, and angular gyri all exhibited comparatively lower R1 in the cortex. Cortical GM R1 varied between 0.65 and 0.8Hz. Cortical-adjacent WM R1 ranged between 1 and 1.2Hz.

Effects of age on R1 in cortical GM and cortical-adjacent WM

Figure 3 visualizes and quantifies regional model results for the ADRC/WRAP cohort. In cortical GM, positive linear associations between age and R1 were found in the insula (t = 5.685, q = 6.280e^{-7}), medial orbitofrontal (t = 3.306, q = 5.608e^{-3}), parahippocampal (t = 4.001, q = 5.860e^{-4}), rostral anterior cingulate (t = 4.416, q = 1.298e^{-4}), superior temporal (t = 2.720, q = 3.245e^{-2}), and transverse temporal (t = 3.562, q = 2.658e^{-3}) ROIs (Figure 3a, Table A3). There were no negative associations with age (Table A3) and no quadratic effects of age (Table A5) on cortical R1. In cortical-adjacent WM, negative quadratic effects of age on R1 were found in all regions except for the precentral, postcentral, pericalcarine, lingual, lateral occipital, and cuneus ROIs. WM regions with the strongest quadratic age effects on R1 included the entorhinal (t = -5.546, q = 1.357e^{-6}), parahippocampal (t = -4.080, q = 3.369e^{-4}), lateral orbitofrontal (t = -4.905, q = 1.928e^{-5}), and medial orbitofrontal (t = -4.471, q = 1.010e^{-4}) ROIs (Figure 3b, Table A6). There were no positive associations between age and R1 in WM (Table A6). Coefficient of determination (R^2) values were higher in models predicting WM R1 (Adjusted

R^2 between 0.1 and 0.28 in significant models) compared to GM R1 (Adjusted R^2 < 0.04). Complete model outputs can be referred to in Tables A3-A8.

Results of analyses testing the linear and quadratic effects of age on cortical GM and cortical-adjacent WM R1 in the ADCP cohort can be found in Figure 4. There were no significant associations between age and R1 in cortical GM, however, at an uncorrected p<0.05 threshold, positive linear associations between age and R1 were found in the insula (t = 2.769, p = 6.322e^{-3}), medial orbitofrontal (t = 2.322, p = 2.156e^{-2}), parahippocampal (t = 2.173, p = 3.133e^{-2}), rostral anterior cingulate (t = 2.028, p = 4.426e^{-2}), and posterior cingulate (t = 4.053, p = 7.999e^{-5}), ROIs (Figure 4a, Table A9). There were no significant negative associations with age (Table A9) and no detectable quadratic effects of age (Table A11) on cortical R1 in ADCP. In cortical-adjacent WM, significant negative linear effects of age on R1 were found in all regions. These included regions often affected by AD pathology, including the lateral orbitofrontal (t = -7.098, q = 1.483e^{-9}), medial orbitofrontal (t = -6.813, q = 3.450e^{-9}), superior frontal (t = -6.575, q = 8.083e^{-9}), supramarginal (t = -5.830, q = 1.187e^{-7}), middle temporal (t = -5.000, q = 3.285e^{-6}), and fusiform (t = -6.575, q = 8.083e^{-9}) ROIs, among others (Figure 4b, Table A10). There were no positive associations between age and R1 in WM. There were no positive associations with age, and no detectable quadratic effects of age in WM. Consistent with the ADRC/WRAP sample, R^2 values tended to be higher in models predicting WM R1 (Adjusted R^2 between 0.04 and 0.22 in significant models, Figure 4b) compared to GM R1 (Adjusted R^2 between 0.01 and 0.16, Figure 4a). Complete outputs of models testing linear and quadratic age effects on cortical GM and WM R1 in the ADCP cohort can be referred to in Tables A9-A14.

Relationships between cortical and WM R1 and cognitive impairment

Population-averaged cortical R1 maps for each diagnostic group scanned under MPnRAGE protocol A can be seen in Figure 5. Visual inspection of the surface maps shows that MCI and dementia participants had higher R1, particularly in the temporal lobe.

Results from regression models and post-hoc t-tests assessing the effects of cognitive impairment on GM and WM R1 in the ADRC/WRAP cohort can be observed in Figure 6. Within cortical GM, individuals with cognitive impairment exhibited significantly higher levels of R1 in the middle temporal (t = 2.782, q = 4.276e^{-2}), parahippocampal (t = 3.461, q = 1.919e^{-2}), and rostral anterior cingulate (t = 3.240, q = 2.113e^{-2}) ROIs. R1 was marginally higher in the cognitively impaired group in the inferior temporal (t = 2.377, p = 1.766e^{-2}), insula (t = 2.418, p = 1.582e^{-2}), and superior temporal (t = 2.159, p = 3.110e^{-2}) ROIs. Bonferroni-corrected post-hoc t-tests in each of these ROIs revealed no significant differences in R1 between the MCI and Dementia participants and that the MCI participants drove the effect of cognitive impairment (Figure 6a). Of note, there were no regions in which cognitively impaired individuals exhibited lower levels of R1 in the cortex compared to unimpaired participants (Table A15).

In cortical-adjacent WM, individuals with cognitive impairment had significantly higher R1 in all regions. These effects were strongest in the entorhinal (t = -8.403, q = 6.083e^{-15}), parahippocampal (t = -7.115, q = 4.026e^{-11}), precuneus (t = -5.315, q = 1.555e^{-6}), temporal pole (t = -5.230, q = 1.816e^{-6}), posterior cingulate (t = -5.187, q = 1.816e^{-6}), and isthmus cingulate (t = -4.999, q = 3.964e^{-6}) ROIs. Analogously to cortical GM, Bonferroni-corrected post-hoc t-tests in each WM ROI revealed no significant differences in R1 between MCI and dementia participants, however R1 tended to be marginally lower in individuals with dementia compared to those with MCI (Figure 6b). There were no regions where individuals with cognitive impairment had higher WM R1 compared to unimpaired individuals (Table A16).

Results from regression models and post-hoc t-tests assessing the effects of cognitive impairment on GM and WM R1 in the ADCP cohort can be observed in Figure 7. Within cortical GM, individuals with cognitive impairment exhibited significantly higher levels of R1 in numerous regions including the inferior temporal (t = 4.596, q = 3.044e^{-4}), parahippocampal (t = 4.314, q = 4.454e^{-4}), middle temporal (t = 4.235, q = 4.454e^{-4}), fusiform (t = 4.066, q = 6.486e^{-4}), temporal pole (t = 3.590, q = 3.029e^{-3}), and insula (t = 3.366, q = 5.464e^{-3}) ROIs. Similarly to the

ADRC/WRAP cohort, Bonferroni-corrected post-hoc t-tests in each of these ROIs revealed no significant differences in R1 between the MCI and Dementia participants (Figure 7a). There were no cortical regions where individuals with cognitive impairment had lower R1 compared to unimpaired individuals (Table A17).

In cortical-adjacent WM, individuals with cognitive impairment had marginally higher R1 only in the entorhinal cortex (t = -2.082, $p = 3.900e^{-2}$). WM ROIs that exhibited significant impairment effects in the ADRC/WRAP cohort were also examined in the ADCP cohort. Bonferroni-corrected post-hoc t-tests revealed that dementia participants had significantly lower R1 compared to MCI and unimpaired individuals, with no significantly differences in R1 between MCI and unimpaired participants (Figure 7b). There were no regions where individuals with cognitive impairment had higher WM R1 compared to unimpaired individuals (Table A18).

Associations between cortical and WM R1 and cognitive performance

Higher cortical R1 was associated with worse performance on the DCCS test in the temporal ($t = -2.766$, $p = 6.445e^{-3}$) and posterior cingulate ($t = -2.621$, $p = 9.743e^{-3}$) ROIs. Additionally, higher R1 in temporal ROI was associated with worse performance on the LS test ($t = -2.834$, $p = 5.321e^{-3}$) (Figure 9a). There were no significant associations between performance on the PC test and regional cortical R1. In cortical-adjacent WM, no significant associations were found between R1 and performance on the DCCS or LS tests, however, higher R1 was associated with better performance on the PC test in the frontal ($t = -2.834$, $p = 5.321e^{-3}$), temporal ($t = -2.834$, $p = 5.321e^{-3}$), and parietal ($t = -2.834$, $p = 5.321e^{-3}$) ROIs (Figure 9b). Full outputs of regression models may be referred to in Tables A19-A24 in the appendix.

DISCUSSION

Regional variation in cortical GM and WM R1

Our single subject and population-averaged cortical R1 maps reflected myelin patterns previously reported in studies of grey matter myeloarchitecture[48,50,51,57,60]. The somatosensory, motor, and visual cortices exhibited the highest myelin levels and the temporal and frontal cortices exhibited relatively lower myelin levels (Figure 2a & 2b). Two distinct temporal regions, the entorhinal cortex and the transverse temporal area, had high levels of R1 in contrast to the rest of the temporal lobe. This is likely due to the relatively unreliable estimation of the pial and GM/WM boundaries in these regions[113,114], and our findings in these regions are consistent with previously-reported T1/T2 ratio surface maps[60]. Cortical R1 patterns were consistent across hemispheres as can be observed in Figure 2a. In contrast, distributions of R1 in cortical-adjacent WM were more uniform across the brain, with cingulate WM exhibiting the highest levels of R1 and visual and orbitofrontal WM revealing the lowest WM R1. Importantly, R1 values in gray and white matter fell within ranges of T1 relaxation times derived through alternative MR protocols and sequences (specifically brain tissue scanned at 3T)[115,116]. These findings provide robust support that MPnRAGE-derived R1 is a sensitive to intraindividual variations in myelin content in both the cortex and WM.

Increases in cortical R1 with aging and cognitive impairment

Investigation of cortical R1 in both the ADRC/WRAP and ADCP samples suggested that myelination remains relatively stable in most regions, with some areas including the insula, parahippocampal gyrus, and medial orbitofrontal cortex showing linear increases with age. We also found that individuals with cognitive impairment exhibited higher R1 compared to unimpaired individuals, controlling for age effects. These results contrast our hypotheses, as well as findings from prior human imaging studies which have identified negative parabolic

trajectories of myelin across the lifespan using the T1w/T2w ratio[56,57,60]. Studies assessing relationships between cortical myelin and AD have yielded mixed results, with one study finding greater cortical myelin in individuals with AD[69], and another finding lower cortical myelin in AD[70]. This study aimed to improve upon prior work by including the largest population of older adults in a cortical myelin study to date, using MPnRAGE with motion correction to derive quantitative R1, and repeating analyses in an independent cohort.

In addition to assessing cortical myelin, our study also identified age and impairment effects on cortical-adjacent WM R1. Our results strongly supported the existing findings that WM myelin decreases parabolically with age and is lower in individuals with MCI and dementia. We likely did not find quadratic age effects in our replication cohort due to the small sample size in ADCP; however, we did find strong linear decreases. Additionally, there were no significant impairment effects in our replication cohort, but post-hoc t-tests revealed that individuals with dementia had significantly lower R1 compared to those without impairment. Unlike our ADRC/WRAP cohort, individuals with MCI in ADCP did not show lower R1 compared to unimpaired participants. With regards to the individual tests of cognition, cortical myelin exhibited different relationships compared to those identified in WM, with GM myelin relating to performance of executive function and working memory, while WM related heavily to processing speed. Prior studies of WM myelin have found strong associations with measures of processing speed in adolescence[117], aging[118,119], as well as in neurodegenerative disease[120]. No studies have yet assessed the role of cortex specific myelin in individual cognitive domains; as such, this is the first to indicate that cortical myelin may be involved in promoting executive function.

Higher cortical R1 with age and cognitive impairment could indicate the complex differential role that myelin plays in the cortex as opposed to in WM. In a prior study, researchers stained hippocampal tissue for myelin from a healthy control, a person with late onset Alzheimer's disease (LOAD), and an individual with early onset Alzheimer's disease (EOAD). The healthy control showed clean, raster-like traversal of myelin-coated axons

throughout layers 3-5 of the cortex, whereas those with LOAD and especially EOAD had greater cortical myelin disorganization[121]. It is possible that our MPnRAGE procedures represent this greater disorganization as higher R1 values. Another possibility may be that in aging and AD, oligodendrocytes compensate for axonal damage and demyelination by repairing and remyelinating the cortex. A study using a multiple sclerosis mouse model found that, after inducing acute demyelination, oligodendrocytes myelinated axons that were previously unmyelinated in addition to the acutely damaged axons, altering the composition and organization of cortical myelin[39]. This may occur in individuals with MCI and dementia, as oligodendrocytes are known to continue remyelinating in AD. Our findings with increased cortical myelin with worse executive function and working memory add support for this hypothesis, as altered patterns of cortical myelin (especially within inhibitory neurons) could negatively impact function within these domains. Future work investigating the interplay between beta-amyloid and phosphorylated tau accumulation will elucidate cortical myelin's role in the AD pathogenesis and progression.

While R1 is highly sensitive to brain myelin, several other biological and physical properties may contribute to tissue relaxometry, including iron concentration, partial volume effects due to cortical thinning with age, variable MR acquisition and scanner parameters, and molecular composition of the cortex, among others. Additionally, some cortical regions including the pre-and-postcentral gyri and cuneus can be <1mm in thickness, potentially leading to signal bias from cerebrospinal fluid outside the brain or adjacent WM. However, our methods attempted to minimize this bias by sampling R1 from the midpoint of the cortical surface. Finally, while this study was performed using large sample sizes and an independent cohort for replication, participants of both cohorts were highly educated and reflected the primarily White/Caucasian demographic of the midwestern United States, which may affect the study's generalizability. The primary focus of this work was to use quantitative R1 mapping derived from the novel MPnRAGE sequence to assess the effects of age and cognitive impairment on

intracortical myelin. Future work will directly explore the impact of AD pathology, including brain amyloid beta and phosphorylated tau, on myelination in the cortex and cortical-adjacent WM.

CONCLUSION

Our findings, contrary to prior studies of cortical myelin throughout the lifespan, suggest that intracortical myelin indexed by R1 remains relatively stable from ages 45 to 90, with some regions in the temporal and frontal cortices exhibiting increases with age. Importantly, these results were maintained when assessed in an independent replication cohort. While our statistical analyses revealed increases in cortical R1 with age in several regions, effect sizes were small and indicated that very little R1 change occurs in the cortex. In contrast, our analyses of cortical-adjacent WM R1 strongly supported findings from prior studies that suggest loss of myelin from middle age through late life, and particularly in individuals with MCI and dementia.

TABLES AND FIGURES

Table 1: Participant Demographics from ADRC/WRAP Cohort

	Cognitively Unimpaired (N=791)	Mild Cognitive Impairment (N=43)	Dementia (N=30)	p value
Age at MRI Scan				< 0.001[1]
Mean (SD)	65.183 (7.711)	72.710 (9.231)	71.998 (8.928)	
Min - Max	45.710 - 90.370	49.850 - 90.210	49.740 - 88.110	
Sex				0.026[2]
Female	524 (66.2%)	20 (46.5%)	18 (60.0%)	
Male	267 (33.8%)	23 (53.5%)	12 (40.0%)	
Education				0.034[1]
Mean (SD)	16.269 (2.548)	15.372 (2.479)	15.467 (3.511)	
Min - Max	8.000 - 25.000	12.000 - 20.000	9.000 - 22.000	
Primary Race				0.934[2]
American Indian or Alaska Native	18 (2.3%)	0 (0.0%)	1 (3.3%)	
Asian	2 (0.3%)	0 (0.0%)	0 (0.0%)	
Black or African American	71 (9.0%)	7 (16.3%)	2 (6.7%)	
Other	1 (0.1%)	0 (0.0%)	0 (0.0%)	
Unknown	2 (0.3%)	0 (0.0%)	0 (0.0%)	
White	697 (88.1%)	36 (83.7%)	27 (90.0%)	
APOE E4 Status				0.003[2]
Non-Carrier	493 (62.3%)	20 (46.5%)	11 (36.7%)	
Carrier	298 (37.7%)	23 (53.5%)	19 63.3%)	

Table 1: Participants were enrolled in the Wisconsin Alzheimer's disease Research Center Clinical Core or the Wisconsin Registry for Alzheimer's Prevention studies at the University of Wisconsin-Madison (Madison, WI).[1]Kruskal-Wallis rank sum test. [2]Pearson's Chi-squared test

Table 2: Participant Demographics from ADCP Cohort

	Cognitively Unimpaired (N=79)	Mild Cognitive Impairment (N=49)	Dementia (N=29)	p value
Age at MRI				< 0.001[1]
Mean (SD)	67.129 (7.010)	71.498 (8.665)	73.645 (8.873)	
Min - Max	55.069 - 86.378	55.047 - 90.889	58.647 - 90.467	
Sex				0.058[2]
Male	32 (40.5%)	30 (61.2%)	12 (41.4%)	
Female	47 (59.5%)	19 (38.8%)	17 (58.6%)	
Education				0.037[1]
Mean (SD)	16.506 (2.347)	15.878 (2.690)	15.069 (2.267)	
Min - Max	12.000 - 24.000	12.000 - 21.000	12.000 - 18.000	
Primary Race				0.097[2]
White	73 (92.4%)	41 (83.7%)	29 (100.0%)	
Black or African American	2 (2.5%)	7 (14.3%)	0 (0.0%)	
American Indian or Alaska Native	2 (2.5%)	0 (0.0%)	0 (0.0%)	
Asian	1 (1.3%)	0 (0.0%)	0 (0.0%)	
Other	1 (1.3%)	1 (2.0%)	0 (0.0%)	

Table 2: Participants were enrolled in the Alzheimer's Disease Connectome Project at the University of Wisconsin-Madison (Madison, WI) or Medical College of Wisconsin (Milwaukee, WI). [1]Kruskal-Wallis rank sum test. [2]Pearson's Chi-squared test

Table 3: Participants with NIH Toolbox Data from ADCP Cohort

	Cognitively Normal (N=75)	Mild Cognitive Impairment (N=44)	Dementia (N=24)	p value
Age				< 0.001[1]
Mean (SD)	66.813 (7.128)	71.250 (8.659)	73.875 (8.358)	
Min - Max	55.000 - 86.000	55.000 - 90.000	58.000 - 86.000	
Sex				0.027[2]
Male	29 (38.7%)	28 (63.6%)	10 (41.7%)	
Female	46 (61.3%)	16 (36.4%)	14 (58.3%)	
Education				0.051[1]
Mean (SD)	16.400 (2.354)	16.182 (2.617)	14.958 (2.236)	
Min - Max	12.000 - 24.000	12.000 - 21.000	12.000 - 18.000	
Primary Race				0.174[2]
White	69 (92.0%)	38 (86.4%)	24 (100.0%)	
Black or African American	2 (2.7%)	6 (13.6%)	0 (0.0%)	
American Indian or Alaska Native	2 (2.7%)	0 (0.0%)	0 (0.0%)	
Asian	1 (1.3%)	0 (0.0%)	0 (0.0%)	
Other	1 (1.3%)	0 (0.0%)	0 (0.0%)	
Study Site				0.271[2]
MCW	31 (41.3%)	12 (27.3%)	10 (41.7%)	
UW	44 (58.7%)	32 (72.7%)	14 58.3%)	

Table 3: Participants were enrolled in the Alzheimer's Disease Connectome Project at the University of Wisconsin-Madison (Madison, WI) or Medical College of Wisconsin (Milwaukee, WI). [1]Kruskal-Wallis rank sum test. [2]Pearson's Chi-squared test

Figure 1: Outline of image processing steps conducted using FSL and Freesurfer and resulting WM parcellation maps and surface meshes.

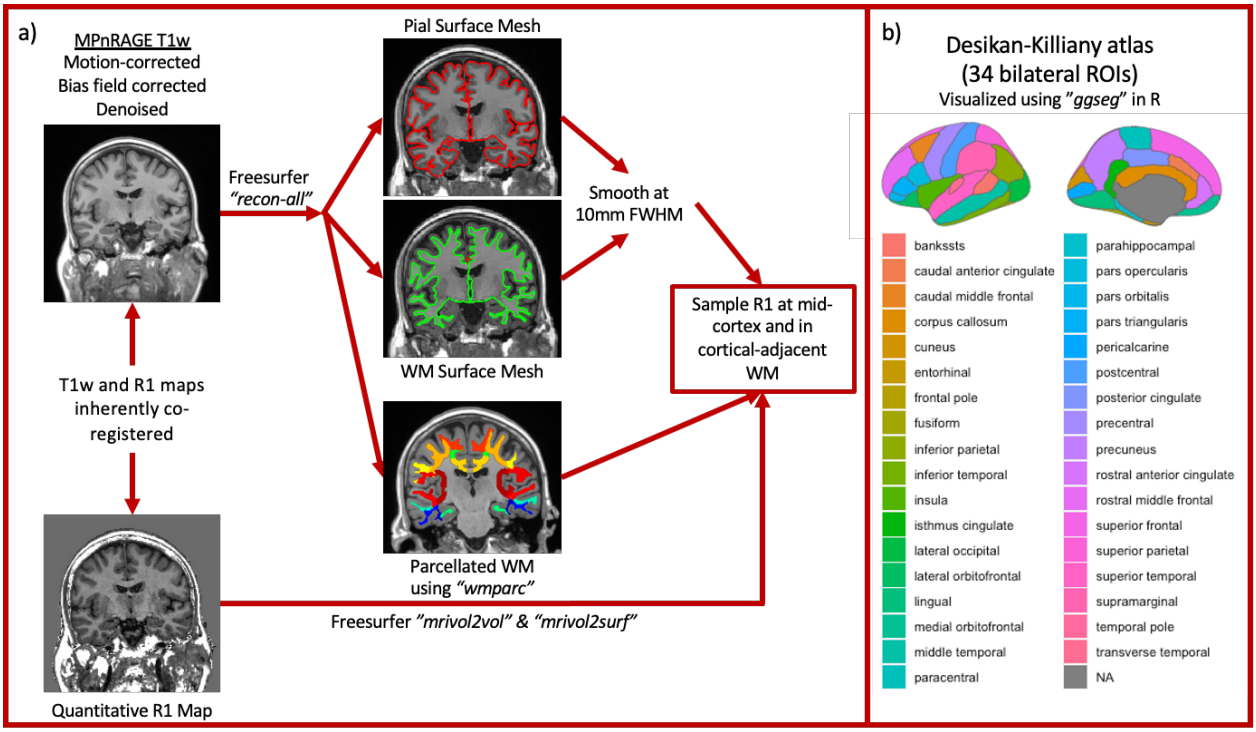

Figure 1: a) Image processing pipeline: T1w images were processed using Advanced Normalization Tools (ANTs) and Freesurfer v6. R1 was sampled at the midpoint of the cortical surface using surface meshes and parcellations produced from Freesurfer for 34 bilaterally-averaged regions of interest (ROI) from the Desikan-Killiany parcellation. b) Regions of interest comprised of bilaterally-averaged regions from the Desikan-Killiany parcellation overlayed onto a brain using the "ggseg" package in R.

Figure 2: Regional Distribution of R1 in cortical GM and WM

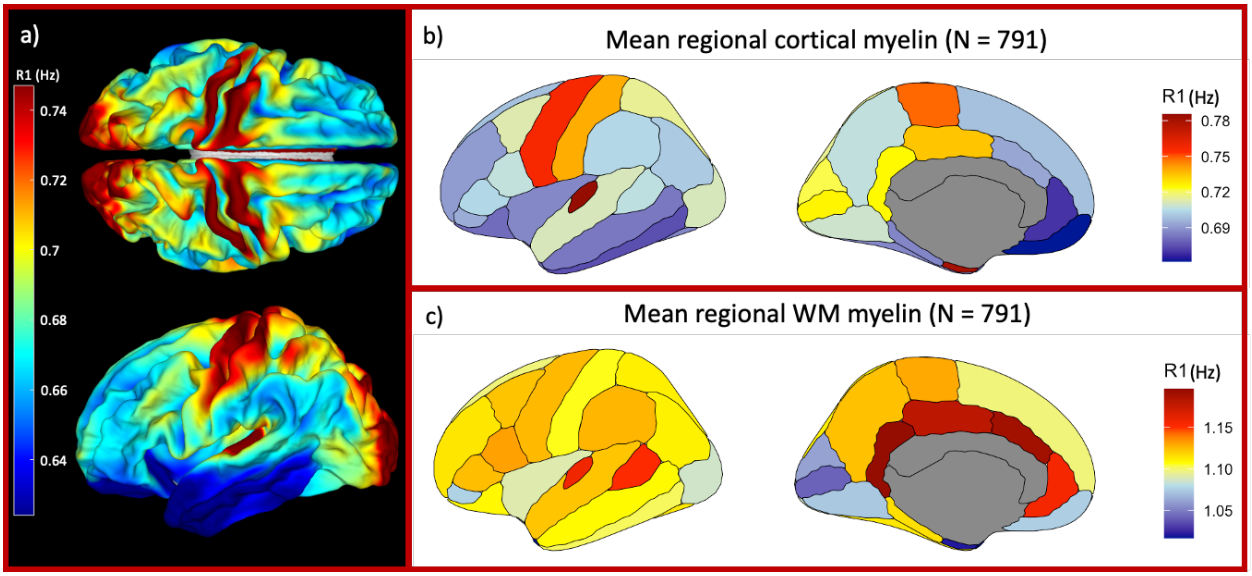

Figure 2: A) Cortical R1 map of a single cognitively unimpaired older adult (age 67). B) Bilaterally averaged R1 in the cortex across 791 cognitively unimpaired participants using the Desikan-Killiany atlas. C) Bilaterally averaged R1 in cortical-adjacent WM across 791 cognitively unimpaired participants parcellated using the Desikan-Killiany atlas.

Figure 3: Effects of Age on Cortical GM and Cortical-Adjacent WM R1 in ADRC/WRAP

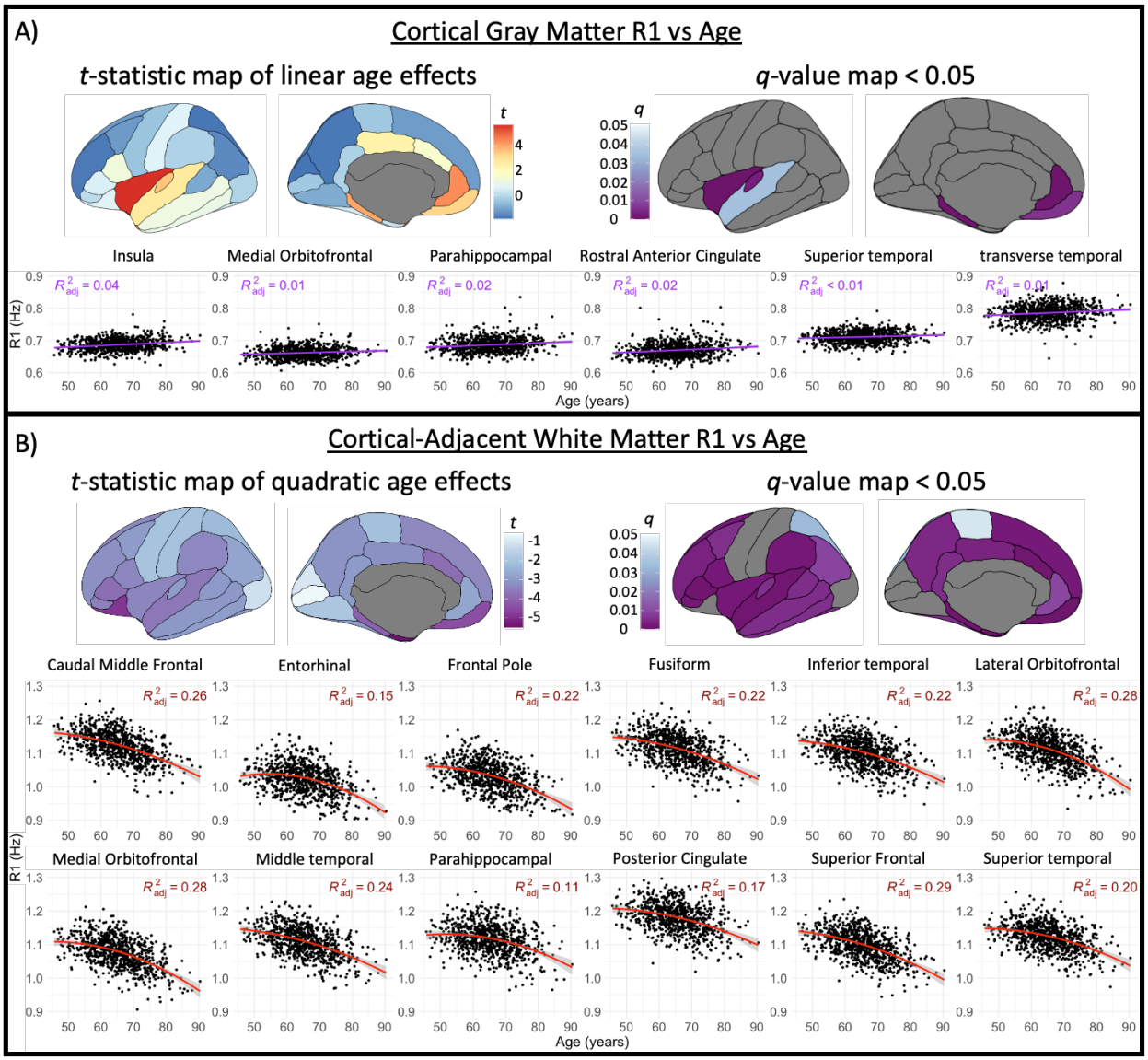

Figure 3: Regression results assessing the effects of age on R1 in the ADRC/WRAP cohort. A) Maps of t-statistics and corresponding FDR-corrected p-values visualizing the linear age effects on cortical GM R1 parcellated by ROIs from the Desikan parcellation. Individual regions with corresponding linear trend lines are plotted below the brain maps using the formula 'y~x'. B) Maps of *t*-statistics and corresponding FDR-corrected p-values visualizing the quadratic age effects on cortical-adjacent WM R1 parcellated by ROIs from the Desikan parcellation. Individual regions with corresponding parabolic trend lines are plotted below the brain maps using the formula 'y~x+x^2'.

Figure 4: Effects of age on cortical GM and cortical-adjacent WM R1 in ADCP

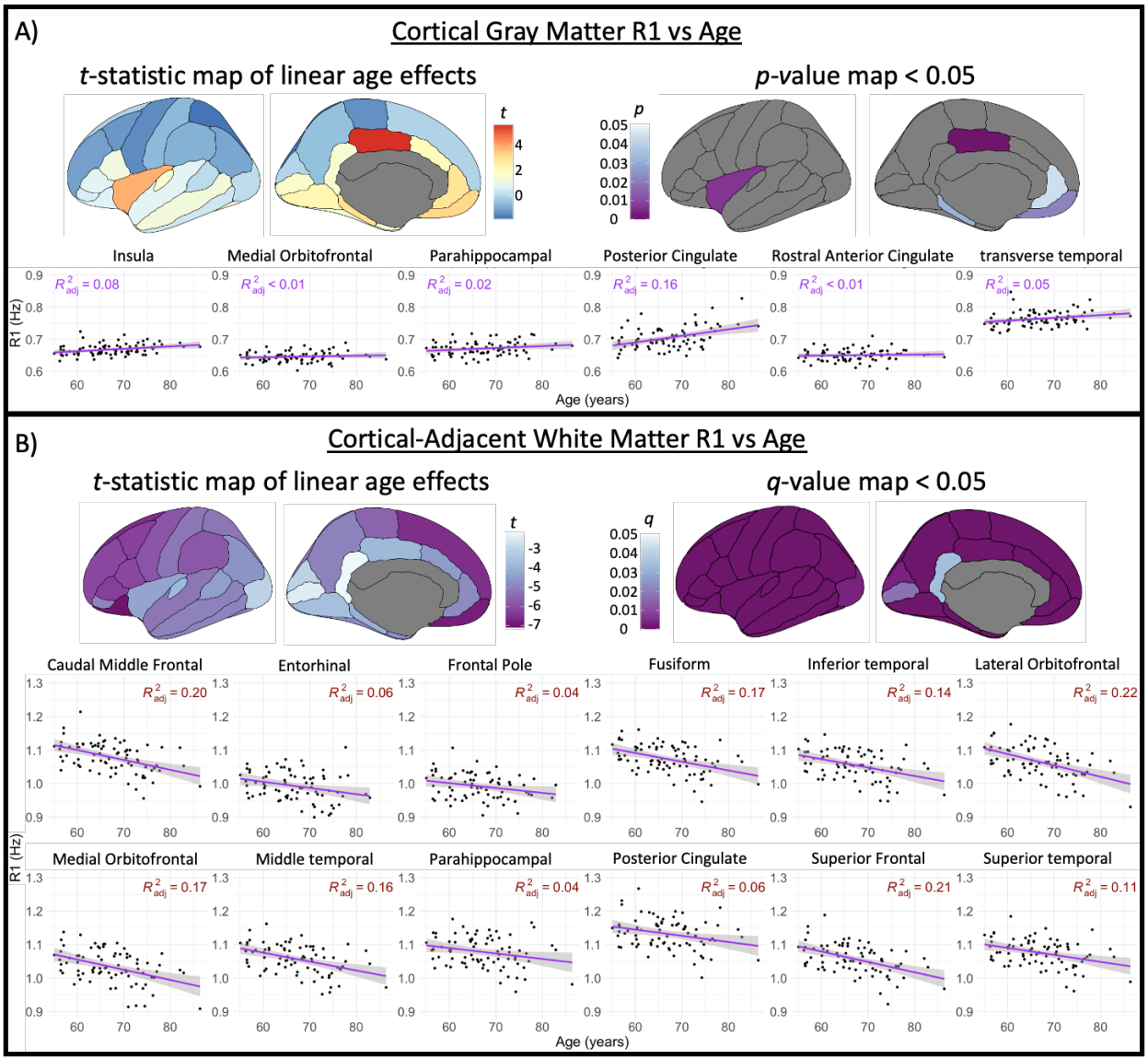

Figure 4: Regression results assessing the effects of age on R1 in the ADCP cohort. A) Maps of *t*-statistics and corresponding *p*-values visualizing the linear age effects on cortical GM R1 parcellated by ROIs from the Desikan parcellation. Individual regions with corresponding linear trend lines are plotted below the brain maps using the formula 'y~x'. B) Maps of *t*-statistics and corresponding FDR-corrected *q*-values visualizing the linear age effects on cortical-adjacent WM R1 parcellated by ROIs from the Desikan parcellation. Individual regions with corresponding linear trend lines are plotted below the brain maps using the formula 'y~x'.

Figure 5: Averaged cortical GM R1 surface maps for each cognitive group scanned under MPnRAGE protocol A

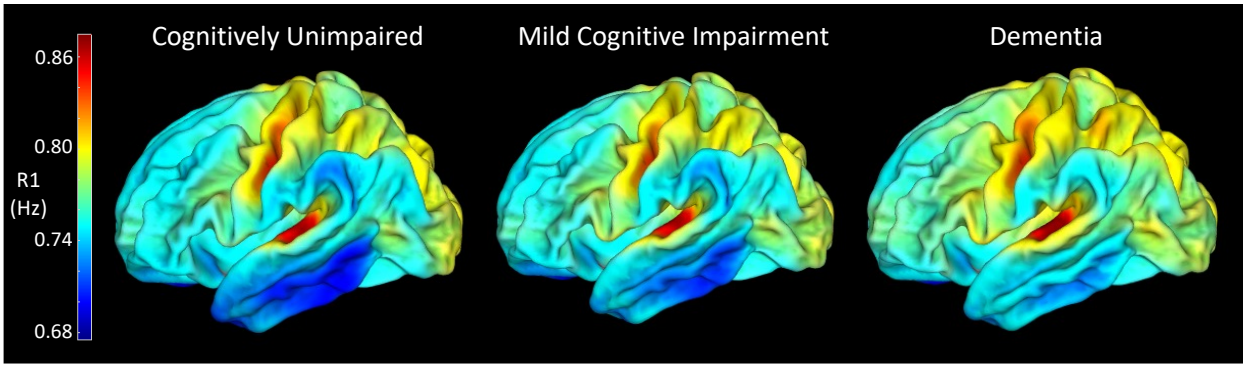

Figure 5: Cortical GM R1 surface maps averaged for each cognitive group scanned under MPnRAGE protocol A in the ADRC/WRAP cohort (Cognitively Unimpaired N = 343, Mild Cognitive Impairment N = 32, Dementia N = 24). Higher R1 can be visually observed in the mild cognitive impairment group, and to a greater degree in the dementia group, as compared to the cognitively unimpaired group. This is most pronounced within the temporal lobe, inferior parietal lobule, and supramarginal gyrus.

Figure 6: Effects of MCI and dementia on cortical and WM R1 in ADRC/WRAP

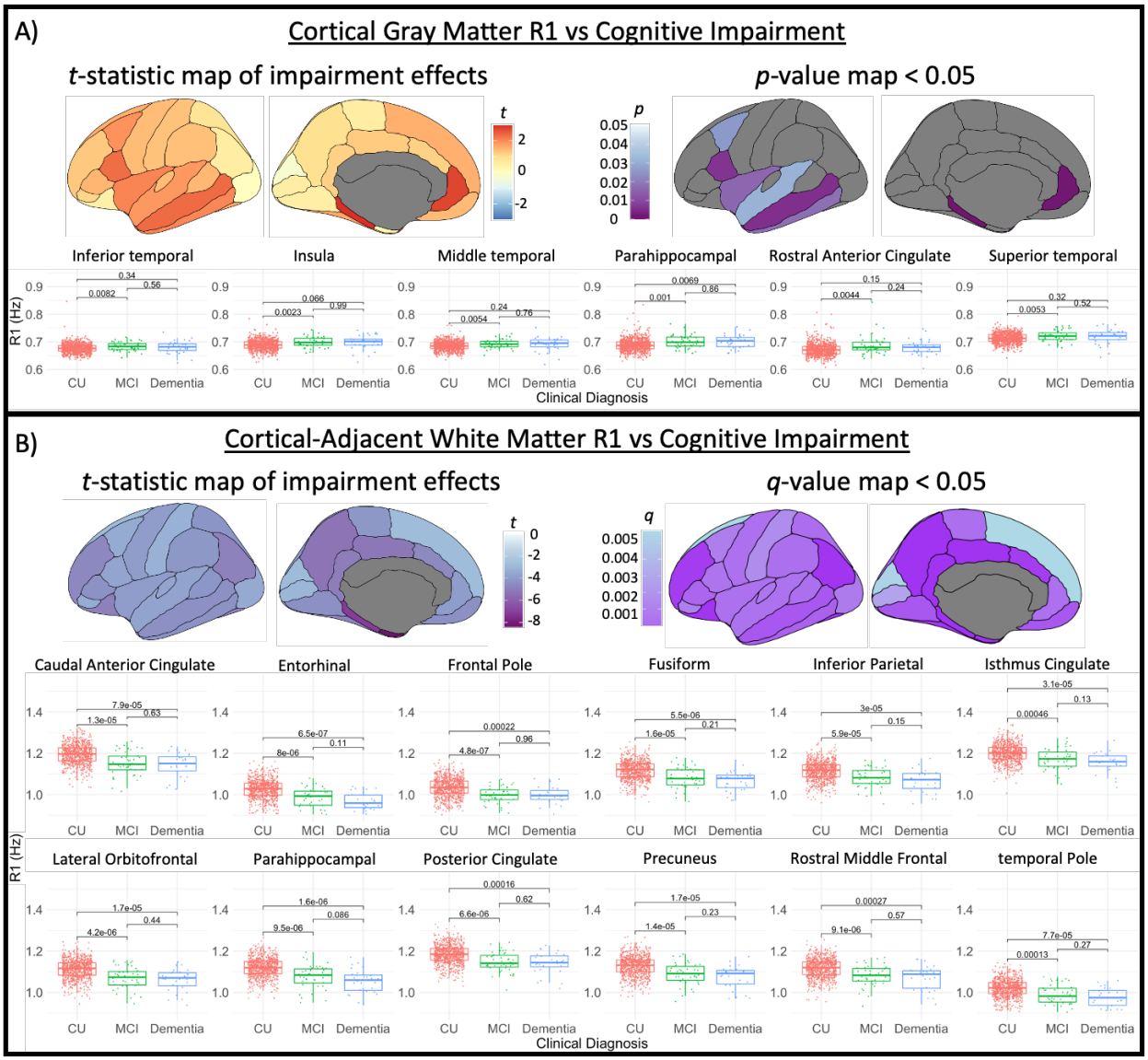

Figure 6: Regression results assessing the effects of cognitive impairment on R1 in the ADRC/WRAP cohort. A) Maps of *t*-statistics and corresponding *p*-values visualizing the effect of impairment on cortical GM R1 parcellated by ROIs from the Desikan parcellation. Individual regions with post-hoc Bonferroni-corrected t-tests comparing diagnostic groups are plotted below the brain maps. B) Maps of *t*-statistics and corresponding FDR-corrected *q*-values visualizing the effect of impairment on cortical-adjacent WM R1 parcellated by ROIs from the Desikan parcellation. Individual regions with post-hoc Bonferroni-corrected t-tests comparing diagnostic groups are plotted below the brain maps.

Figure 7: Effects of MCI and dementia on cortical and WM R1 in ADCP

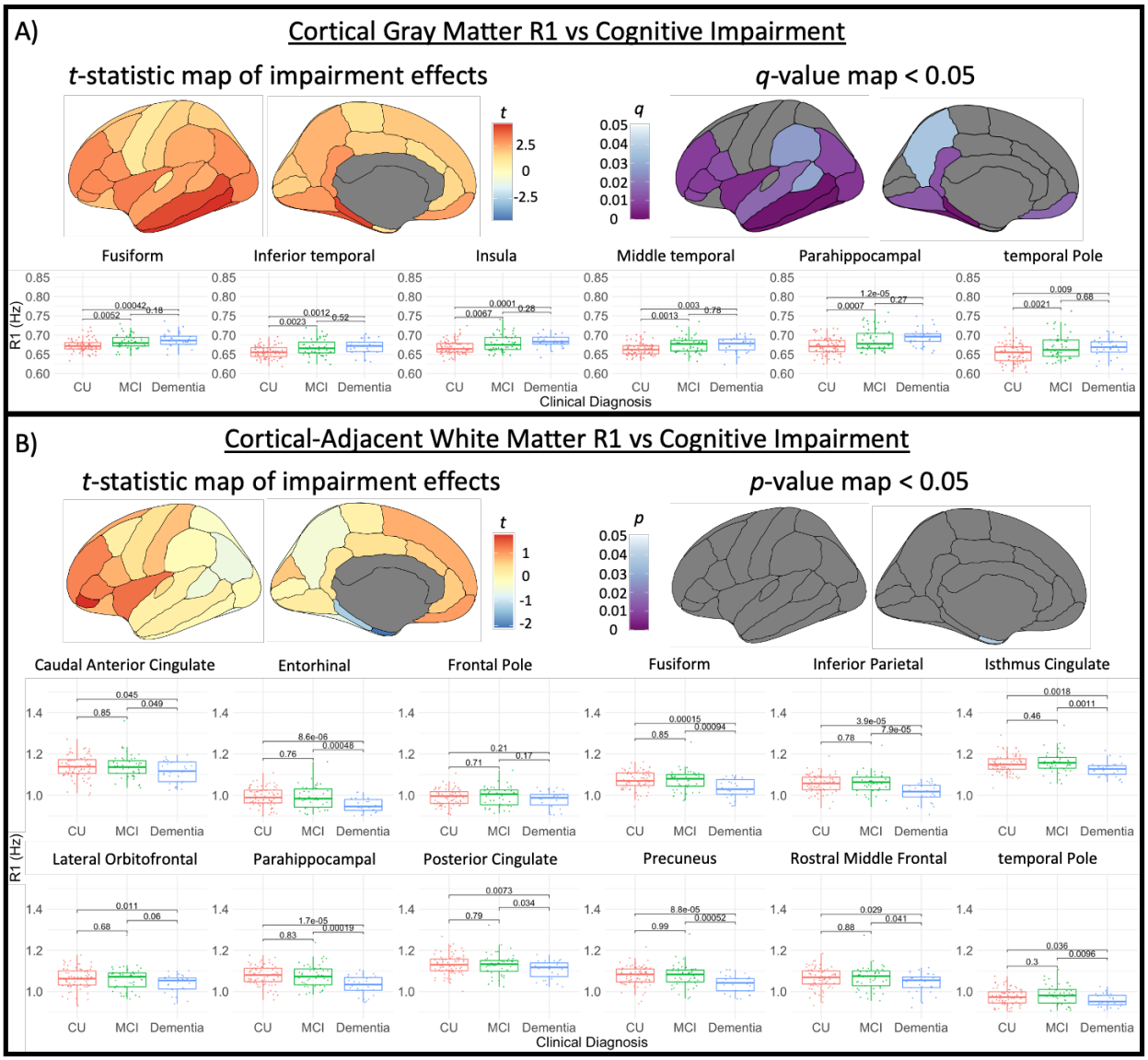

Figure 7: Regression results assessing the effects of cognitive impairment on R1 in the ADCP cohort. A) Maps of *t*-statistics and corresponding FDR-corrected *q*-values visualizing the effect of impairment on cortical GM R1 parcellated by ROIs from the Desikan parcellation. Individual regions with post-hoc Bonferroni-corrected t-tests comparing diagnostic groups are plotted below the brain maps. B) Maps of *t*-statistics and corresponding *p*-values visualizing the effect of impairment on cortical-adjacent WM R1 parcellated by ROIs from the Desikan parcellation. Individual regions with post-hoc Bonferroni-corrected t-tests comparing diagnostic groups are plotted below the brain maps.

Figure 8: Composite ROIs for Cognitive Testing Analysis

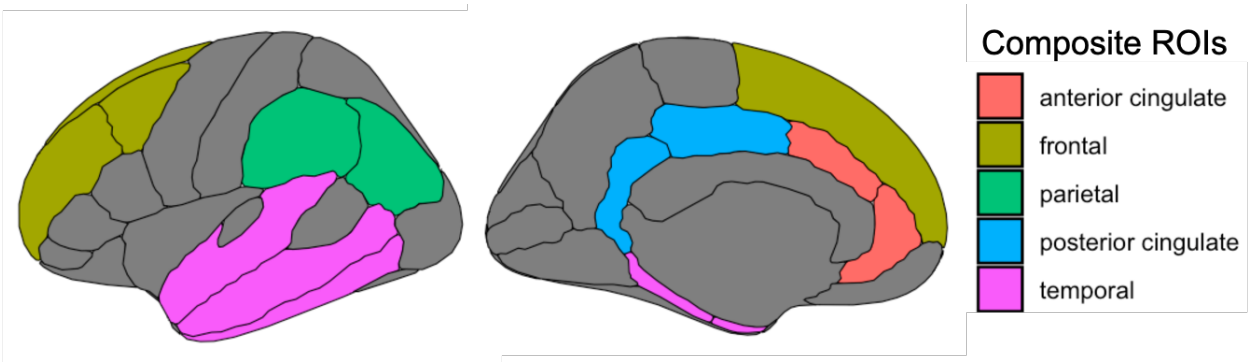

Figure 8: Composite regions of interest comprised of regions from the Desikan-Killiany parcellation overlayed onto a brain using the “ggseg” package in R. Anterior cingulate is comprised of the rostral and caudal anterior cingulate ROIs. Frontal is comprised of the superior frontal, and rostral and caudal middle frontal ROIs. Parietal is comprised of the supramarginal and inferior parietal ROIs. Posterior cingulate is comprised of the isthmus and posterior cingulate ROIs. Temporal is comprised of the entorhinal, parahippocampal, superior, middle, and inferior temporal ROIs.

Figure 9: Associations between cortical GM and cortical-adjacent WM R1 on NIH Toolbox performance

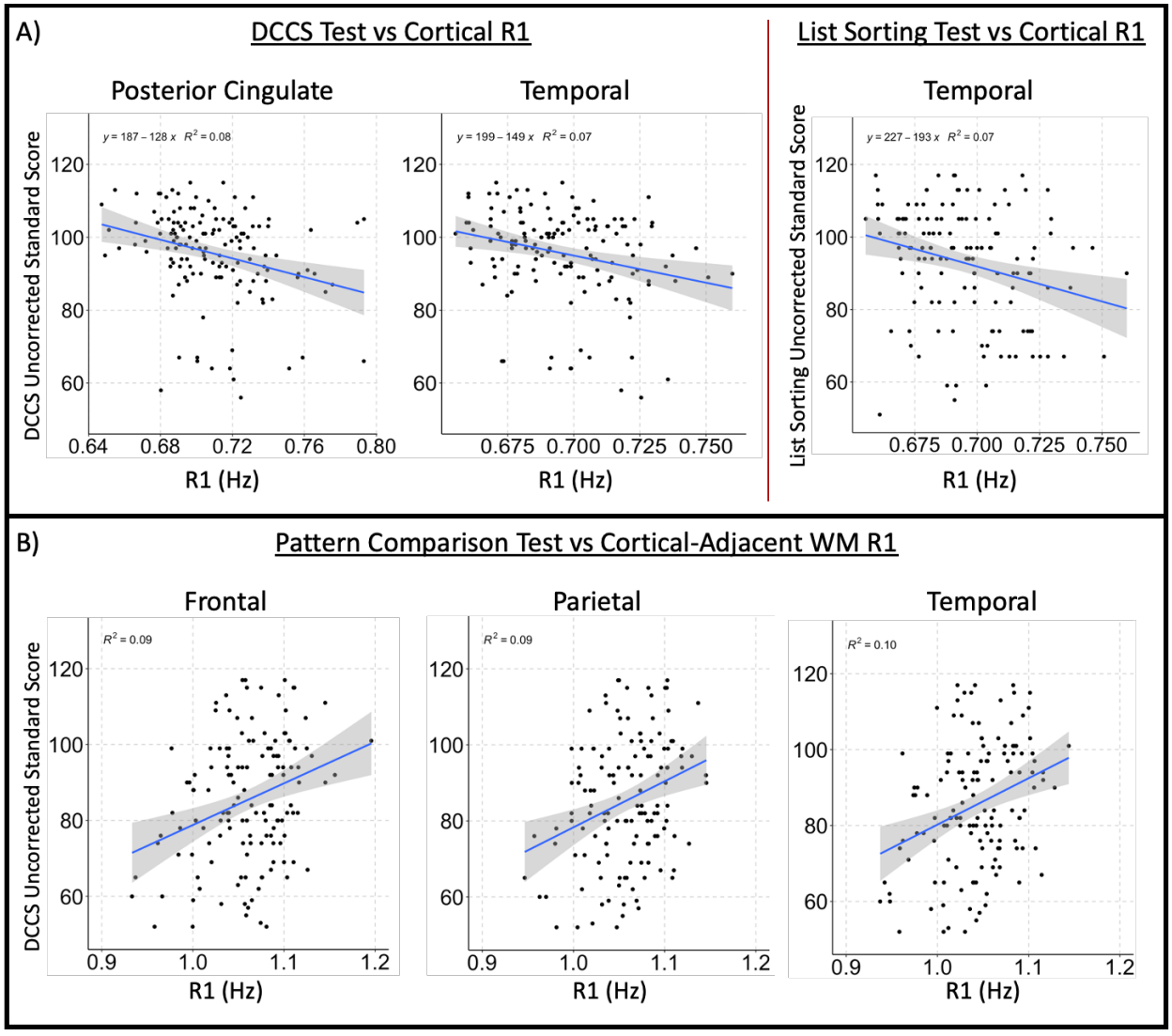

Figure 9: Plots of significant composite regional associations between cognitive performance and R1. A) Regression plots of associations between dimensional change card sort test uncorrected standard scores against posterior cingulate and temporal cortical R1 and list sorting test uncorrected standard scores against temporal cortical R1. B) Regression plots of associations between pattern comparison test uncorrected standard scores against temporal, parietal, and frontal WM R1. Linear trend lines are plotted using the formula 'y~x'.

ACKNOWLEDGEMENTS & FUNDING

We thank the WRAP, ADRC, and ADCP study participants for volunteering their time and energy for our studies. We also thank the staff of the Wisconsin ADRC for their hard work in supporting this study's efforts. Data were collected under the following grants from the NIH National Institute of Aging: R01AG037639 (Bendlin), R01AG027161 (Johnson), P50AG033514 (Asthana), U01AG051216 (Li, Bendlin). MR imaging at UW-Madison was supported by a core grant to the Waisman Center from the National Institute of Child Health and Human Development (P50 HD105353). Akshay Kohli and Kao Lee Yang are both students in the Neuroscience Training Program (NIH/NINDS T32 NS105602). Funding sources did not contribute to the study conceptualization, design, execution, and analysis.

Chapter 3: Effects of sex and APOE E4 positivity on cortical and white matter myelin as assessed by quantitative relaxometry

Effects of sex and APOE E4 positivity on cortical and white matter myelin as assessed by quantitative relaxometry

ABSTRACT

Prevalence of Alzheimer's disease (AD) is higher in women and in individuals who carry the E4 allele variant of the Apolipoprotein (APOE) gene. Prior studies have employed diffusion MRI to identify whether there are relationships between these risk factors of AD and white matter myelin and microstructure. However, researcher have yet to expand these investigations to the cortex which also contains myelin and is selectively targeted by AD pathology. In the following study, we employed the novel MPnRAGE MRI sequence to derive quantitative R1, a metric sensitive to myelin, to explore whether levels of cortical myelin differ by sex and in carriers of the APOE E4 allele. We hypothesized that women would have lower regional cortical myelin, that E4 carriers would exhibit lower levels of myelin, and that women with the E4 allele would exhibit exacerbated effects compared to non-carriers. While we found that women had marginally lower cortical myelin in a few brain regions, no relationships were found with APOE status, and the marginal APOE-by-sex interaction effects indicated males with APOE E4 had higher R1 in WM than male non-carriers. These findings suggest that myelination of the cortex remains consistent across sex and that the E4 allele does not negatively impact cortical myelin. Future work should aim to expand our understanding of cortical myelin in the context of other AD risk factors such as cardiovascular health and family history of AD, as well as biomarkers of AD pathology.

INTRODUCTION

The prevalence of Alzheimer's disease (AD) is substantially higher in women as compared to men, as 66% of all AD diagnoses are in women. While some research suggests this may be attributed to women, on average, living longer than men[13,122], it is important to explore all avenues to understand why disproportionally affects women. A study using diffusion tensor imaging (DTI) to investigate sex differences in white matter myelin and microstructure revealed that women show reduced fractional anisotropy (FA) in temporal, cingulate, and precentral regions[123]. Another study expanded upon this through advanced multi-shell diffusion imaging methods such as Hybrid Diffusion Imaging (HYDI), Neurite Orientation Dispersion and Density Imaging (NODDI), and q-space imaging. These researchers found that while the age-related changes did not differ by sex, men had higher NODDI-derived intra-axonal volume fraction in numerous white matter (WM) regions of interest (ROI) including the fornix, corona radiata, cingulum, and uncinate fasciculus[124]. These alterations in white matter integrity have yet to be expanded to studies of the cortex, and although methods such as T1/T2 ratio mapping have recently attempted to elucidate relationships with age[56,57,60], cognition[55,56,69], and Alzheimer's disease[69,70], they have yet to be applied to study sex differences.

In addition to sex, evidence has also linked apolipoprotein E (APOE) genotype to greater risk of developing Alzheimer's disease, as individuals with at least one E4 allele variant of the APOE gene are diagnosed at higher rates than those with the E3 or E2 variants. In fact, individuals with APOE E4 heterozygosity have 3 times the risk, and those with APOE E4 homozygosity have 12 times the risk of developing AD compared to those with two E3 alleles[125,126]. One meta-analysis found that among individuals in the United States with a diagnosis of AD, 56% were heterozygous and 11% were homozygous for the E4 allele[127]. An additional study found that 65% of 1770 individuals with an AD diagnosis enrolled in Alzheimer's disease research centers across the United States had at least one E4 allele[128].

As the APOE gene is known to be involved in cholesterol transport and lipid metabolism in the brain[129,130], it is reasonable to assume it may influence the production and/or maintenance of myelin. Indeed, research has identified alterations in white matter integrity in individuals who are carriers of the APOE E4 allele. One study identified lower myelin content in late-myelinating WM in carriers of the E4 allele[131], another found altered DTI metrics (lower FA, higher MD) in E4 carriers (particularly those with a family history of AD)[82], and a third identified lower myelin water fraction (MWF) was lower in normal appearing WM in E4 carriers[132]. These studies all conclude that APOE genotype contributes to altered WM myelin and structural integrity, however, as is the case with sex differences, no study to date has yet identified whether these relationships hold true with cortex-specific myelin.

Early post-mortem observations made by Heiko and Eva Braak noted the intriguing inverse patterns of cortical myelogenesis compared to that of AD pathology development[76]. While work has been conducted to assess the relationships between risk factors of AD (such as sex and APOE genotype) and white matter myelin and structural integrity, no studies to date have expanded this to myelin in the cortex. Here we employ quantitative relaxometry *in vivo* to better understand how cortex-specific myelin may differ by sex well as those with the APOE E4 genotype in cognitively unimpaired individuals. We hypothesized that 1) women would exhibit lower levels of myelin in both WM and cortical gray matter (GM) as compared to men, 2) carriers of the APOE E4 genotype would have lower myelin content compared to non-carriers, and 3) APOE E4 genotype would moderate the effect of sex on myelin content such that women who carry the E4 allele will exhibit lower myelin than non-carriers. This study is the first to employ R1 mapping to investigate sex differences and APOE genotype on cortical myelin *in vivo*.

METHODS

Participant Sample

Participants included 791 individuals (mean age = 65.18; 66.25% female; 37.7% APOE E4 carriers) with a diagnosis of cognitively unimpaired enrolled in the Wisconsin Alzheimer's Disease Research Center (ADRC) and Wisconsin Registry for Alzheimer's Prevention (WRAP) studies who underwent MPnRAGE MRI and genotyping for APOE E4 carrier determination.

Institutional approvals and consent

All protocols for the ADRC and WRAP studies were approved by the University of Wisconsin Health Science Institutional Review Board. Written informed consent was provided by all enrolled participants.

APOE genotyping

APOE genotyping procedures are describe previously[133]. In brief, DNA was extracted from blood samples collected from participants at the time of the study visit and E2, E3, and E4 allele variants were determined through polymerase chain reaction (PCR) testing. Individuals were classified as "APOE positive" if they were heterozygous or homozygous for the E4 variant.

MRI acquisition

The ADRC and WRAP studies took place at the University of Wisconsin-Madison on 3T MRI scanners from GE Healthcare. Acquisitions on the Discovery MR750 systems utilized a 32 channel receive-only head coil from Nova Medical (Wilmington, MA) and those on the Signa Premiere systems used the vendor supplied 48 channel receive only head coil. All MPnRAGE acquisitions included whole brain coverage with 1.0mm isotropic spatial resolution and lasted 9 minutes. Minor variations in protocol occurred throughout this study, including switching from

sagittal to axial orientations as well as changes of the second flip angle (degree and number of views). Details of all protocols are presented in Table B1 in appendix B.

MRI image reconstruction, processing, and harmonization

All MPnRAGE images were reconstructed to 1.0mm isotropic spatial resolution with self-navigated retrospective motion correction[74] to produce a T1-weighted (T1w) image with conventional MPRAGE-like contrast and a quantitative R1 map[73]. The T1w images were processed with the *recon-all* script from Freesurfer version 6.0.0[68]. R1 was sampled at the midpoint of the cortex at each vertex using Freesurfer's *mri_vol2surf* command and mapped to the "fsaverage" templated with *mri_surf2surf* which included 10mm of smoothing along the surface with the "—fwhm-trg" option.

The Desikan-Killiany (DK) atlas was used to compute regions of interest (ROIs) cortical and cortical-adjacent WM R1 measurements. The WM ROIs are given in the "/mri/wmparc.mgz" output file of *recon-all*, which were determined based on the nearest cortical ROI of each white matter voxel within 5 mm of the white/gray matter boundary. This resulted in 34 independent ROIs for cortical GM R1 and 34 ROIs for cortical-adjacent WM R1. Cortical surface meshes and WM segmentations were visually inspected to ensure accurate tissue delineation. Full processing steps are depicted in Figure B1.

As multiple MPnRAGE protocols were implemented across the ADRC and WRAP cohorts, data harmonization was required to pool these data for statistical analysis of R1. Harmonization was performed using ComBat, a tool originally developed for large gene sets[109] and subsequently adapted for neuroimaging data[110–112]. We applied ComBat independently to each regression model estimated for cortical GM R1 and cortical-adjacent WM R1. To minimize bias from extreme outliers, R1 values beyond 3 x interquartile range for each ROI were removed before harmonization was initiated.

Statistical Analysis

Main effect of sex on regional R1

To test the hypothesis that cortical GM and WM myelin is lower in women, multiple regression models were employed per ROI for both cortical GM and WM R1 (34 total models for each tissue). The outcome measure for each ROI's model was mean regional R1; the main predictor of interest included sex, and age at MRI visit was included as a covariate in each model. In models investigating WM R1, a quadratic age term was included as a covariate, as prior assessments of age effects in myelin were found to be quadratic in WM (see Chapter 2). FDR-corrected *p*-values (*q*-values) were deemed significant at 0.05; Benjamini-Hochberg FDR adjustment was performed per group of 34 tests for cortical GM and cortical-adjacent WM separately.

Main effect of APOE E4 positivity on regional R1

To assess the effect of APOE E4 positivity on cortical GM and WM myelin, multiple regression models were employed per ROI for both cortical GM and WM R1 (34 total models for each tissue). The outcome measure for each ROI's model was mean regional R1; the main predictor of interest included APOE E4 positivity, and age at MRI visit and sex were included as covariates. As mentioned above, age^2 was included as a covariate in models assessing WM myelin. Resulting FDR-corrected *p*-values (*q*-values) were deemed significant at 0.05; Benjamini-Hochberg FDR adjustment was performed per group of 34 tests for cortical GM and cortical-adjacent WM separately.

Interaction between APOE E4 positivity and sex on regional R1

Finally, to determine whether APOE E4 moderated the relationship between sex and myelin, multiple linear regression models were employed per ROI for both cortical GM and WM R1 (34 total models for each tissue). The outcome measure for each ROI's model was mean

R1; the main predictor of interest was the interaction between APOE E4 positivity and sex, and covariates included age or age^2. Resulting FDR-corrected *p*-values (*q*-values) were deemed significant at 0.05; Benjamini-Hochberg FDR adjustment was performed per group of 34 tests for GM and WM separately.

RESULTS

Effects of sex on regional cortical GM and cortical-adjacent WM R1

Regions with significant effects of sex on cortical R1 and cortical-adjacent WM R1 are visualized in Figure 1. Within the cortex, no significant associations were identified between sex and R1 at an FDR-corrected threshold of $q<0.05$ while controlling for age effects. However, at an exploratory $p<0.05$ threshold, women had lower R1 in the pericalcarine (t = -2.557, p = 1.075e^{-02}), parahippocampal (t = -2.527, p = 1.171e^{-02}), and cuneus (t = -2.307, p = 2.132e^{-02}) ROIs. In contrast, cortical-adjacent WM exhibited strong sex-differences in R1, with women exhibiting lower R1 in numerous regions in the posterior, temporal, and cingulate WM. Specifically lower R1 in women was found in the cuneus (t = -7.560, q = 3.825e^{-12}), lateral occipital (t = -6.565, q = 1.609e^{-09}), lingual (t = -6.465, q = 2.014e^{-09}), pericalcarine (t = -6.300, q = 3.684e^{-09}), inferior parietal (t = -6.285, q = 3.684e^{-09}), isthmus cingulate (t = -6.082, q = 1.047e^{-08}), superior parietal (t = -6.035, q = 1.188e^{-08}), precuneus (t = -5.948, q = 1.734e^{-08}), parahippocampal (t = -5.546, q = 1.506e^{-07}), caudal anterior cingulate (t = -5.278, q = 5.739e^{-07}), posterior cingulate (t = -5.123, q = 1.170e^{-06}), and supramarginal (t = -4.909, q = 3.148e^{-06}) ROIs, among others. In total, 32/34 WM ROIs exhibited significantly higher R1 in men than women. Complete outputs of regression models can be observed in Tables B2 and B3.

Effects of APOE E4 positivity on regional cortical GM and cortical-adjacent WM R1

Regions with significant effects of APOE E4 on cortical R1 and cortical-adjacent WM R1 are visualized in Figure 2. There were no regional differences in R1 between APOE E4 carriers and non-carriers in the cortex. Within cortical-adjacent WM, the only relationship identified was lower R1 in the transverse temporal ROI in APOE E4 carriers compared to non-carriers at an uncorrected $p<0.05$ threshold (t = -2.426, p = 1.549 e^{-02}). Full outputs of regression models are found in Tables B4 and B5.

Interaction effects of APOE E4 positivity on regional cortical GM and cortical-adjacent WM R1

Regions with APOE-by-sex interaction effects on cortical R1 and cortical-adjacent WM R1 are visualized in Figure 3. There was a marginal sex-by-APOE interaction effect on R1 in the transverse temporal ROI in cortical GM (Figure 3a). In cortical-adjacent WM, 18/34 ROIs exhibited marginal interaction effects (at an uncorrected $p<0.05$ threshold), with male carriers exhibiting higher R1 than male non-carriers. In contrast, female carriers and non-carriers had no differences in R1 in any WM ROIs. These regions include the inferior parietal (t = -2.108, p = 3.531e^{-02}), lingual (t = -2.477, p = 1.347e^{-02}), precuneus (t = -2.469, p = 1.377e^{-02}), superior parietal (t = -2.567, p = 1.044e^{-02}), superior temporal (t = -2.176, p = 2.988e^{-02}), and supramarginal (t = -2.162, p = 3.091e^{-02}), among others. None of these regions survived correction for multiple comparisons. Full outputs of models assessing the APOE-by-sex interaction are presented in Tables B6 and B7.

DISCUSSION

The goal of this study was to better characterize differences in cortical GM and cortical-adjacent WM R1, a metric sensitive to brain myelin, between men and women, as well as

amongst individuals who carry the APOE E4 allele. While we hypothesized that the cortex would reflect the relationships typically found between WM microstructure and these risk factors of AD, our analyses revealed relatively minor differences. Of the two risk factors assessed, sex exhibited the largest alterations in cortical myelin, albeit only surviving a less stringent statistical threshold without correcting for multiple comparisons, and carriers of the APOE E4 genotype had no alterations in cortical R1 compared to non-carriers. Additionally, sex did not moderate the effect of APOE on cortical R1. The null findings observed within the cortex could be due to the relatively low amount of variance observed in R1 signal, especially compared to that observed within WM. That being said, significant effects of age on cortical R1 are exhibited (as may be seen in Chapter 2), suggesting that alterations do occur, and are detectable, in older adults. Another possibility is that while R1 is highly sensitive to brain myelin, tissue properties such as iron, water, and other macromolecules can alter R1. These obscurities could be exacerbated in the cortex, where myelin is relatively minimal in presence, especially with regards to WM, where myelin comprises nearly 90% of tissue[52].

Sex differences in brain myelination are routinely studied across development, aging, and disease, and often lead to conflicting findings. One study in rodents revealed that male mice exhibited higher density of oligodendrocytes and myelin in numerous white matter structures (particularly the corpus callosum) as compared to that of female mice, and when castrated, the male mice displayed the female phenotype[134]. Another study that leveraged R1 mapping, in tandem with DWI-derived FA, assessed sex differences in adolescents with depression. They identified higher R1 in the corpus callosum and uncinate fasciculus in individuals with depression that was significantly moderated by sex, such that females with depression had elevated R1 compared to non-depressed females. Importantly, they did not find differences in FA, suggesting R1 was a more sensitive metric to myelin-specific alterations in depression[135]. These findings exist in opposition which is commonly observed in studies of sex differences. It is possible that the presence of different sex hormones throughout development and the lifespan

drive the altered patterns of myelin cortically and subcortically. Other studies have suggested the g-ratio, or the ratio between the axon diameter and total fiber diameter, indicating the thickness of the myelin sheath. Increased g-ratio in men, specifically manifesting during adolescence, could also drive these observed sex effects on R1, as it has been identified that men have more densely packed fiber tracts than women[136]. Still, higher g-ratio in men has also been attributed to the presence of testosterone and other androgenic hormones[137]. Studies of hormonal changes in post-menopausal women have noted the alterations in catabolism of lipids in the brain. The utilization of lipids as an energy source could have implications in the higher rates of Alzheimer's disease in women, and as such, our strong findings with lower levels of R1 in white matter

There are additional extraneous factors that may have contributed to the sex differences observed in this study. As is displayed in Table 1, mean age did not significantly differ by sex, and analyses controlled for the effects of age, reducing the likelihood that age played a role in the major differences in R1 identified in WM. It is possible that the higher average number of years of education obtained by males may have led to increased levels of myelin earlier in life, as prior associations have been found between education and myelin content in the frontal cortices[138]. Future studies should examine the role that education may play in degeneration of myelin, as well as the interactive effects that sex and education could have on brain myelin. Finally, cardiovascular risk and related ischemic injury often impacts the integrity of white matter tissue, which typically presents as WM hypointensities on T1-weighted scans. While the use of cortical-adjacent WM ROIs reduces the impact of such insult on averaged WM R1 signal, it is possible that differences in overall cardiovascular health were present between males and females, thus driving some of the sex differences detected. Future studies could remedy this by incorporating a measure of cardiovascular health such as the Framingham score[122] or through T2-FLAIR-derived WM hyperintensity load.

In addition to the effects of sex on myelin, we also examined the impact APOE E4 genotype has on myelin. Given the involvement of APOE in cholesterol metabolism and lipid transport[139], as well as prior studies that have identified relationships between APOE and white matter microstructure and myelin[82,131,132], our overall lack of findings are surprising. While lower R1 in the transverse temporal was identified in WM, we expected APOE E4 carriers to exhibit greatly reduced levels of R1 through WM regions, especially within WM regions that myelinate later in life such as within the temporal and frontal cortices. Sex has also shown to moderate the APOE-related risk of developing Alzheimer's disease, however, we identified marginal sex-by-APOE interaction effects within WM, with male APOE E4 carriers exhibiting higher R1 than male non-carriers. These results are not consistent with prior literature, which suggest women with the APOE E4 allele tend to have greater risk of developing AD than men[84]. An additional study of young adults found that male APOE E4 carriers exhibit reduced white matter volume compared to female carriers, although both showed reduced volume compared to non-carriers[140]. Although we did not measure volume in this study, higher R1 would be indicative of greater myelin density and thus greater volume, contrasting these prior reports. Still, our results did not survive correction, and as such, should not be used to interpret that male E4 carriers are "protected" from myelin injury. It's possible that by grouping all individuals without the E4 variant of the APOE gene, we reduced the sensitivity to other myelin and/or microstructural alterations that may be present in individuals with E2 or E3 variants. Additional work attempting to elucidate the role that APOE plays on integrity of brain myelin could utilize polygenic risk scores, particularly because the E2 allele has shown to have protective effects in the brain[141,142]. Moreover, future studies should examine these effects in participants with impairment due to Alzheimer's disease.

CONCLUSION

Cortical myelin appears to be consistent across sex and APOE genotype, with minimal sex effects and no significant effects of APOE E4 on cortical R1. Similarly, carriers of the APOE E4 allele did not exhibit altered WM R1 as compared to non-carriers. In contrast, major sex differences were identified in cortical-adjacent WM, with men having drastically higher R1 in almost all WM regions indexed as compared to women. Finally, no significant sex-by-APOE interactions were identified in GM, however, male APOE E4 carriers exhibited higher R1 than male non-carriers in WM. These results largely do not support our hypotheses, with the exception of sex differences in WM. Future work should aim to elucidate the potential causes of WM myelin sex differences, identify the longitudinal trajectories of myelin in men and women, and determine whether sex moderates the relationships between markers of AD pathology and WM myelination.

TABLES AND FIGURES

Table 1: Participant Demographics by Sex

	Female (N=524)	Male (N=267)	p value
Age at Baseline MRI Scan			0.364[1]
Mean (SD)	65.057 (7.429)	65.430 (8.245)	
Min - Max	46.840 - 90.370	45.710 - 87.960	
APOE E4 Status			0.395[2]
Non-Carrier	321 (61.3%)	172 (64.4%)	
Carrier	203 (38.7%)	95 (35.6%)	
Education			< 0.001[1]
Mean (SD)	15.893 (2.389)	17.007 (2.689)	
Min - Max	10.000 - 24.000	8.000 - 25.000	
Clinical Diagnosis			
Cognitively Unimpaired	524 (100.0%)	267 (100.0%)	
Mild Cognitive Impairment	0 (0.0%)	0 (0.0%)	
Dementia	0 (0.0%)	0 (0.0%)	
Primary Race			0.255[2]
American Indian or Alaska Native	16 (3.1%)	2 (0.7%)	
Asian	1 (0.2%)	1 (0.4%)	
Black or African American	47 (9.0%)	24 (9.0%)	
Other	1 (0.2%)	0 (0.0%)	
Unknown	1 (0.2%)	1 (0.4%)	
White	458 (87.4%)	239 (89.5%)	

1. Kruskal-Wallis rank sum test
2. Fisher's Exact Test for Count Data

Figure 1: Main effects of sex on cortical GM and cortical-adjacent WM R1

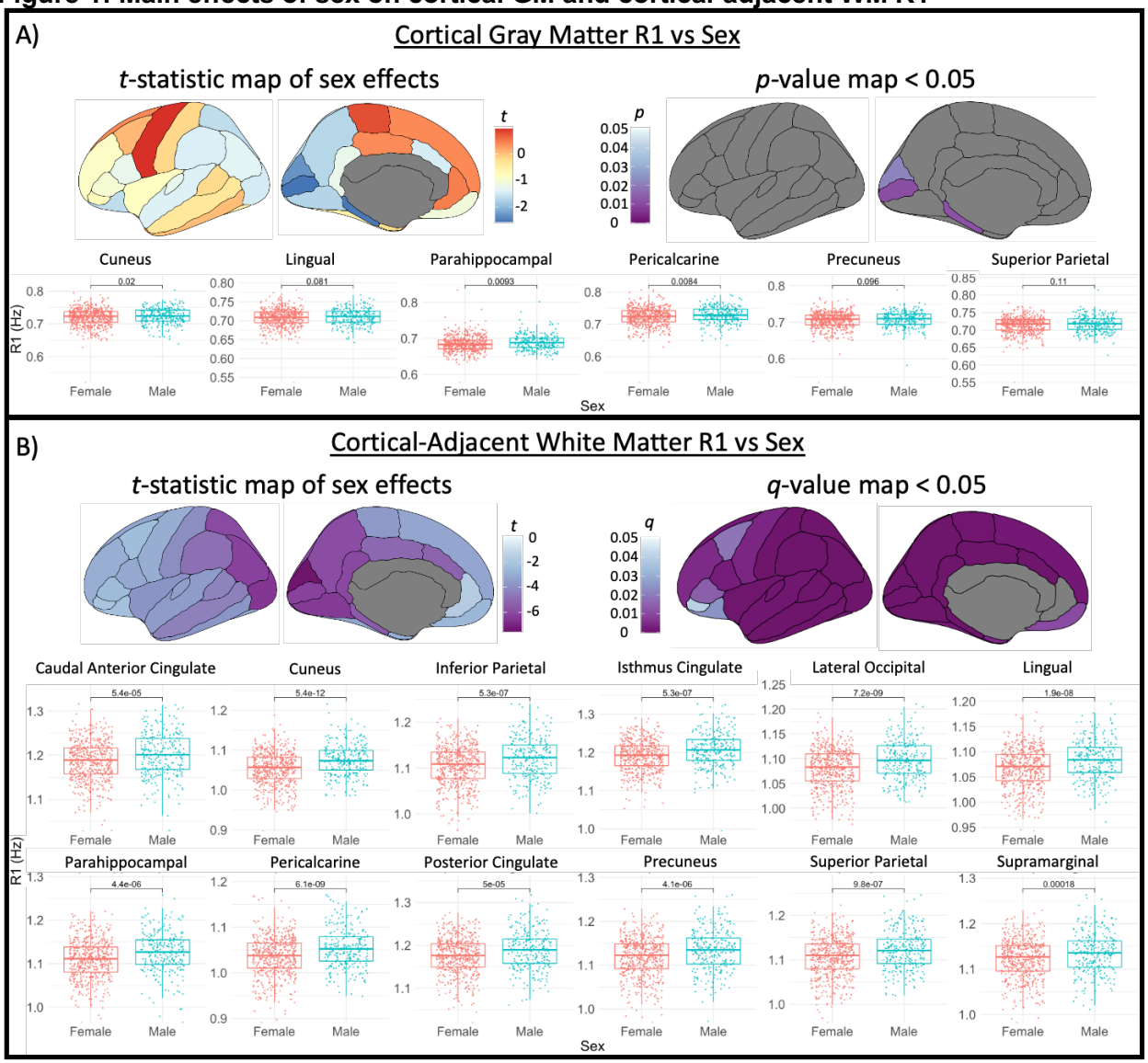

Figure 1: Regression results assessing the effects of sex on R1. A) Maps of t-statistics and corresponding FDR-corrected p-values visualizing the sex effects on cortical GM R1 (controlling for linear age effects) parcellated by ROIs from the Desikan parcellation. B) Maps of *t*-statistics and corresponding FDR-corrected p-values visualizing the sex effects on cortical-adjacent WM R1 (controlling for quadratic age effects) parcellated by ROIs from the Desikan parcellation. Individual regions with t-tests assessing sex differences are plotted below the brain maps.

Figure 2: Main effects of APOE E4 genotype on cortical GM and cortical-adjacent WM R1

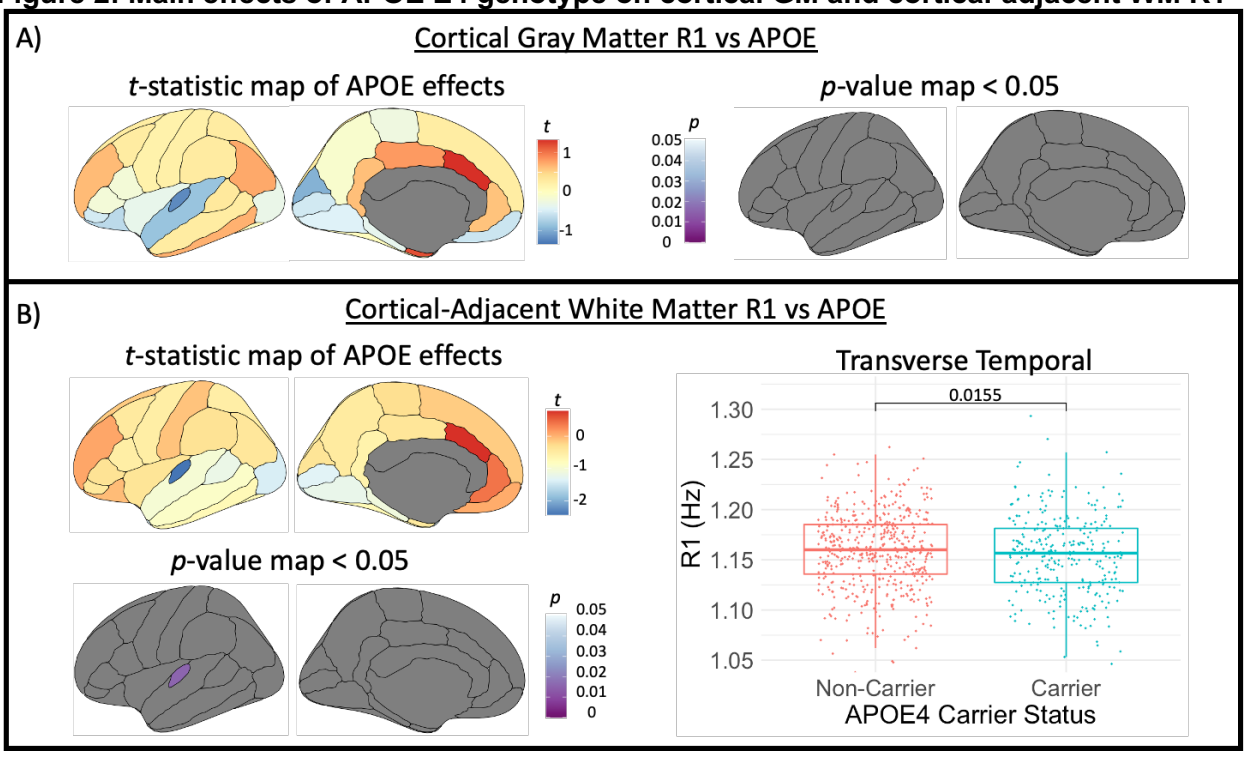

Figure 2: Regression results assessing the effects of APOE E4 positivity on R1. A) Maps of t-statistics and corresponding FDR-corrected p-values visualizing the APOE effects on cortical GM R1 (controlling for linear age effects) parcellated by ROIs from the Desikan parcellation. B) Maps of *t*-statistics and corresponding FDR-corrected p-values visualizing the APOE effects on cortical-adjacent WM R1 (controlling for quadratic age effects) parcellated by ROIs from the Desikan parcellation. Individual regions with t-tests assessing sex differences are plotted below the brain maps.

Figure 3: Interaction effects of sex and APOE E4 genotype on cortical GM and cortical-adjacent WM R1

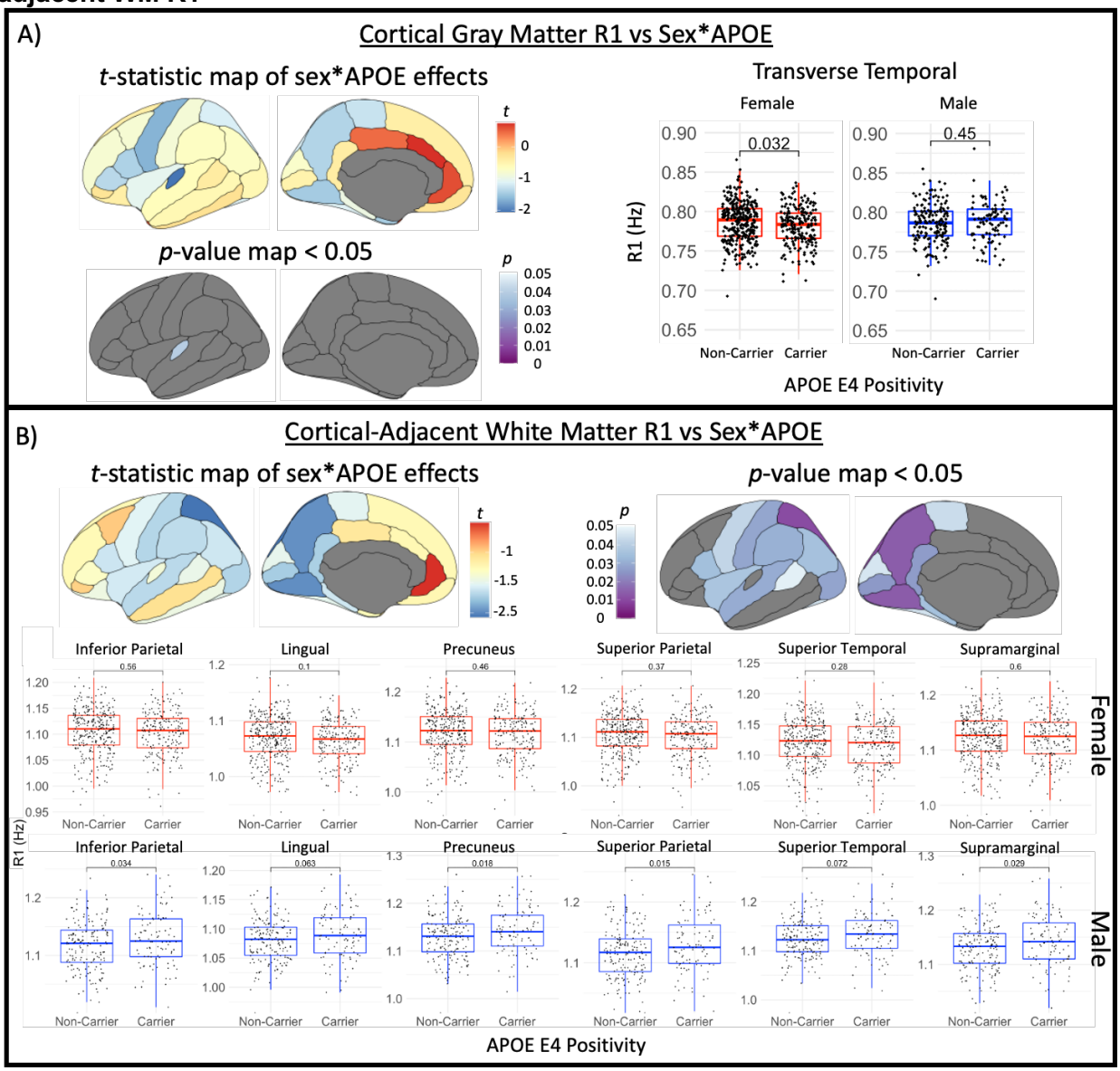

Figure 3: Regression results assessing the interaction effects between sex and APOE E4 positivity on R1. A) Maps of t-statistics and corresponding FDR-corrected p-values visualizing the sex-by-APOE effects on cortical GM R1 (controlling for linear age effects) parcellated by ROIs from the Desikan parcellation. B) Maps of *t*-statistics and corresponding FDR-corrected p-values visualizing the sex-by-APOE effects on cortical-adjacent WM R1 (controlling for quadratic age effects) parcellated by ROIs from the Desikan parcellation. Individual regions with t-tests assessing sex differences are plotted below the brain maps.

ACKNOWLEDGEMENTS & FUNDING

We thank the WRAP and ADRC study participants for volunteering their time and energy for our studies. We also thank the staff of the Wisconsin ADRC for their hard work in supporting this study's efforts. Data were collected under the following grants from the NIH National Institute of Aging: R01AG037639 (Bendlin), R01AG027161 (Johnson), P50AG033514 (Asthana). MR imaging at UW-Madison was supported by a core grant to the Waisman Center from the National Institute of Child Health and Human Development (P50 HD105353). Akshay Kohli is a student in the Neuroscience Training Program (NIH/NINDS T32 NS105602). Funding sources did not contribute to the study conceptualization, design, execution, and analysis.

Chapter 4: Alterations in cortical and white matter myelin are associated with amyloid, tau, and neurodegeneration in individuals across the Alzheimer's disease continuum

Alterations in cortical and white matter myelin are associated with amyloid, tau, and neurodegeneration in individuals across the Alzheimer's disease continuum

Prepared following guidelines for the journal Alzheimer's and Dementia

Authors: Akshay Kohli, Margo Heston, Kao Lee Yang, Steven R Kecskemeti, Rebecca L Koscik, Tobey J Betthauser, Jennifer M Oh, Richard Batrla, Gwendlyn Kollmorgen, Norbert Wild, Katharina Buck, Cynthia M Carlsson, Henrik Zetterberg, Kaj Blennow, Ozioma Okonkwo, Sterling C Johnson, Sanjay Asthana, Andrew L Alexander, Barbara B Bendlin

ABSTRACT

INTRODUCTION: This study investigated relationships between myelin and cerebrospinal fluid (CSF) markers of amyloid, tau, and neurodegeneration in older adults, and explored spatial distributions of cortical myelin and Alzheimer's disease (AD) pathology in a case study.

METHODS: MPnRAGE-derived R1 and CSF was acquired from 400 adults ages 47 to 90 years. CSF amyloid beta (Aß)42, Aß40, $pTau_{181}$, tTau, neurogranin, and neurofilament light were measured using the NeuroToolKit. A single subject underwent amyloid and tau PET imaging. FDR-adjusted and unadjusted multiple regressions were used to assess relationships between R1 and AD pathology.

RESULTS: Elevated CSF biomarker levels of AD pathology and neurodegeneration are associated with lower cortical and white matter R1. Spatial distribution of cortical R1 inversely mirrors that of amyloid and tau deposition in a single individual.

DISCUSSION: Myelin is linked to CSF AD pathology and neurodegeneration. MRI and PET imaging demonstrated that regions with lower cortical myelin had higher amyloid and tau pathology.

Keywords: magnetic resonance imaging, relaxometry, myelin, cerebrospinal fluid biomarkers, amyloid, tau, neurodegeneration

Research in Context:

Systematic Review: The authors utilized PubMed and Google Scholar to index articles investigating cortical myelin in the context of Alzheimer's disease (AD) biomarkers. Few studies have been conducted on this topic; this study takes novel approaches by using quantitative relaxometry in combination with PET imaging and cerebrospinal fluid (CSF) biomarkers of AD and neurodegeneration.

Interpretation: Our results show that 1) lower regional cortical and white matter myelin content is associated with elevated CSF levels of AD pathology and neurodegeneration and 2) the spatial distribution of cortical myelin inversely mirrors that of amyloid and tau.

Future Directions: These results provide support for further investigations of myelin in AD. Longitudinal studies are warranted to understand whether change in myelin over time is associated with earlier development of pathology and/or earlier onset of clinical symptoms.

INTRODUCTION

A key feature of early Alzheimer's disease (AD) is the aggregation of pathological proteins, amyloid beta (Aß) and tau, nonuniformly across the cortical surface. Prior observations of post-mortem brains suggest that regions with prolonged and typically lower levels of cortical myelin may be more susceptible to AD pathology[41,42,76], however, this has yet to be fully demonstrated *in vivo*. Although research has found significant impacts of AD-related pathology and neurodegeneration on brain white matter (WM) microstructure and connectivity, the role of intracortical myelin in AD remains relatively understudied.

Prior work has utilized the MRI-derived T1/T2 ratio to study myelin in the cortex in individuals across the AD continuum. One such study found higher T1-weighted (T1w)/T2-weighted (T2w) ratios in numerous cortical regions in individuals with an AD diagnosis[69], while another found that individuals with AD pathology had lower T1w/T2w ratios in several cortical regions[70]. It is possible these incongruent findings are attributed to variable MRI acquisition parameters as well as the biological ambiguity of the T1w/T2w ratio. Additional work has suggested that individuals who maintain high levels of cortical myelin (as assessed through diffusion imaging) are more resistant to tau pathology over time[143]. More evidence indicates that the breakdown of oligodendrocytes and myelin sheaths may be an early occurrence in AD-related pathology[62,80] and neurodegeneration[32,61,75]. Studies of intracortical myelin in AD show promise in identifying individual susceptibility of disease pathogenesis and progression.

R1, a quantitative measure of the tissue longitudinal relaxation rate, is a metric highly sensitive to myelin that can be applied to studies of the neocortex[51,52,97]. Researchers have employed R1 mapping to study myelination of the striate cortex[98], the human brainstem[99], as well as lifetime maturation and degeneration[36,100]. To study cortical and white matter myelin in the context of AD, we employ the novel T1w magnetization-prepared *n* rapid acquisition gradient echo (MPnRAGE) MRI sequence with motion-correction[73,74]. MPnRAGE[73] is a

variation of the MPRAGE[102] sequence which includes additional sampling over many time points to allow for precise estimation of R1.

The goals of this study were to leverage R1 mapping in tandem with AD pathology cerebrospinal fluid (CSF) biomarkers to 1) establish the associations between CSF measures of amyloid and tau burden on cortical myelin, and 2) determine the extent to which cortical myelin is related to biomarkers of neurodegeneration. In a case study, we further utilized amyloid and tau PET imaging with R1 mapping to replicate post-mortem observations of the spatial distributions of cortical myelin and AD pathology *in vivo*. This study expands upon the growing literature into the relationships between brain myelin and AD, and is the first to employ MPnRAGE-based R1 mapping to investigate cortical and WM myelin in a large older adult population well characterized for AD biomarkers.

METHODS

Participant Sample

T1-weighted MPnRAGE MRI was acquired from 400 older adults aged 47 to 90 years (mean age = 65.92, standard deviation [SD] = 7.68 years; 65.5% female) enrolled in the Wisconsin Alzheimer's Disease Research Center clinical core (ADRC, n = 235), Wisconsin Registry for Alzheimer's Prevention (WRAP, n = 152), or affiliated studies (see supporting information; n = 13). CSF for each participant was acquired at study visits prior to MRI (mean = 2.30, SD = 2.56 years prior to MRI). A full breakdown of corresponding studies from which MRI and CSF data was used, as well as full descriptions of variable enrollment criteria and study procedures can be found in appendix C. Demographic characteristics for all participants are available in Table 1.

Clinical Diagnosis

Consensus conference of participant cognitive performance and functional ability were conducted at each visit. Diagnosis of mild cognitive impairment (MCI) or dementia were assigned based on National Institute on Aging-Alzheimer's Association (NIA-AA) criteria[15,104] without confirmation from imaging or fluid biomarkers; n = 7 had a dementia diagnosis, n = 18 had an MCI diagnosis, and n = 375 were cognitively unimpaired (CU).

Institutional approvals and consent

All study protocols were approved by the University of Wisconsin Health Science Institutional Review Board. Written informed consent was provided by all participants enrolled in this study.

MPnRAGE MRI acquisition, processing, and harmonization

Participants underwent MPnRAGE MRI via a General Electric 3T Discovery MR750 (Waukesha, WI) with a 32 channel receive-only head coil (Nova Medical, Wilmington, MA) or a General Electric 3T Signa Premier scanner using a 48 channel receive-only head coil at the University of Wisconsin. T1w structural scans were acquired via the MPnRAGE[73] sequence, a variation of the MPRAGE[102] sequence that allows for sampling over a large number of time points, n, along the inversion recovery curve. Four variations of the MPnRAGE sequence were used over the course of the study (Table C1 in supporting information). T1-weighted images were reconstructed with motion-correction[74], underwent 6 iterations of bias field correction and total variation denoising via ANTs[105]. Quantitative T1 maps were constructed into composite images (?) by estimating T1 in each voxel using methods described previously[74]. Quantitative R1 maps were produced by taking the reciprocal of the T1 maps using FSL[106]. As the R1 maps are inherently registered to the T1w composite images, no co-registration was required prior to

subsequent processing and analyses. All T1w images and R1 maps were visually inspected for quality assurance.

As multiple MPnRAGE protocols were implemented across the ADRC and WRAP cohorts, data harmonization was required to pool these data for statistical analysis of R1. Harmonization was performed using ComBat, a tool originally developed for large gene sets[109] and subsequently adapted for neuroimaging data[110–112]. In the present study, ComBat was independently applied to each regression model estimated for cortical GM R1 and cortical-adjacent WM R1. To minimize bias from extreme outliers, R1 values beyond 3 x interquartile range for each ROI were removed before harmonization was initiated.

For each participant, T1w composite images were processed through the *recon-all* function in Freesurfer v6[68]. In brief, structural scans underwent GM and WM tissue segmentation, as well as surface estimation at the boundary of GM and WM and at the pial surface. To estimate cortical GM R1, quantitative R1 values were sampled at the midpoint between these two surfaces. Resulting R1 surface meshes were resampled into Freesurfer template space and smoothed via a 10mm full width at half maximum Gaussian kernel (in geodesic distance)[56]. Mean R1 was extracted for each region of interest (ROI) according to the Desikan atlas.[107] Similarly, to estimate WM R1, quantitative R1 values were extracted from each subject's *wmparc* file, which parcellates WM according to the closest cortical ROI in the Desikan atlas. This processing resulted in 34 ROIs for cortical GM R1 and 34 ROIs for WM R1. The *ggseg* package in R was used for data visualization of each ROI in the Desikan atlas. All surface meshes and WM segmentations were visually inspected to ensure accurate delineation of the tissue of interest. Full processing steps are described and visualized in Figure C1 in Appendix C.

Cerebrospinal fluid collection, assays, and biomarker positivity determination

A complete description of CSF biomarker collection, assaying, and positivity threshold determination procedures are described previously[144]. In brief, CSF was acquired in the morning following an 8-12 hour fast via a Sprotte 24 or 25-gauge spinal needle. CSF was stored in 1.5mL polypropylene tubes at -80$^{\circ C}$ within 30 minutes of collection. CSF was assayed at the Clinical Neurochemistry Lab at the University of Gothenburg. Elecsys Aß (1-42) CSF, Elecsys tau phosphorylated at threonine 181 ($pTau_{181}$) CSF, Elecsys Total-Tau (tTau) CSF were measured using a cobas e 601 analyzer. Aβ (1-40) CSF, neurogranin, and neurofilament light protein (NfL) were assayed on a cobas e411 analyzer.

Case study participant characteristics

A female participant (age 67) enrolled in the WRAP study was selected for the case analysis to visually compare the spatial distribution of amyloid, tau, and cortical myelin *in vivo*. This participant had a family history of late-onset AD, was non-Hispanic white, completed 18 years of education, only spoke English, and was positive for apolipoprotein E (APOE) ε4 heterozygosity. Cognitive testing was performed within 10 days of PET and MRI scans in which they scored a 30 on the Mini Mental State Exam (MMSE). This individual was medicated for asthma, hypertension, and depression. This individual had no extended hospital stays or prior head trauma, and self-reported regular high levels of aerobic physical activity.

Case study [18F]MK6240 and [11C]PiB PET image acquisition and processing

The participant underwent T1-weighted MPnRAGE MRI, [18F]MK6240 PET for assessment of tau burden, and [11C]Pittsburgh Compound B (PiB) PET for measurement of amyloid load. MRI, tau PET, and amyloid PET were acquired within 11 days of each other. Amyloid and tau PET measures from a WRAP visit ~2 years prior indicated high levels of brain

amyloid and tau burden. Cortical R1 surface map estimation methods were performed as previously discussed. Procedures for MK6240 PET image acquisition, processing, derivation of standardized uptake value ratios (SUVR), and determination of tau positivity are fully described elsewhere[145,146]. Similarly, procedures for PiB PET imaging acquisition, processing, derivation of distribution volume ratios (DVR), and determination of amyloid positivity have been described in prior reports[146,147]. In brief, PiB and MK6240 images were summed, co-registered to the individual's T1-weighted MRI scan, and smoothed via a $6mm^3$ Gaussian kernel. PIB DVR and MK6240 SUVR were calculated using the cerebellum as a reference region. The threshold for amyloid positivity was set at a DVR > 1.19 averaged across 8 bilateral regions typically affected by early amyloid pathology[148]. Tau positivity was set at a threshold of SUVR > 1.27 in the bilateral parahippocampal gyrus[146]. Resulting R1, PiB DVR, and MK6240 SUVR values were then sampled from the center of the cortical surface as described in the previous section. Finally, R1, PiB DVR, and MK6240 SUVR surface meshes were displayed for visual comparison using the Computational Anatomy Toolbox for SPM12.

Statistical analysis and data visualization

Multivariate linear regression modeling was used to assess relationships between cortical and cortical-adjacent R1 and biomarkers of amyloid, tau, and neurodegeneration. Models were estimated in R version 4.1.1 using the "lmSupport" package for each bilaterally averaged ROI (34) for cortical GM and cortical-adjacent WM independently, with regional R1 as the outcome of interest in each model. The main effect of interest in each model was either CSF-derived Aβ42/40 ratio (with a higher ratio corresponding to less brain amyloid burden), $pTau_{181}$ (log-transformed), neurogranin (log-transformed), NfL (log-transformed), or tTau (log-transformed). CSF biomarker measures were transformed accordingly to ensure assumptions of the linear model framework were satisfied. Covariates in each model included age, sex, APOE

ε4 carrier status, and time (in years) between LP and MRI. In models assessing cortical-adjacent WM R1, a quadratic age term was included in each model as prior work within this dataset found a significant quadratic effect of age on R1 in WM, but not cortical GM. T-statistics for each model were displayed using the "ggseg" package. Due to the exploratory nature of this study, analyses were conducted with a *p*-value threshold of 0.05 without corrections for multiple comparisons, and *q*-value < 0.05 after Benjamini-Hochberg FDR corrections.

RESULTS

Associations between CSF biomarkers of AD and R1

Higher CSF Aβ42/40 ratio was significantly associated with higher cortical GM R1 in the superior parietal (t = 3.295, q = 3.330e^{-2}), inferior parietal (t = 3.117, q = 3.330e^{-2}), supramarginal (t = 2.904, q = 3.618e^{-2}), and precuneus (t = 2.875, q = 3.618e^{-2}). Additional relationships were found at an exploratory p<0.05 threshold in the banks of the superior temporal sulcus (t = 2.447, p = 1.485e^{-2}), postcentral (t = 2.383, p = 1.764e^{-2}), cuneus (t = 2.370, p = 1.826e^{-2}), and lateral occipital (t = 2.332, p = 2.022e^{-2}) regions. While a few regions in the frontal and temporal cortices showed negative relationships between R1 and CSF Aβ42/40 (Figure 1a), none of these reached significance at an uncorrected p<0.05 threshold. In cortical-adjacent WM, no significant regional relationships were found between CSF Aβ42/40 ratio and R1 after FDR-correction for multiple comparisons. However, at an uncorrected p<0.05 threshold, the lateral occipital (t = 2.749, p = 6.263e^{-3}), inferior parietal (t = 2.417, p = 1.610e^{-2}), inferior temporal (t = 2.187, p = 2.930e^{-2}), superior parietal (t = 2.181, p = 2.978e^{-2}), banks of the superior temporal sulcus (t = 2.127, p = 3.406e^{-2}), among others (Figure 1b) showed similar positive associations between CSF Aβ42/40 ratio and R1.

Regional effects of CSF $pTau_{181}$ on cortical GM R1 were uniformly negative. The inferior parietal (t = -3.356, q = 2.947e^{-2}), supramarginal (t = -3.074, q = 3.672e^{-2}), lateral occipital (t = -2.962, q = 3.672e^{-2}), and superior temporal (t = -2.827, q = 4.194e^{-2}) ROIs survived FDR-correction for multiple comparisons. Additional areas that showed negative relationships at an exploratory p<0.05 threshold included the pars orbitalis (t = -2.692, p = 7.405e^{-3}), superior parietal (t = -2.627, p = 8.948e^{-3}), precuneus (t = -2.495, p = 1.301e^{-2}), transverse temporal (t = -2.451, p = 1.467e^{-2}), and cuneus (t = -2.433, p = 1.542e^{-2}), among others (Figure 1c). Relationships with cortical-adjacent WM R1 were also uniformly negative, with a greater number of regions reaching FDR-correction, namely the lateral occipital (t = -3.356, q = 2.947e^{-2}), frontal pole (t = -3.356, q = 2.947e^{-2}), inferior parietal (t = -3.356, q = 2.947e^{-2}), banks of the superior temporal sulcus (t = -3.356, q = 2.947e^{-2}), middle temporal (t = -3.356, q = 2.947e^{-2}), among others (Figure 1d). In total 27/34 bilateral ROIs exhibited significant relationships with CSF $pTau_{181}$. Full outputs for regression models assessing relationships with CSF Aβ42/40 ratio and $pTau_{181}$ can be found in appendix C (Tables C2-5).

Relationships between CSF biomarkers of neurodegeneration and R1

Higher CSF neurogranin was significantly associated with lower cortical GM R1 in the inferior parietal (t = -3.066, q = 3.890e^{-2}), superior temporal (t = -2.914, q = 3.890e^{-2}), lateral occipital (t = -2.896, q = 3.890e^{-2}), supramarginal (t = -2.852, q = 3.890e^{-2}), and pars orbitalis (t = -2.698, q = 4.950e^{-2}) ROIs. Cortical R1 in the precuneus, lingual, cuneus, pars triangularis, superior parietal, and frontal pole ROIs, among others, were negatively associated with CSF neurogranin at an exploratory p<0.05 threshold (Figure 2a). Cortical-adjacent WM R1 exhibited stronger negative associations with CSF neurogranin as compared to cortex, with 29/34 regions surviving multiple comparisons correction. Among these regions, the lateral occipital (t = -4.806, q = 7.449e^{-5}), frontal pole (t = -3.866, q = 2.254e^{-3}), inferior parietal (t = -3.747, q = 2.331e^{-3}),

banks of the superior temporal sulcus (t = -3.656, q = 2.477e^{-3}), and middle temporal (t = -3.386, q = 4.501e^{-3}) ROIs exhibited the strongest relationships (Figure 2b).

No regions showed significant relationships between CSF NFL and cortical GM R1 after FDR-correction for multiple comparisons, however, higher NFL was associated with higher cortical R1 in the parahippocampal (t = 2.668, p = 7.945e^{-3}) and entorhinal ROIs (t = 2.195, p = 2.878e^{-2}) at an exploratory p<0.05 threshold. Additional regions with trending relationships are plotted in Figure 2c. R1 in cortical-adjacent WM was negatively associated with CSF NFL in the lateral occipital (t = -3.006, p = 2.818e^{-3}), frontal pole (t = -2.518, p = 1.221e^{-2}), banks of the superior temporal sulcus (t = -2.476, p = 1.372e^{-2}), inferior parietal (t = -2.415, p = 1.620e^{-2}), and caudal middle frontal (t = -2.372, p = 1.817e^{-2}) ROIs, among others, without FDR-correction for multiple comparisons (Figure 2d).

After FDR-correction, elevated CSF tTau was significantly associated with lower cortical GM R1 in the inferior parietal (t = -3.275, q = 3.108e^{-2}), supramarginal (t = -3.015, q = 3.108e^{-2}), and the lateral occipital (t = -3.014, q = 3.108e^{-2}). Moreover, CSF tTau was associated with the superior temporal (t = -2.754, p = 6.152e^{-3}), cuneus (t = -2.698, p = 4.950e^{-2}), and precuneus (t = -2.698, p = 4.950e^{-2}) at the exploratory p<0.05 threshold (Figure 2e). Cortical-adjacent WM R1 was also negatively associated with CSF tTau, with 28/34 regions surviving FDR-correction for multiple comparisons. These regions included the lateral occipital (t = -4.716, q = 1.139e^{-4}), frontal pole (t = -4.080, q = 9.258e^{-4}), inferior parietal (t = -3.660, q = 3.249e^{-3}), banks of the superior temporal sulcus (t = -3.551, q = 3.654e^{-3}), and middle temporal (t = -3.278, q = 5.884e^{-3}) ROIs, among others (Figure 2f). Full outputs of regression models assessing relationships between CSF neurogranin, NFL, and tTau and R1 can be found in appendix C (Tables C6-11).

Case study: visual comparison between cortical myelin, amyloid, and tau in a single subject

Surface maps of cortical R1, amyloid plaque burden ([11C]PiB PET DVR), and tau burden ([18F]MK6240 PET SUVR) can be found in Figure 3. Motor, somatosensory, and lateral occipital regions exhibited the highest levels of R1. Inferior temporal, inferior frontal, precuneus, and supramarginal regions had the lowest levels of R1. Values of R1 in this participant ranged from ~0.62Hz in the medial orbitofrontal and rostral anterior cingulate cortices to ~0.72Hz in the motor and somatosensory regions.

High amyloid plaque load was evident throughout the individual's neocortex, with the highest PiB DVR located in the middle frontal, medial frontal, anterior and posterior cingulate, precuneus, inferior parietal, supramarginal, angular, and middle temporal gyri. Areas such as the motor, somatosensory, and posterior occipital cortices exhibited the lowest PiB binding. Amyloid levels were consistent across hemispheres. This participant had a global PiB DVR of 1.69 and a visual rating of 3, indicating they were positive for amyloid plaques.

High tau burden can be observed in distinct regions of the cortex including the lateral and medial prefrontal, inferior parietal, supramarginal, posterior cingulate, precuneus, inferior and middle temporal, fusiform, parahippocampal, and entorhinal regions. This individual had a MK6240 SUVR in the bilateral parahippocampal gyrus of 1.68 (1.79 – left; 1.57 – right) and was classified as Braak stage 6 according to a visual reading (SCJ). While MK6240 SUVR far surpassed the threshold for positivity, tau burden appeared to be exacerbated in the left hemisphere as can be observed in the axial view of Figure 2, specifically in the precuneus, superior parietal, and inferior parietal regions.

DISCUSSION

Higher frontal, occipital, and inferior parietal myelin linked to reduced AD pathology and neurodegeneration

Elevated CSF levels of both AD pathology (lower Aβ42/40 ratio and higher $pTau_{181}$) and neurodegeneration (higher neurogranin, NfL, and tTau) were linked to reduced myelin content in both the cortex and cortical-adjacent WM. Our findings in WM add support to prior diffusion imaging studies that suggest lower CSF amyloid and elevated CSF pTau are associated with decreases in WM integrity in individuals across the AD clinical spectrum[67,149–151]. In particular, we found that decreased parietal, occipital, and temporal myelin was linked with elevated amyloid pathology, and elevated pTau was strongly associated with global WM demyelination.

With regards to biomarkers of neurodegeneration, neurogranin and tTau exhibited the strongest negative relationships with myelin out of all biomarkers tested. Despite the role that NfL plays as a key cytoplasmic protein in large-caliber myelinated axons, as well as its prior associations with axonal degeneration in AD[87,88], it demonstrated the weakest associations with myelin content out of all neurodegeneration markers tested. It is likely that because R1 was assessed in the cortex and in cortical-adjacent WM, our measures did not include possible demyelination of large association or commissural fiber tracts. Still, negative associations between NfL and myelin were found in several areas typically affected in AD, including parietal, middle temporal, and frontal WM. Future work should aim to investigate R1 within major WM fiber bundles to further elucidate structural connectivity as it relates to biomarkers of neurodegeneration.

As mentioned previously, two studies[69,70] to date have attempted to assess relationships between cortical myelin and AD pathology *in vivo*, relying on the T1/T2 ratio as an index of myelin content. These studies present contrasting results, with one identifying higher cortical T1/T2 ratios in individuals with greater AD pathology[69] and the other revealing lower T1/T2

ratios in individuals across the AD continuum[70], leading to inconclusive interpretations about the role cortical myelin plays in the AD pathological cascade. Here we clarified this role by employing cortical R1 mapping in the context of AD biomarkers. Our findings, both on the single subject and group level, supported those of Luo et al.[70] in that lower cortical myelin was associated with greater pathology in individuals across the AD continuum. Interestingly, our results also identified the inferior parietal lobule (IPL) as a region with strong associations between myelination and pathology, in both the cortex and adjacent WM. The IPL is known to be a highly interconnected region, with involvement in memory retrieval, spatial processing, and executive function, in addition to being a node in the default mode network (DMN)[152,153]. Given the prior reports of tau accumulation in the IPL in preclinical AD[40,154], it is possible that reduced myelination of the IPL or surrounding WM may lead to susceptibility of developing AD pathology and could have strong negative impacts on cognitive performance. However, without longitudinal assessment, we cannot infer the temporal relationship between myelination and development of pathology.

While directionality of effects was consistent across GM and WM ROIs, cortical myelin showed stronger relationships with CSF amyloid levels and WM exhibited stronger associations with CSF pTau. These results suggest that cortical myelin may be more sensitive to damage from amyloid toxicity, while larger and substantially more myelinated afferent or efferent fiber tracts in WM could be more susceptible to damage from pathological tau. One advantage afforded through the utilization of the Desikan parcellation to study myelin in cortical-adjacent WM, as opposed to traditional tractography approaches, was the ability to directly compare the effects of these biomarkers spatially for both the cortex and WM. Here we see that regional effects were similar between the cortex and nearby WM, however, relationships tended to be stronger and more widespread in WM, likely due to increased sensitivity of R1 to the greater myelin content present in WM.

Case study: Cortical myelin inversely mirrors spatial distribution of pathological amyloid plaque and tau tangles *in vivo.*

Observations made at the single subject level reinforced findings from ROI-based analyses assessing relationships between CSF levels of AD pathology. Regional patterns of cortical R1 in a single older adult reflected patterns of cortical myelination reported previously[51,52,56,60,155]. With regards to AD pathology, neocortical distribution of amyloid burden followed stereotypical patterns of plaque accumulation[146,147], and distribution and intensity of tau tangles suggest this participant was in the late Braak stages[76,156]. Although amyloid plaques and tau tangles encumbered much of the cortex, regions with the highest levels of cortical myelin such as the pre-and-postcentral gyrus were spared from such pathology. In contrast, the inferior and medial temporal, inferior parietal, and prefrontal regions had high AD pathology and relatively low myelin. Opposing spatial patterns between myelin and AD pathology were consistent with both amyloid and tau. However, regions with elevated myelin and higher tau are in almost complete contradiction, reinforcing the idea that cortical tau and myelin may be linked.

Interestingly, despite heavy pathological load, this individual remained cognitively unimpaired at the time of assessment. Prior work has identified that greater WM tissue integrity (as assessed through diffusion imaging) is associated with higher cognitive reserve and resilience[32,151,157]. While we cannot directly infer the role that cortical myelin has in cognitive reserve and resilience, it is possible that substantial myelination and/or continuous repair of myelin by oligodendrocytes could be compensating for this pathology to maintain cognitive function[39]. Still, given this participant has a family history of AD, as well as overwhelming pathology, it is more likely than not that they will progress to the clinical syndromic stages of AD. This case analysis emphasizes the importance of incorporating markers of brain myelin into studies of AD, as the contrasting similarities in the spatial distribution cortical myelin to AD pathology cannot be overlooked. Of note, this is the first MRI and PET-driven *in vivo*

demonstration of the post-mortem observations made by Heiko and Eva Braak[76] suggesting links between cortical myelination and AD.

Limitations

While quantitative R1 mapping has been shown to be a highly sensitive index of brain myelination, other macromolecules present in brain tissue can influence R1[36,50,71,72,158]. As cortical tissue has far less myelin compared to that of WM, and work has shown a large portion coats axons of inhibitory interneurons[159,160], it is reasonable to expect that cortical R1 may exhibit different, and potentially less sensitive, relationships with biomarkers of AD pathology and neurodegeneration than R1 in WM. Beyond the imaging metrics, our population was enriched for family history of AD, highly educated, and primarily of Caucasian descent, limiting the generalizability of these findings. Finally, due to the longitudinal nature of the larger WRAP and ADRC parent studies, some participants underwent lumbar puncture procedures years prior to MPnRAGE MRI acquisition. While we included the time between LP and MRI as a covariate in all models, future work should aim to acquire these metrics in closer proximity to limit effects of aging and pathological accumulation.

CONCLUSION

This novel work, through the inclusion of a large cohort well characterized for biomarkers of AD pathology and neurodegeneration, application of the novel high-fidelity MPnRAGE MRI sequence to derive a relaxometry metric sensitive to myelin, and an *in vivo* comparison of the spatial distribution of cortical myelin alongside amyloid and tau PET, provided robust support for studying myelin in AD. Through our approaches, we identified that the spatial patterns of cortical myelin indeed do mirror that of AD pathology *in vivo*, and that elevated CSF levels of AD pathology and neurodegeneration are associated with decreased myelin in both the cortex and

cortical-adjacent WM. In particular, the IPL consistently showed strong relationships with these biomarkers, adding credence for future investigations of the role of the IPL in AD pathogenesis and progression.

TABLES AND FIGURES

Table 1: Participant Demographics and Characteristics

	Dementia (N=7)	MCI (N=18)	Unimpaired (N=375)	Total (N=400)
Age at Baseline MRI Scan (years)				
Mean (SD)	72.534 (7.425)	71.224 (10.253)	65.539 (7.417)	65.917 (7.684)
Sex				
Female	5 (71.4%)	8 (44.4%)	249 (66.4%)	262 (65.5%)
Male	2 (28.6%)	10 (55.6%)	126 (33.6%)	138 (34.5%)
APOE ε4 Status				
Non-Carrier	2 (28.6%)	9 (50.0%)	237 (63.2%)	248 (62.0%)
Carrier	5 (71.4%)	9 (50.0%)	138 (36.8%)	152 (38.0%)
Education				
Mean (SD)	15.571 (3.457)	16.056 (2.287)	16.347 (2.347)	16.320 (2.363)
Time b/w LP and MRI (years)				
Mean (SD)	3.029 (2.504)	1.566 (2.774)	2.320 (2.547)	2.298 (2.557)
Primary Race				
American Indian or Alaska Native	0 (0.0%)	0 (0.0%)	3 (0.8%)	3 (0.8%)
Asian	0 (0.0%)	0 (0.0%)	1 (0.3%)	1 (0.2%)
Black or African American	0 (0.0%)	1 (5.6%)	14 (3.7%)	15 (3.8%)
Other	0 (0.0%)	0 (0.0%)	1 (0.3%)	1 (0.2%)
White	7 (100.0%)	17 (94.4%)	356 (94.9%)	380 (95.0%)
CSF Aβ42/40 Ratio				
Mean (SD)	0.034 (0.018)	0.045 (0.020)	0.064 (0.017)	0.062 (0.018)
CSF $pTau_{181}$ (pg/mL)				
Mean (SD)	40.566 (25.233)	24.844 (12.392)	17.958 (6.710)	18.664 (8.302)
CSF tTau (pg/mL)				
Mean (SD)	393.786 (200.317)	266.133 (116.935)	204.572 (71.376)	210.654 (81.996)
CSF NfL (pg/mL)				
Mean (SD)	199.780 (61.848)	140.752 (68.070)	98.362 (68.013)	102.044 (69.561)
CSF Neurogranin (pg/mL)				
Mean (SD)	1230.243 (679.053)	952.128 (449.126)	794.275 (306.012)	809.008 (327.941)

Table 1: Participants were enrolled in the Wisconsin Alzheimer's disease Research Center Clinical Core or the Wisconsin Registry for Alzheimer's Prevention studies at the University of Wisconsin-Madison (Madison, WI). Abbreviations: MCI, mild cognitive impairment; AD,

Alzheimer's disease; ADRC, Alzheimer's Disease Research Center; WRAP, Wisconsin Registry for Alzheimer's prevention; LP, lumbar puncture; MRI, magnetic resonance imaging; APOE, apolipoprotein E; $pTau_{181}$, Tau phosphorylated at threonine 181; tTau, total Tau; Aβ, amyloid-beta; NfL, neurofilament light chain protein.

Figure 1: Relationships between AD pathology and R1

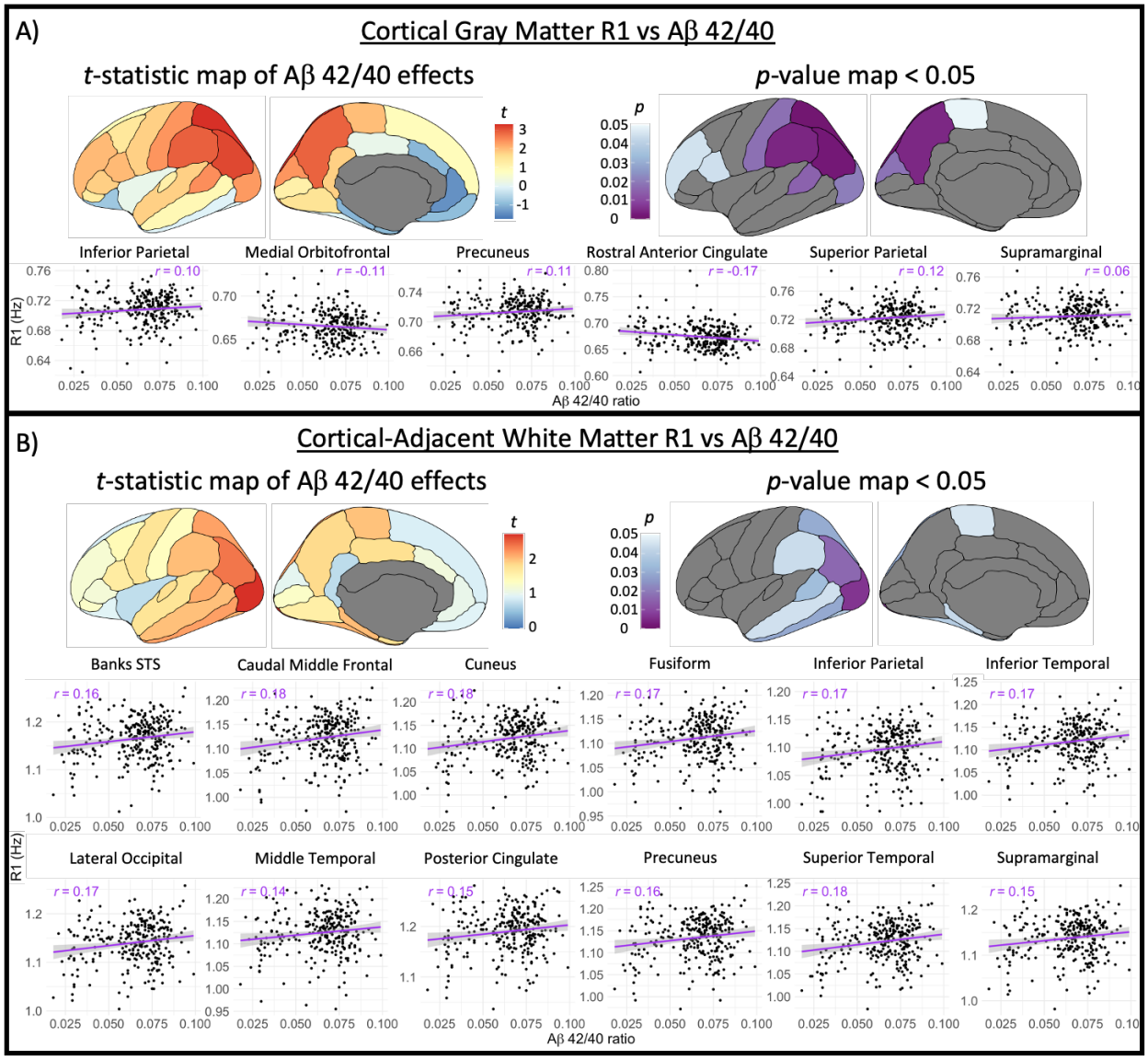

Figure 1: Regression results assessing the effects of AD pathology on R1. Maps of *t*-statistics and corresponding *p*-values visualizing the effects of CSF Aβ42/40 on A) cortical GM R1 and B) cortical-adjacent WM R1 parcellated by ROIs from the Desikan parcellation. Maps of *t*-statistics and corresponding *p*-values or *q*-values visualizing the effects of CSF $pTau_{181}$ on C) cortical GM R1 and D) cortical-adjacent WM R1 parcellated by ROIs from the Desikan parcellation. Individual regions with corresponding linear trend lines are plotted below the brain maps in each panel using the formula 'y~x'. Abbreviations: Aβ, amyloid-beta; $pTau_{181}$, tau phosphorylated at threonine 181; Banks STS, banks of the superior temporal sulcus.

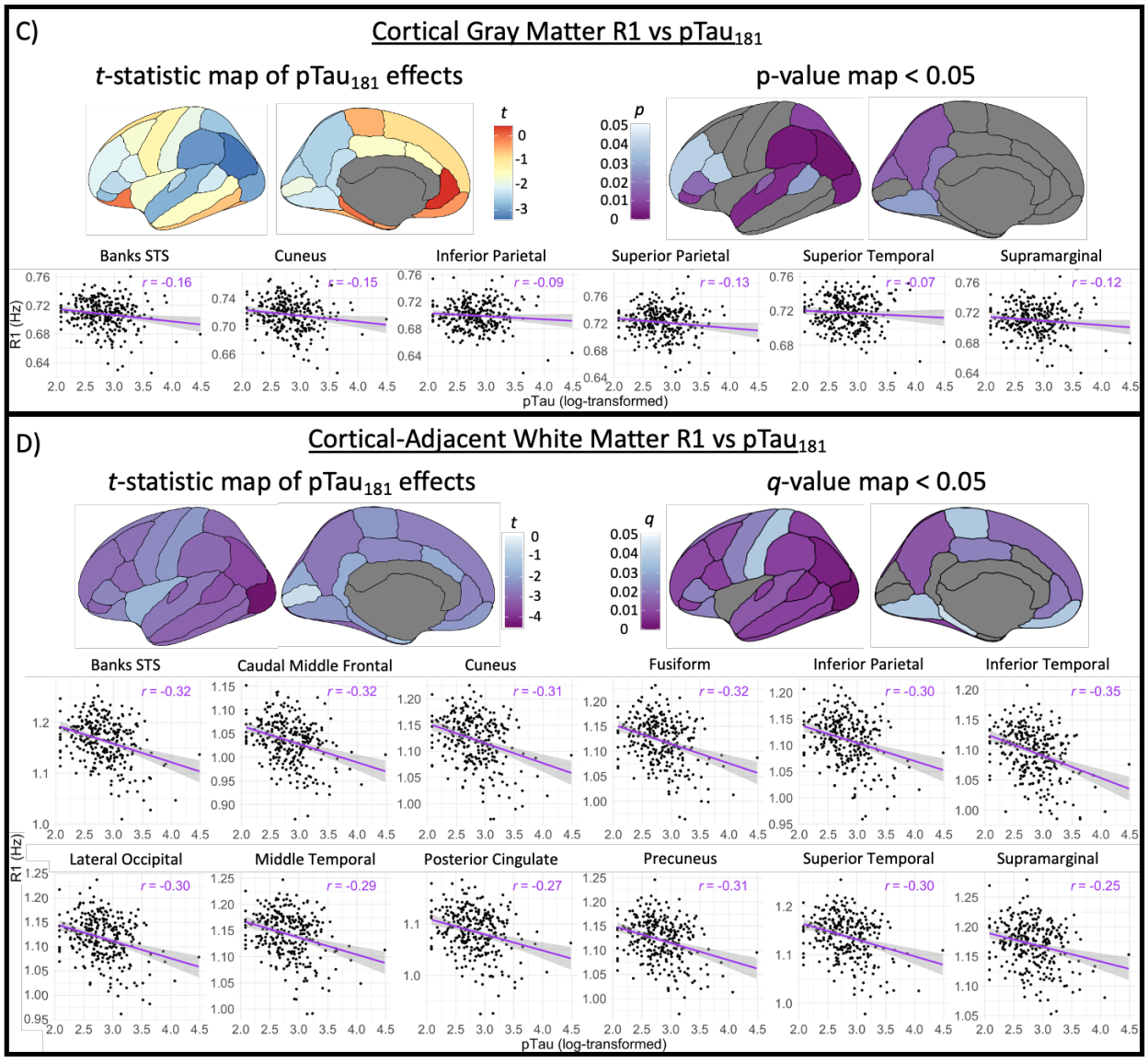

Figure 1 continued

Figure 2: Relationships between CSF markers of neurodegeneration and R1

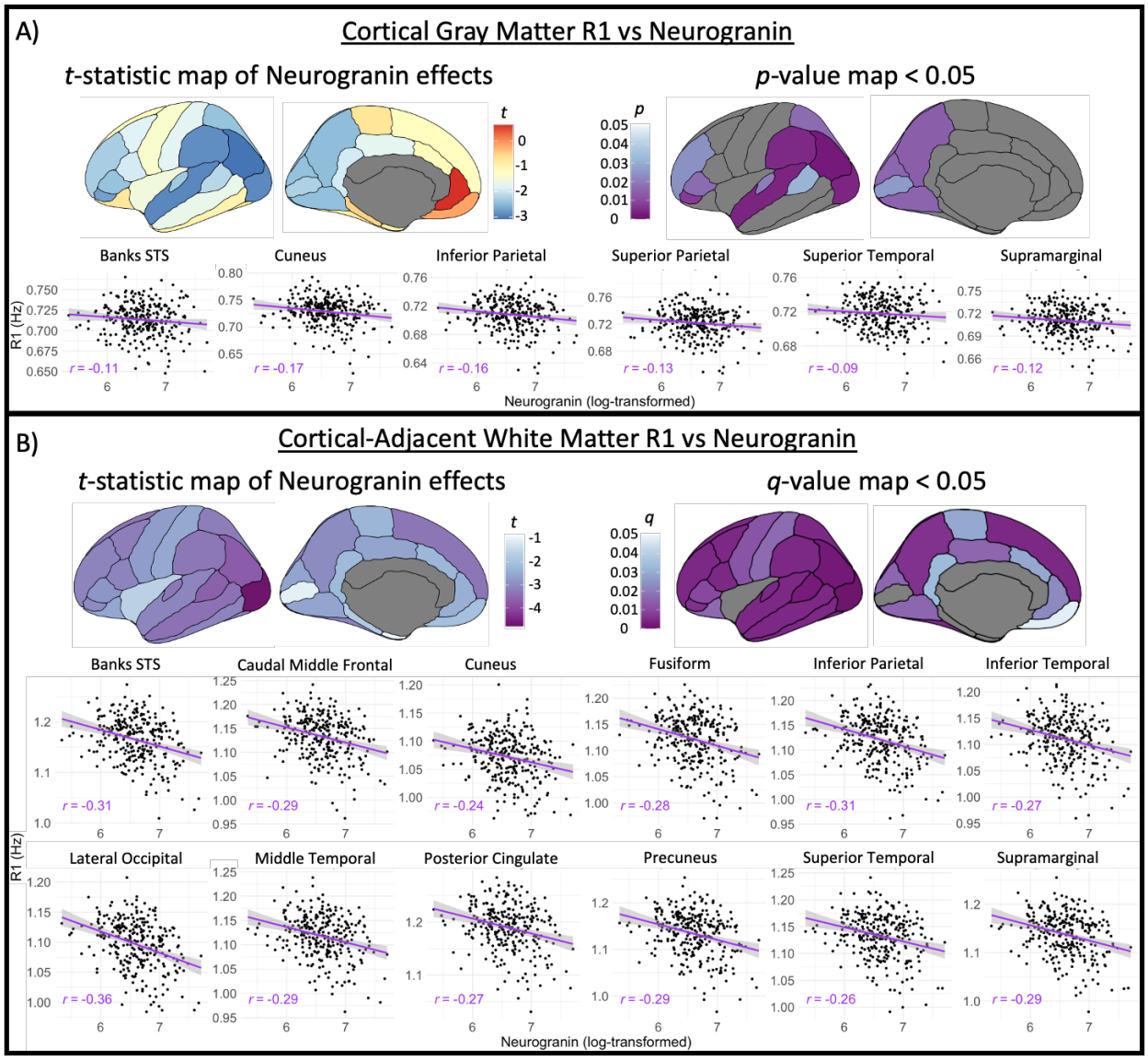

Figure 2: Regression results assessing the effects of AD pathology on R1. Maps of *t*-statistics and corresponding *p*-values or *q*-values visualizing the effects of CSF Neurogranin on A) cortical GM R1 and B) cortical-adjacent WM R1 parcellated by ROIs from the Desikan parcellation. Maps of *t*-statistics and corresponding *p*-values visualizing the effects of CSF NfL on C) cortical GM R1 and D) cortical-adjacent WM R1 parcellated by ROIs from the Desikan parcellation. Maps of *t*-statistics and corresponding *p*-values or *q*-values visualizing the effects of CSF tTau on E) cortical GM R1 and F) cortical-adjacent WM R1 parcellated by ROIs from the

Desikan parcellation. Individual regions with corresponding linear trend lines are plotted below the brain maps in each panel using the formula ‘y~x’. Abbreviations: Banks STS, banks of the superior temporal sulcus; NfL, neurofilament light chain protein; tTau, total Tau.

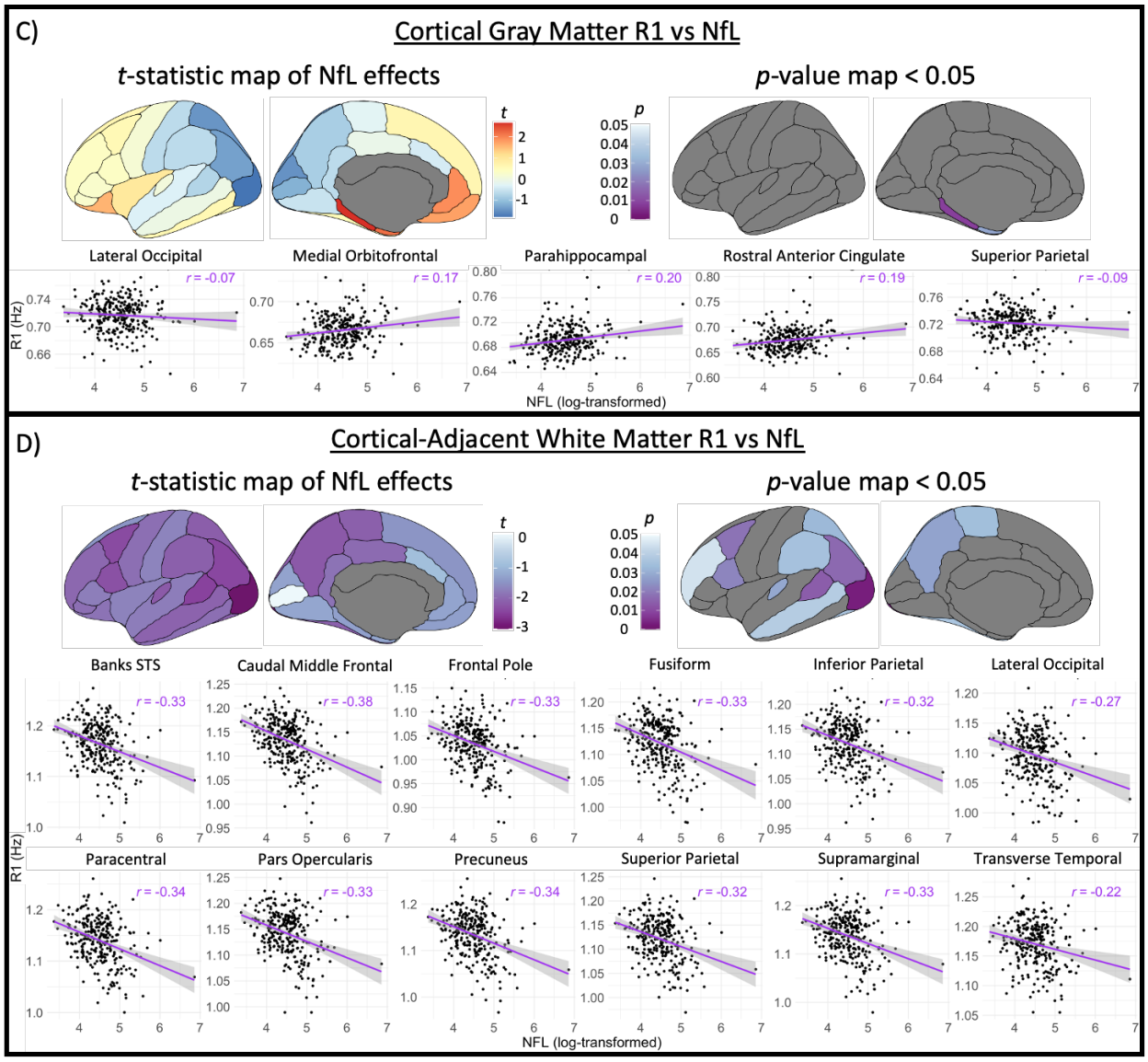

Figure 2 continued

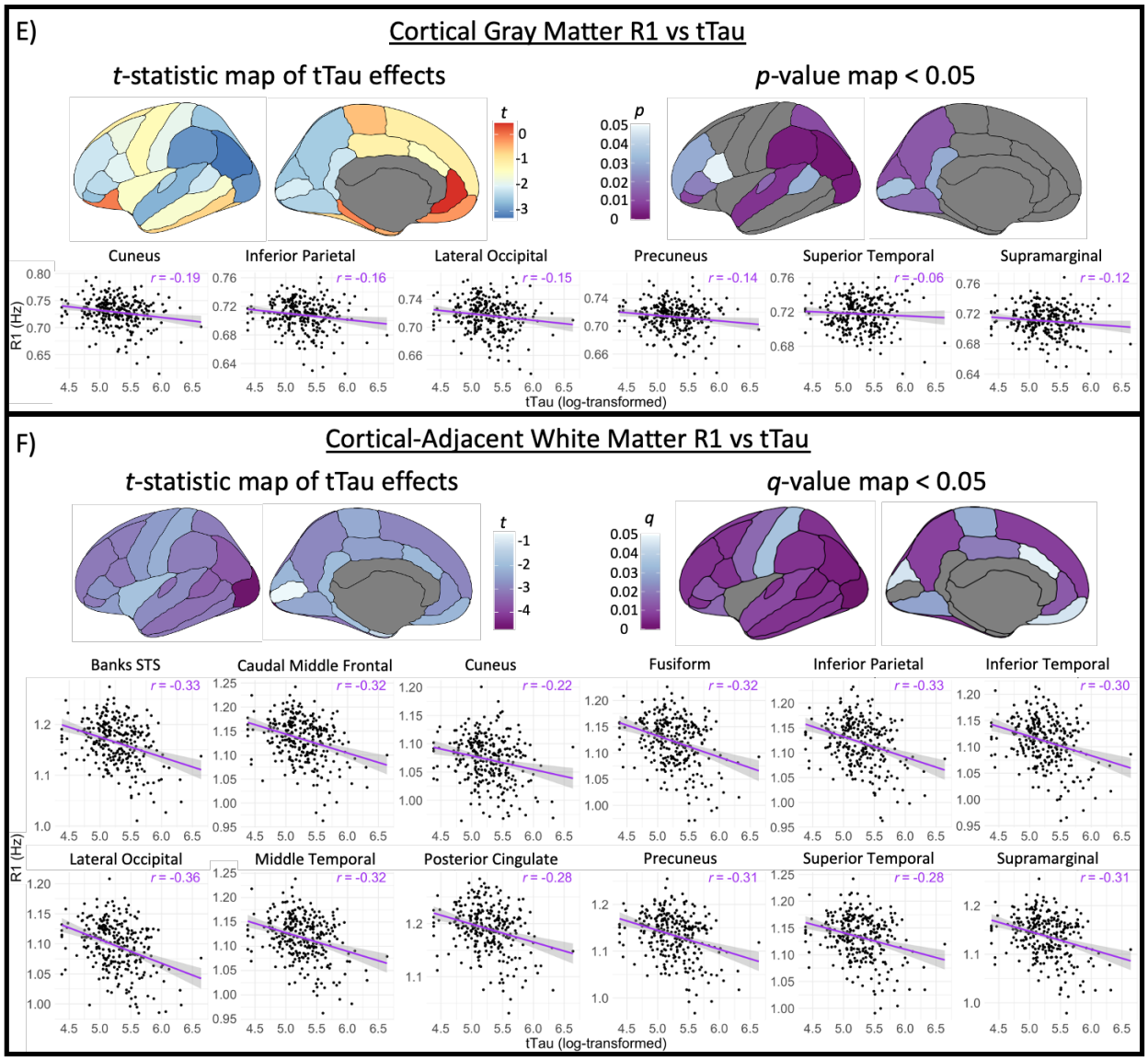

Figure 2 continued

Figure 3: Single subject visualization of cortical myelin, amyloid, and tau *in vivo*

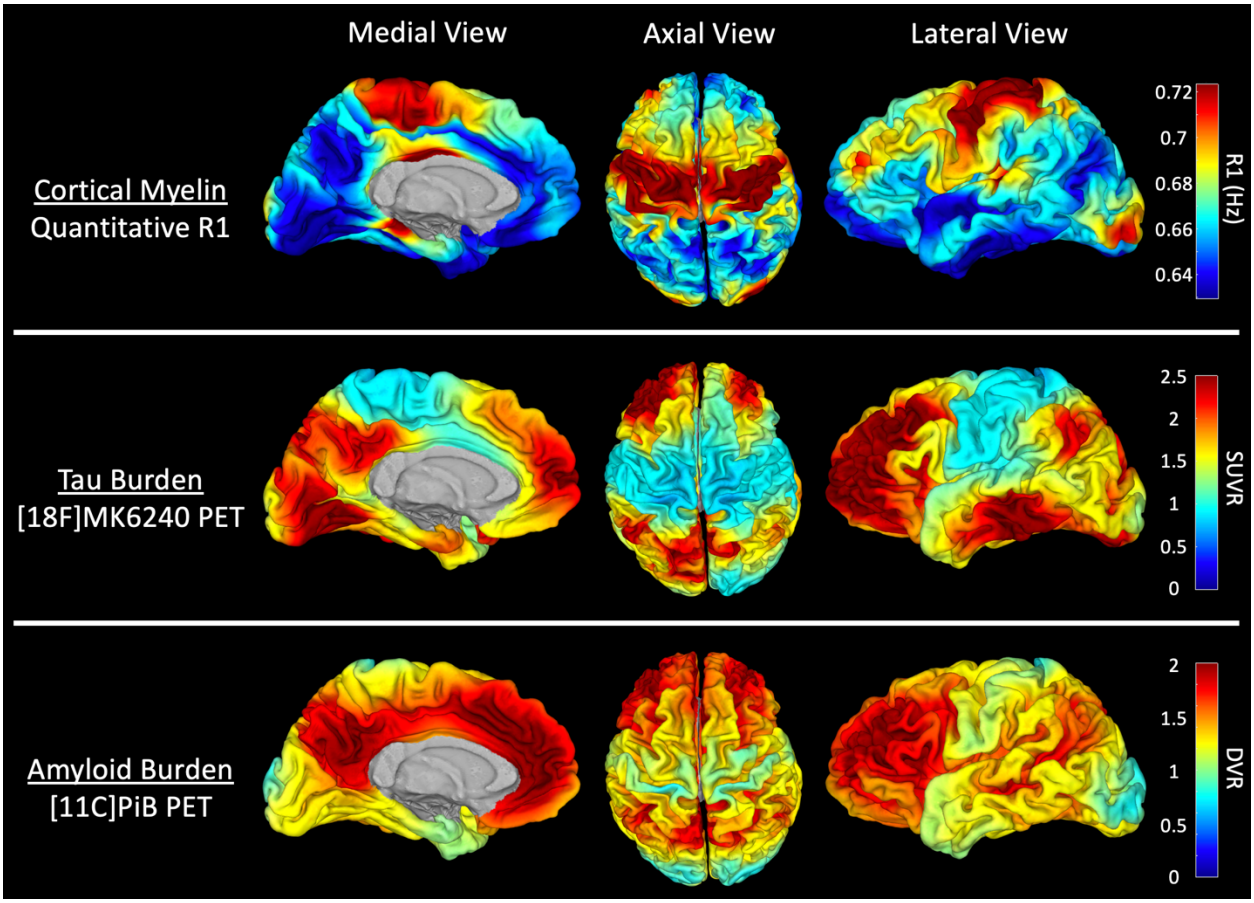

Figure 3: Top row: Quantitative R1 map indexing myelin content at the center of cortical gray matter. Higher R1 indicates greater myelin content. Middle row: [18F]MK6240 PET SUVR map indexing tau burden at the center of cortical gray matter. Bottom row: [11C] PiB PET DVR map indexing amyloid burden at the center of cortical gray matter. Participant was 67 years old, female, and diagnosed as cognitively unimpaired. Abbreviations: PET, positron emission tomography; SUVR, standardized uptake value ratio; DVR, distribution volume ratio; PiB, Pittsburgh compound B.

ACKNOWLEDGEMENTS & FUNDING

MR imaging at UW-Madison was supported in part by a core grant to the Waisman Center from the National Institute of Child Health and Human Development (P50HD105353). Akshay Kohli and Kao Lee Yang are both students in the Neuroscience Training Program (NIH/NINDS T32 NS105602). Data were collected under the following grants from the NIH National Institute of Aging: R01AG037639 (Bendlin), R01AG062285 (Bendlin), R01AG027161 (Johnson), P50AG033514 (Asthana), R01AG062167 (Okonkwo). Henrik Zetterberg is a Wallenberg Scholar supported by grants from the Swedish Research Council (#2018-02532), the European Research Council (#681712), the Swedish state under the agreement between the Swedish government and the County Councils, the ALF-agreement (#ALFGBG-720931), the Alzheimer Drug Discovery Foundation (ADDF), USA (#201809-2016862), and the UK Dementia Research Institute at UCL. Kaj Blennow is supported by the Swedish Research Council (#2017-00915), the Alzheimer Drug Discovery Foundation (ADDF), USA (#RDAPB-201809-2016615), the Swedish Alzheimer Foundation (#AF-742881), Hjärnfonden, Sweden (#FO2017-0243), the Swedish state under the agreement between the Swedish government and the County Councils, the ALF-agreement (#ALFGBG-715986), and European Union Joint Program for Neurodegenerative Disorders (JPND2019-466-236). ELECSYS is a registered trademark of Roche. The NeuroToolKit is a panel of exploratory robust prototype immunoassays intended for research use only. The authors would like to thank the research participants for their commitment to our research studies as well as the staff of the Wisconsin ADRC for their assistance with data collection, organization, and management. Funding sources were not involved in study conceptualization, design, execution, and analysis.

Chapter 5: Conclusions, Broader Implications, and Future Directions

Summary of Findings

This dissertation provided an initial examination of the role that cortical myelin may play in healthy and diseased aging through the use of quantitative relaxometry. In the first aim, trajectories of R1 were identified across two independent populations of cognitively unimpaired older adults between the ages of 45 and 90. Within the cortex, increases in R1 were identified in late-myelinating regions in the temporal and frontal cortices, although effect sizes were minimal. In comparison, R1 in white matter showed strong decreases globally, with the quadratic model fitting the data better in the ADRC/WRAP dataset, and linear decreases identified in the ADCP cohort. Additionally, alterations in R1 were assessed between diagnostic groups. Individuals with cognitive impairment were found to have higher cortical R1 in the temporal and frontal regions, which are typically impacted in AD. In contrast, R1 was significantly lower in individuals with cognitive impairment globally in WM. Results pertaining to cortical alterations in cognitive impairment were replicated in the ADCP cohort, whereas WM did not show significant differences; however, when the impairment group was stratified by MCI or dementia status, it was found that. Finally, a closer examination of the relationships between cortical and WM myelin and performance on test of executive function, working memory, and processing speed was performed. Higher cortical R1 was significantly associated with worse performance on tests of executive function and working memory, whereas lower WM R1 was associated with worse performance on tests of processing speed. The findings of strong positive associations between processing speed and WM R1 were consistent with prior studies, while the results showing negative associations between cortical R1 and executive function and working memory add novel insight into the differential role cortical myelin may play in maintaining cognition as compared to WM.

The second aim explored the impacts of sex and APOE genotype on cortical and WM tissue relaxation. Analysis of cortex revealed that minimal alterations are exhibited in the cortex between males and females, carriers of the APOE E4 allele do not have altered R1 as

compared to non-carriers, and there was no significant interaction between sex and APOE on R1. Within WM, males had globally higher R1 compared to females, and while there were minimal effects of APOE E4 genotype on WM R1, significant interaction effects were detected indicated male E4 carriers had higher R1 than male non-carriers. These analyses expanded upon the existing knowledgebase of genetic influences on cortical myelination in addition to WM.

Within the third aim, cross-sectional associations between CSF biomarkers of AD pathology and neurodegeneration and cortical R1 were investigated. Higher cortical R1 was significantly associated with reduced CSF biomarkers of amyloid, tau, and neurodegeneration, primarily in the posterior cortices of the brain, with the strongest effects in the inferior parietal, cingulate, and superior temporal regions. Interestingly, directionality of effects was consistent between the cortex and WM, and while the cortical R1 showed stronger associations with amyloid burden, WM R1 had stronger relationships with phosphorylated tau. With regards to markers of neurodegeneration, NFL solely related to R1 within WM, consistent with the fact that NFL is present in large caliber myelinated axons which are likely not present in the cortex. In contrast, neurogranin and total tau showed strong relationships with both cortical and WM R1. These findings support the idea that myelin is sensitive to early pathological change in AD (and in regionally distinct ways). Finally, in an effort to replicate the original post-mortem observations made by Heiko and Eva Braak, a single subject case study was presented using PET-derived maps of amyloid and tau burden in relation to a cortical R1 map. Visually, maps of AD pathology inversely mirrored the spatial distribution of cortical myelin (as indexed by R1), suggesting these patterns can be detected *in vivo*. The strongest visual congruency could be observed within the inferior parietal lobule and supramarginal gyrus, regions that showed significant associations with CSF biomarkers in the aforementioned analyses. Although this participant had intensive amyloid and tau burden, they remained cognitively unimpaired, and while research indicates this individual will likely develop the clinical syndromic effects of AD in the future, it remains up for

debate as to why they are resistant to the toxicity of the plaque and tangle burden present in their brain.

Broader Implications for Clinical and Translational Studies

While the work presented in this dissertation does not directly test myelin therapies or other clinical interventions, it adds to the existing knowledgebase of the role myelin plays in the pathogenesis and progression of AD, and presents possible targets for future applications of these treatments. A growing body of research has been assessing the effects of amyloid therapies on resulting brain morphometry and myelin integrity in mouse models. One such study, published in 2010, assessed the impact of a recombinant adeno-associated viral vector therapy expressing an Aβ42 antibody in a transgenic mouse model of AD. Researchers found that expression of this antibody led to an increase in the expression of oligodendrocyte and myelin markers, suggesting clearing pathological Aβ may restore myelin integrity, and thus reduce the impact of myelin disruption early in the AD pathological process[161]. Recent work as of 2021 has taken an alternative therapeutic approach by inducing oligodendrocyte precursor cell differentiation via Clemastine, an H1-anthistiamine. Researchers found that treatment by this antihistamine increased levels of myelin in the cortex and hippocampus, which ultimately led to an improvement in memory-related cognitive function in an amyloid precursor protein/presenilin-1 (APP/PS1) mouse model of AD[162].

As more studies investigate the potential therapeutic aspects that pharmaceutical interventions stimulating myelin repair could have in reducing risk of developing AD pathology, the findings within this dissertation 1) provide a comprehensive overview of the impact cortex-specific myelin has in normal aging, cognition, and AD pathological processes, 2) identified regions susceptible to AD pathology in direct comparison to the spatial distribution of AD, and 3) directly compared cortical myelin to myelin within adjacent WM. Overall, the results, primarily

from the first and third aims of this dissertation, suggest that cortical and white matter myelin may play differential roles in maintaining normal cognitive function. Given the close inverse spatial distributions of cortical myelin and AD pathology, it is possible that by targeting regions that typically myelinate later in life such as the temporal, inferior parietal, posterior cingulate, and frontal cortices,

Future Directions

The MPnRAGE sequence is extremely powerful, and while this dissertation is the first to utilize MPnRAGE-derived R1 to study aging and AD-related risk factors and pathologies, there are other ways to leverage this sequence to assess AD in vivo. The MPnRAGE sequence also allows for the quantification of proton density, a measure sensitive to fat concentration[163,164], and therefore myelin. Further investigations should utilize proton density as a potential imaging marker of myelin and determine whether it provides additional utility beyond R1 mapping. Beyond myelin-related assessments, MPnRAGE implements intrinsic motion-correction that has shown to produce higher contrast and less blurring between GM and WM than traditional techniques[73,74]. The amount of motion exhibited over the duration of the scan can be recorded and output as a motion map – these maps may serve as a potential marker of aging or impacts of AD-related pathology. Were these maps to be employed in such a context, it is possible they could identify patients with AD (or other neurodegenerative diseases) through increased motion, prior to the onset of clinically detectable cognitive impairment.

While the primary focus of this work was to characterize cortical myelin in the context of aging and AD, analyses within each aim also examined R1 in cortical-adjacent WM to compare findings as well as sensitivity of the R1 measurement to alterations in myelin content. Throughout this dissertation, stronger effects were observed in WM as compared to the cortex, with strong global decreases in R1 with age, sex differences in a majority of WM, and more pronounced associations with AD pathology and cognition. Although these findings are not

necessarily surprising, this was the first time these assessments had been made through *in vivo* R1 mapping. Although it was important to investigate R1 in the cortex due to the strong post-mortem observations myelin and AD pathology, it is likely that R1 will have stronger utility in studies of WM solely due to the relative abundance of myelin as compared to the cortex. Future work utilizing the MPnRAGE R1 maps should focus more on WM, including assessing integrity of known tracts through atlas-based ROI analyses (JHU[165] or IIT[33]), or by combining DTI-based tractography with R1 to more precisely measure myelin in specific tracts.

Prior studies have utilized R1 mapping in tandem with other diffusion-based metrics to examine different aspects of tissue integrity[35,67]. Such metrics as fractional anisotropy, mean diffusivity, myelin water fraction, among others, can help elucidate how brain tissue is changing at various stages of the disease, while also helping to validate what components of tissue R1 is reflecting. Given the wide use of DWI and DTI in Alzheimer's disease, future studies may benefit from combining such methodology with tissue relaxometry, and as relaxometry tends to be less sensitive to variations in MRI scanners and acquisition protocols, it could help in the development of clinically applicable cutoffs and thresholds to aid in diagnosis.

Another possible future study could involve either taking the ratio of the R1 in the cortical GM and adjacent WM, or directly indexing R1 at the GM/WM boundary. Prior work has leveraged standard T1-weighted imaging techniques to measure GM/WM contrast, with a reduced GM/WM contrast suggests possible neurodegeneration, and may serve as an early marker of disease. One study has utilized this method as a way of differentiating individuals aging normally from those who may be undergoing accelerated or diseased aging, while another used the GM/WM contrast to study developmental alterations in microstructure in toddlers with autism spectrum disorder[166]. By expanding upon this methodology through R1 mapping, it's possible that researchers may identify myelin-specific alterations occurring at the GM/WM tissue boundary. When applied to studies of AD pathogenesis and progression, this

metric could provide useful insight to the breakdown of myelinated axons traversing between the cortex and WM.

As previously mentioned, while R1 is highly sensitive to brain myelin, other tissue components and macromolecules can impact the longitudinal relaxation rate. In the context of aging, the accumulation of iron in cortical and subcortical tissue is commonly observed, and this occurrence is even more pronounced in individuals with AD. Iron is known to be highly colocalized with myelin in brain tissue [58,121], and as such, it is likely that some alterations in R1 that were identified in these analyses could also be driven by iron. That being said, future work should utilize quantitative imaging metrics such as T2*[167], which has greater sensitive to iron than T1, to either control for the effects of iron, or examine iron and myelin simultaneously. Elucidating the complex relationships between iron and myelin *in* vivo could prove valuable in identifying microstructural change earlier in the disease, and may also aid in identifying potential targets for treatment intervention.

In addition to iron, neuroinflammation is another phenomenon exhibited in aging and AD that may play an influential role in R1. In chapter 5, the relationships between R1 and biomarkers of AD-specific pathology and neurodegeneration assayed via the Roche NeuroToolKit were explored, in which increased R1 in both the cortex and WM were associated with reduced CSF levels of pathology. The Roche NeuroToolKit also provides measures of biomarkers of glial activity, including interleukin-6 (IL-6), chitinase-3-like protein 1 (YKL-40), glial fibrillary acidic protein (GFAP), and soluble triggering receptor expressed on myeloid cells 2 (sTREM2). Each of these biomarkers have shown associations with markers of AD pathology[144], as well as are linked with alterations in WM microstructure (as assessed through DWI)[88]. Currently, CSF measures of these biomarkers are highly sensitive to the presence of these phenomena, but do not provide any regional specificity as to which regions are undergoing the greatest inflammation. Determining associations between R1 and these inflammatory markers

would greatly increase our understanding of which brain regions are most impacted by inflammation in aging and AD.

The second aim of this dissertation examined the role of sex and APOE genotype on cortical myelin content. Major sex differences were identified in brain white matter, and prior studies have suggested the role that menopause may play in altering metabolism of lipids in the brain. As such, a future study could utilize quantitative relaxometry to determine the direct role that hormonal fluctuations exhibited in menopause may play in altering brain white matter microstructure and myelin content. Additionally, while APOE was included as a binary variable in regression models to assess the effect of the E4 genotype on cortical myelin content, recent work has developed risk scores that may be more sensitive to the variable risk that APOE and other genes may have on developing AD[168]. Future studies should examine the relationship between these risk scores and brain myelin.

The overwhelming majority (~90%) of participants included in analyses within this dissertation were Caucasian, highly educated, and of high socioeconomic backgrounds. As AD is known to disproportionately affect individuals from minority backgrounds, it is imperative that future studies increase recruitment efforts from these populations. In addition, covariates included in models within this dissertation such as years of education, could be further expanded up on such as quality and access to educational resources. Along this line, recent work in the field has developed indices, including the area deprivation index[169,170], that can be used as composite metric of the relative disadvantage based on a variety of socioeconomic, health, environmental, and other factors that could contribute to an individual's increased risk of developing AD-related pathology. Studies should examine this index in relation to brain myelination to understand how persons from disadvantaged backgrounds may be susceptible to brain health issues.

Finally, longitudinal analyses are critical to determine the temporal relationships between brain demyelination (or remyelination) and AD pathology buildup in the brain. Studies presented

in throughout the three aims were solely cross-sectional, and while the large sample sizes and robust statistical methods revealed strong associations with age, cognition, and pathology, it is unclear whether alterations in myelin precede the changes seen in the other biomarkers tested and the decline in cognition typically found with age. As more scans are collected within the ADRC and WRAP cohorts, determining changes in relaxometry over time will help elucidate the timeline of myelin change, and could prove valuable in understanding disease trajectories, as well as evaluating the therapeutic impact of pharmaceutical interventions. In addition, validating these findings by staining myelin in cortical tissue post-mortem would both provide verification that R1 is sensitive to the subtle changes in myelin content even in non-WM tissue.

In sum, this research contributes to the scholarship suggesting brain myelin content contributes age-related changes in myelin, genetic influences on brain myelin, and its close relationships with AD pathology. These studies provide an initial examination of cortical myelin in individuals with and without AD that may lend insight into what may lead to the selective vulnerability of certain brain regions to develop AD pathology, neurodegeneration, and subsequent cognitive decline.

References

1. Tomasi, D. & Volkow, N. D. Aging and functional brain networks. *Molecular Psychiatry* **17**, 549–558 (2012).
2. Raz, N. *et al.* Regional Brain Changes in Aging Healthy Adults: General Trends, Individual Differences and Modifiers. *Cerebral Cortex* **15**, 1676–1689 (2005).
3. Aboud, K. S. *et al.* Structural covariance across the lifespan: Brain development and aging through the lens of inter-network relationships. *Human Brain Mapping* **40**, 125–136 (2019).
4. Fletcher, E. *et al.* β-amyloid, hippocampal atrophy and their relation to longitudinal brain change in cognitively normal individuals. *Neurobiol Aging* **40**, 173–180 (2016).
5. Horn, J. L. & Cattell, R. B. Age differences in fluid and crystallized intelligence. *Acta Psychologica* **26**, 107–129 (1967).
6. Tadayon, E., Pascual-Leone, A. & Santarnecchi, E. Differential Contribution of Cortical Thickness, Surface Area, and Gyrification to Fluid and Crystallized Intelligence. *Cerebral Cortex* **30**, 215–225 (2020).
7. Harrington, K. D. *et al.* The effect of preclinical Alzheimer's disease on age-related changes in intelligence in cognitively normal older adults. *Intelligence* **70**, 22–29 (2018).
8. Yuan, P., Voelkle, M. C. & Raz, N. Fluid intelligence and gross structural properties of the cerebral cortex in middle-aged and older adults: A multi-occasion longitudinal study. *Neuroimage* **172**, 21–30 (2018).
9. Gazes, Y. *et al.* fMRI-guided white matter connectivity in fluid and crystallized cognitive abilities in healthy adults. *Neuroimage* **215**, 116809 (2020).
10. Brenowitz, W. D. *et al.* Mixed neuropathologies and estimated rates of clinical progression in a large autopsy sample. *Alzheimer's & Dementia* **13**, 654–662 (2017).
11. Baum, L. W. Sex, hormones, and Alzheimer's disease. *J Gerontol A Biol Sci Med Sci* **60**, 736–43 (2005).
12. Bendlin, B. B. *et al.* Midlife predictors of Alzheimer's disease. *Maturitas* **65**, 131–137 (2010).
13. Hebert, L. E., Scherr, P. A., McCann, J. J., Beckett, L. A. & Evans, D. A. Is the risk of developing Alzheimer's disease greater for women than for men? *Am J Epidemiol* **153**, 132–136 (2001).
14. Manly, J. J. *et al.* Endogenous estrogen levels and Alzheimer's disease among postmenopausal women. *Neurology* **54**, 833–7 (2000).
15. McKhann, G. M. *et al.* The diagnosis of dementia due to Alzheimer's disease: recommendations from the National Institute on Aging-Alzheimer's Association workgroups on diagnostic guidelines for Alzheimer's disease. *Alzheimer's & dementia* **7**, 263–269 (2011).
16. Nasreddine, Z. S. *et al.* The Montreal Cognitive Assessment, MoCA: a brief screening tool for mild cognitive impairment. *J Am Geriatr Soc* **53**, 695–699 (2005).
17. Ciesielska, N. *et al.* Is the Montreal Cognitive Assessment (MoCA) test better suited than the Mini-Mental State Examination (MMSE) in mild cognitive impairment (MCI)

detection among people aged over 60? Meta-analysis. *Psychiatr Pol* **50**, 1039–1052 (2016).
18. Buckley, R. F. *et al.* Computerized cognitive testing for use in clinical trials: a comparison of the NIH Toolbox and Cogstate C3 batteries. *J Prev Alzheimers Dis* **4**, 3 (2017).
19. Heaton, R. K. *et al.* Reliability and validity of composite scores from the NIH Toolbox Cognition Battery in adults. *Journal of the International Neuropsychological Society* **20**, 588–598 (2014).
20. Weintraub, S. *et al.* The cognition battery of the NIH toolbox for assessment of neurological and behavioral function: validation in an adult sample. *Journal of the International Neuropsychological Society* **20**, 567–578 (2014).
21. Hackett, K. *et al.* Utility of the NIH Toolbox for assessment of prodromal Alzheimer's disease and dementia. *Alzheimer's & Dementia: Diagnosis, Assessment & Disease Monitoring* **10**, 764–772 (2018).
22. Snitz, B. E. *et al.* Associations between NIH Toolbox Cognition Battery and in vivo brain amyloid and tau pathology in non-demented older adults. *Alzheimer's & Dementia: Diagnosis, Assessment & Disease Monitoring* **12**, e12018 (2020).
23. Parsey, C. M., Bagger, J. E., Trittschuh, E. H. & Hanson, A. J. Utility of the iPad NIH Toolbox Cognition Battery in a clinical trial of older adults. *J Am Geriatr Soc* **69**, 3519–3528 (2021).
24. Cunningham, A. B. Montreal Cognitive Assessment (MoCA) and National Institutes of Health Toolbox (NIH-TB) Cognition Battery Among Healthy Older Adults. (2019).
25. Carlozzi, N. E. *et al.* NIH toolbox cognitive battery (NIHTB-CB): the NIHTB pattern comparison processing speed test. *Journal of the International Neuropsychological Society* **20**, 630–641 (2014).
26. Carlozzi, N. E., Beaumont, J. L., Tulsky, D. S. & Gershon, R. C. The NIH toolbox pattern comparison processing speed test: normative data. *Archives of Clinical Neuropsychology* **30**, 359–368 (2015).
27. Saher, G. *et al.* High cholesterol level is essential for myelin membrane growth. *Nat Neurosci* **8**, 468–475 (2005).
28. Boggs, J. M. Myelin basic protein: a multifunctional protein. *Cellular and Molecular Life Sciences CMLS* **63**, 1945–1961 (2006).
29. Traka, M. *et al.* A genetic mouse model of adult-onset, pervasive central nervous system demyelination with robust remyelination. *Brain* **133**, 3017–3029 (2010).
30. Kuhn, S., Gritti, L., Crooks, D. & Dombrowski, Y. Oligodendrocytes in Development, Myelin Generation and Beyond. *Cells* doi:10.3390/cells8111424.
31. Bendlin, B. B. *et al.* White matter in aging and cognition: a cross-sectional study of microstructure in adults aged eighteen to eighty-three. *Dev Neuropsychol* **35**, 257–277 (2010).
32. Bartzokis, G. Age-related myelin breakdown: a developmental model of cognitive decline and Alzheimer's disease. *Neurobiology of Aging* **25**, 5–18 (2004).
33. Varentsova, A., Zhang, S. & Arfanakis, K. Development of a high angular resolution diffusion imaging human brain template. *Neuroimage* **91**, 177–186 (2014).
34. Heath, F., Hurley, S. A., Johansen-Berg, H. & Sampaio-Baptista, C. Advances in noninvasive myelin imaging. *Developmental Neurobiology* **78**, 136–151 (2018).

35. Aggarwal, N. *et al.* Spatiotemporal dynamics of nonhuman primate white matter development during the first year of life. *Neuroimage* **231**, 117825 (2021).
36. Moody, J. F. *et al.* Longitudinal assessment of early-life white matter development with quantitative relaxometry in nonhuman primates. *Neuroimage* **251**, 118989 (2022).
37. Tomassy, G. S. *et al.* Distinct profiles of myelin distribution along single axons of pyramidal neurons in the neocortex. *Science* **344**, 319–324 (2014).
38. Hughes, E. G., Orthmann-Murphy, J. L., Langseth, A. J. & Bergles, D. E. Myelin remodeling through experience-dependent oligodendrogenesis in the adult somatosensory cortex. *Nat Neurosci* **21**, 696–706 (2018).
39. Orthmann-Murphy, J. *et al.* Remyelination alters the pattern of myelin in the cerebral cortex. *Elife* **9**, e56621 (2020).
40. Lowe, V. J. *et al.* Widespread brain tau and its association with ageing, Braak stage and Alzheimer's dementia. *Brain* **141**, 271–287 (2018).
41. Braak, H. & Braak, E. Frequency of stages of Alzheimer-related lesions in different age categories. *Neurobiol Aging* **18**, 351–357 (1997).
42. Braak, H. *et al.* Staging of brain pathology related to sporadic Parkinson's disease. *Neurobiol Aging* **24**, 197–211 (2003).
43. Miller, D. J. *et al.* Prolonged myelination in human neocortical evolution. *Proceedings of the National Academy of Sciences* **109**, 16480–16485 (2012).
44. O'Brien, J. S. & Sampson, E. L. Lipid composition of the normal human brain: gray matter, white matter, and myelin. *J Lipid Res* **6**, 537–544 (1965).
45. Lake, E. M. R. *et al.* Altered intracortical myelin staining in the dorsolateral prefrontal cortex in severe mental illness. *Eur Arch Psychiatry Clin Neurosci* **267**, 369–376 (2017).
46. Nieuwenhuys, R. & Broere, C. A. J. A map of the human neocortex showing the estimated overall myelin content of the individual architectonic areas based on the studies of Adolf Hopf. *Brain Structure and Function* **222**, 465–480 (2017).
47. Nieuwenhuys, R. The myeloarchitectonic studies on the human cerebral cortex of the Vogt–Vogt school, and their significance for the interpretation of functional neuroimaging data. *Brain Structure and Function* **218**, 303–352 (2013).
48. Rowley, C. D. *et al.* Assessing intracortical myelin in the living human brain using myelinated cortical thickness. *Front Neurosci* **9**, 396 (2015).
49. Uddin, M. N., Figley, T. D., Marrie, R. A., Figley, C. R. & Group, for the C. S. Can T1w/T2w ratio be used as a myelin-specific measure in subcortical structures? Comparisons between FSE-based T1w/T2w ratios, GRASE-based T1w/T2w ratios and multi-echo GRASE-based myelin water fractions. *NMR in Biomedicine* **31**, e3868 (2018).
50. Deoni, S. C. L., Dean 3rd, D. C., Remer, J., Dirks, H. & O'Muircheartaigh, J. Cortical maturation and myelination in healthy toddlers and young children. *Neuroimage* **115**, 147–161 (2015).
51. Bock, N. A., Kocharyan, A., Liu, J. v & Silva, A. C. Visualizing the entire cortical myelination pattern in marmosets with magnetic resonance imaging. *Journal of Neuroscience Methods* **185**, 15–22 (2009).
52. Lutti, A., Dick, F., Sereno, M. I. & Weiskopf, N. Using high-resolution quantitative mapping of R1 as an index of cortical myelination. *Neuroimage* **93**, 176–188 (2014).

53. Shafee, R., Buckner, R. L. & Fischl, B. Gray matter myelination of 1555 human brains using partial volume corrected MRI images. *Neuroimage* **105**, 473–485 (2015).
54. Arshad, M., Stanley, J. A. & Raz, N. Test–retest reliability and concurrent validity of in vivo myelin content indices: Myelin water fraction and calibrated T1w/T2w image ratio. *Hum Brain Mapp* **38**, 1780–1790 (2017).
55. Grydeland, H., Westlye, L. T., Walhovd, K. B. & Fjell, A. M. Intracortical Posterior Cingulate Myelin Content Relates to Error Processing: Results from T1- and T2-Weighted MRI Myelin Mapping and Electrophysiology in Healthy Adults. *Cerebral Cortex* **26**, 2402–2410 (2015).
56. Grydeland, H., Walhovd, K. B., Tamnes, C. K., Westlye, L. T. & Fjell, A. M. Intracortical Myelin Links with Performance Variability across the Human Lifespan: Results from T1- and T2-Weighted MRI Myelin Mapping and Diffusion Tensor Imaging. *The Journal of Neuroscience* **33**, 18618 LP – 18630 (2013).
57. Glasser, M. F., Goyal, M. S., Preuss, T. M., Raichle, M. E. & van Essen, D. C. Trends and properties of human cerebral cortex: Correlations with cortical myelin content. *Neuroimage* **93**, 165–175 (2014).
58. Stüber, C. *et al.* Myelin and iron concentration in the human brain: A quantitative study of MRI contrast. *Neuroimage* **93**, 95–106 (2014).
59. Koenig, S. H. Cholesterol of myelin is the determinant of gray-white contrast in MRI of brain. *Magnetic Resonance in Medicine* **20**, 285–291 (1991).
60. Glasser, M. F. & van Essen, D. C. 1Mapping human cortical areas in vivo based on myelin content as revealed by T1- and T2-weighted MRI. *J Neurosci* **31**, 11597–11616 (2011).
61. Bartzokis, G. Alzheimer's disease as homeostatic responses to age-related myelin breakdown. *Neurobiol Aging* **32**, 1341–1371 (2011).
62. Bartzokis, G., Lu, P. H. & Mintz, J. Human brain myelination and amyloid beta deposition in Alzheimer's disease. *Alzheimer's & Dementia* **3**, 122–125 (2007).
63. Vogt, N. M. *et al.* Cortical Microstructural Alterations in Mild Cognitive Impairment and Alzheimer's Disease Dementia. *Cerebral Cortex* (2020) doi:10.1093/cercor/bhz286.
64. Lankford, C. L. & Does, M. D. On the inherent precision of mcDESPOT. *Magn Reson Med* **69**, 127–136 (2013).
65. Bouhrara, M. *et al.* Adult brain aging investigated using BMC-mcDESPOT–based myelin water fraction imaging. *Neurobiol Aging* **85**, 131–139 (2020).
66. Kitzler, H. H. *et al.* Deficient MWF mapping in multiple sclerosis using 3D whole-brain multi-component relaxation MRI. *Neuroimage* **59**, 2670–2677 (2012).
67. Dean, D. C. *et al.* Association of amyloid pathology with myelin alteration in preclinical Alzheimer disease. *JAMA Neurology* **74**, 41–49 (2017).
68. Fischl, B. FreeSurfer. *Neuroimage* **62**, 774–781 (2012).
69. Pelkmans, W. *et al.* Gray matter T1-w/T2-w ratios are higher in Alzheimer's disease. *Human Brain Mapping* **40**, 3900–3909 (2019).
70. Luo, X. *et al. Application of T1-/T2-Weighted Ratio Mapping to Elucidate Intracortical Demyelination Process in the Alzheimer's Disease Continuum*. *Frontiers in Neuroscience* vol. 13 904 (2019).
71. Deoni, S. C. L. Quantitative relaxometry of the brain. *Top Magn Reson Imaging* **21**, 101–113 (2010).

72. Koenig, S. H., Brown III, R. D., Spiller, M. & Lundbom, N. Relaxometry of brain: Why white matter appears bright in MRI. *Magnetic Resonance in Medicine* **14**, 482–495 (1990).
73. Kecskemeti, S. *et al.* MPnRAGE: A technique to simultaneously acquire hundreds of differently contrasted MPRAGE images with applications to quantitative T1 mapping. *Magnetic Resonance in Medicine* **75**, 1040–1053 (2016).
74. Kecskemeti, S. & Alexander, A. L. Three-dimensional motion-corrected T1 relaxometry with MPnRAGE. *Magnetic Resonance in Medicine* **84**, 2400–2411 (2020).
75. Bartzokis, G. *et al.* Heterogeneous age-related breakdown of white matter structural integrity: implications for cortical "disconnection" in aging and Alzheimer's disease. *Neurobiology of Aging* **25**, 843–851 (2004).
76. Braak, H. & Braak, E. Development of Alzheimer-related neurofibrillary changes in the neocortex inversely recapitulates cortical myelogenesis. *Acta Neuropathologica* **92**, 197–201 (1996).
77. Haast, R. A. M., Ivanov, D., Formisano, E. & Uludağ, K. Reproducibility and Reliability of Quantitative and Weighted T(1) and T(2)(∗) Mapping for Myelin-Based Cortical Parcellation at 7 Tesla. *Front Neuroanat* **10**, 112 (2016).
78. Marner, L., Nyengaard, J. R., Tang, Y. & Pakkenberg, B. Marked loss of myelinated nerve fibers in the human brain with age. *Journal of Comparative Neurology* **462**, 144–152 (2003).
79. Callaghan, M. F. *et al.* Widespread age-related differences in the human brain microstructure revealed by quantitative magnetic resonance imaging. *Neurobiology of Aging* **35**, 1862–1872 (2014).
80. Bartzokis, G. *et al.* Multimodal Magnetic Resonance Imaging Assessment of White Matter Aging Trajectories Over the Lifespan of Healthy Individuals. *Biological Psychiatry* **72**, 1026–1034 (2012).
81. Poirier, J. Apolipoprotein E and cholesterol metabolism in the pathogenesis and treatment of Alzheimer's disease. *Trends Mol Med* **9**, 94–101 (2003).
82. Adluru, N. *et al.* White matter microstructure in late middle-age: Effects of apolipoprotein E4 and parental family history of Alzheimer's disease. *Neuroimage Clin* **4**, 730–742 (2014).
83. Westlye, L. T., Reinvang, I., Rootwelt, H. & Espeseth, T. Effects of APOE on brain white matter microstructure in healthy adults. *Neurology* **79**, 1961 LP – 1969 (2012).
84. Altmann, A., Tian, L., Henderson, V. W., Greicius, M. D. & Investigators, A. D. N. I. Sex modifies the APOE-related risk of developing Alzheimer disease. *Annals of Neurology* **75**, 563–573 (2014).
85. Mack, C. M., Boehm, G. W., Berrebi, A. S. & Denenberg, V. H. Sex differences in the distribution of axon types within the genu of the rat corpus callosum. *Brain Res* **697**, 152–156 (1995).
86. Liu, F., Vidarsson, L., Winter, J. D., Tran, H. & Kassner, A. Sex differences in the human corpus callosum microstructure: a combined T2 myelin-water and diffusion tensor magnetic resonance imaging study. *Brain Res* **1343**, 37–45 (2010).

87. Merluzzi, A. P. *et al.* Differential effects of neurodegeneration biomarkers on subclinical cognitive decline. *Alzheimer's & Dementia: Translational Research & Clinical Interventions* **5**, 129–138 (2019).
88. Racine, A. M. *et al.* Association of longitudinal white matter degeneration and cerebrospinal fluid biomarkers of neurodegeneration, inflammation and Alzheimer's disease in late-middle-aged adults. *Brain Imaging and Behavior* **13**, 41–52 (2019).
89. Nasrabady, S. E., Rizvi, B., Goldman, J. E. & Brickman, A. M. White matter changes in Alzheimer's disease: a focus on myelin and oligodendrocytes. *Acta Neuropathologica Communications* **6**, 22 (2018).
90. Salat, D. H. *et al.* Regional white matter volume differences in nondemented aging and Alzheimer's disease. *Neuroimage* **44**, 1247–1258 (2009).
91. de Groot, M. *et al.* Tract-specific white matter degeneration in aging: the Rotterdam Study. *Alzheimer's & Dementia* **11**, 321–330 (2015).
92. Amlien, I. K. & Fjell, A. M. Diffusion tensor imaging of white matter degeneration in Alzheimer's disease and mild cognitive impairment. *Neuroscience* **276**, 206–215 (2014).
93. Alves, G. S. *et al.* Different patterns of white matter degeneration using multiple diffusion indices and volumetric data in mild cognitive impairment and Alzheimer patients. *PLoS One* **7**, e52859 (2012).
94. Grydeland, H., Westlye, L. T., Walhovd, K. B. & Fjell, A. M. Improved prediction of Alzheimer's disease with longitudinal white matter/gray matter contrast changes. *Hum Brain Mapp* **34**, 2775–2785 (2013).
95. Nakamura, K., Chen, J. T., Ontaneda, D., Fox, R. J. & Trapp, B. D. T1-/T2-weighted ratio differs in demyelinated cortex in multiple sclerosis. *Annals of Neurology* **82**, 635–639 (2017).
96. Rowley, C. D. *et al.* Altered Intracortical T1-Weighted/T2-Weighted Ratio Signal in Huntington's Disease. *Frontiers in Neuroscience* vol. 12 805 (2018).
97. Vymazal, J. *et al.* Magnetic resonance imaging of brain iron in health and disease. *J Neurol Sci* **134**, 19–26 (1995).
98. Sereno, M. I., Lutti, A., Weiskopf, N. & Dick, F. Mapping the Human Cortical Surface by Combining Quantitative T1 with Retinotopy†. *Cerebral Cortex* **23**, 2261–2268 (2012).
99. Lambert, C. *et al.* Characterizing Aging in the Human Brainstem Using Quantitative Multimodal MRI Analysis. *Frontiers in Human Neuroscience* vol. 7 462 (2013).
100. Yeatman, J. D., Wandell, B. A. & Mezer, A. A. Lifespan maturation and degeneration of human brain white matter. *Nat Commun* **5**, 4932 (2014).
101. Deoni, S. C. L., Rutt, B. K., Arun, T., Pierpaoli, C. & Jones, D. K. Gleaning multicomponent T1 and T2 information from steady-state imaging data. *Magnetic Resonance in Medicine: An Official Journal of the International Society for Magnetic Resonance in Medicine* **60**, 1372–1387 (2008).
102. Mugler, J. P. & Brookeman, J. R. Three-dimensional magnetization-prepared rapid gradient-echo imaging (3D MP RAGE). *Magn Reson Med* **15**, 152–7 (1990).
103. Kecskemeti, S., Freeman, A., Travers, B. G. & Alexander, A. L. FreeSurfer based cortical mapping and T1-relaxometry with MPnRAGE: Test-retest reliability with and without retrospective motion correction. *Neuroimage* **242**, 118447 (2021).

104. Albert, M. S. *et al.* The diagnosis of mild cognitive impairment due to Alzheimer's disease: recommendations from the National Institute on Aging-Alzheimer's Association workgroups on diagnostic guidelines for Alzheimer's disease. *Alzheimer's & dementia* **7**, 270–279 (2011).
105. Tustison, N. J. *et al.* N4ITK: improved N3 bias correction. *IEEE Trans Med Imaging* **29**, 1310–1320 (2010).
106. Jenkinson, M., Beckmann, C. F., Behrens, T. E. J., Woolrich, M. W. & Smith, S. M. FSL. *Neuroimage* **62**, 782–790 (2012).
107. Desikan, R. S. *et al.* An automated labeling system for subdividing the human cerebral cortex on MRI scans into gyral based regions of interest. *Neuroimage* **31**, 968–980 (2006).
108. Mowinckel, A. M. & Vidal-Piñeiro, D. Visualization of Brain Statistics With R Packages ggseg and ggseg3d. *Advances in Methods and Practices in Psychological Science* **3**, 466–483 (2020).
109. Johnson, W. E., Li, C. & Rabinovic, A. Adjusting batch effects in microarray expression data using empirical Bayes methods. *Biostatistics* **8**, 118–127 (2007).
110. Fortin, J.-P. *et al.* Harmonization of cortical thickness measurements across scanners and sites. *Neuroimage* **167**, 104–120 (2018).
111. Fortin, J.-P. *et al.* Harmonization of multi-site diffusion tensor imaging data. *Neuroimage* **161**, 149–170 (2017).
112. Yu, M. *et al.* Statistical harmonization corrects site effects in functional connectivity measurements from multi-site fMRI data. *Hum Brain Mapp* **39**, 4213–4227 (2018).
113. Velázquez, J., Mateos, J., Pasaye, E. H., Barrios, F. A. & Marquez-Flores, J. A. Cortical Thickness Estimation: A Comparison of FreeSurfer and Three Voxel-Based Methods in a Test–Retest Analysis and a Clinical Application. *Brain Topography* **34**, 430–441 (2021).
114. Han, X. *et al.* Reliability of MRI-derived measurements of human cerebral cortical thickness: the effects of field strength, scanner upgrade and manufacturer. *Neuroimage* **32**, 180–194 (2006).
115. Bojorquez, J. Z. *et al.* What are normal relaxation times of tissues at 3 T? *Magnetic Resonance Imaging* **35**, 69–80 (2017).
116. Parry, A. *et al.* White matter and lesion T1 relaxation times increase in parallel and correlate with disability in multiple sclerosis. *Journal of Neurology* **249**, 1279–1286 (2002).
117. Chevalier, N. *et al.* Myelination is associated with processing speed in early childhood: preliminary insights. *PLoS One* **10**, e0139897 (2015).
118. Lu, P. H. *et al.* Age-related slowing in cognitive processing speed is associated with myelin integrity in a very healthy elderly sample. *J Clin Exp Neuropsychol* **33**, 1059–1068 (2011).
119. Lu, P. H. *et al.* Myelin breakdown mediates age-related slowing in cognitive processing speed in healthy elderly men. *Brain and Cognition* **81**, 131–138 (2013).
120. Abel, S. *et al.* Myelin damage in normal appearing white matter contributes to impaired cognitive processing speed in multiple sclerosis. *Journal of Neuroimaging* **30**, 205–211 (2020).

121. Bulk, M. *et al.* Postmortem MRI and histology demonstrate differential iron accumulation and cortical myelin organization in early- and late-onset Alzheimer's disease. *Neurobiology of Aging* **62**, 231–242 (2018).
122. Chêne, G. *et al.* Gender and incidence of dementia in the Framingham Heart Study from mid-adult life. *Alzheimer's & Dementia* **11**, 310–320 (2015).
123. Hsu, J.-L. *et al.* Gender differences and age-related white matter changes of the human brain: A diffusion tensor imaging study. *Neuroimage* **39**, 566–577 (2008).
124. Kodiweera, C., Alexander, A. L., Harezlak, J., McAllister, T. W. & Wu, Y.-C. Age effects and sex differences in human brain white matter of young to middle-aged adults: A DTI, NODDI, and q-space study. *Neuroimage* **128**, 180–192 (2016).
125. Michaelson, D. M. APOE ε4: The most prevalent yet understudied risk factor for Alzheimer's disease. *Alzheimer's & Dementia* **10**, 861–868 (2014).
126. Holtzman, D. M., Herz, J. & Bu, G. Apolipoprotein E and apolipoprotein E receptors: normal biology and roles in Alzheimer disease. *Cold Spring Harb Perspect Med* **2**, a006312 (2012).
127. Ward, A. *et al.* Prevalence of apolipoprotein E4 genotype and homozygotes (APOE e4/4) among patients diagnosed with Alzheimer's disease: a systematic review and meta-analysis. *Neuroepidemiology* **38**, 1–17 (2012).
128. Mayeux, R. *et al.* Utility of the apolipoprotein E genotype in the diagnosis of Alzheimer's disease. *New England Journal of Medicine* **338**, 506–511 (1998).
129. Leduc, V., Jasmin-Bélanger, S. & Poirier, J. APOE and cholesterol homeostasis in Alzheimer's disease. *Trends in Molecular Medicine* **16**, 469–477 (2010).
130. Dufouil, C. *et al.* APOE genotype, cholesterol level, lipid-lowering treatment, and dementia: the Three-City Study. *Neurology* **64**, 1531–1538 (2005).
131. Bartzokis, G. *et al.* Apolipoprotein E Genotype and Age-Related Myelin Breakdown in Healthy Individuals: Implications for Cognitive Decline and Dementia. *Archives of General Psychiatry* **63**, 63–72 (2006).
132. Park, M. *et al.* Brain myelin water fraction is associated with APOE4 allele status in patients with cognitive impairment. *Journal of Neuroimaging* **32**, 521–529 (2022).
133. Johnson, S. C. *et al.* The effect of TOMM40 poly-T length on gray matter volume and cognition in middle-aged persons with APOE ε3/ε3 genotype. *Alzheimer's & Dementia* **7**, 456–465 (2011).
134. Cerghet, M., Skoff, R. P., Swamydas, M. & Bessert, D. Sexual dimorphism in the white matter of rodents. *Journal of the Neurological Sciences* **286**, 76–80 (2009).
135. Ho, T. C. *et al.* Sex differences in myelin content of white matter tracts in adolescents with depression. *Neuropsychopharmacology* **46**, 2295–2303 (2021).
136. Perrin, J. S. *et al.* Sex differences in the growth of white matter during adolescence. *Neuroimage* **45**, 1055–1066 (2009).
137. Perrin, J. S. *et al.* Growth of White Matter in the Adolescent Brain: Role of Testosterone and Androgen Receptor. *The Journal of Neuroscience* **28**, 9519 LP – 9524 (2008).
138. Flynn, S. W. *et al.* Abnormalities of myelination in schizophrenia detected in vivo with MRI, and post-mortem with analysis of oligodendrocyte proteins. *Mol Psychiatry* **8**, 811–820 (2003).

139. Mahley, R. W. Central nervous system lipoproteins: ApoE and regulation of cholesterol metabolism. *Arterioscler Thromb Vasc Biol* **36**, 1305–1315 (2016).
140. Takeuchi, H. *et al.* Sex-Dependent Effects of the APOE ε4 Allele on Behavioral Traits and White Matter Structures in Young Adults. *Cerebral Cortex* **31**, 672–680 (2021).
141. Shinohara, M. *et al.* APOE2 is associated with longevity independent of Alzheimer's disease. *Elife* **9**, e62199 (2020).
142. Conejero-Goldberg, C. *et al.* APOE2 enhances neuroprotection against Alzheimer's disease through multiple molecular mechanisms. *Mol Psychiatry* **19**, 1243–1250 (2014).
143. Rubinski, A. *et al.* Higher levels of myelin are associated with higher resistance against tau pathology in Alzheimer's disease. *medRxiv* (2022).
144. Van Hulle, C. *et al.* An examination of a novel multipanel of CSF biomarkers in the Alzheimer's disease clinical and pathological continuum. *Alzheimer's & Dementia* **17**, 431–445 (2021).
145. Betthauser, T. J. *et al.* In vivo characterization and quantification of neurofibrillary tau PET radioligand 18F-MK-6240 in humans from Alzheimer disease dementia to young controls. *Journal of Nuclear Medicine* **60**, 93–99 (2019).
146. Betthauser, T. J. *et al.* Amyloid and tau imaging biomarkers explain cognitive decline from late middle-age. *Brain* **143**, 320–335 (2020).
147. Johnson, S. C. *et al.* Amyloid burden and neural function in people at risk for Alzheimer's Disease. *Neurobiol Aging* **35**, 576–584 (2014).
148. Racine, A. M. *et al.* Associations between Performance on an Abbreviated CogState Battery, Other Measures of Cognitive Function, and Biomarkers in People at Risk for Alzheimer's Disease. *J Alzheimers Dis* **54**, 1395–1408 (2016).
149. Gold, B. T. *et al.* White matter integrity is associated with cerebrospinal fluid markers of Alzheimer's disease in normal adults. *Neurobiol Aging* **35**, 2263–2271 (2014).
150. Bendlin, B. B. *et al.* CSF T-Tau/Aβ42 Predicts White Matter Microstructure in Healthy Adults at Risk for Alzheimer's Disease. *PLoS ONE* **7**, e37720 (2012).
151. Molinuevo, J. L. *et al.* White matter changes in preclinical Alzheimer's disease: a magnetic resonance imaging-diffusion tensor imaging study on cognitively normal older people with positive amyloid β protein 42 levels. *Neurobiology of Aging* **35**, 2671–2680 (2014).
152. Greicius, M. D., Srivastava, G., Reiss, A. L. & Menon, V. Default-mode network activity distinguishes Alzheimer's disease from healthy aging: evidence from functional MRI. *Proceedings of the National Academy of Sciences* **101**, 4637–4642 (2004).
153. Zhong, Y. *et al.* Altered effective connectivity patterns of the default mode network in Alzheimer's disease: An fMRI study. *Neuroscience Letters* **578**, 171–175 (2014).
154. Schultz, S. A. *et al.* Widespread distribution of tauopathy in preclinical Alzheimer's disease. *Neurobiology of Aging* **72**, 177–185 (2018).
155. Marques, J. P., Khabipova, D. & Gruetter, R. Studying cyto and myeloarchitecture of the human cortex at ultra-high field with quantitative imaging: R1, R2* and magnetic susceptibility. *Neuroimage* **147**, 152–163 (2017).
156. Schöll, M. *et al.* PET Imaging of Tau Deposition in the Aging Human Brain. *Neuron* **89**, 971–982 (2016).

157. Arenaza-Urquijo, E. M. *et al.* Specific Anatomic Associations Between White Matter Integrity and Cognitive Reserve in Normal and Cognitively Impaired Elders. *The American Journal of Geriatric Psychiatry* **19**, 33–42 (2011).
158. Nürnberger, L. *et al.* Longitudinal changes of cortical microstructure in Parkinson's disease assessed with T1 relaxometry. *NeuroImage: Clinical* **13**, 405–414 (2017).
159. Zonouzi, M. *et al.* Individual oligodendrocytes show bias for inhibitory axons in the neocortex. *Cell Rep* **27**, 2799–2808 (2019).
160. Benamer, N., Vidal, M., Balia, M. & Angulo, M. C. Myelination of parvalbumin interneurons shapes the function of cortical sensory inhibitory circuits. *Nat Commun* **11**, 5151 (2020).
161. Desai, M. K. *et al.* Early Oligodendrocyte/Myelin Pathology in Alzheimer's Disease Mice Constitutes a Novel Therapeutic Target. *The American Journal of Pathology* **177**, 1422–1435 (2010).
162. Chen, J.-F. *et al.* Enhancing myelin renewal reverses cognitive dysfunction in a murine model of Alzheimer's disease. *Neuron* **109**, 2292-2307.e5 (2021).
163. Reeder, S. B., Hu, H. H. & Sirlin, C. B. Proton density fat-fraction: a standardized MR-based biomarker of tissue fat concentration. *Journal of magnetic resonance imaging: JMRI* **36**, 1011 (2012).
164. Hagiwara, A. *et al.* SyMRI of the brain: rapid quantification of relaxation rates and proton density, with synthetic MRI, automatic brain segmentation, and myelin measurement. *Invest Radiol* **52**, 647 (2017).
165. Zhang, W., Olivi, A., Hertig, S. J., van Zijl, P. & Mori, S. Automated fiber tracking of human brain white matter using diffusion tensor imaging. *Neuroimage* **42**, 771–777 (2008).
166. Godel, M. *et al.* Altered Gray-White Matter Boundary Contrast in Toddlers at Risk for Autism Relates to Later Diagnosis of Autism Spectrum Disorder. *Front Neurosci* **15**, 669194 (2021).
167. Torlasco, C. *et al.* Role of T1 mapping as a complementary tool to T2* for non-invasive cardiac iron overload assessment. *PLoS One* **13**, e0192890–e0192890 (2018).
168. Cruchaga, C. *et al.* Polygenic risk score of sporadic late-onset Alzheimer's disease reveals a shared architecture with the familial and early-onset forms. *Alzheimer's & Dementia* **14**, 205–214 (2018).
169. Hu, J., Kind, A. J. H. & Nerenz, D. Area deprivation index predicts readmission risk at an urban teaching hospital. *American Journal of Medical Quality* **33**, 493–501 (2018).
170. Zuelsdorff, M. *et al.* The Area Deprivation Index: a novel tool for harmonizable risk assessment in Alzheimer's disease research. *Alzheimer's & Dementia: Translational Research & Clinical Interventions* **6**, e12039 (2020).

Appendix A

Table A1: Breakdown of ADRC/WRAP participants by MPnRAGE sequence.

	A (N=399)	B (N=97)	C (N=142)	D (N=226)	p value
Age at Baseline MRI Scan					< 0.001[1]
Mean (SD)	64.990 (9.125)	64.920 (6.775)	68.176 (6.894)	66.091 (6.980)	
Min - Max	45.710 - 90.370	50.360 - 82.080	48.570 - 85.320	46.850 - 88.060	
Sex					0.352[2]
Female	247 (61.9%)	66 (68.0%)	97 (68.3%)	152 (67.3%)	
Male	152 (38.1%)	31 (32.0%)	45 (31.7%)	74 (32.7%)	
Clinical Diagnosis					< 0.001[2]
Cognitively Unimpaired	343 (86.0%)	94 (96.9%)	140 (98.6%)	214 (94.7%)	
Mild Cognitive Impairment	32 (8.0%)	2 (2.1%)	1 (0.7%)	8 (3.5%)	
Dementia	24 (6.0%)	1 (1.0%)	1 (0.7%)	4 (1.8%)	

1. Kruskal-Wallis rank sum test
2. Pearson's Chi-squared test

Table A2: MPnRAGE acquisition parameters for each protocol used.

Protocol	N1	N2	Alpha1	Alpha2	TD
A	325/326	111/112	4	6	237/242
B	304	81/82	4	8	505
C	304	81/82	4	8	502/503
D	325	51/61	4	8	505

Table A3: Outputs of multiple regression models testing linear effect of age on regional cortical GM R1 in ADRC/WRAP

ROI	Predictor	Estimate	Std. Error	T-Statistic	pUncorrected	pFDR
bankssts	Intercept	0.712	0.006	114.058	0.000e+00	0.000e+00
	Age	-0.000	0.000	-1.006	3.148e-01	5.097e-01
	Sex	-0.000	0.002	-0.188	8.507e-01	9.163e-01
caudal anterior cingulate	Intercept	0.680	0.010	65.806	1.294e-320	1.375e-320
	Age	0.000	0.000	1.588	1.127e-01	2.936e-01
	Sex	-0.004	0.003	-1.459	1.449e-01	4.810e-01
caudal middle frontal	Intercept	0.720	0.006	114.352	0.000e+00	0.000e+00
	Age	-0.000	0.000	-1.249	2.119e-01	4.414e-01
	Sex	0.000	0.002	0.057	9.549e-01	9.817e-01
cuneus	Intercept	0.739	0.008	91.908	0.000e+00	0.000e+00
	Age	-0.000	0.000	-1.900	5.776e-02	2.020e-01
	Sex	-0.005	0.002	-2.307	2.132e-02	2.416e-01
entorhinal	Intercept	0.778	0.015	51.427	1.005e-253	1.005e-253
	Age	0.000	0.000	0.288	7.733e-01	8.764e-01
	Sex	-0.001	0.004	-0.263	7.927e-01	8.984e-01
frontal pole	Intercept	0.683	0.007	103.883	0.000e+00	0.000e+00
	Age	-0.000	0.000	-1.150	2.507e-01	4.654e-01
	Sex	-0.002	0.002	-1.134	2.571e-01	5.463e-01
fusiform	Intercept	0.684	0.005	125.072	0.000e+00	0.000e+00
	Age	0.000	0.000	0.424	6.715e-01	8.235e-01
	Sex	-0.001	0.001	-0.548	5.837e-01	8.269e-01
inferior parietal	Intercept	0.712	0.007	107.922	0.000e+00	0.000e+00
	Age	-0.000	0.000	-1.553	1.209e-01	2.936e-01
	Sex	-0.002	0.002	-1.347	1.785e-01	4.810e-01
inferior temporal	Intercept	0.669	0.005	127.780	0.000e+00	0.000e+00
	Age	0.000	0.000	1.022	3.070e-01	5.097e-01
	Sex	0.000	0.001	0.023	9.817e-01	9.817e-01
insula	Intercept	0.656	0.006	118.233	0.000e+00	0.000e+00

ROI	Predictor	Estimate	Std. Error	T-Statistic	pUncorrected	pFDR
	Age	0.000	0.000	5.685	1.847e-08	6.280e-07
	Sex	-0.001	0.001	-0.843	3.994e-01	6.466e-01
isthmus cingulate	Intercept	0.728	0.008	87.735	0.000e+00	0.000e+00
	Age	-0.000	0.000	-0.195	8.456e-01	9.070e-01
	Sex	-0.003	0.002	-1.248	2.122e-01	4.810e-01
lateral occipital	Intercept	0.713	0.007	103.380	0.000e+00	0.000e+00
	Age	-0.000	0.000	-0.151	8.803e-01	9.070e-01
	Sex	-0.002	0.002	-1.474	1.410e-01	4.810e-01
lateral orbitofrontal	Intercept	0.679	0.005	131.294	0.000e+00	0.000e+00
	Age	0.000	0.000	0.650	5.159e-01	7.545e-01
	Sex	-0.002	0.001	-1.630	1.034e-01	4.810e-01
lingual	Intercept	0.717	0.007	104.227	0.000e+00	0.000e+00
	Age	-0.000	0.000	-0.946	3.443e-01	5.321e-01
	Sex	-0.003	0.002	-1.720	8.583e-02	4.810e-01
medial orbitofrontal	Intercept	0.645	0.005	117.752	0.000e+00	0.000e+00
	Age	0.000	0.000	3.306	9.897e-04	5.608e-03
	Sex	-0.001	0.001	-1.093	2.749e-01	5.498e-01
middle temporal	Intercept	0.678	0.005	132.673	0.000e+00	0.000e+00
	Age	0.000	0.000	1.127	2.601e-01	4.654e-01
	Sex	-0.000	0.001	-0.371	7.109e-01	8.375e-01
paracentral	Intercept	0.751	0.007	106.899	0.000e+00	0.000e+00
	Age	-0.000	0.000	-0.408	6.835e-01	8.235e-01
	Sex	0.001	0.002	0.775	4.385e-01	6.720e-01
parahippocampal	Intercept	0.663	0.007	98.974	0.000e+00	0.000e+00
	Age	0.000	0.000	4.001	6.894e-05	5.860e-04
	Sex	-0.004	0.002	-2.527	1.171e-02	1.991e-01
pars opercularis	Intercept	0.701	0.006	125.477	0.000e+00	0.000e+00
	Age	0.000	0.000	1.269	2.048e-01	4.414e-01
	Sex	-0.002	0.001	-1.265	2.064e-01	4.810e-01
pars orbitalis	Intercept	0.695	0.006	118.647	0.000e+00	0.000e+00
	Age	0.000	0.000	0.042	9.667e-01	9.667e-01

ROI	Predictor	Estimate	Std. Error	T-Statistic	pUncorrected	pFDR
	Sex	-0.001	0.001	-0.748	4.546e-01	6.720e-01
pars triangularis	Intercept	0.701	0.006	121.611	0.000e+00	0.000e+00
	Age	0.000	0.000	0.543	5.871e-01	7.985e-01
	Sex	-0.001	0.001	-1.015	3.105e-01	5.865e-01
pericalcarine	Intercept	0.732	0.008	86.602	0.000e+00	0.000e+00
	Age	-0.000	0.000	-0.382	7.024e-01	8.235e-01
	Sex	-0.005	0.002	-2.557	1.075e-02	1.991e-01
postcentral	Intercept	0.735	0.007	112.235	0.000e+00	0.000e+00
	Age	0.000	0.000	0.624	5.326e-01	7.545e-01
	Sex	-0.000	0.002	-0.173	8.624e-01	9.163e-01
posterior cingulate	Intercept	0.704	0.013	56.069	1.039e-273	1.070e-273
	Age	0.000	0.000	2.398	1.670e-02	7.097e-02
	Sex	0.001	0.003	0.366	7.143e-01	8.375e-01
precentral	Intercept	0.759	0.007	108.901	0.000e+00	0.000e+00
	Age	-0.000	0.000	-0.476	6.339e-01	8.235e-01
	Sex	0.002	0.002	0.937	3.492e-01	6.249e-01
precuneus	Intercept	0.720	0.007	108.168	0.000e+00	0.000e+00
	Age	-0.000	0.000	-1.837	6.663e-02	2.020e-01
	Sex	-0.003	0.002	-1.707	8.827e-02	4.810e-01
rostral anterior cingulate	Intercept	0.640	0.007	95.836	0.000e+00	0.000e+00
	Age	0.000	0.000	4.416	1.145e-05	1.298e-04
	Sex	0.001	0.002	0.453	6.510e-01	8.375e-01
rostral middle frontal	Intercept	0.702	0.006	117.016	0.000e+00	0.000e+00
	Age	-0.000	0.000	-1.806	7.129e-02	2.020e-01
	Sex	-0.001	0.001	-0.884	3.771e-01	6.411e-01
superior frontal	Intercept	0.705	0.006	122.628	0.000e+00	0.000e+00
	Age	-0.000	0.000	-1.226	2.207e-01	4.414e-01
	Sex	0.001	0.001	0.379	7.046e-01	8.375e-01
superior parietal	Intercept	0.730	0.007	104.456	0.000e+00	0.000e+00
	Age	-0.000	0.000	-1.863	6.277e-02	2.020e-01
	Sex	-0.003	0.002	-1.631	1.032e-01	4.810e-01

ROI	Predictor	Estimate	Std. Error	T-Statistic	pUncorrected	pFDR
superior temporal	Intercept	0.697	0.006	123.326	0.000e+00	0.000e+00
	Age	0.000	0.000	2.720	6.680e-03	3.245e-02
	Sex	-0.002	0.001	-1.417	1.568e-01	4.810e-01
supramarginal	Intercept	0.706	0.006	118.047	0.000e+00	0.000e+00
	Age	-0.000	0.000	-0.166	8.684e-01	9.070e-01
	Sex	-0.002	0.001	-1.432	1.525e-01	4.810e-01
temporal pole	Intercept	0.650	0.007	99.606	0.000e+00	0.000e+00
	Age	0.000	0.000	4.763	2.267e-06	3.854e-05
	Sex	0.001	0.002	0.499	6.182e-01	8.375e-01
transverse temporal	Intercept	0.760	0.008	97.902	0.000e+00	0.000e+00
	Age	0.000	0.000	3.562	3.909e-04	2.658e-03
	Sex	-0.002	0.002	-1.254	2.102e-01	4.810e-01

Table A4: Outputs of multiple regression models testing linear effect of age on regional cortical-adjacent WM R1 in ADRC/WRAP

ROI	Predictor	Estimate	Std. Error	T-Statistic	pUncorrected	pFDR
bankssts	Intercept	1.315	0.012	110.499	0.000e+00	0.000e+00
	Age	-0.002	0.000	-13.352	8.313e-37	1.346e-36
	Sex	-0.012	0.003	-4.088	4.800e-05	1.166e-04
caudal anterior cingulate	Intercept	1.368	0.013	106.960	0.000e+00	0.000e+00
	Age	-0.003	0.000	-13.366	7.122e-37	1.211e-36
	Sex	-0.016	0.003	-4.971	8.167e-07	2.777e-06
caudal middle frontal	Intercept	1.306	0.011	116.688	0.000e+00	0.000e+00
	Age	-0.003	0.000	-16.392	3.488e-52	1.977e-51
	Sex	-0.006	0.003	-2.209	2.746e-02	3.219e-02
cuneus	Intercept	1.175	0.012	98.947	0.000e+00	0.000e+00
	Age	-0.002	0.000	-8.584	4.857e-17	5.161e-17
	Sex	-0.022	0.003	-7.508	1.625e-13	5.525e-12
entorhinal	Intercept	1.170	0.013	90.877	0.000e+00	0.000e+00
	Age	-0.002	0.000	-11.428	4.282e-28	5.824e-28
	Sex	-0.008	0.003	-2.483	1.325e-02	1.733e-02
frontal pole	Intercept	1.205	0.012	96.877	0.000e+00	0.000e+00
	Age	-0.003	0.000	-14.415	5.585e-42	1.266e-41
	Sex	0.000	0.003	0.139	8.898e-01	8.898e-01
fusiform	Intercept	1.291	0.012	108.960	0.000e+00	0.000e+00
	Age	-0.003	0.000	-14.831	4.551e-44	1.289e-43
	Sex	-0.009	0.003	-3.038	2.463e-03	3.988e-03
inferior parietal	Intercept	1.288	0.012	107.877	0.000e+00	0.000e+00
	Age	-0.003	0.000	-14.216	5.363e-41	1.073e-40
	Sex	-0.018	0.003	-6.078	1.896e-09	1.289e-08
inferior temporal	Intercept	1.277	0.012	110.811	0.000e+00	0.000e+00
	Age	-0.003	0.000	-14.982	7.740e-45	2.392e-44
	Sex	-0.010	0.003	-3.552	4.052e-04	8.104e-04
insula	Intercept	1.209	0.010	115.986	0.000e+00	0.000e+00

ROI	Predictor	Estimate	Std. Error	T-Statistic	pUncorrected	pFDR
	Age	-0.002	0.000	-11.024	2.208e-26	2.780e-26
	Sex	-0.009	0.003	-3.610	3.256e-04	6.919e-04
isthmus cingulate	Intercept	1.328	0.012	109.940	0.000e+00	0.000e+00
	Age	-0.002	0.000	-10.208	4.608e-23	5.222e-23
	Sex	-0.017	0.003	-5.854	7.043e-09	3.421e-08
lateral occipital	Intercept	1.218	0.011	108.647	0.000e+00	0.000e+00
	Age	-0.002	0.000	-11.071	1.401e-26	1.832e-26
	Sex	-0.018	0.003	-6.498	1.438e-10	2.445e-09
lateral orbitofrontal	Intercept	1.307	0.012	111.424	0.000e+00	0.000e+00
	Age	-0.003	0.000	-16.949	3.568e-55	6.066e-54
	Sex	-0.005	0.003	-1.905	5.714e-02	6.267e-02
lingual	Intercept	1.200	0.011	107.214	0.000e+00	0.000e+00
	Age	-0.002	0.000	-10.582	1.465e-24	1.718e-24
	Sex	-0.017	0.003	-6.337	3.931e-10	4.455e-09
medial orbitofrontal	Intercept	1.274	0.012	107.552	0.000e+00	0.000e+00
	Age	-0.003	0.000	-16.759	3.787e-54	3.665e-53
	Sex	-0.007	0.003	-2.314	2.092e-02	2.634e-02
middle temporal	Intercept	1.294	0.011	113.947	0.000e+00	0.000e+00
	Age	-0.003	0.000	-16.022	3.208e-50	1.558e-49
	Sex	-0.012	0.003	-4.198	3.003e-05	7.854e-05
paracentral	Intercept	1.292	0.012	112.258	0.000e+00	0.000e+00
	Age	-0.002	0.000	-13.879	2.432e-39	4.594e-39
	Sex	-0.010	0.003	-3.519	4.575e-04	8.642e-04
parahippocampal	Intercept	1.248	0.013	97.450	0.000e+00	0.000e+00
	Age	-0.002	0.000	-9.763	2.482e-21	2.722e-21
	Sex	-0.016	0.003	-5.214	2.367e-07	8.942e-07
pars opercularis	Intercept	1.311	0.011	116.702	0.000e+00	0.000e+00
	Age	-0.003	0.000	-15.889	1.591e-49	6.762e-49
	Sex	-0.008	0.003	-2.897	3.871e-03	5.722e-03
pars orbitalis	Intercept	1.254	0.011	109.959	0.000e+00	0.000e+00
	Age	-0.003	0.000	-15.677	2.044e-48	7.722e-48

ROI	Predictor	Estimate	Std. Error	T-Statistic	pUncorrected	pFDR
	Sex	-0.005	0.003	-1.817	6.961e-02	7.396e-02
pars triangularis	Intercept	1.314	0.011	115.674	0.000e+00	0.000e+00
	Age	-0.003	0.000	-16.748	4.312e-54	3.665e-53
	Sex	-0.006	0.003	-2.246	2.495e-02	3.030e-02
pericalcarine	Intercept	1.150	0.013	90.744	0.000e+00	0.000e+00
	Age	-0.001	0.000	-7.735	3.153e-14	3.153e-14
	Sex	-0.019	0.003	-6.277	5.699e-10	4.844e-09
postcentral	Intercept	1.248	0.011	114.599	0.000e+00	0.000e+00
	Age	-0.002	0.000	-12.744	5.877e-34	8.688e-34
	Sex	-0.010	0.003	-3.862	1.216e-04	2.756e-04
posterior cingulate	Intercept	1.339	0.012	110.747	0.000e+00	0.000e+00
	Age	-0.002	0.000	-12.635	1.867e-33	2.645e-33
	Sex	-0.014	0.003	-4.880	1.286e-06	3.975e-06
precentral	Intercept	1.285	0.011	118.017	0.000e+00	0.000e+00
	Age	-0.002	0.000	-14.528	1.523e-42	3.983e-42
	Sex	-0.008	0.003	-2.856	4.400e-03	6.233e-03
precuneus	Intercept	1.314	0.012	107.631	0.000e+00	0.000e+00
	Age	-0.003	0.000	-15.055	3.302e-45	1.123e-44
	Sex	-0.017	0.003	-5.708	1.618e-08	6.876e-08
rostral anterior cingulate	Intercept	1.315	0.012	105.831	0.000e+00	0.000e+00
	Age	-0.002	0.000	-12.860	1.700e-34	2.627e-34
	Sex	-0.005	0.003	-1.486	1.377e-01	1.419e-01
rostral middle frontal	Intercept	1.308	0.012	111.122	0.000e+00	0.000e+00
	Age	-0.003	0.000	-16.430	2.182e-52	1.484e-51
	Sex	-0.008	0.003	-2.697	7.157e-03	9.734e-03
superior frontal	Intercept	1.301	0.011	114.202	0.000e+00	0.000e+00
	Age	-0.003	0.000	-17.748	1.530e-59	5.202e-58
	Sex	-0.008	0.003	-2.986	2.913e-03	4.502e-03
superior parietal	Intercept	1.288	0.012	108.023	0.000e+00	0.000e+00
	Age	-0.003	0.000	-14.254	3.485e-41	7.406e-41
	Sex	-0.017	0.003	-5.873	6.296e-09	3.421e-08

ROI	Predictor	Estimate	Std. Error	T-Statistic	pUncorrected	pFDR
superior temporal	Intercept	1.276	0.011	117.162	0.000e+00	0.000e+00
	Age	-0.002	0.000	-13.857	3.085e-39	5.521e-39
	Sex	-0.009	0.003	-3.322	9.353e-04	1.674e-03
supramarginal	Intercept	1.303	0.012	110.007	0.000e+00	0.000e+00
	Age	-0.003	0.000	-14.473	2.846e-42	6.912e-42
	Sex	-0.013	0.003	-4.652	3.863e-06	1.095e-05
temporal pole	Intercept	1.148	0.012	94.292	0.000e+00	0.000e+00
	Age	-0.002	0.000	-10.671	6.336e-25	7.694e-25
	Sex	-0.006	0.003	-2.067	3.907e-02	4.428e-02
transverse temporal	Intercept	1.252	0.011	112.721	0.000e+00	0.000e+00
	Age	-0.001	0.000	-8.208	9.188e-16	9.466e-16
	Sex	-0.009	0.003	-3.237	1.257e-03	2.137e-03

Table A5: Outputs of multiple regression models testing quadratic effects of age on regional cortical GM R1 in ADRC/WRAP

ROI	Predictor	Estimate	Std. Error	T-Statistic	pUncorrected	pFDR
bankssts	Intercept	0.729	0.039	18.901	5.751e-66	1.304e-65
	Age	-0.001	0.001	-0.524	6.003e-01	8.432e-01
	Age^2	0.000	0.000	0.446	6.558e-01	8.325e-01
	Sex	-0.000	0.002	-0.155	8.765e-01	9.210e-01
caudal anterior cingulate	Intercept	0.750	0.064	11.783	1.315e-29	1.397e-29
	Age	-0.002	0.002	-0.998	3.186e-01	8.432e-01
	Age^2	0.000	0.000	1.127	2.599e-01	8.325e-01
	Sex	-0.003	0.003	-1.374	1.699e-01	5.227e-01
caudal middle frontal	Intercept	0.742	0.039	19.094	4.632e-67	1.211e-66
	Age	-0.001	0.001	-0.688	4.914e-01	8.432e-01
	Age^2	0.000	0.000	0.591	5.545e-01	8.325e-01
	Sex	0.000	0.002	0.099	9.210e-01	9.210e-01
cuneus	Intercept	0.811	0.050	16.345	6.496e-52	7.888e-52
	Age	-0.002	0.002	-1.616	1.065e-01	7.956e-01
	Age^2	0.000	0.000	1.470	1.419e-01	8.234e-01
	Sex	-0.004	0.002	-2.196	2.837e-02	3.215e-01
entorhinal	Intercept	0.644	0.093	6.903	1.050e-11	1.050e-11
	Age	0.004	0.003	1.476	1.404e-01	7.956e-01
	Age^2	-0.000	0.000	-1.458	1.453e-01	8.234e-01
	Sex	-0.001	0.004	-0.368	7.128e-01	8.357e-01
frontal pole	Intercept	0.697	0.041	17.145	3.212e-56	4.550e-56
	Age	-0.001	0.001	-0.427	6.696e-01	8.432e-01
	Age^2	0.000	0.000	0.337	7.362e-01	8.325e-01
	Sex	-0.002	0.002	-1.106	2.690e-01	5.380e-01
fusiform	Intercept	0.722	0.034	21.374	2.903e-80	3.290e-79
	Age	-0.001	0.001	-1.095	2.738e-01	8.432e-01
	Age^2	0.000	0.000	1.132	2.579e-01	8.325e-01
	Sex	-0.001	0.001	-0.465	6.421e-01	8.227e-01

ROI	Predictor	Estimate	Std. Error	T-Statistic	pUncorrected	pFDR
inferior parietal	Intercept	0.748	0.041	18.348	7.427e-63	1.403e-62
	Age	-0.001	0.001	-1.006	3.149e-01	8.432e-01
	Age^2	0.000	0.000	0.886	3.761e-01	8.325e-01
	Sex	-0.002	0.002	-1.279	2.013e-01	5.227e-01
inferior temporal	Intercept	0.721	0.032	22.328	6.655e-86	1.131e-84
	Age	-0.002	0.001	-1.549	1.218e-01	7.956e-01
	Age^2	0.000	0.000	1.635	1.024e-01	8.234e-01
	Sex	0.000	0.001	0.141	8.877e-01	9.210e-01
insula	Intercept	0.683	0.034	19.916	9.092e-72	3.864e-71
	Age	-0.000	0.001	-0.332	7.396e-01	8.671e-01
	Age^2	0.000	0.000	0.785	4.326e-01	8.325e-01
	Sex	-0.001	0.001	-0.784	4.333e-01	6.696e-01
isthmus cingulate	Intercept	0.760	0.051	14.826	5.139e-44	5.636e-44
	Age	-0.001	0.002	-0.652	5.143e-01	8.432e-01
	Age^2	0.000	0.000	0.639	5.230e-01	8.325e-01
	Sex	-0.002	0.002	-1.200	2.306e-01	5.227e-01
lateral occipital	Intercept	0.807	0.042	19.003	1.517e-66	3.684e-66
	Age	-0.003	0.001	-2.253	2.451e-02	7.183e-01
	Age^2	0.000	0.000	2.248	2.482e-02	7.604e-01
	Sex	-0.002	0.002	-1.311	1.903e-01	5.227e-01
lateral orbitofrontal	Intercept	0.659	0.032	20.639	6.108e-76	5.192e-75
	Age	0.001	0.001	0.678	4.983e-01	8.432e-01
	Age^2	-0.000	0.000	-0.628	5.302e-01	8.325e-01
	Sex	-0.002	0.001	-1.671	9.514e-02	5.227e-01
lingual	Intercept	0.758	0.042	17.857	3.988e-60	6.457e-60
	Age	-0.001	0.001	-1.064	2.875e-01	8.432e-01
	Age^2	0.000	0.000	0.992	3.213e-01	8.325e-01
	Sex	-0.003	0.002	-1.644	1.006e-01	5.227e-01
medial orbitofrontal	Intercept	0.628	0.034	18.575	4.069e-64	8.138e-64
	Age	0.001	0.001	0.756	4.497e-01	8.432e-01
	Age^2	-0.000	0.000	-0.496	6.200e-01	8.325e-01

ROI	Predictor	Estimate	Std. Error	T-Statistic	pUncorrected	pFDR
	Sex	-0.002	0.001	-1.125	2.608e-01	5.380e-01
middle temporal	Intercept	0.727	0.032	23.069	2.515e-90	8.551e-89
	Age	-0.001	0.001	-1.491	1.365e-01	7.956e-01
	Age^2	0.000	0.000	1.585	1.134e-01	8.234e-01
	Sex	-0.000	0.001	-0.255	7.984e-01	9.049e-01
paracentral	Intercept	0.770	0.043	17.765	1.332e-59	2.059e-59
	Age	-0.001	0.001	-0.494	6.211e-01	8.432e-01
	Age^2	0.000	0.000	0.464	6.430e-01	8.325e-01
	Sex	0.001	0.002	0.806	4.204e-01	6.696e-01
parahippocampal	Intercept	0.707	0.041	17.104	5.405e-56	7.351e-56
	Age	-0.001	0.001	-0.768	4.424e-01	8.432e-01
	Age^2	0.000	0.000	1.089	2.766e-01	8.325e-01
	Sex	-0.004	0.002	-2.441	1.485e-02	2.754e-01
pars opercularis	Intercept	0.711	0.035	20.615	8.103e-76	5.510e-75
	Age	-0.000	0.001	-0.210	8.336e-01	9.042e-01
	Age^2	0.000	0.000	0.312	7.554e-01	8.325e-01
	Sex	-0.002	0.001	-1.238	2.161e-01	5.227e-01
pars orbitalis	Intercept	0.702	0.036	19.392	9.288e-69	3.158e-68
	Age	-0.000	0.001	-0.189	8.503e-01	9.042e-01
	Age^2	0.000	0.000	0.193	8.472e-01	9.002e-01
	Sex	-0.001	0.001	-0.732	4.646e-01	6.868e-01
pars triangularis	Intercept	0.690	0.036	19.369	1.258e-68	3.888e-68
	Age	0.000	0.001	0.359	7.193e-01	8.671e-01
	Age^2	-0.000	0.000	-0.317	7.510e-01	8.325e-01
	Sex	-0.001	0.001	-1.035	3.012e-01	5.689e-01
pericalcarine	Intercept	0.835	0.052	16.035	2.838e-50	3.327e-50
	Age	-0.003	0.002	-2.034	4.225e-02	7.183e-01
	Age^2	0.000	0.000	2.010	4.473e-02	7.604e-01
	Sex	-0.005	0.002	-2.410	1.620e-02	2.754e-01
postcentral	Intercept	0.762	0.040	18.834	1.373e-65	2.918e-65
	Age	-0.001	0.001	-0.623	5.337e-01	8.432e-01

ROI	Predictor	Estimate	Std. Error	T-Statistic	pUncorrected	pFDR
	Age^2	0.000	0.000	0.674	5.004e-01	8.325e-01
	Sex	-0.000	0.002	-0.124	9.012e-01	9.210e-01
posterior cingulate	Intercept	0.763	0.078	9.826	1.529e-21	1.575e-21
	Age	-0.001	0.002	-0.568	5.702e-01	8.432e-01
	Age^2	0.000	0.000	0.761	4.471e-01	8.325e-01
	Sex	0.001	0.003	0.420	6.742e-01	8.227e-01
precentral	Intercept	0.757	0.043	17.567	1.596e-58	2.359e-58
	Age	0.000	0.001	0.020	9.841e-01	9.841e-01
	Age^2	-0.000	0.000	-0.058	9.539e-01	9.617e-01
	Sex	0.002	0.002	0.929	3.529e-01	6.315e-01
precuneus	Intercept	0.744	0.041	18.086	2.140e-61	3.829e-61
	Age	-0.001	0.001	-0.729	4.665e-01	8.432e-01
	Age^2	0.000	0.000	0.585	5.588e-01	8.325e-01
	Sex	-0.003	0.002	-1.659	9.747e-02	5.227e-01
rostral anterior cingulate	Intercept	0.696	0.041	16.878	9.238e-55	1.208e-54
	Age	-0.001	0.001	-1.009	3.132e-01	8.432e-01
	Age^2	0.000	0.000	1.364	1.730e-01	8.325e-01
	Sex	0.001	0.002	0.550	5.823e-01	8.057e-01
rostral middle frontal	Intercept	0.717	0.037	19.331	2.050e-68	5.808e-68
	Age	-0.001	0.001	-0.539	5.897e-01	8.432e-01
	Age^2	0.000	0.000	0.398	6.909e-01	8.325e-01
	Sex	-0.001	0.001	-0.852	3.944e-01	6.696e-01
superior frontal	Intercept	0.724	0.036	20.371	2.209e-74	1.252e-73
	Age	-0.001	0.001	-0.619	5.359e-01	8.432e-01
	Age^2	0.000	0.000	0.524	6.005e-01	8.325e-01
	Sex	0.001	0.001	0.416	6.775e-01	8.227e-01
superior parietal	Intercept	0.775	0.043	17.956	1.130e-60	1.921e-60
	Age	-0.002	0.001	-1.198	2.313e-01	8.432e-01
	Age^2	0.000	0.000	1.054	2.924e-01	8.325e-01
	Sex	-0.003	0.002	-1.551	1.213e-01	5.227e-01
superior temporal	Intercept	0.699	0.035	20.006	2.769e-72	1.345e-71

ROI	Predictor	Estimate	Std. Error	T-Statistic	pUncorrected	pFDR
	Age	0.000	0.001	0.167	8.671e-01	9.042e-01
	Age^2	0.000	0.000	0.048	9.617e-01	9.617e-01
	Sex	-0.002	0.001	-1.409	1.592e-01	5.227e-01
supramarginal	Intercept	0.722	0.037	19.534	1.423e-69	5.376e-69
	Age	-0.001	0.001	-0.446	6.561e-01	8.432e-01
	Age^2	0.000	0.000	0.434	6.646e-01	8.325e-01
	Sex	-0.002	0.001	-1.396	1.631e-01	5.227e-01
temporal pole	Intercept	0.671	0.040	16.648	1.554e-53	1.957e-53
	Age	-0.000	0.001	-0.154	8.776e-01	9.042e-01
	Age^2	0.000	0.000	0.533	5.942e-01	8.325e-01
	Sex	0.001	0.002	0.536	5.924e-01	8.057e-01
transverse temporal	Intercept	0.745	0.048	15.542	1.071e-47	1.214e-47
	Age	0.001	0.001	0.588	5.568e-01	8.432e-01
	Age^2	-0.000	0.000	-0.307	7.590e-01	8.325e-01
	Sex	-0.002	0.002	-1.272	2.037e-01	5.227e-01

Table A6: Outputs of multiple regression models testing quadratic effects of age on regional cortical-adjacent WM R1 in ADRC/WRAP

ROI	Predictor	Estimate	Std. Error	T-Statistic	pUncorrected	pFDR
bankssts	Intercept	1.098	0.073	15.009	5.774e-45	1.155e-44
	Age	0.004	0.002	1.930	5.401e-02	1.054e-01
	Age^2	-0.000	0.000	-3.001	2.775e-03	4.946e-03
	Sex	-0.013	0.003	-4.315	1.802e-05	4.376e-05
caudal anterior cingulate	Intercept	1.072	0.078	13.672	2.471e-38	3.000e-38
	Age	0.007	0.002	2.757	5.973e-03	3.385e-02
	Age^2	-0.000	0.000	-3.836	1.352e-04	6.742e-04
	Sex	-0.016	0.003	-5.278	1.688e-07	5.739e-07
caudal middle frontal	Intercept	1.107	0.069	16.075	1.721e-50	1.170e-49
	Age	0.003	0.002	1.624	1.048e-01	1.423e-01
	Age^2	-0.000	0.000	-2.937	3.416e-03	5.138e-03
	Sex	-0.007	0.003	-2.426	1.549e-02	1.816e-02
cuneus	Intercept	1.104	0.073	15.036	4.176e-45	8.874e-45
	Age	0.001	0.002	0.304	7.609e-01	8.085e-01
	Age^2	-0.000	0.000	-0.987	3.240e-01	3.338e-01
	Sex	-0.022	0.003	-7.560	1.125e-13	3.825e-12
entorhinal	Intercept	0.743	0.078	9.507	2.315e-20	2.315e-20
	Age	0.011	0.002	4.607	4.759e-06	1.618e-04
	Age^2	-0.000	0.000	-5.546	3.992e-08	1.357e-06
	Sex	-0.009	0.003	-2.923	3.565e-03	4.662e-03
frontal pole	Intercept	0.951	0.076	12.447	1.355e-32	1.486e-32
	Age	0.005	0.002	2.217	2.691e-02	7.290e-02
	Age^2	-0.000	0.000	-3.376	7.719e-04	2.242e-03
	Sex	-0.000	0.003	-0.105	9.166e-01	9.166e-01
fusiform	Intercept	1.077	0.073	14.783	8.051e-44	1.244e-43
	Age	0.004	0.002	1.786	7.455e-02	1.207e-01
	Age^2	-0.000	0.000	-2.975	3.024e-03	4.946e-03
	Sex	-0.009	0.003	-3.260	1.164e-03	1.885e-03

ROI	Predictor	Estimate	Std. Error	T-Statistic	pUncorrected	pFDR
inferior parietal	Intercept	1.089	0.073	14.820	5.226e-44	8.461e-44
	Age	0.004	0.002	1.605	1.088e-01	1.423e-01
	Age^2	-0.000	0.000	-2.744	6.213e-03	8.450e-03
	Sex	-0.018	0.003	-6.285	5.417e-10	3.684e-09
inferior temporal	Intercept	1.073	0.071	15.143	1.191e-45	2.892e-45
	Age	0.004	0.002	1.710	8.773e-02	1.297e-01
	Age^2	-0.000	0.000	-2.910	3.714e-03	5.261e-03
	Sex	-0.011	0.003	-3.770	1.757e-04	3.514e-04
insula	Intercept	0.995	0.064	15.546	9.966e-48	4.061e-47
	Age	0.005	0.002	2.502	1.257e-02	5.040e-02
	Age^2	-0.000	0.000	-3.390	7.325e-04	2.242e-03
	Sex	-0.010	0.003	-3.869	1.181e-04	2.510e-04
isthmus cingulate	Intercept	1.110	0.074	14.945	1.215e-44	2.174e-44
	Age	0.005	0.002	2.150	3.185e-02	7.290e-02
	Age^2	-0.000	0.000	-2.971	3.055e-03	4.946e-03
	Sex	-0.018	0.003	-6.082	1.848e-09	1.047e-08
lateral occipital	Intercept	1.141	0.069	16.463	1.485e-52	1.683e-51
	Age	0.001	0.002	0.255	7.990e-01	8.232e-01
	Age^2	-0.000	0.000	-1.135	2.568e-01	2.728e-01
	Sex	-0.018	0.003	-6.565	9.465e-11	1.609e-09
lateral orbitofrontal	Intercept	0.961	0.071	13.451	2.843e-37	3.333e-37
	Age	0.008	0.002	3.529	4.413e-04	7.502e-03
	Age^2	-0.000	0.000	-4.905	1.134e-06	1.928e-05
	Sex	-0.006	0.003	-2.282	2.275e-02	2.495e-02
lingual	Intercept	1.073	0.069	15.540	1.075e-47	4.061e-47
	Age	0.002	0.002	1.015	3.104e-01	3.643e-01
	Age^2	-0.000	0.000	-1.860	6.331e-02	6.944e-02
	Sex	-0.018	0.003	-6.465	1.777e-10	2.014e-09
medial orbitofrontal	Intercept	0.954	0.072	13.199	4.454e-36	5.048e-36
	Age	0.007	0.002	3.115	1.906e-03	1.296e-02
	Age^2	-0.000	0.000	-4.471	8.914e-06	1.010e-04

ROI	Predictor	Estimate	Std. Error	T-Statistic	pUncorrected	pFDR
	Sex	-0.008	0.003	-2.659	8.003e-03	1.008e-02
middle temporal	Intercept	1.086	0.070	15.559	8.557e-48	4.061e-47
	Age	0.004	0.002	1.728	8.431e-02	1.297e-01
	Age^2	-0.000	0.000	-3.012	2.675e-03	4.946e-03
	Sex	-0.012	0.003	-4.426	1.096e-05	2.866e-05
paracentral	Intercept	1.145	0.071	16.132	8.584e-51	7.296e-50
	Age	0.002	0.002	0.992	3.214e-01	3.643e-01
	Age^2	-0.000	0.000	-2.100	3.608e-02	4.381e-02
	Sex	-0.010	0.003	-3.669	2.595e-04	4.902e-04
parahippocampal	Intercept	0.933	0.078	11.897	3.927e-30	4.172e-30
	Age	0.008	0.002	3.287	1.057e-03	8.984e-03
	Age^2	-0.000	0.000	-4.080	4.955e-05	3.369e-04
	Sex	-0.017	0.003	-5.546	3.987e-08	1.506e-07
pars opercularis	Intercept	1.083	0.069	15.693	1.723e-48	9.764e-48
	Age	0.004	0.002	2.081	3.775e-02	8.022e-02
	Age^2	-0.000	0.000	-3.357	8.248e-04	2.242e-03
	Sex	-0.009	0.003	-3.151	1.690e-03	2.498e-03
pars orbitalis	Intercept	1.014	0.070	14.487	2.469e-42	3.358e-42
	Age	0.005	0.002	2.216	2.700e-02	7.290e-02
	Age^2	-0.000	0.000	-3.476	5.367e-04	2.028e-03
	Sex	-0.006	0.003	-2.076	3.822e-02	4.061e-02
pars triangularis	Intercept	1.051	0.070	15.100	1.977e-45	4.481e-45
	Age	0.005	0.002	2.480	1.334e-02	5.040e-02
	Age^2	-0.000	0.000	-3.829	1.388e-04	6.742e-04
	Sex	-0.007	0.003	-2.537	1.139e-02	1.383e-02
pericalcarine	Intercept	1.105	0.078	14.101	2.007e-40	2.527e-40
	Age	-0.000	0.002	-0.030	9.760e-01	9.760e-01
	Age^2	-0.000	0.000	-0.584	5.596e-01	5.596e-01
	Sex	-0.020	0.003	-6.300	4.948e-10	3.684e-09
postcentral	Intercept	1.114	0.067	16.583	3.405e-53	5.789e-52
	Age	0.002	0.002	1.006	3.147e-01	3.643e-01

ROI	Predictor	Estimate	Std. Error	T-Statistic	pUncorrected	pFDR
	Age^2	-0.000	0.000	-2.023	4.341e-02	5.089e-02
	Sex	-0.011	0.003	-4.006	6.764e-05	1.533e-04
posterior cingulate	Intercept	1.107	0.074	14.902	2.017e-44	3.429e-44
	Age	0.005	0.002	2.146	3.216e-02	7.290e-02
	Age^2	-0.000	0.000	-3.162	1.628e-03	3.460e-03
	Sex	-0.015	0.003	-5.123	3.784e-07	1.170e-06
precentral	Intercept	1.154	0.067	17.178	2.088e-56	7.099e-55
	Age	0.002	0.002	0.822	4.115e-01	4.513e-01
	Age^2	-0.000	0.000	-1.980	4.808e-02	5.449e-02
	Sex	-0.008	0.003	-2.997	2.811e-03	3.982e-03
precuneus	Intercept	1.085	0.075	14.452	3.678e-42	4.810e-42
	Age	0.004	0.002	1.892	5.892e-02	1.054e-01
	Age^2	-0.000	0.000	-3.099	2.009e-03	4.018e-03
	Sex	-0.018	0.003	-5.948	4.079e-09	1.734e-08
rostral anterior cingulate	Intercept	1.110	0.076	14.515	1.781e-42	2.523e-42
	Age	0.004	0.002	1.684	9.267e-02	1.313e-01
	Age^2	-0.000	0.000	-2.714	6.794e-03	8.884e-03
	Sex	-0.005	0.003	-1.684	9.255e-02	9.535e-02
rostral middle frontal	Intercept	1.082	0.072	14.953	1.113e-44	2.102e-44
	Age	0.004	0.002	1.855	6.397e-02	1.087e-01
	Age^2	-0.000	0.000	-3.173	1.568e-03	3.460e-03
	Sex	-0.008	0.003	-2.934	3.442e-03	4.662e-03
superior frontal	Intercept	1.072	0.070	15.315	1.569e-46	4.342e-46
	Age	0.004	0.002	1.902	5.759e-02	1.054e-01
	Age^2	-0.000	0.000	-3.326	9.232e-04	2.242e-03
	Sex	-0.009	0.003	-3.238	1.256e-03	1.941e-03
superior parietal	Intercept	1.125	0.074	15.310	1.660e-46	4.342e-46
	Age	0.002	0.002	1.105	2.694e-01	3.392e-01
	Age^2	-0.000	0.000	-2.243	2.515e-02	3.167e-02
	Sex	-0.018	0.003	-6.035	2.446e-09	1.188e-08
superior temporal	Intercept	1.036	0.067	15.514	1.474e-47	5.012e-47

ROI	Predictor	Estimate	Std. Error	T-Statistic	pUncorrected	pFDR
	Age	0.005	0.002	2.522	1.186e-02	5.040e-02
	Age^2	-0.000	0.000	-3.639	2.917e-04	1.240e-03
	Sex	-0.010	0.003	-3.602	3.359e-04	6.011e-04
supramarginal	Intercept	1.064	0.073	14.630	4.758e-43	7.034e-43
	Age	0.005	0.002	2.165	3.073e-02	7.290e-02
	Age^2	-0.000	0.000	-3.328	9.162e-04	2.242e-03
	Sex	-0.014	0.003	-4.909	1.111e-06	3.148e-06
temporal pole	Intercept	0.833	0.074	11.201	4.019e-27	4.141e-27
	Age	0.008	0.002	3.412	6.767e-04	7.669e-03
	Age^2	-0.000	0.000	-4.280	2.102e-05	1.787e-04
	Sex	-0.007	0.003	-2.393	1.694e-02	1.920e-02
transverse temporal	Intercept	1.055	0.068	15.434	3.784e-47	1.170e-46
	Age	0.005	0.002	2.269	2.353e-02	7.290e-02
	Age^2	-0.000	0.000	-2.931	3.476e-03	5.138e-03
	Sex	-0.009	0.003	-3.456	5.774e-04	9.816e-04

Table A7: Outputs of multiple regression models testing linear and quadratic age effects on cortical GM R1 in ADRC/WRAP

ROI	Model	R^2	Adjusted R^2	F-Statistic	p-value	df	logLikelihood	AIC	BIC	# obs
bankssts	Linear	0.001	-0.001	0.52	5.95e-01	2	1,961.03	-3,914.06	-3,895.38	790
	Quadratic	0.002	-0.002	0.41	7.44e-01	3	1,961.13	-3,912.26	-3,888.90	790
caudal anterior cingulate	Linear	0.006	0.004	2.38	9.35e-02	2	1,551.60	-3,095.20	-3,076.55	783
	Quadratic	0.008	0.004	2.01	1.11e-01	3	1,552.24	-3,094.48	-3,071.16	783
caudal middle frontal	Linear	0.002	-0.001	0.78	4.57e-01	2	1,954.88	-3,901.75	-3,883.06	790
	Quadratic	0.002	-0.001	0.64	5.90e-01	3	1,955.05	-3,900.10	-3,876.74	790
cuneus	Linear	0.011	0.008	4.36	1.30e-02	2	1,761.43	-3,514.86	-3,496.17	790
	Quadratic	0.014	0.010	3.63	1.27e-02	3	1,762.52	-3,515.03	-3,491.67	790
entorhinal	Linear	0.000	-0.002	0.08	9.25e-01	2	1,261.15	-2,514.30	-2,495.62	789
	Quadratic	0.003	-0.001	0.76	5.16e-01	3	1,262.22	-2,514.43	-2,491.08	789
frontal pole	Linear	0.003	0.001	1.27	2.80e-01	2	1,920.17	-3,832.33	-3,813.65	790
	Quadratic	0.003	-0.000	0.89	4.48e-01	3	1,920.22	-3,830.45	-3,807.09	790
fusiform	Linear	0.001	-0.002	0.25	7.82e-01	2	2,065.46	-4,122.92	-4,104.23	790
	Quadratic	0.002	-0.002	0.59	6.21e-01	3	2,066.10	-4,122.21	-4,098.85	790
inferior parietal	Linear	0.005	0.003	2.06	1.28e-01	2	1,917.52	-3,827.04	-3,808.35	790
	Quadratic	0.006	0.002	1.64	1.79e-01	3	1,917.91	-3,825.83	-3,802.47	790
inferior temporal	Linear	0.001	-0.001	0.52	5.93e-01	2	2,100.16	-4,192.33	-4,173.64	790
	Quadratic	0.005	0.001	1.24	2.94e-01	3	2,101.50	-4,193.01	-4,169.65	790
insula	Linear	0.041	0.038	16.64	8.38e-08	2	2,054.22	-4,100.44	-4,081.75	790
	Quadratic	0.041	0.038	11.29	2.94e-07	3	2,054.53	-4,099.06	-4,075.70	790
isthmus cingulate	Linear	0.002	-0.001	0.79	4.53e-01	2	1,730.47	-3,452.93	-3,434.26	787
	Quadratic	0.003	-0.001	0.66	5.74e-01	3	1,730.67	-3,451.34	-3,428.00	787
lateral occipital	Linear	0.003	0.000	1.09	3.36e-01	2	1,882.46	-3,756.92	-3,738.23	790
	Quadratic	0.009	0.005	2.42	6.51e-02	3	1,884.99	-3,759.99	-3,736.63	790
lateral orbitofrontal	Linear	0.004	0.001	1.56	2.10e-01	2	2,108.12	-4,208.24	-4,189.55	789
	Quadratic	0.004	0.001	1.17	3.19e-01	3	2,108.32	-4,206.63	-4,183.28	789
lingual	Linear	0.005	0.002	1.89	1.52e-01	2	1,884.90	-3,761.80	-3,743.11	790
	Quadratic	0.006	0.002	1.59	1.91e-01	3	1,885.39	-3,760.79	-3,737.43	790

ROI	Model	R^2	Adjusted R^2	F-Statistic	p-value	df	logLikelihood	AIC	BIC	# obs
medial orbitofrontal	Linear	0.015	0.013	6.14	2.25e-03	2	2,062.58	-4,117.17	-4,098.49	789
	Quadratic	0.016	0.012	4.17	6.04e-03	3	2,062.71	-4,115.42	-4,092.06	789
middle temporal	Linear	0.002	-0.001	0.71	4.90e-01	2	2,119.87	-4,231.75	-4,213.06	790
	Quadratic	0.005	0.001	1.31	2.68e-01	3	2,121.13	-4,232.27	-4,208.91	790
paracentral	Linear	0.001	-0.002	0.39	6.77e-01	2	1,866.51	-3,725.01	-3,706.33	789
	Quadratic	0.001	-0.003	0.33	8.02e-01	3	1,866.61	-3,723.23	-3,699.87	789
parahippocampal	Linear	0.028	0.026	11.45	1.26e-05	2	1,906.24	-3,804.49	-3,785.80	790
	Quadratic	0.030	0.026	8.03	2.84e-05	3	1,906.84	-3,803.68	-3,780.32	790
pars opercularis	Linear	0.004	0.002	1.64	1.94e-01	2	2,049.35	-4,090.69	-4,072.00	790
	Quadratic	0.004	0.000	1.13	3.37e-01	3	2,049.39	-4,088.79	-4,065.43	790
pars orbitalis	Linear	0.001	-0.002	0.28	7.55e-01	2	2,012.03	-4,016.05	-3,997.36	790
	Quadratic	0.001	-0.003	0.20	8.96e-01	3	2,012.05	-4,014.09	-3,990.73	790
pars triangularis	Linear	0.002	-0.001	0.68	5.09e-01	2	2,024.03	-4,040.05	-4,021.36	790
	Quadratic	0.002	-0.002	0.48	6.94e-01	3	2,024.08	-4,038.15	-4,014.79	790
pericalcarine	Linear	0.008	0.006	3.32	3.67e-02	2	1,722.00	-3,436.01	-3,417.32	790
	Quadratic	0.013	0.010	3.57	1.38e-02	3	1,724.03	-3,438.06	-3,414.70	790
postcentral	Linear	0.001	-0.002	0.21	8.08e-01	2	1,923.64	-3,839.28	-3,820.59	790
	Quadratic	0.001	-0.003	0.29	8.30e-01	3	1,923.87	-3,837.73	-3,814.37	790
posterior cingulate	Linear	0.008	0.005	2.93	5.38e-02	2	1,385.68	-2,763.36	-2,744.77	771
	Quadratic	0.008	0.004	2.15	9.28e-02	3	1,385.97	-2,761.94	-2,738.71	771
precentral	Linear	0.001	-0.001	0.56	5.70e-01	2	1,874.31	-3,740.63	-3,721.94	790
	Quadratic	0.001	-0.002	0.38	7.70e-01	3	1,874.32	-3,738.63	-3,715.27	790
precuneus	Linear	0.008	0.005	3.07	4.70e-02	2	1,910.52	-3,813.03	-3,794.34	790
	Quadratic	0.008	0.004	2.16	9.15e-02	3	1,910.69	-3,811.37	-3,788.01	790
rostral anterior cingulate	Linear	0.024	0.022	9.81	6.16e-05	2	1,905.60	-3,803.20	-3,784.51	789
	Quadratic	0.027	0.023	7.17	9.41e-05	3	1,906.53	-3,803.06	-3,779.71	789
rostral middle frontal	Linear	0.005	0.002	1.98	1.38e-01	2	1,992.86	-3,977.71	-3,959.02	790
	Quadratic	0.005	0.001	1.37	2.49e-01	3	1,992.94	-3,975.87	-3,952.51	790
superior frontal	Linear	0.002	-0.000	0.83	4.35e-01	2	2,023.96	-4,039.91	-4,021.23	789
	Quadratic	0.002	-0.001	0.65	5.85e-01	3	2,024.09	-4,038.19	-4,014.83	789
superior parietal	Linear	0.008	0.005	3.00	5.06e-02	2	1,872.50	-3,737.00	-3,718.31	790

ROI	Model	R^2	Adjusted R^2	F-Statistic	p-value	df	logLikelihood	AIC	BIC	# obs
	Quadratic	0.009	0.005	2.37	6.95e-02	3	1,873.06	-3,736.11	-3,712.75	790
superior temporal	Linear	0.012	0.010	4.80	8.49e-03	2	2,040.00	-4,072.00	-4,053.31	790
	Quadratic	0.012	0.008	3.19	2.30e-02	3	2,040.00	-4,070.00	-4,046.64	790
supramarginal	Linear	0.003	0.000	1.03	3.56e-01	2	1,995.46	-3,982.92	-3,964.24	790
	Quadratic	0.003	-0.001	0.75	5.22e-01	3	1,995.56	-3,981.11	-3,957.75	790
temporal pole	Linear	0.028	0.026	11.42	1.29e-05	2	1,926.60	-3,845.21	-3,826.52	790
	Quadratic	0.029	0.025	7.70	4.48e-05	3	1,926.75	-3,843.49	-3,820.13	790
transverse temporal	Linear	0.018	0.016	7.24	7.66e-04	2	1,789.22	-3,570.44	-3,551.75	790
	Quadratic	0.018	0.014	4.85	2.37e-03	3	1,789.27	-3,568.54	-3,545.18	790

Abbreviations: df = degrees of freedom; AIC = Akaike Information Criterion; BIC = Bayesian Information Criterion; # obs = number of observations

Table A8: Outputs of multiple regression models testing linear and quadratic age effects on cortical-adjacent WM R1 in ADRC/WRAP

ROI	Model	R^2	Adjusted R^2	F-Statistic	p-value	df	logLikelihood	AIC	BIC	# obs
bankssts	Linear	0.196	0.194	96.29	3.85e-38	2	1,452.93	-2,897.86	-2,879.17	791
	Quadratic	0.205	0.202	67.85	4.98e-39	3	1,457.43	-2,904.86	-2,881.50	791
caudal anterior cingulate	Linear	0.203	0.201	100.21	1.67e-39	2	1,395.83	-2,783.67	-2,764.98	791
	Quadratic	0.217	0.214	72.88	1.34e-41	3	1,403.16	-2,796.32	-2,772.95	791
caudal middle frontal	Linear	0.257	0.255	136.04	1.78e-51	2	1,501.44	-2,994.88	-2,976.19	791
	Quadratic	0.265	0.262	94.44	3.27e-52	3	1,505.75	-3,001.50	-2,978.14	791
cuneus	Linear	0.139	0.137	63.59	2.51e-26	2	1,454.63	-2,901.26	-2,882.57	791
	Quadratic	0.140	0.137	42.71	1.40e-25	3	1,455.12	-2,900.24	-2,876.88	791
entorhinal	Linear	0.147	0.145	67.77	6.93e-28	2	1,390.50	-2,773.00	-2,754.31	791
	Quadratic	0.179	0.176	57.14	2.01e-33	3	1,405.66	-2,801.33	-2,777.96	791
frontal pole	Linear	0.209	0.207	104.00	8.27e-41	2	1,417.79	-2,827.58	-2,808.88	791
	Quadratic	0.220	0.217	74.05	3.43e-42	3	1,423.47	-2,836.95	-2,813.58	791
fusiform	Linear	0.224	0.222	113.62	4.41e-44	2	1,456.69	-2,905.38	-2,886.69	791
	Quadratic	0.232	0.230	79.45	6.66e-45	3	1,461.11	-2,912.22	-2,888.86	791
inferior parietal	Linear	0.230	0.228	117.61	2.02e-45	2	1,450.60	-2,893.21	-2,874.51	791
	Quadratic	0.237	0.234	81.56	5.95e-46	3	1,454.37	-2,898.74	-2,875.37	791
inferior temporal	Linear	0.230	0.228	117.39	2.39e-45	2	1,478.33	-2,948.66	-2,929.97	791
	Quadratic	0.238	0.235	81.82	4.42e-46	3	1,482.57	-2,955.13	-2,931.76	791
insula	Linear	0.144	0.142	66.41	2.23e-27	2	1,557.89	-3,107.78	-3,089.09	791
	Quadratic	0.157	0.153	48.69	7.15e-29	3	1,563.63	-3,117.25	-3,093.89	791
isthmus cingulate	Linear	0.147	0.145	67.91	6.19e-28	2	1,441.07	-2,874.15	-2,855.45	791
	Quadratic	0.156	0.153	48.66	7.42e-29	3	1,445.49	-2,880.97	-2,857.60	791
lateral occipital	Linear	0.170	0.168	80.80	1.21e-32	2	1,499.90	-2,991.81	-2,973.11	791
	Quadratic	0.172	0.168	54.31	6.50e-32	3	1,500.55	-2,991.10	-2,967.73	791
lateral orbitofrontal	Linear	0.269	0.267	144.79	2.80e-54	2	1,464.51	-2,921.03	-2,902.34	791
	Quadratic	0.290	0.288	107.37	2.83e-58	3	1,476.43	-2,942.85	-2,919.49	791
lingual	Linear	0.159	0.157	74.57	2.18e-30	2	1,501.39	-2,994.77	-2,976.08	791
	Quadratic	0.163	0.160	51.02	3.85e-30	3	1,503.12	-2,996.24	-2,972.87	791

ROI	Model	R^2	Adjusted R^2	F-Statistic	p-value	df	logLikelihood	AIC	BIC	# obs
medial orbitofrontal	Linear	0.265	0.263	142.30	1.74e-53	2	1,456.92	-2,905.84	-2,887.15	791
	Quadratic	0.284	0.281	103.81	1.25e-56	3	1,466.84	-2,923.68	-2,900.32	791
middle temporal	Linear	0.256	0.254	135.69	2.30e-51	2	1,490.29	-2,972.58	-2,953.88	791
	Quadratic	0.265	0.262	94.41	3.38e-52	3	1,494.82	-2,979.64	-2,956.28	791
paracentral	Linear	0.205	0.203	101.43	6.33e-40	2	1,479.28	-2,950.55	-2,931.86	791
	Quadratic	0.209	0.206	69.38	8.11e-40	3	1,481.49	-2,952.97	-2,929.61	791
parahippocampal	Linear	0.132	0.130	60.11	5.04e-25	2	1,394.69	-2,781.37	-2,762.68	791
	Quadratic	0.150	0.147	46.42	1.25e-27	3	1,402.97	-2,795.93	-2,772.56	791
pars opercularis	Linear	0.247	0.245	129.45	2.45e-49	2	1,498.37	-2,988.74	-2,970.05	791
	Quadratic	0.258	0.255	91.18	1.20e-50	3	1,503.99	-2,997.99	-2,974.62	791
pars orbitalis	Linear	0.239	0.237	123.95	1.57e-47	2	1,486.47	-2,964.93	-2,946.24	791
	Quadratic	0.251	0.248	87.83	5.04e-49	3	1,492.49	-2,974.98	-2,951.62	791
pars triangularis	Linear	0.265	0.263	141.99	2.17e-53	2	1,489.50	-2,970.99	-2,952.30	791
	Quadratic	0.278	0.276	101.19	2.11e-55	3	1,496.80	-2,983.59	-2,960.23	791
pericalcarine	Linear	0.110	0.107	48.53	1.33e-20	2	1,403.07	-2,798.14	-2,779.44	791
	Quadratic	0.110	0.107	32.44	8.92e-20	3	1,403.24	-2,796.48	-2,773.11	791
postcentral	Linear	0.182	0.180	87.58	4.50e-35	2	1,522.87	-3,037.73	-3,019.04	791
	Quadratic	0.186	0.183	59.98	6.28e-35	3	1,524.92	-3,039.84	-3,016.47	791
posterior cingulate	Linear	0.187	0.184	90.36	4.66e-36	2	1,440.59	-2,873.18	-2,854.49	791
	Quadratic	0.197	0.194	64.26	3.60e-37	3	1,445.58	-2,881.17	-2,857.80	791
precentral	Linear	0.216	0.214	108.71	2.02e-42	2	1,523.32	-3,038.65	-3,019.96	791
	Quadratic	0.220	0.217	74.05	3.41e-42	3	1,525.29	-3,040.58	-3,017.21	791
precuneus	Linear	0.245	0.243	127.72	9.03e-49	2	1,432.58	-2,857.16	-2,838.47	791
	Quadratic	0.254	0.251	89.28	9.95e-50	3	1,437.38	-2,864.76	-2,841.39	791
rostral anterior cingulate	Linear	0.175	0.173	83.40	1.39e-33	2	1,418.77	-2,829.55	-2,810.86	791
	Quadratic	0.182	0.179	58.51	3.78e-34	3	1,422.46	-2,834.92	-2,811.55	791
rostral middle frontal	Linear	0.259	0.257	137.67	5.26e-52	2	1,461.63	-2,915.27	-2,896.57	791
	Quadratic	0.268	0.266	96.19	4.79e-53	3	1,466.66	-2,923.32	-2,899.96	791
superior frontal	Linear	0.290	0.288	160.82	2.69e-59	2	1,487.40	-2,966.80	-2,948.11	791
	Quadratic	0.300	0.297	112.27	1.62e-60	3	1,492.92	-2,975.84	-2,952.47	791
superior parietal	Linear	0.229	0.227	116.98	3.26e-45	2	1,451.39	-2,894.78	-2,876.09	791

ROI	Model	R^2	Adjusted R^2	F-Statistic	p-value	df	logLikelihood	AIC	BIC	# obs
	Quadratic	0.234	0.231	80.07	3.29e-45	3	1,453.91	-2,897.82	-2,874.46	791
superior temporal	Linear	0.203	0.201	100.53	1.30e-39	2	1,523.35	-3,038.70	-3,020.01	791
	Quadratic	0.216	0.213	72.47	2.15e-41	3	1,529.95	-3,049.90	-3,026.54	791
supramarginal	Linear	0.225	0.223	114.07	3.09e-44	2	1,456.78	-2,905.56	-2,886.87	791
	Quadratic	0.235	0.232	80.71	1.57e-45	3	1,462.31	-2,914.62	-2,891.25	791
temporal pole	Linear	0.129	0.127	58.60	1.88e-24	2	1,435.07	-2,862.14	-2,843.45	791
	Quadratic	0.149	0.146	46.03	2.05e-27	3	1,444.17	-2,878.34	-2,854.98	791
transverse temporal	Linear	0.089	0.086	38.33	1.30e-16	2	1,507.25	-3,006.50	-2,987.80	791
	Quadratic	0.099	0.095	28.67	1.35e-17	3	1,511.54	-3,013.08	-2,989.72	791

Abbreviations: df = degrees of freedom; AIC = Akaike Information Criterion; BIC = Bayesian Information Criterion; # obs = number of observations

Table A9: Outputs of multiple regression models testing linear effect of age on regional cortical GM R1 in ADCP

ROI	Predictor	Estimate	Std. Error	T-Statistic	pUncorrected	pFDR
bankssts	Intercept	0.686	0.014	49.793	7.591e-97	1.434e-96
	Age	-0.000	0.000	-0.015	9.881e-01	9.911e-01
	Sex	0.001	0.003	0.249	8.036e-01	8.735e-01
caudal anterior cingulate	Intercept	0.638	0.027	23.632	4.331e-53	4.602e-53
	Age	0.001	0.000	1.405	1.622e-01	6.128e-01
	Sex	-0.010	0.006	-1.669	9.718e-02	4.688e-01
caudal middle frontal	Intercept	0.715	0.013	56.176	1.709e-104	2.905e-103
	Age	-0.000	0.000	-0.983	3.272e-01	6.821e-01
	Sex	-0.004	0.003	-1.481	1.407e-01	4.783e-01
cuneus	Intercept	0.715	0.017	42.105	2.148e-86	3.043e-86
	Age	-0.000	0.000	-0.110	9.126e-01	9.729e-01
	Sex	-0.007	0.004	-1.707	8.980e-02	4.688e-01
entorhinal	Intercept	0.734	0.034	21.430	4.565e-48	4.703e-48
	Age	0.000	0.000	0.970	3.338e-01	6.821e-01
	Sex	0.013	0.008	1.606	1.103e-01	4.688e-01
frontal pole	Intercept	0.660	0.015	44.148	2.534e-89	3.746e-89
	Age	-0.000	0.000	-0.106	9.157e-01	9.729e-01
	Sex	-0.002	0.003	-0.675	5.004e-01	8.110e-01
fusiform	Intercept	0.666	0.013	52.660	2.199e-100	1.068e-99
	Age	0.000	0.000	0.944	3.467e-01	6.821e-01
	Sex	0.002	0.003	0.527	5.989e-01	8.110e-01
inferior parietal	Intercept	0.693	0.014	50.636	6.634e-98	1.790e-97
	Age	-0.000	0.000	-0.797	4.268e-01	6.910e-01
	Sex	-0.002	0.003	-0.525	6.000e-01	8.110e-01
inferior temporal	Intercept	0.658	0.013	50.347	1.522e-97	3.450e-97
	Age	0.000	0.000	0.195	8.460e-01	9.729e-01
	Sex	0.004	0.003	1.397	1.644e-01	4.783e-01
insula	Intercept	0.638	0.013	47.876	2.225e-94	3.782e-94

ROI	Predictor	Estimate	Std. Error	T-Statistic	pUncorrected	pFDR
	Age	0.001	0.000	2.769	6.322e-03	1.075e-01
	Sex	0.001	0.003	0.465	6.425e-01	8.110e-01
isthmus cingulate	Intercept	0.695	0.017	41.695	8.581e-86	1.167e-85
	Age	0.000	0.000	1.036	3.020e-01	6.821e-01
	Sex	-0.005	0.004	-1.284	2.011e-01	5.260e-01
lateral occipital	Intercept	0.700	0.015	46.686	8.371e-93	1.294e-92
	Age	0.000	0.000	0.011	9.911e-01	9.911e-01
	Sex	-0.003	0.003	-0.967	3.350e-01	7.119e-01
lateral orbitofrontal	Intercept	0.660	0.013	51.356	8.518e-99	3.185e-98
	Age	0.000	0.000	0.403	6.873e-01	8.655e-01
	Sex	-0.002	0.003	-0.724	4.702e-01	8.110e-01
lingual	Intercept	0.681	0.014	48.856	1.190e-95	2.129e-95
	Age	0.000	0.000	1.561	1.207e-01	5.863e-01
	Sex	-0.009	0.003	-2.648	8.935e-03	3.038e-01
medial orbitofrontal	Intercept	0.614	0.017	36.725	4.462e-78	5.619e-78
	Age	0.001	0.000	2.322	2.156e-02	2.443e-01
	Sex	0.001	0.004	0.226	8.212e-01	8.735e-01
middle temporal	Intercept	0.656	0.013	50.064	3.451e-97	7.333e-97
	Age	0.000	0.000	0.891	3.745e-01	6.821e-01
	Sex	0.003	0.003	1.022	3.083e-01	6.988e-01
paracentral	Intercept	0.752	0.015	51.203	1.314e-98	4.061e-98
	Age	-0.000	0.000	-1.072	2.853e-01	6.821e-01
	Sex	-0.002	0.003	-0.720	4.724e-01	8.110e-01
parahippocampal	Intercept	0.647	0.018	36.641	6.125e-78	7.437e-78
	Age	0.001	0.000	2.173	3.133e-02	2.663e-01
	Sex	-0.006	0.004	-1.463	1.456e-01	4.783e-01
pars opercularis	Intercept	0.678	0.013	51.445	6.606e-99	2.808e-98
	Age	0.000	0.000	0.818	4.145e-01	6.910e-01
	Sex	-0.000	0.003	-0.025	9.799e-01	9.799e-01
pars orbitalis	Intercept	0.677	0.014	47.142	2.067e-93	3.347e-93
	Age	0.000	0.000	0.329	7.422e-01	9.012e-01

ROI	Predictor	Estimate	Std. Error	T-Statistic	pUncorrected	pFDR
	Sex	-0.004	0.003	-1.191	2.353e-01	5.714e-01
pars triangularis	Intercept	0.680	0.013	50.534	8.886e-98	2.158e-97
	Age	0.000	0.000	0.492	6.237e-01	8.314e-01
	Sex	-0.002	0.003	-0.533	5.946e-01	8.110e-01
pericalcarine	Intercept	0.698	0.019	36.251	2.685e-77	3.148e-77
	Age	0.000	0.000	1.161	2.476e-01	6.821e-01
	Sex	-0.007	0.004	-1.647	1.016e-01	4.688e-01
postcentral	Intercept	0.735	0.014	53.117	6.237e-101	3.534e-100
	Age	-0.000	0.000	-0.569	5.700e-01	8.314e-01
	Sex	-0.001	0.003	-0.377	7.065e-01	8.283e-01
posterior cingulate	Intercept	0.613	0.026	23.699	3.074e-53	3.371e-53
	Age	0.001	0.000	4.053	7.999e-05	2.720e-03
	Sex	-0.003	0.006	-0.430	6.679e-01	8.110e-01
precentral	Intercept	0.760	0.014	54.781	6.837e-103	5.811e-102
	Age	-0.000	0.000	-1.133	2.592e-01	6.821e-01
	Sex	-0.001	0.003	-0.464	6.432e-01	8.110e-01
precuneus	Intercept	0.703	0.014	50.625	6.845e-98	1.790e-97
	Age	-0.000	0.000	-0.474	6.358e-01	8.314e-01
	Sex	-0.006	0.003	-1.739	8.399e-02	4.688e-01
rostral anterior cingulate	Intercept	0.552	0.050	10.967	4.816e-21	4.816e-21
	Age	0.001	0.001	2.028	4.426e-02	3.010e-01
	Sex	0.019	0.012	1.642	1.025e-01	4.688e-01
rostral middle frontal	Intercept	0.684	0.013	53.960	6.242e-102	4.245e-101
	Age	-0.000	0.000	-0.878	3.812e-01	6.821e-01
	Sex	-0.001	0.003	-0.225	8.221e-01	8.735e-01
superior frontal	Intercept	0.688	0.012	58.508	4.295e-107	1.460e-105
	Age	-0.000	0.000	-0.147	8.836e-01	9.729e-01
	Sex	-0.002	0.003	-0.626	5.320e-01	8.110e-01
superior parietal	Intercept	0.720	0.014	51.322	9.369e-99	3.185e-98
	Age	-0.000	0.000	-1.417	1.586e-01	6.128e-01
	Sex	-0.004	0.003	-1.383	1.688e-01	4.783e-01

ROI	Predictor	Estimate	Std. Error	T-Statistic	pUncorrected	pFDR
superior temporal	Intercept	0.690	0.014	50.027	3.848e-97	7.696e-97
	Age	0.000	0.000	0.482	6.307e-01	8.314e-01
	Sex	0.001	0.003	0.453	6.515e-01	8.110e-01
supramarginal	Intercept	0.697	0.013	55.143	2.602e-103	2.949e-102
	Age	-0.000	0.000	-0.664	5.080e-01	7.851e-01
	Sex	0.000	0.003	0.163	8.708e-01	8.972e-01
temporal pole	Intercept	0.622	0.019	32.897	1.527e-71	1.731e-71
	Age	0.000	0.000	1.891	6.049e-02	3.428e-01
	Sex	0.008	0.004	1.754	8.146e-02	4.688e-01
transverse temporal	Intercept	0.750	0.018	40.788	1.917e-84	2.507e-84
	Age	0.000	0.000	1.068	2.874e-01	6.821e-01
	Sex	-0.002	0.004	-0.494	6.217e-01	8.110e-01

Table A10: Outputs of multiple regression models testing linear effect of age on regional cortical-adjacent WM R1 in ADCP

ROI	Predictor	Estimate	Std. Error	T-Statistic	pUncorrected	pFDR
bankssts	Intercept	1.214	0.031	39.415	2.369e-82	4.239e-82
	Age	-0.002	0.000	-4.390	2.098e-05	2.853e-05
	Sex	0.009	0.007	1.257	2.106e-01	4.812e-01
caudal anterior cingulate	Intercept	1.290	0.036	35.659	2.593e-76	3.265e-76
	Age	-0.002	0.001	-4.496	1.356e-05	2.005e-05
	Sex	0.005	0.008	0.589	5.564e-01	7.007e-01
caudal middle frontal	Intercept	1.249	0.030	42.180	1.665e-86	7.578e-86
	Age	-0.003	0.000	-6.295	3.051e-09	2.075e-08
	Sex	0.010	0.007	1.444	1.508e-01	4.732e-01
cuneus	Intercept	1.117	0.029	38.327	1.187e-80	1.834e-80
	Age	-0.001	0.000	-3.005	3.106e-03	3.399e-03
	Sex	-0.014	0.007	-2.102	3.714e-02	4.492e-01
entorhinal	Intercept	1.142	0.036	31.480	5.622e-69	5.622e-69
	Age	-0.002	0.001	-4.631	7.675e-06	1.186e-05
	Sex	-0.003	0.008	-0.405	6.860e-01	7.775e-01
frontal pole	Intercept	1.153	0.032	35.966	7.962e-77	1.041e-76
	Age	-0.003	0.000	-5.685	6.392e-08	2.173e-07
	Sex	0.013	0.007	1.700	9.111e-02	4.492e-01
fusiform	Intercept	1.208	0.031	39.522	1.617e-82	3.234e-82
	Age	-0.002	0.000	-4.902	2.381e-06	4.261e-06
	Sex	0.005	0.007	0.712	4.778e-01	6.248e-01
inferior parietal	Intercept	1.188	0.031	38.214	1.790e-80	2.646e-80
	Age	-0.002	0.000	-4.654	6.967e-06	1.128e-05
	Sex	0.004	0.007	0.516	6.069e-01	7.369e-01
inferior temporal	Intercept	1.188	0.030	40.204	1.462e-83	3.314e-83
	Age	-0.002	0.000	-4.961	1.832e-06	3.664e-06
	Sex	0.008	0.007	1.191	2.356e-01	4.812e-01
insula	Intercept	1.164	0.028	41.293	3.383e-85	1.150e-84

ROI	Predictor	Estimate	Std. Error	T-Statistic	pUncorrected	pFDR
	Age	-0.002	0.000	-4.288	3.169e-05	4.144e-05
	Sex	0.006	0.007	0.995	3.213e-01	5.202e-01
isthmus cingulate	Intercept	1.224	0.035	34.734	9.515e-75	1.078e-74
	Age	-0.001	0.000	-2.132	3.461e-02	3.461e-02
	Sex	-0.006	0.008	-0.779	4.374e-01	5.949e-01
lateral occipital	Intercept	1.117	0.027	41.227	4.235e-85	1.309e-84
	Age	-0.001	0.000	-2.995	3.199e-03	3.399e-03
	Sex	-0.005	0.006	-0.822	4.126e-01	5.845e-01
lateral orbitofrontal	Intercept	1.277	0.033	39.251	4.245e-82	7.216e-82
	Age	-0.003	0.000	-7.098	4.362e-11	1.483e-09
	Sex	0.008	0.008	1.047	2.970e-01	5.049e-01
lingual	Intercept	1.129	0.026	43.145	6.712e-88	5.705e-87
	Age	-0.001	0.000	-3.650	3.586e-04	4.064e-04
	Sex	-0.011	0.006	-1.894	6.007e-02	4.492e-01
medial orbitofrontal	Intercept	1.236	0.032	38.447	7.673e-81	1.242e-80
	Age	-0.003	0.000	-6.813	2.029e-10	3.449e-09
	Sex	0.008	0.007	1.110	2.689e-01	4.812e-01
middle temporal	Intercept	1.191	0.030	39.918	3.992e-83	8.483e-83
	Age	-0.002	0.000	-5.000	1.546e-06	3.285e-06
	Sex	0.011	0.007	1.571	1.183e-01	4.492e-01
paracentral	Intercept	1.238	0.029	42.170	1.724e-86	7.578e-86
	Age	-0.002	0.000	-5.601	9.537e-08	2.948e-07
	Sex	0.008	0.007	1.214	2.266e-01	4.812e-01
parahippocampal	Intercept	1.203	0.034	35.414	6.694e-76	8.128e-76
	Age	-0.002	0.000	-4.026	8.890e-05	1.119e-04
	Sex	-0.002	0.008	-0.315	7.535e-01	8.092e-01
pars opercularis	Intercept	1.248	0.030	42.075	2.375e-86	8.972e-86
	Age	-0.003	0.000	-6.158	6.132e-09	2.984e-08
	Sex	0.014	0.007	2.005	4.669e-02	4.492e-01
pars orbitalis	Intercept	1.169	0.031	38.170	2.100e-80	2.856e-80
	Age	-0.002	0.000	-4.934	2.071e-06	3.912e-06

ROI	Predictor	Estimate	Std. Error	T-Statistic	pUncorrected	pFDR
	Sex	0.008	0.007	1.118	2.652e-01	4.812e-01
pars triangularis	Intercept	1.252	0.031	40.431	6.613e-84	1.606e-83
	Age	-0.003	0.000	-6.309	2.838e-09	2.075e-08
	Sex	0.012	0.007	1.702	9.076e-02	4.492e-01
pericalcarine	Intercept	1.081	0.033	33.043	8.399e-72	8.924e-72
	Age	-0.001	0.000	-2.399	1.764e-02	1.817e-02
	Sex	-0.009	0.008	-1.174	2.422e-01	4.812e-01
postcentral	Intercept	1.196	0.027	44.189	2.220e-89	3.774e-88
	Age	-0.002	0.000	-5.241	5.190e-07	1.298e-06
	Sex	0.005	0.006	0.850	3.965e-01	5.845e-01
posterior cingulate	Intercept	1.258	0.036	34.658	1.283e-74	1.407e-74
	Age	-0.002	0.001	-3.840	1.791e-04	2.175e-04
	Sex	0.004	0.008	0.417	6.773e-01	7.775e-01
precentral	Intercept	1.228	0.027	45.214	8.354e-91	2.840e-89
	Age	-0.002	0.000	-5.900	2.226e-08	9.460e-08
	Sex	0.009	0.006	1.388	1.670e-01	4.732e-01
precuneus	Intercept	1.225	0.032	38.175	2.066e-80	2.856e-80
	Age	-0.002	0.000	-5.005	1.512e-06	3.285e-06
	Sex	-0.000	0.007	-0.007	9.944e-01	9.944e-01
rostral anterior cingulate	Intercept	1.262	0.036	35.367	8.012e-76	9.393e-76
	Age	-0.002	0.000	-4.804	3.659e-06	6.220e-06
	Sex	0.012	0.008	1.396	1.648e-01	4.732e-01
rostral middle frontal	Intercept	1.242	0.032	39.440	2.167e-82	4.093e-82
	Age	-0.003	0.000	-6.158	6.143e-09	2.984e-08
	Sex	0.015	0.007	2.002	4.703e-02	4.492e-01
superior frontal	Intercept	1.233	0.029	42.375	8.660e-87	5.889e-86
	Age	-0.003	0.000	-6.575	7.132e-10	8.083e-09
	Sex	0.011	0.007	1.568	1.189e-01	4.492e-01
superior parietal	Intercept	1.205	0.030	40.715	2.473e-84	6.468e-84
	Age	-0.002	0.000	-5.237	5.267e-07	1.298e-06
	Sex	0.002	0.007	0.248	8.044e-01	8.288e-01

ROI	Predictor	Estimate	Std. Error	T-Statistic	pUncorrected	pFDR
superior temporal	Intercept	1.207	0.028	43.206	5.481e-88	5.705e-87
	Age	-0.002	0.000	-5.234	5.345e-07	1.298e-06
	Sex	0.010	0.006	1.570	1.185e-01	4.492e-01
supramarginal	Intercept	1.232	0.029	42.160	1.783e-86	7.578e-86
	Age	-0.002	0.000	-5.830	3.142e-08	1.187e-07
	Sex	0.008	0.007	1.226	2.222e-01	4.812e-01
temporal pole	Intercept	1.113	0.035	31.646	2.785e-69	2.869e-69
	Age	-0.002	0.000	-4.478	1.460e-05	2.068e-05
	Sex	0.007	0.008	0.882	3.790e-01	5.845e-01
transverse temporal	Intercept	1.208	0.030	40.900	1.304e-84	3.695e-84
	Age	-0.002	0.000	-3.791	2.147e-04	2.517e-04
	Sex	0.002	0.007	0.304	7.616e-01	8.092e-01

Table A11: Outputs of multiple regression models testing quadratic effects of age on regional cortical GM R1 in ADCP

ROI	Predictor	Estimate	Std. Error	T-Statistic	pUncorrected	pFDR
bankssts	Intercept	0.607	0.098	6.204	4.909e-09	1.283e-08
	Age	0.002	0.003	0.806	4.218e-01	7.313e-01
	Age^2	-0.000	0.000	-0.809	4.200e-01	6.878e-01
	Sex	0.001	0.003	0.261	7.947e-01	8.800e-01
caudal anterior cingulate	Intercept	0.553	0.192	2.881	4.538e-03	4.822e-03
	Age	0.003	0.005	0.540	5.903e-01	8.506e-01
	Age^2	-0.000	0.000	-0.443	6.583e-01	8.589e-01
	Sex	-0.010	0.006	-1.658	9.940e-02	4.701e-01
caudal middle frontal	Intercept	0.602	0.090	6.671	4.371e-10	1.651e-09
	Age	0.003	0.003	1.197	2.331e-01	6.331e-01
	Age^2	-0.000	0.000	-1.269	2.065e-01	6.116e-01
	Sex	-0.004	0.003	-1.465	1.450e-01	4.927e-01
cuneus	Intercept	0.480	0.120	4.019	9.140e-05	1.072e-04
	Age	0.007	0.003	1.974	5.013e-02	6.331e-01
	Age^2	-0.000	0.000	-1.987	4.871e-02	6.116e-01
	Sex	-0.007	0.004	-1.694	9.226e-02	4.701e-01
entorhinal	Intercept	0.676	0.244	2.772	6.272e-03	6.462e-03
	Age	0.002	0.007	0.306	7.597e-01	8.907e-01
	Age^2	-0.000	0.000	-0.240	8.108e-01	9.344e-01
	Sex	0.013	0.008	1.605	1.106e-01	4.701e-01
frontal pole	Intercept	0.575	0.106	5.418	2.294e-07	3.250e-07
	Age	0.002	0.003	0.791	4.302e-01	7.313e-01
	Age^2	-0.000	0.000	-0.800	4.248e-01	6.878e-01
	Sex	-0.002	0.003	-0.663	5.084e-01	8.141e-01
fusiform	Intercept	0.761	0.090	8.476	1.825e-14	6.205e-13
	Age	-0.003	0.003	-0.998	3.196e-01	6.345e-01
	Age^2	0.000	0.000	1.067	2.878e-01	6.116e-01
	Sex	0.002	0.003	0.512	6.096e-01	8.141e-01

ROI	Predictor	Estimate	Std. Error	T-Statistic	pUncorrected	pFDR
inferior parietal	Intercept	0.577	0.097	5.940	1.845e-08	3.690e-08
	Age	0.003	0.003	1.156	2.497e-01	6.331e-01
	Age^2	-0.000	0.000	-1.214	2.266e-01	6.116e-01
	Sex	-0.002	0.003	-0.508	6.119e-01	8.141e-01
inferior temporal	Intercept	0.720	0.093	7.751	1.182e-12	1.528e-11
	Age	-0.002	0.003	-0.664	5.075e-01	7.843e-01
	Age^2	0.000	0.000	0.679	4.979e-01	7.695e-01
	Sex	0.004	0.003	1.385	1.682e-01	4.927e-01
insula	Intercept	0.530	0.094	5.609	9.291e-08	1.504e-07
	Age	0.004	0.003	1.343	1.814e-01	6.331e-01
	Age^2	-0.000	0.000	-1.153	2.509e-01	6.116e-01
	Sex	0.001	0.003	0.483	6.301e-01	8.141e-01
isthmus cingulate	Intercept	0.488	0.117	4.151	5.478e-05	6.898e-05
	Age	0.006	0.003	1.848	6.649e-02	6.331e-01
	Age^2	-0.000	0.000	-1.780	7.705e-02	6.116e-01
	Sex	-0.005	0.004	-1.267	2.072e-01	5.419e-01
lateral occipital	Intercept	0.594	0.106	5.582	1.055e-07	1.630e-07
	Age	0.003	0.003	1.001	3.182e-01	6.345e-01
	Age^2	-0.000	0.000	-1.003	3.174e-01	6.348e-01
	Sex	-0.003	0.003	-0.952	3.424e-01	7.276e-01
lateral orbitofrontal	Intercept	0.617	0.092	6.738	3.071e-10	1.305e-09
	Age	0.001	0.003	0.508	6.119e-01	8.506e-01
	Age^2	-0.000	0.000	-0.482	6.308e-01	8.589e-01
	Sex	-0.002	0.003	-0.715	4.757e-01	8.141e-01
lingual	Intercept	0.575	0.099	5.815	3.424e-08	6.057e-08
	Age	0.003	0.003	1.186	2.373e-01	6.331e-01
	Age^2	-0.000	0.000	-1.080	2.817e-01	6.116e-01
	Sex	-0.008	0.003	-2.634	9.318e-03	3.168e-01
medial orbitofrontal	Intercept	0.765	0.118	6.465	1.289e-09	3.984e-09
	Age	-0.004	0.003	-1.129	2.607e-01	6.331e-01
	Age^2	0.000	0.000	1.294	1.976e-01	6.116e-01

ROI	Predictor	Estimate	Std. Error	T-Statistic	pUncorrected	pFDR
	Sex	0.001	0.004	0.208	8.356e-01	8.800e-01
middle temporal	Intercept	0.654	0.093	7.003	7.443e-11	4.218e-10
	Age	0.000	0.003	0.087	9.305e-01	9.447e-01
	Age^2	-0.000	0.000	-0.026	9.796e-01	9.796e-01
	Sex	0.003	0.003	1.019	3.098e-01	7.022e-01
paracentral	Intercept	0.638	0.104	6.123	7.424e-09	1.578e-08
	Age	0.003	0.003	1.027	3.058e-01	6.345e-01
	Age^2	-0.000	0.000	-1.105	2.710e-01	6.116e-01
	Sex	-0.002	0.003	-0.705	4.821e-01	8.141e-01
parahippocampal	Intercept	0.613	0.126	4.875	2.698e-06	3.669e-06
	Age	0.002	0.004	0.423	6.732e-01	8.506e-01
	Age^2	-0.000	0.000	-0.272	7.856e-01	9.344e-01
	Sex	-0.006	0.004	-1.454	1.480e-01	4.927e-01
pars opercularis	Intercept	0.576	0.093	6.167	5.930e-09	1.344e-08
	Age	0.003	0.003	1.148	2.527e-01	6.331e-01
	Age^2	-0.000	0.000	-1.094	2.757e-01	6.116e-01
	Sex	-0.000	0.003	-0.009	9.927e-01	9.927e-01
pars orbitalis	Intercept	0.672	0.102	6.571	7.384e-10	2.511e-09
	Age	0.000	0.003	0.069	9.447e-01	9.447e-01
	Age^2	-0.000	0.000	-0.047	9.628e-01	9.796e-01
	Sex	-0.004	0.003	-1.187	2.371e-01	5.758e-01
pars triangularis	Intercept	0.592	0.096	6.190	5.281e-09	1.283e-08
	Age	0.003	0.003	0.965	3.359e-01	6.345e-01
	Age^2	-0.000	0.000	-0.933	3.521e-01	6.651e-01
	Sex	-0.002	0.003	-0.519	6.043e-01	8.141e-01
pericalcarine	Intercept	0.525	0.136	3.853	1.713e-04	1.941e-04
	Age	0.005	0.004	1.353	1.779e-01	6.331e-01
	Age^2	-0.000	0.000	-1.276	2.040e-01	6.116e-01
	Sex	-0.007	0.004	-1.631	1.049e-01	4.701e-01
postcentral	Intercept	0.693	0.099	7.039	6.103e-11	4.150e-10
	Age	0.001	0.003	0.385	7.005e-01	8.506e-01

ROI	Predictor	Estimate	Std. Error	T-Statistic	pUncorrected	pFDR
	Age^2	-0.000	0.000	-0.426	6.708e-01	8.589e-01
	Sex	-0.001	0.003	-0.370	7.119e-01	8.346e-01
posterior cingulate	Intercept	0.588	0.184	3.190	1.728e-03	1.895e-03
	Age	0.002	0.005	0.419	6.755e-01	8.506e-01
	Age^2	-0.000	0.000	-0.139	8.899e-01	9.760e-01
	Sex	-0.003	0.006	-0.426	6.704e-01	8.141e-01
precentral	Intercept	0.680	0.099	6.895	1.325e-10	6.436e-10
	Age	0.002	0.003	0.739	4.611e-01	7.465e-01
	Age^2	-0.000	0.000	-0.820	4.137e-01	6.878e-01
	Sex	-0.001	0.003	-0.452	6.522e-01	8.141e-01
precuneus	Intercept	0.571	0.098	5.807	3.563e-08	6.057e-08
	Age	0.004	0.003	1.320	1.889e-01	6.331e-01
	Age^2	-0.000	0.000	-1.356	1.771e-01	6.116e-01
	Sex	-0.006	0.003	-1.724	8.674e-02	4.701e-01
rostral anterior cingulate	Intercept	0.698	0.359	1.947	5.341e-02	5.341e-02
	Age	-0.003	0.010	-0.269	7.886e-01	8.937e-01
	Age^2	0.000	0.000	0.410	6.821e-01	8.589e-01
	Sex	0.019	0.012	1.632	1.048e-01	4.701e-01
rostral middle frontal	Intercept	0.664	0.090	7.356	1.077e-11	9.155e-11
	Age	0.000	0.003	0.161	8.725e-01	9.270e-01
	Age^2	-0.000	0.000	-0.222	8.245e-01	9.344e-01
	Sex	-0.001	0.003	-0.221	8.252e-01	8.800e-01
superior frontal	Intercept	0.646	0.084	7.728	1.348e-12	1.528e-11
	Age	0.001	0.002	0.486	6.279e-01	8.506e-01
	Age^2	-0.000	0.000	-0.497	6.199e-01	8.589e-01
	Sex	-0.002	0.003	-0.617	5.379e-01	8.141e-01
superior parietal	Intercept	0.584	0.099	5.875	2.543e-08	4.803e-08
	Age	0.004	0.003	1.286	2.004e-01	6.331e-01
	Age^2	-0.000	0.000	-1.388	1.671e-01	6.116e-01
	Sex	-0.004	0.003	-1.366	1.739e-01	4.927e-01
superior temporal	Intercept	0.532	0.097	5.460	1.879e-07	2.778e-07

ROI	Predictor	Estimate	Std. Error	T-Statistic	pUncorrected	pFDR
	Age	0.005	0.003	1.670	9.704e-02	6.331e-01
	Age^2	-0.000	0.000	-1.640	1.031e-01	6.116e-01
	Sex	0.002	0.003	0.479	6.327e-01	8.141e-01
supramarginal	Intercept	0.571	0.089	6.386	1.941e-09	5.499e-09
	Age	0.003	0.003	1.371	1.725e-01	6.331e-01
	Age^2	-0.000	0.000	-1.420	1.576e-01	6.116e-01
	Sex	0.001	0.003	0.184	8.541e-01	8.800e-01
temporal pole	Intercept	0.611	0.135	4.539	1.138e-05	1.488e-05
	Age	0.001	0.004	0.211	8.331e-01	9.137e-01
	Age^2	-0.000	0.000	-0.080	9.362e-01	9.796e-01
	Sex	0.008	0.004	1.749	8.228e-02	4.701e-01
transverse temporal	Intercept	0.537	0.130	4.139	5.744e-05	6.975e-05
	Age	0.006	0.004	1.725	8.655e-02	6.331e-01
	Age^2	-0.000	0.000	-1.654	1.001e-01	6.116e-01
	Sex	-0.002	0.004	-0.473	6.369e-01	8.141e-01

Table A12: Outputs of multiple regression models testing quadratic effects of age on regional cortical-adjacent WM R1 in ADCP

ROI	Predictor	Estimate	Std. Error	T-Statistic	pUncorrected	pFDR
bankssts	Intercept	1.331	0.219	6.070	9.659e-09	7.280e-08
	Age	-0.005	0.006	-0.841	4.018e-01	9.592e-01
	Age^2	0.000	0.000	0.537	5.918e-01	9.943e-01
	Sex	0.009	0.007	1.246	2.146e-01	4.776e-01
caudal anterior cingulate	Intercept	1.244	0.258	4.830	3.291e-06	4.144e-06
	Age	-0.001	0.007	-0.134	8.937e-01	9.592e-01
	Age^2	-0.000	0.000	-0.178	8.586e-01	9.943e-01
	Sex	0.005	0.008	0.590	5.559e-01	7.000e-01
caudal middle frontal	Intercept	1.254	0.211	5.949	1.769e-08	7.280e-08
	Age	-0.003	0.006	-0.464	6.430e-01	9.592e-01
	Age^2	0.000	0.000	0.028	9.777e-01	9.943e-01
	Sex	0.010	0.007	1.439	1.523e-01	4.776e-01
cuneus	Intercept	0.988	0.207	4.766	4.332e-06	5.260e-06
	Age	0.002	0.006	0.417	6.773e-01	9.592e-01
	Age^2	-0.000	0.000	-0.627	5.315e-01	9.943e-01
	Sex	-0.014	0.007	-2.089	3.837e-02	4.605e-01
entorhinal	Intercept	1.204	0.258	4.660	6.815e-06	7.724e-06
	Age	-0.004	0.007	-0.564	5.738e-01	9.592e-01
	Age^2	0.000	0.000	0.243	8.084e-01	9.943e-01
	Sex	-0.003	0.008	-0.407	6.843e-01	7.755e-01
frontal pole	Intercept	0.829	0.227	3.655	3.532e-04	3.532e-04
	Age	0.007	0.006	1.042	2.989e-01	9.592e-01
	Age^2	-0.000	0.000	-1.443	1.512e-01	9.943e-01
	Sex	0.013	0.007	1.727	8.616e-02	4.605e-01
fusiform	Intercept	1.291	0.218	5.932	1.927e-08	7.280e-08
	Age	-0.004	0.006	-0.724	4.702e-01	9.592e-01
	Age^2	0.000	0.000	0.385	7.010e-01	9.943e-01
	Sex	0.005	0.007	0.704	4.825e-01	6.310e-01

ROI	Predictor	Estimate	Std. Error	T-Statistic	pUncorrected	pFDR
inferior parietal	Intercept	1.162	0.221	5.249	5.028e-07	7.775e-07
	Age	-0.001	0.006	-0.206	8.368e-01	9.592e-01
	Age^2	-0.000	0.000	-0.117	9.072e-01	9.943e-01
	Sex	0.004	0.007	0.516	6.069e-01	7.369e-01
inferior temporal	Intercept	1.268	0.210	6.028	1.192e-08	7.280e-08
	Age	-0.004	0.006	-0.729	4.672e-01	9.592e-01
	Age^2	0.000	0.000	0.385	7.004e-01	9.943e-01
	Sex	0.008	0.007	1.182	2.392e-01	4.776e-01
insula	Intercept	1.197	0.201	5.963	1.653e-08	7.280e-08
	Age	-0.003	0.006	-0.464	6.432e-01	9.592e-01
	Age^2	0.000	0.000	0.167	8.675e-01	9.943e-01
	Sex	0.006	0.007	0.989	3.241e-01	5.247e-01
isthmus cingulate	Intercept	1.268	0.251	5.055	1.215e-06	1.721e-06
	Age	-0.002	0.007	-0.328	7.436e-01	9.592e-01
	Age^2	0.000	0.000	0.180	8.572e-01	9.943e-01
	Sex	-0.006	0.008	-0.779	4.374e-01	5.949e-01
lateral occipital	Intercept	1.104	0.193	5.720	5.441e-08	1.542e-07
	Age	-0.001	0.005	-0.140	8.892e-01	9.592e-01
	Age^2	-0.000	0.000	-0.068	9.456e-01	9.943e-01
	Sex	-0.005	0.006	-0.818	4.147e-01	5.875e-01
lateral orbitofrontal	Intercept	1.130	0.231	4.884	2.591e-06	3.403e-06
	Age	0.001	0.007	0.145	8.849e-01	9.592e-01
	Age^2	-0.000	0.000	-0.639	5.235e-01	9.943e-01
	Sex	0.008	0.008	1.054	2.936e-01	4.991e-01
lingual	Intercept	1.073	0.186	5.760	4.481e-08	1.385e-07
	Age	0.000	0.005	0.048	9.621e-01	9.621e-01
	Age^2	-0.000	0.000	-0.302	7.634e-01	9.943e-01
	Sex	-0.011	0.006	-1.884	6.146e-02	4.605e-01
medial orbitofrontal	Intercept	0.981	0.228	4.300	3.030e-05	3.219e-05
	Age	0.004	0.006	0.654	5.143e-01	9.592e-01
	Age^2	-0.000	0.000	-1.131	2.599e-01	9.943e-01

ROI	Predictor	Estimate	Std. Error	T-Statistic	pUncorrected	pFDR
	Sex	0.008	0.007	1.127	2.615e-01	4.776e-01
middle temporal	Intercept	1.407	0.212	6.643	5.070e-10	9.656e-09
	Age	-0.008	0.006	-1.376	1.709e-01	9.592e-01
	Age^2	0.000	0.000	1.030	3.045e-01	9.943e-01
	Sex	0.011	0.007	1.556	1.219e-01	4.605e-01
paracentral	Intercept	1.246	0.209	5.960	1.675e-08	7.280e-08
	Age	-0.003	0.006	-0.429	6.685e-01	9.592e-01
	Age^2	0.000	0.000	0.041	9.676e-01	9.943e-01
	Sex	0.008	0.007	1.209	2.284e-01	4.776e-01
parahippocampal	Intercept	1.048	0.242	4.336	2.622e-05	2.876e-05
	Age	0.003	0.007	0.368	7.137e-01	9.592e-01
	Age^2	-0.000	0.000	-0.649	5.175e-01	9.943e-01
	Sex	-0.002	0.008	-0.304	7.612e-01	8.088e-01
pars opercularis	Intercept	1.182	0.211	5.598	9.798e-08	2.380e-07
	Age	-0.001	0.006	-0.114	9.092e-01	9.592e-01
	Age^2	-0.000	0.000	-0.314	7.541e-01	9.943e-01
	Sex	0.014	0.007	2.004	4.686e-02	4.605e-01
pars orbitalis	Intercept	1.171	0.218	5.365	2.935e-07	5.252e-07
	Age	-0.002	0.006	-0.349	7.273e-01	9.592e-01
	Age^2	0.000	0.000	0.007	9.943e-01	9.943e-01
	Sex	0.008	0.007	1.114	2.669e-01	4.776e-01
pars triangularis	Intercept	1.256	0.221	5.692	6.218e-08	1.626e-07
	Age	-0.003	0.006	-0.454	6.503e-01	9.592e-01
	Age^2	0.000	0.000	0.017	9.867e-01	9.943e-01
	Sex	0.012	0.007	1.696	9.190e-02	4.605e-01
pericalcarine	Intercept	1.093	0.233	4.690	6.015e-06	7.052e-06
	Age	-0.001	0.007	-0.218	8.277e-01	9.592e-01
	Age^2	0.000	0.000	0.052	9.588e-01	9.943e-01
	Sex	-0.009	0.008	-1.171	2.434e-01	4.776e-01
postcentral	Intercept	1.201	0.193	6.227	4.380e-09	4.964e-08
	Age	-0.002	0.005	-0.387	6.991e-01	9.592e-01

ROI	Predictor	Estimate	Std. Error	T-Statistic	pUncorrected	pFDR
	Age^2	0.000	0.000	0.024	9.810e-01	9.943e-01
	Sex	0.005	0.006	0.847	3.983e-01	5.875e-01
posterior cingulate	Intercept	1.263	0.259	4.883	2.602e-06	3.403e-06
	Age	-0.002	0.007	-0.285	7.764e-01	9.592e-01
	Age^2	0.000	0.000	0.018	9.855e-01	9.943e-01
	Sex	0.004	0.008	0.415	6.786e-01	7.755e-01
precentral	Intercept	1.281	0.193	6.621	5.680e-10	9.656e-09
	Age	-0.004	0.005	-0.684	4.948e-01	9.592e-01
	Age^2	0.000	0.000	0.276	7.832e-01	9.943e-01
	Sex	0.009	0.006	1.380	1.696e-01	4.776e-01
precuneus	Intercept	1.202	0.229	5.256	4.880e-07	7.775e-07
	Age	-0.002	0.006	-0.243	8.085e-01	9.592e-01
	Age^2	-0.000	0.000	-0.105	9.169e-01	9.943e-01
	Sex	-0.000	0.007	-0.005	9.957e-01	9.957e-01
rostral anterior cingulate	Intercept	1.308	0.254	5.143	8.146e-07	1.204e-06
	Age	-0.004	0.007	-0.513	6.089e-01	9.592e-01
	Age^2	0.000	0.000	0.180	8.574e-01	9.943e-01
	Sex	0.012	0.008	1.389	1.670e-01	4.776e-01
rostral middle frontal	Intercept	1.219	0.224	5.431	2.159e-07	4.588e-07
	Age	-0.002	0.006	-0.321	7.489e-01	9.592e-01
	Age^2	-0.000	0.000	-0.107	9.152e-01	9.943e-01
	Sex	0.015	0.007	1.997	4.759e-02	4.605e-01
superior frontal	Intercept	1.197	0.207	5.777	4.128e-08	1.385e-07
	Age	-0.002	0.006	-0.282	7.782e-01	9.592e-01
	Age^2	-0.000	0.000	-0.174	8.619e-01	9.943e-01
	Sex	0.011	0.007	1.565	1.196e-01	4.605e-01
superior parietal	Intercept	1.106	0.211	5.249	5.031e-07	7.775e-07
	Age	0.001	0.006	0.111	9.120e-01	9.592e-01
	Age^2	-0.000	0.000	-0.475	6.352e-01	9.943e-01
	Sex	0.002	0.007	0.254	7.995e-01	8.237e-01
superior temporal	Intercept	1.107	0.199	5.570	1.117e-07	2.532e-07

ROI	Predictor	Estimate	Std. Error	T-Statistic	pUncorrected	pFDR
	Age	0.001	0.006	0.141	8.884e-01	9.592e-01
	Age^2	-0.000	0.000	-0.505	6.142e-01	9.943e-01
	Sex	0.010	0.006	1.573	1.177e-01	4.605e-01
supramarginal	Intercept	1.122	0.208	5.395	2.556e-07	5.112e-07
	Age	0.001	0.006	0.128	8.982e-01	9.592e-01
	Age^2	-0.000	0.000	-0.534	5.940e-01	9.943e-01
	Sex	0.008	0.007	1.230	2.204e-01	4.776e-01
temporal pole	Intercept	1.057	0.251	4.221	4.156e-05	4.282e-05
	Age	-0.001	0.007	-0.087	9.310e-01	9.592e-01
	Age^2	-0.000	0.000	-0.224	8.228e-01	9.943e-01
	Sex	0.007	0.008	0.883	3.788e-01	5.854e-01
transverse temporal	Intercept	1.132	0.210	5.381	2.729e-07	5.155e-07
	Age	0.001	0.006	0.103	9.184e-01	9.592e-01
	Age^2	-0.000	0.000	-0.367	7.144e-01	9.943e-01
	Sex	0.002	0.007	0.308	7.582e-01	8.088e-01

Table A13: Outputs of multiple regression models testing linear and quadratic age effects on cortical GM R1 in ADCP

ROI	Model	R^2	Adjusted R^2	F-Statistic	p-value	df	logLikelihood	AIC	BIC	# obs
bankssts	Linear	0.000	-0.013	0.03	9.69e-01	2	394.06	-780.12	-767.89	157
	Quadratic	0.005	-0.015	0.24	8.69e-01	3	394.39	-778.79	-763.51	157
caudal anterior cingulate	Linear	0.033	0.021	2.65	7.41e-02	2	288.42	-568.83	-556.61	157
	Quadratic	0.034	0.016	1.82	1.46e-01	3	288.52	-567.03	-551.75	157
caudal middle frontal	Linear	0.018	0.006	1.45	2.39e-01	2	406.36	-804.73	-792.50	157
	Quadratic	0.029	0.010	1.50	2.16e-01	3	407.19	-804.37	-789.09	157
cuneus	Linear	0.019	0.006	1.46	2.36e-01	2	361.05	-714.10	-701.87	157
	Quadratic	0.043	0.025	2.31	7.88e-02	3	363.05	-716.10	-700.82	157
entorhinal	Linear	0.021	0.008	1.62	2.02e-01	2	250.92	-493.83	-481.61	157
	Quadratic	0.021	0.002	1.09	3.55e-01	3	250.95	-491.89	-476.61	157
frontal pole	Linear	0.003	-0.010	0.23	7.96e-01	2	381.28	-754.56	-742.33	157
	Quadratic	0.007	-0.012	0.37	7.78e-01	3	381.61	-753.21	-737.93	157
fusiform	Linear	0.007	-0.006	0.54	5.84e-01	2	407.33	-806.66	-794.43	157
	Quadratic	0.014	-0.005	0.74	5.30e-01	3	407.91	-805.82	-790.54	157
inferior parietal	Linear	0.005	-0.008	0.42	6.60e-01	2	394.99	-781.97	-769.75	157
	Quadratic	0.015	-0.004	0.77	5.12e-01	3	395.74	-781.48	-766.20	157
inferior temporal	Linear	0.013	-0.000	0.98	3.79e-01	2	402.35	-796.70	-784.48	157
	Quadratic	0.016	-0.004	0.80	4.94e-01	3	402.59	-795.17	-779.89	157
insula	Linear	0.048	0.035	3.85	2.34e-02	2	399.32	-790.65	-778.42	157

ROI	Model	R^2	Adjusted R^2	F-Statistic	p-value	df	logLikelihood	AIC	BIC	# obs
	Quadratic	0.056	0.037	3.01	3.19e-02	3	400.00	-790.00	-774.72	157
isthmus cingulate	Linear	0.019	0.007	1.51	2.24e-01	2	364.15	-720.31	-708.08	157
	Quadratic	0.039	0.020	2.08	1.05e-01	3	365.76	-721.52	-706.24	157
lateral occipital	Linear	0.006	-0.007	0.47	6.24e-01	2	380.80	-753.60	-741.37	157
	Quadratic	0.013	-0.007	0.65	5.83e-01	3	381.31	-752.63	-737.34	157
lateral orbitofrontal	Linear	0.005	-0.008	0.38	6.86e-01	2	404.80	-801.60	-789.37	157
	Quadratic	0.006	-0.013	0.33	8.05e-01	3	404.92	-799.84	-784.55	157
lingual	Linear	0.063	0.051	5.20	6.52e-03	2	392.24	-776.49	-764.26	157
	Quadratic	0.070	0.052	3.86	1.07e-02	3	392.84	-775.68	-760.40	157
medial orbitofrontal	Linear	0.034	0.021	2.70	7.07e-02	2	363.68	-719.36	-707.13	157
	Quadratic	0.044	0.026	2.36	7.35e-02	3	364.53	-719.06	-703.78	157
middle temporal	Linear	0.011	-0.002	0.83	4.36e-01	2	401.84	-795.68	-783.46	157
	Quadratic	0.011	-0.009	0.55	6.47e-01	3	401.84	-793.68	-778.40	157
paracentral	Linear	0.010	-0.003	0.76	4.68e-01	2	384.05	-760.10	-747.87	157
	Quadratic	0.018	-0.002	0.92	4.35e-01	3	384.67	-759.35	-744.06	157
parahippocampal	Linear	0.047	0.035	3.79	2.46e-02	2	355.08	-702.17	-689.94	157
	Quadratic	0.047	0.029	2.54	5.86e-02	3	355.12	-700.24	-684.96	157
pars opercularis	Linear	0.004	-0.009	0.34	7.12e-01	2	401.06	-794.13	-781.90	157
	Quadratic	0.012	-0.007	0.63	5.99e-01	3	401.67	-793.35	-778.07	157
pars orbitalis	Linear	0.010	-0.002	0.81	4.46e-01	2	387.56	-767.13	-754.90	157
	Quadratic	0.010	-0.009	0.54	6.56e-01	3	387.56	-765.13	-749.85	157

ROI	Model	R^2	Adjusted R^2	F-Statistic	p-value	df	logLikelihood	AIC	BIC	# obs
pars triangularis	Linear	0.004	-0.009	0.29	7.47e-01	2	397.67	-787.33	-775.11	157
	Quadratic	0.009	-0.010	0.49	6.93e-01	3	398.11	-786.22	-770.94	157
pericalcarine	Linear	0.028	0.016	2.25	1.09e-01	2	341.53	-675.07	-662.84	157
	Quadratic	0.039	0.020	2.05	1.10e-01	3	342.36	-674.73	-659.45	157
postcentral	Linear	0.003	-0.010	0.21	8.08e-01	2	393.31	-778.62	-766.39	157
	Quadratic	0.004	-0.016	0.20	8.95e-01	3	393.40	-776.81	-761.52	157
posterior cingulate	Linear	0.100	0.089	8.57	2.95e-04	2	295.02	-582.03	-569.81	157
	Quadratic	0.100	0.083	5.69	1.02e-03	3	295.03	-580.05	-564.77	157
precentral	Linear	0.009	-0.004	0.70	4.97e-01	2	392.86	-777.72	-765.49	157
	Quadratic	0.013	-0.006	0.69	5.59e-01	3	393.20	-776.41	-761.13	157
precuneus	Linear	0.020	0.007	1.56	2.14e-01	2	392.85	-777.71	-765.48	157
	Quadratic	0.031	0.012	1.66	1.79e-01	3	393.79	-777.58	-762.30	157
rostral anterior cingulate	Linear	0.039	0.026	3.10	4.80e-02	2	190.46	-372.91	-360.69	157
	Quadratic	0.040	0.021	2.11	1.01e-01	3	190.54	-371.09	-355.80	157
rostral middle frontal	Linear	0.005	-0.008	0.39	6.74e-01	2	407.11	-806.21	-793.99	157
	Quadratic	0.005	-0.014	0.28	8.41e-01	3	407.13	-804.26	-788.98	157
superior frontal	Linear	0.003	-0.010	0.20	8.19e-01	2	418.94	-829.88	-817.65	157
	Quadratic	0.004	-0.015	0.21	8.86e-01	3	419.07	-828.13	-812.85	157
superior parietal	Linear	0.023	0.010	1.78	1.73e-01	2	391.13	-774.27	-762.04	157
	Quadratic	0.035	0.016	1.83	1.43e-01	3	392.12	-774.23	-758.95	157
superior temporal	Linear	0.003	-0.010	0.20	8.20e-01	2	393.84	-779.69	-767.46	157

ROI	Model	R^2	Adjusted R^2	F-Statistic	p-value	df	logLikelihood	AIC	BIC	# obs
	Quadratic	0.020	0.001	1.03	3.81e-01	3	395.21	-780.42	-765.14	157
supramarginal	Linear	0.003	-0.010	0.25	7.81e-01	2	407.58	-807.17	-794.94	157
	Quadratic	0.016	-0.003	0.84	4.75e-01	3	408.61	-807.22	-791.94	157
temporal pole	Linear	0.038	0.025	3.02	5.18e-02	2	344.34	-680.67	-668.45	157
	Quadratic	0.038	0.019	2.00	1.16e-01	3	344.34	-678.68	-663.40	157
transverse temporal	Linear	0.010	-0.003	0.75	4.72e-01	2	348.75	-689.49	-677.27	157
	Quadratic	0.027	0.008	1.42	2.39e-01	3	350.14	-690.28	-675.00	157

Abbreviations: df = degrees of freedom; AIC = Akaike Information Criterion; BIC = Bayesian Information Criterion; # obs = number of observations

Table A14: Outputs of multiple regression models testing linear and quadratic age effects on cortical-adjacent WM R1 in ADCP

ROI	Model	R^2	Adjusted R^2	F-Statistic	p-value	df	logLikelihood	AIC	BIC	# obs
bankssts	Linear	0.126	0.115	11.11	3.12e-05	2	267.61	-527.22	-515.00	157
	Quadratic	0.128	0.111	7.47	1.07e-04	3	267.76	-525.52	-510.24	157
caudal anterior cingulate	Linear	0.122	0.110	10.66	4.60e-05	2	242.48	-476.96	-464.74	157
	Quadratic	0.122	0.105	7.07	1.75e-04	3	242.50	-475.00	-459.72	157
caudal middle frontal	Linear	0.222	0.212	22.01	3.90e-09	2	273.92	-539.83	-527.61	157
	Quadratic	0.222	0.207	14.58	2.11e-08	3	273.92	-537.83	-522.55	157
cuneus	Linear	0.074	0.062	6.14	2.71e-03	2	276.42	-544.85	-532.62	157
	Quadratic	0.076	0.058	4.21	6.81e-03	3	276.63	-543.25	-527.97	157
entorhinal	Linear	0.122	0.111	10.73	4.35e-05	2	241.98	-475.97	-463.74	157
	Quadratic	0.123	0.105	7.13	1.63e-04	3	242.01	-474.03	-458.75	157
frontal pole	Linear	0.196	0.186	18.79	5.00e-08	2	261.42	-514.85	-502.62	157
	Quadratic	0.207	0.191	13.31	9.17e-08	3	262.48	-514.97	-499.69	157
fusiform	Linear	0.142	0.131	12.76	7.46e-06	2	268.84	-529.69	-517.46	157
	Quadratic	0.143	0.126	8.51	2.91e-05	3	268.92	-527.84	-512.56	157
inferior parietal	Linear	0.128	0.117	11.33	2.57e-05	2	266.25	-524.50	-512.28	157
	Quadratic	0.128	0.111	7.51	1.01e-04	3	266.26	-522.52	-507.24	157
inferior temporal	Linear	0.152	0.141	13.76	3.16e-06	2	274.23	-540.45	-528.23	157
	Quadratic	0.152	0.136	9.18	1.28e-05	3	274.30	-538.60	-523.32	157
insula	Linear	0.117	0.106	10.23	6.73e-05	2	281.61	-555.23	-543.00	157

ROI	Model	R^2	Adjusted R^2	F-Statistic	p-value	df	logLikelihood	AIC	BIC	# obs
	Quadratic	0.117	0.100	6.79	2.51e-04	3	281.63	-553.26	-537.98	157
isthmus cingulate	Linear	0.031	0.018	2.43	9.13e-02	2	246.60	-485.19	-472.97	157
	Quadratic	0.031	0.012	1.62	1.87e-01	3	246.61	-483.23	-467.95	157
lateral occipital	Linear	0.057	0.044	4.62	1.13e-02	2	287.83	-567.66	-555.43	157
	Quadratic	0.057	0.038	3.06	3.00e-02	3	287.83	-565.66	-550.38	157
lateral orbitofrontal	Linear	0.258	0.248	26.77	1.05e-10	2	259.10	-510.20	-497.97	157
	Quadratic	0.260	0.245	17.92	5.11e-10	3	259.31	-508.62	-493.33	157
lingual	Linear	0.092	0.081	7.83	5.77e-04	2	293.31	-578.62	-566.39	157
	Quadratic	0.093	0.075	5.22	1.85e-03	3	293.36	-576.71	-561.43	157
medial orbitofrontal	Linear	0.244	0.234	24.85	4.42e-10	2	260.94	-513.88	-501.66	157
	Quadratic	0.250	0.236	17.03	1.36e-09	3	261.60	-513.19	-497.91	157
middle temporal	Linear	0.160	0.149	14.69	1.45e-06	2	272.67	-537.35	-525.12	157
	Quadratic	0.166	0.150	10.15	3.89e-06	3	273.22	-536.43	-521.15	157
paracentral	Linear	0.183	0.173	17.30	1.67e-07	2	275.26	-542.53	-530.30	157
	Quadratic	0.183	0.167	11.46	8.05e-07	3	275.26	-540.53	-525.25	157
parahippocampal	Linear	0.095	0.084	8.11	4.49e-04	2	252.25	-496.51	-484.28	157
	Quadratic	0.098	0.080	5.53	1.25e-03	3	252.47	-494.94	-479.66	157
pars opercularis	Linear	0.226	0.216	22.47	2.74e-09	2	273.65	-539.29	-527.07	157
	Quadratic	0.226	0.211	14.92	1.43e-08	3	273.70	-537.39	-522.11	157
pars orbitalis	Linear	0.149	0.138	13.50	3.96e-06	2	268.56	-529.13	-516.90	157
	Quadratic	0.149	0.133	8.94	1.70e-05	3	268.56	-527.13	-511.85	157

ROI	Model	R^2	Adjusted R^2	F-Statistic	p-value	df	logLikelihood	AIC	BIC	# obs
pars triangularis	Linear	0.228	0.218	22.69	2.32e-09	2	266.85	-525.70	-513.47	157
	Quadratic	0.228	0.212	15.03	1.27e-08	3	266.85	-523.70	-508.42	157
pericalcarine	Linear	0.041	0.029	3.31	3.90e-02	2	258.20	-508.40	-496.17	157
	Quadratic	0.041	0.022	2.20	9.09e-02	3	258.20	-506.40	-491.12	157
postcentral	Linear	0.160	0.149	14.70	1.43e-06	2	287.95	-567.90	-555.68	157
	Quadratic	0.160	0.144	9.74	6.41e-06	3	287.95	-565.90	-550.62	157
posterior cingulate	Linear	0.091	0.079	7.70	6.47e-04	2	241.89	-475.79	-463.56	157
	Quadratic	0.091	0.073	5.10	2.15e-03	3	241.89	-473.79	-458.51	157
precentral	Linear	0.201	0.191	19.41	3.03e-08	2	287.39	-566.79	-554.56	157
	Quadratic	0.202	0.186	12.89	1.49e-07	3	287.43	-564.87	-549.59	157
precuneus	Linear	0.141	0.130	12.65	8.18e-06	2	261.18	-514.36	-502.14	157
	Quadratic	0.141	0.124	8.38	3.39e-05	3	261.19	-512.38	-497.09	157
rostral anterior cingulate	Linear	0.148	0.137	13.34	4.55e-06	2	244.53	-481.06	-468.84	157
	Quadratic	0.148	0.131	8.85	1.91e-05	3	244.55	-479.09	-463.81	157
rostral middle frontal	Linear	0.226	0.216	22.46	2.76e-09	2	264.15	-520.30	-508.08	157
	Quadratic	0.226	0.211	14.88	1.50e-08	3	264.16	-518.31	-503.03	157
superior frontal	Linear	0.239	0.229	24.15	7.53e-10	2	276.60	-545.19	-532.97	157
	Quadratic	0.239	0.224	16.01	4.20e-09	3	276.61	-543.22	-527.94	157
superior parietal	Linear	0.154	0.143	14.03	2.54e-06	2	273.98	-539.95	-527.73	157
	Quadratic	0.155	0.139	9.38	9.95e-06	3	274.09	-538.18	-522.90	157
superior temporal	Linear	0.171	0.161	15.94	5.12e-07	2	283.03	-558.05	-545.83	157

ROI	Model	R^2	Adjusted R^2	F-Statistic	p-value	df	logLikelihood	AIC	BIC	# obs
	Quadratic	0.173	0.157	10.66	2.10e-06	3	283.16	-556.31	-541.03	157
supramarginal	Linear	0.195	0.185	18.67	5.48e-08	2	275.98	-543.96	-531.73	157
	Quadratic	0.197	0.181	12.49	2.39e-07	3	276.12	-542.25	-526.97	157
temporal pole	Linear	0.124	0.113	10.93	3.63e-05	2	246.84	-485.68	-473.45	157
	Quadratic	0.125	0.107	7.26	1.38e-04	3	246.86	-483.73	-468.45	157
transverse temporal	Linear	0.088	0.076	7.43	8.32e-04	2	274.20	-540.40	-528.17	157
	Quadratic	0.089	0.071	4.97	2.56e-03	3	274.27	-538.54	-523.26	157

Abbreviations: df = degrees of freedom; AIC = Akaike Information Criterion; BIC = Bayesian Information Criterion; # obs = number of observations

Table A15: Outputs of multiple regression models testing effect of cognitive impairment on regional cortical GM R1 in ADRC/WRAP

ROI	Predictor	Estimate	Std. Error	T-Statistic	pUncorrected	pFDR
bankssts	Intercept	0.714	0.006	119.482	0.000e+00	0.000e+00
	Age	-0.000	0.000	-0.900	3.684e-01	5.465e-01
	Impairment	0.005	0.003	1.731	8.386e-02	2.046e-01
	Sex	-0.000	0.001	-0.282	7.780e-01	9.121e-01
caudal anterior cingulate	Intercept	0.679	0.010	68.720	0.000e+00	0.000e+00
	Age	0.000	0.000	1.998	4.603e-02	1.565e-01
	Impairment	0.006	0.004	1.370	1.712e-01	2.544e-01
	Sex	-0.004	0.002	-1.615	1.067e-01	2.419e-01
caudal middle frontal	Intercept	0.719	0.006	119.762	0.000e+00	0.000e+00
	Age	-0.000	0.000	-0.820	4.124e-01	5.465e-01
	Impairment	0.006	0.003	2.235	2.567e-02	1.091e-01
	Sex	-0.000	0.001	-0.216	8.287e-01	9.191e-01
cuneus	Intercept	0.743	0.008	97.936	0.000e+00	0.000e+00
	Age	-0.000	0.000	-2.063	3.940e-02	1.488e-01
	Impairment	-0.001	0.003	-0.324	7.459e-01	7.925e-01
	Sex	-0.005	0.002	-2.651	8.184e-03	9.275e-02
entorhinal	Intercept	0.774	0.014	53.938	6.906e-278	6.906e-278
	Age	0.000	0.000	0.810	4.179e-01	5.465e-01
	Impairment	0.002	0.006	0.249	8.035e-01	8.278e-01
	Sex	-0.002	0.004	-0.566	5.713e-01	7.770e-01
frontal pole	Intercept	0.684	0.006	108.957	0.000e+00	0.000e+00
	Age	-0.000	0.000	-0.826	4.091e-01	5.465e-01
	Impairment	0.004	0.003	1.436	1.513e-01	2.450e-01
	Sex	-0.003	0.002	-1.991	4.677e-02	2.388e-01
fusiform	Intercept	0.686	0.005	132.743	0.000e+00	0.000e+00
	Age	0.000	0.000	0.587	5.575e-01	7.020e-01
	Impairment	0.004	0.002	1.934	5.348e-02	1.818e-01
	Sex	-0.000	0.001	-0.285	7.761e-01	9.121e-01

ROI	Predictor	Estimate	Std. Error	T-Statistic	pUncorrected	pFDR
inferior parietal	Intercept	0.714	0.006	114.454	0.000e+00	0.000e+00
	Age	-0.000	0.000	-1.424	1.547e-01	3.287e-01
	Impairment	0.002	0.003	0.686	4.931e-01	5.925e-01
	Sex	-0.003	0.002	-1.655	9.834e-02	2.388e-01
inferior temporal	Intercept	0.670	0.005	134.292	0.000e+00	0.000e+00
	Age	0.000	0.000	1.309	1.909e-01	3.818e-01
	Impairment	0.005	0.002	2.377	1.766e-02	8.578e-02
	Sex	0.000	0.001	0.160	8.726e-01	9.271e-01
insula	Intercept	0.657	0.005	124.147	0.000e+00	0.000e+00
	Age	0.000	0.000	6.298	4.816e-10	1.637e-08
	Impairment	0.006	0.002	2.418	1.582e-02	8.578e-02
	Sex	-0.001	0.001	-1.082	2.796e-01	4.527e-01
isthmus cingulate	Intercept	0.728	0.008	93.736	0.000e+00	0.000e+00
	Age	0.000	0.000	0.154	8.775e-01	9.041e-01
	Impairment	0.005	0.003	1.367	1.721e-01	2.544e-01
	Sex	-0.002	0.002	-1.286	1.989e-01	3.381e-01
lateral occipital	Intercept	0.716	0.006	110.274	0.000e+00	0.000e+00
	Age	-0.000	0.000	-0.163	8.704e-01	9.041e-01
	Impairment	0.000	0.003	0.010	9.919e-01	9.919e-01
	Sex	-0.003	0.002	-1.781	7.522e-02	2.388e-01
lateral orbitofrontal	Intercept	0.680	0.005	137.837	0.000e+00	0.000e+00
	Age	0.000	0.000	0.910	3.630e-01	5.465e-01
	Impairment	0.001	0.002	0.547	5.842e-01	6.407e-01
	Sex	-0.002	0.001	-2.026	4.311e-02	2.388e-01
lingual	Intercept	0.719	0.006	110.870	0.000e+00	0.000e+00
	Age	-0.000	0.000	-0.829	4.076e-01	5.465e-01
	Impairment	0.002	0.003	0.602	5.470e-01	6.199e-01
	Sex	-0.003	0.002	-1.839	6.623e-02	2.388e-01
medial orbitofrontal	Intercept	0.645	0.005	122.861	0.000e+00	0.000e+00
	Age	0.000	0.000	3.801	1.541e-04	8.732e-04
	Impairment	0.004	0.002	1.690	9.147e-02	2.046e-01

ROI	Predictor	Estimate	Std. Error	T-Statistic	pUncorrected	pFDR
	Sex	-0.002	0.001	-1.318	1.879e-01	3.381e-01
middle temporal	Intercept	0.678	0.005	138.249	0.000e+00	0.000e+00
	Age	0.000	0.000	1.483	1.383e-01	3.235e-01
	Impairment	0.006	0.002	2.782	5.526e-03	4.276e-02
	Sex	-0.000	0.001	-0.351	7.258e-01	9.121e-01
paracentral	Intercept	0.753	0.007	112.935	0.000e+00	0.000e+00
	Age	-0.000	0.000	-0.423	6.725e-01	7.691e-01
	Impairment	0.002	0.003	0.673	5.011e-01	5.925e-01
	Sex	0.001	0.002	0.779	4.362e-01	6.448e-01
parahippocampal	Intercept	0.663	0.006	104.666	0.000e+00	0.000e+00
	Age	0.000	0.000	4.614	4.553e-06	3.870e-05
	Impairment	0.010	0.003	3.461	5.644e-04	1.919e-02
	Sex	-0.005	0.002	-2.896	3.879e-03	6.594e-02
pars opercularis	Intercept	0.701	0.005	131.130	0.000e+00	0.000e+00
	Age	0.000	0.000	1.913	5.612e-02	1.735e-01
	Impairment	0.006	0.002	2.739	6.288e-03	4.276e-02
	Sex	-0.002	0.001	-1.673	9.466e-02	2.388e-01
pars orbitalis	Intercept	0.695	0.006	123.499	0.000e+00	0.000e+00
	Age	0.000	0.000	0.419	6.754e-01	7.691e-01
	Impairment	0.003	0.002	1.301	1.935e-01	2.741e-01
	Sex	-0.002	0.001	-1.311	1.902e-01	3.381e-01
pars triangularis	Intercept	0.701	0.006	126.818	0.000e+00	0.000e+00
	Age	0.000	0.000	1.240	2.154e-01	3.860e-01
	Impairment	0.004	0.002	1.751	8.029e-02	2.046e-01
	Sex	-0.002	0.001	-1.722	8.546e-02	2.388e-01
pericalcarine	Intercept	0.736	0.008	92.330	0.000e+00	0.000e+00
	Age	-0.000	0.000	-0.415	6.786e-01	7.691e-01
	Impairment	0.002	0.003	0.666	5.054e-01	5.925e-01
	Sex	-0.006	0.002	-2.958	3.185e-03	6.594e-02
postcentral	Intercept	0.734	0.006	117.397	0.000e+00	0.000e+00
	Age	0.000	0.000	1.239	2.157e-01	3.860e-01

ROI	Predictor	Estimate	Std. Error	T-Statistic	pUncorrected	pFDR
	Impairment	0.004	0.003	1.574	1.158e-01	2.187e-01
	Sex	-0.000	0.002	-0.204	8.380e-01	9.191e-01
posterior cingulate	Intercept	0.704	0.012	58.599	4.349e-298	4.481e-298
	Age	0.001	0.000	2.811	5.050e-03	2.146e-02
	Impairment	0.008	0.005	1.459	1.451e-01	2.450e-01
	Sex	0.000	0.003	0.046	9.630e-01	9.895e-01
precentral	Intercept	0.759	0.007	114.218	0.000e+00	0.000e+00
	Age	-0.000	0.000	-0.100	9.208e-01	9.208e-01
	Impairment	0.005	0.003	1.671	9.518e-02	2.046e-01
	Sex	0.001	0.002	0.781	4.348e-01	6.448e-01
precuneus	Intercept	0.723	0.006	114.787	0.000e+00	0.000e+00
	Age	-0.000	0.000	-1.867	6.226e-02	1.764e-01
	Impairment	0.003	0.003	1.128	2.597e-01	3.532e-01
	Sex	-0.003	0.002	-1.944	5.216e-02	2.388e-01
rostral anterior cingulate	Intercept	0.640	0.007	97.111	0.000e+00	0.000e+00
	Age	0.000	0.000	4.889	1.212e-06	1.374e-05
	Impairment	0.009	0.003	3.240	1.243e-03	2.113e-02
	Sex	0.001	0.002	0.710	4.781e-01	6.773e-01
rostral middle frontal	Intercept	0.702	0.006	122.285	0.000e+00	0.000e+00
	Age	-0.000	0.000	-1.467	1.427e-01	3.235e-01
	Impairment	0.004	0.003	1.491	1.364e-01	2.441e-01
	Sex	-0.002	0.001	-1.554	1.206e-01	2.506e-01
superior frontal	Intercept	0.705	0.006	127.746	0.000e+00	0.000e+00
	Age	-0.000	0.000	-0.836	4.032e-01	5.465e-01
	Impairment	0.004	0.002	1.844	6.546e-02	2.023e-01
	Sex	-0.000	0.001	-0.013	9.895e-01	9.895e-01
superior parietal	Intercept	0.732	0.007	110.349	0.000e+00	0.000e+00
	Age	-0.000	0.000	-1.830	6.755e-02	1.767e-01
	Impairment	0.003	0.003	1.012	3.117e-01	4.076e-01
	Sex	-0.003	0.002	-1.820	6.918e-02	2.388e-01
superior temporal	Intercept	0.697	0.005	128.484	0.000e+00	0.000e+00

ROI	Predictor	Estimate	Std. Error	T-Statistic	pUncorrected	pFDR
	Age	0.000	0.000	3.367	7.951e-04	3.862e-03
	Impairment	0.005	0.002	2.159	3.110e-02	1.175e-01
	Sex	-0.002	0.001	-1.817	6.957e-02	2.388e-01
supramarginal	Intercept	0.706	0.006	123.929	0.000e+00	0.000e+00
	Age	0.000	0.000	0.252	8.014e-01	8.790e-01
	Impairment	0.004	0.002	1.601	1.098e-01	2.187e-01
	Sex	-0.002	0.001	-1.740	8.215e-02	2.388e-01
temporal pole	Intercept	0.648	0.006	102.837	0.000e+00	0.000e+00
	Age	0.001	0.000	5.567	3.467e-08	5.894e-07
	Impairment	0.008	0.003	2.951	3.250e-03	3.683e-02
	Sex	0.001	0.002	0.441	6.591e-01	8.619e-01
transverse temporal	Intercept	0.760	0.007	102.393	0.000e+00	0.000e+00
	Age	0.000	0.000	4.158	3.533e-05	2.402e-04
	Impairment	0.005	0.003	1.665	9.628e-02	2.046e-01
	Sex	-0.003	0.002	-1.534	1.253e-01	2.506e-01

Table A16: Outputs of multiple regression models testing effect of cognitive impairment on regional cortical-adjacent WM R1 in ADRC/WRAP

ROI	Predictor	Estimate	Std. Error	T-Statistic	pUncorrected	pFDR
bankssts	Intercept	1.128	0.071	15.933	2.925e-50	5.525e-50
	Age	0.003	0.002	1.595	1.111e-01	1.731e-01
	Age^2	-0.000	0.000	-2.695	7.168e-03	1.108e-02
	Impairment	-0.022	0.005	-4.156	3.564e-05	6.345e-05
	Sex	-0.011	0.003	-3.782	1.661e-04	4.034e-04
caudal anterior cingulate	Intercept	1.090	0.073	14.868	1.183e-44	1.490e-44
	Age	0.006	0.002	2.719	6.671e-03	4.536e-02
	Age^2	-0.000	0.000	-3.873	1.156e-04	6.551e-04
	Impairment	-0.026	0.006	-4.610	4.643e-06	1.316e-05
	Sex	-0.015	0.003	-4.815	1.736e-06	6.123e-06
caudal middle frontal	Intercept	1.114	0.064	17.397	2.785e-58	3.156e-57
	Age	0.003	0.002	1.668	9.572e-02	1.678e-01
	Age^2	-0.000	0.000	-3.085	2.100e-03	5.127e-03
	Impairment	-0.017	0.005	-3.414	6.694e-04	7.848e-04
	Sex	-0.006	0.003	-2.197	2.832e-02	3.439e-02
cuneus	Intercept	1.101	0.068	16.176	1.427e-51	3.732e-51
	Age	0.001	0.002	0.407	6.839e-01	7.143e-01
	Age^2	-0.000	0.000	-1.139	2.551e-01	2.628e-01
	Impairment	-0.014	0.005	-2.805	5.149e-03	5.305e-03
	Sex	-0.021	0.003	-7.371	3.989e-13	1.356e-11
entorhinal	Intercept	0.752	0.073	10.262	2.200e-23	2.200e-23
	Age	0.011	0.002	4.881	1.258e-06	4.277e-05
	Age^2	-0.000	0.000	-5.953	3.837e-09	1.305e-07
	Impairment	-0.046	0.006	-8.403	1.789e-16	6.083e-15
	Sex	-0.008	0.003	-2.453	1.437e-02	2.124e-02
frontal pole	Intercept	0.997	0.073	13.736	5.902e-39	6.473e-39
	Age	0.004	0.002	1.690	9.143e-02	1.678e-01
	Age^2	-0.000	0.000	-2.890	3.944e-03	7.058e-03

ROI	Predictor	Estimate	Std. Error	T-Statistic	pUncorrected	pFDR
	Impairment	-0.026	0.005	-4.821	1.693e-06	5.919e-06
	Sex	0.000	0.003	0.078	9.376e-01	9.376e-01
fusiform	Intercept	1.088	0.068	16.081	4.670e-51	1.059e-50
	Age	0.004	0.002	1.795	7.299e-02	1.678e-01
	Age^2	-0.000	0.000	-3.094	2.039e-03	5.127e-03
	Impairment	-0.025	0.005	-4.815	1.741e-06	5.919e-06
	Sex	-0.008	0.003	-2.924	3.545e-03	6.026e-03
inferior parietal	Intercept	1.102	0.071	15.519	4.665e-48	6.896e-48
	Age	0.003	0.002	1.502	1.335e-01	1.973e-01
	Age^2	-0.000	0.000	-2.679	7.518e-03	1.111e-02
	Impairment	-0.026	0.005	-4.843	1.516e-06	5.919e-06
	Sex	-0.017	0.003	-5.766	1.133e-08	7.704e-08
inferior temporal	Intercept	1.088	0.065	16.640	4.293e-54	1.825e-53
	Age	0.003	0.002	1.653	9.869e-02	1.678e-01
	Age^2	-0.000	0.000	-2.951	3.250e-03	6.500e-03
	Impairment	-0.021	0.005	-4.330	1.668e-05	3.544e-05
	Sex	-0.010	0.003	-3.501	4.880e-04	1.106e-03
insula	Intercept	1.026	0.062	16.441	5.229e-53	1.616e-52
	Age	0.004	0.002	2.090	3.695e-02	1.256e-01
	Age^2	-0.000	0.000	-3.000	2.778e-03	5.903e-03
	Impairment	-0.018	0.005	-3.933	9.072e-05	1.286e-04
	Sex	-0.008	0.003	-3.038	2.454e-03	4.635e-03
isthmus cingulate	Intercept	1.146	0.074	15.524	4.398e-48	6.797e-48
	Age	0.004	0.002	1.696	9.024e-02	1.678e-01
	Age^2	-0.000	0.000	-2.506	1.240e-02	1.686e-02
	Impairment	-0.028	0.006	-4.999	6.996e-07	3.964e-06
	Sex	-0.016	0.003	-5.148	3.263e-07	1.387e-06
lateral occipital	Intercept	1.136	0.065	17.529	4.914e-59	8.379e-58
	Age	0.001	0.002	0.394	6.933e-01	7.143e-01
	Age^2	-0.000	0.000	-1.340	1.807e-01	1.920e-01
	Impairment	-0.017	0.005	-3.465	5.573e-04	6.767e-04

ROI	Predictor	Estimate	Std. Error	T-Statistic	pUncorrected	pFDR
	Sex	-0.018	0.003	-6.530	1.122e-10	1.907e-09
lateral orbitofrontal	Intercept	0.996	0.069	14.488	1.034e-42	1.212e-42
	Age	0.007	0.002	3.188	1.484e-03	1.357e-02
	Age^2	-0.000	0.000	-4.632	4.177e-06	7.101e-05
	Impairment	-0.026	0.005	-4.935	9.606e-07	4.666e-06
	Sex	-0.005	0.003	-1.734	8.319e-02	9.753e-02
lingual	Intercept	1.106	0.066	16.675	2.751e-54	1.336e-53
	Age	0.001	0.002	0.574	5.662e-01	6.417e-01
	Age^2	-0.000	0.000	-1.424	1.548e-01	1.698e-01
	Impairment	-0.022	0.005	-4.391	1.270e-05	2.879e-05
	Sex	-0.017	0.003	-5.968	3.505e-09	2.979e-08
medial orbitofrontal	Intercept	0.999	0.069	14.428	2.084e-42	2.362e-42
	Age	0.005	0.002	2.619	8.963e-03	5.079e-02
	Age^2	-0.000	0.000	-4.031	6.056e-05	4.929e-04
	Impairment	-0.023	0.005	-4.413	1.147e-05	2.879e-05
	Sex	-0.006	0.003	-2.212	2.724e-02	3.430e-02
middle temporal	Intercept	1.123	0.066	17.023	3.287e-56	2.235e-55
	Age	0.003	0.002	1.277	2.020e-01	2.642e-01
	Age^2	-0.000	0.000	-2.620	8.957e-03	1.269e-02
	Impairment	-0.022	0.005	-4.396	1.238e-05	2.879e-05
	Sex	-0.011	0.003	-3.986	7.290e-05	1.907e-04
paracentral	Intercept	1.163	0.071	16.469	3.677e-53	1.250e-52
	Age	0.002	0.002	0.778	4.365e-01	5.300e-01
	Age^2	-0.000	0.000	-1.902	5.748e-02	6.980e-02
	Impairment	-0.022	0.005	-4.134	3.919e-05	6.345e-05
	Sex	-0.008	0.003	-2.872	4.185e-03	6.776e-03
parahippocampal	Intercept	0.952	0.076	12.535	3.197e-33	3.397e-33
	Age	0.007	0.002	3.167	1.597e-03	1.357e-02
	Age^2	-0.000	0.000	-3.987	7.249e-05	4.929e-04
	Impairment	-0.041	0.006	-7.115	2.368e-12	4.026e-11
	Sex	-0.015	0.003	-4.808	1.801e-06	6.123e-06

ROI	Predictor	Estimate	Std. Error	T-Statistic	pUncorrected	pFDR
pars opercularis	Intercept	1.105	0.068	16.250	5.674e-52	1.608e-51
	Age	0.004	0.002	1.798	7.253e-02	1.678e-01
	Age^2	-0.000	0.000	-3.084	2.111e-03	5.127e-03
	Impairment	-0.019	0.005	-3.675	2.529e-04	3.307e-04
	Sex	-0.007	0.003	-2.295	2.199e-02	2.991e-02
pars orbitalis	Intercept	1.053	0.067	15.831	1.027e-49	1.838e-49
	Age	0.004	0.002	1.748	8.079e-02	1.678e-01
	Age^2	-0.000	0.000	-3.058	2.294e-03	5.200e-03
	Impairment	-0.017	0.005	-3.383	7.488e-04	8.486e-04
	Sex	-0.004	0.003	-1.608	1.082e-01	1.187e-01
pars triangularis	Intercept	1.089	0.068	16.011	1.109e-50	2.357e-50
	Age	0.004	0.002	1.989	4.706e-02	1.455e-01
	Age^2	-0.000	0.000	-3.361	8.108e-04	3.446e-03
	Impairment	-0.022	0.005	-4.302	1.884e-05	3.768e-05
	Sex	-0.005	0.003	-1.713	8.706e-02	9.867e-02
pericalcarine	Intercept	1.080	0.073	14.806	2.429e-44	2.949e-44
	Age	0.001	0.002	0.335	7.374e-01	7.374e-01
	Age^2	-0.000	0.000	-0.983	3.257e-01	3.257e-01
	Impairment	-0.017	0.005	-3.016	2.638e-03	2.803e-03
	Sex	-0.019	0.003	-6.161	1.109e-09	1.257e-08
postcentral	Intercept	1.137	0.066	17.203	3.288e-57	2.795e-56
	Age	0.001	0.002	0.680	4.967e-01	5.823e-01
	Age^2	-0.000	0.000	-1.692	9.093e-02	1.053e-01
	Impairment	-0.016	0.005	-3.201	1.421e-03	1.559e-03
	Sex	-0.009	0.003	-3.122	1.857e-03	3.946e-03
posterior cingulate	Intercept	1.158	0.074	15.736	3.291e-49	5.595e-49
	Age	0.003	0.002	1.458	1.451e-01	2.056e-01
	Age^2	-0.000	0.000	-2.460	1.410e-02	1.844e-02
	Impairment	-0.029	0.006	-5.187	2.670e-07	1.816e-06
	Sex	-0.013	0.003	-4.112	4.306e-05	1.220e-04
precentral	Intercept	1.174	0.067	17.529	4.929e-59	8.379e-58

ROI	Predictor	Estimate	Std. Error	T-Statistic	pUncorrected	pFDR
	Age	0.001	0.002	0.530	5.963e-01	6.540e-01
	Age^2	-0.000	0.000	-1.682	9.287e-02	1.053e-01
	Impairment	-0.020	0.005	-3.933	9.081e-05	1.286e-04
	Sex	-0.006	0.003	-2.213	2.719e-02	3.430e-02
precuneus	Intercept	1.111	0.073	15.127	5.323e-46	6.961e-46
	Age	0.004	0.002	1.591	1.120e-01	1.731e-01
	Age^2	-0.000	0.000	-2.826	4.818e-03	8.191e-03
	Impairment	-0.029	0.006	-5.313	1.372e-07	1.555e-06
	Sex	-0.016	0.003	-5.172	2.883e-07	1.387e-06
rostral anterior cingulate	Intercept	1.087	0.072	15.190	2.512e-46	3.416e-46
	Age	0.005	0.002	2.170	3.027e-02	1.144e-01
	Age^2	-0.000	0.000	-3.282	1.071e-03	3.641e-03
	Impairment	-0.021	0.005	-3.952	8.396e-05	1.286e-04
	Sex	-0.005	0.003	-1.519	1.291e-01	1.330e-01
rostral middle frontal	Intercept	1.117	0.072	15.601	1.723e-48	2.790e-48
	Age	0.003	0.002	1.383	1.670e-01	2.271e-01
	Age^2	-0.000	0.000	-2.703	7.018e-03	1.108e-02
	Impairment	-0.025	0.005	-4.625	4.326e-06	1.316e-05
	Sex	-0.007	0.003	-2.306	2.137e-02	2.991e-02
superior frontal	Intercept	1.092	0.065	16.900	1.616e-55	9.157e-55
	Age	0.003	0.002	1.755	7.956e-02	1.678e-01
	Age^2	-0.000	0.000	-3.296	1.022e-03	3.641e-03
	Impairment	-0.014	0.005	-2.773	5.682e-03	5.682e-03
	Sex	-0.008	0.003	-2.978	2.985e-03	5.342e-03
superior parietal	Intercept	1.139	0.071	15.988	1.476e-50	2.952e-50
	Age	0.002	0.002	0.977	3.289e-01	4.142e-01
	Age^2	-0.000	0.000	-2.150	3.187e-02	4.013e-02
	Impairment	-0.023	0.005	-4.202	2.927e-05	5.529e-05
	Sex	-0.016	0.003	-5.462	6.161e-08	3.491e-07
superior temporal	Intercept	1.058	0.064	16.530	1.708e-53	6.452e-53
	Age	0.004	0.002	2.298	2.177e-02	1.057e-01

ROI	Predictor	Estimate	Std. Error	T-Statistic	pUncorrected	pFDR
	Age^2	-0.000	0.000	-3.456	5.751e-04	2.793e-03
	Impairment	-0.018	0.005	-3.725	2.078e-04	2.826e-04
	Sex	-0.008	0.003	-3.070	2.209e-03	4.418e-03
supramarginal	Intercept	1.085	0.071	15.291	7.339e-47	1.040e-46
	Age	0.004	0.002	1.944	5.227e-02	1.481e-01
	Age^2	-0.000	0.000	-3.125	1.836e-03	5.127e-03
	Impairment	-0.022	0.005	-4.135	3.898e-05	6.345e-05
	Sex	-0.013	0.003	-4.242	2.456e-05	7.591e-05
temporal pole	Intercept	0.848	0.070	12.144	1.993e-31	2.053e-31
	Age	0.007	0.002	3.489	5.094e-04	8.660e-03
	Age^2	-0.000	0.000	-4.462	9.190e-06	1.042e-04
	Impairment	-0.027	0.005	-5.230	2.137e-07	1.816e-06
	Sex	-0.004	0.003	-1.535	1.250e-01	1.328e-01
transverse temporal	Intercept	1.066	0.066	16.091	4.149e-51	1.008e-50
	Age	0.004	0.002	2.219	2.677e-02	1.138e-01
	Age^2	-0.000	0.000	-2.907	3.746e-03	7.058e-03
	Impairment	-0.018	0.005	-3.653	2.750e-04	3.463e-04
	Sex	-0.008	0.003	-2.798	5.250e-03	8.114e-03

Table A17: Outputs of multiple regression models testing effect of cognitive impairment on regional cortical GM R1 in ADCP

ROI	Predictor	Estimate	Std. Error	T-Statistic	pUncorrected	pFDR
bankssts	Intercept	0.714	0.006	119.482	0.000e+00	0.000e+00
	Age	-0.000	0.000	-0.900	3.684e-01	5.465e-01
	Impairment	0.005	0.003	1.731	8.386e-02	2.046e-01
	Sex	-0.000	0.001	-0.282	7.780e-01	9.121e-01
caudal anterior cingulate	Intercept	0.679	0.010	68.720	0.000e+00	0.000e+00
	Age	0.000	0.000	1.998	4.603e-02	1.565e-01
	Impairment	0.006	0.004	1.370	1.712e-01	2.544e-01
	Sex	-0.004	0.002	-1.615	1.067e-01	2.419e-01
caudal middle frontal	Intercept	0.719	0.006	119.762	0.000e+00	0.000e+00
	Age	-0.000	0.000	-0.820	4.124e-01	5.465e-01
	Impairment	0.006	0.003	2.235	2.567e-02	1.091e-01
	Sex	-0.000	0.001	-0.216	8.287e-01	9.191e-01
cuneus	Intercept	0.743	0.008	97.936	0.000e+00	0.000e+00
	Age	-0.000	0.000	-2.063	3.940e-02	1.488e-01
	Impairment	-0.001	0.003	-0.324	7.459e-01	7.925e-01
	Sex	-0.005	0.002	-2.651	8.184e-03	9.275e-02
entorhinal	Intercept	0.774	0.014	53.938	6.906e-278	6.906e-278
	Age	0.000	0.000	0.810	4.179e-01	5.465e-01
	Impairment	0.002	0.006	0.249	8.035e-01	8.278e-01
	Sex	-0.002	0.004	-0.566	5.713e-01	7.770e-01
frontal pole	Intercept	0.684	0.006	108.957	0.000e+00	0.000e+00
	Age	-0.000	0.000	-0.826	4.091e-01	5.465e-01
	Impairment	0.004	0.003	1.436	1.513e-01	2.450e-01
	Sex	-0.003	0.002	-1.991	4.677e-02	2.388e-01
fusiform	Intercept	0.686	0.005	132.743	0.000e+00	0.000e+00
	Age	0.000	0.000	0.587	5.575e-01	7.020e-01
	Impairment	0.004	0.002	1.934	5.348e-02	1.818e-01
	Sex	-0.000	0.001	-0.285	7.761e-01	9.121e-01

ROI	Predictor	Estimate	Std. Error	T-Statistic	pUncorrected	pFDR
inferior parietal	Intercept	0.714	0.006	114.454	0.000e+00	0.000e+00
	Age	-0.000	0.000	-1.424	1.547e-01	3.287e-01
	Impairment	0.002	0.003	0.686	4.931e-01	5.925e-01
	Sex	-0.003	0.002	-1.655	9.834e-02	2.388e-01
inferior temporal	Intercept	0.670	0.005	134.292	0.000e+00	0.000e+00
	Age	0.000	0.000	1.309	1.909e-01	3.818e-01
	Impairment	0.005	0.002	2.377	1.766e-02	8.578e-02
	Sex	0.000	0.001	0.160	8.726e-01	9.271e-01
insula	Intercept	0.657	0.005	124.147	0.000e+00	0.000e+00
	Age	0.000	0.000	6.298	4.816e-10	1.637e-08
	Impairment	0.006	0.002	2.418	1.582e-02	8.578e-02
	Sex	-0.001	0.001	-1.082	2.796e-01	4.527e-01
isthmus cingulate	Intercept	0.728	0.008	93.736	0.000e+00	0.000e+00
	Age	0.000	0.000	0.154	8.775e-01	9.041e-01
	Impairment	0.005	0.003	1.367	1.721e-01	2.544e-01
	Sex	-0.002	0.002	-1.286	1.989e-01	3.381e-01
lateral occipital	Intercept	0.716	0.006	110.274	0.000e+00	0.000e+00
	Age	-0.000	0.000	-0.163	8.704e-01	9.041e-01
	Impairment	0.000	0.003	0.010	9.919e-01	9.919e-01
	Sex	-0.003	0.002	-1.781	7.522e-02	2.388e-01
lateral orbitofrontal	Intercept	0.680	0.005	137.837	0.000e+00	0.000e+00
	Age	0.000	0.000	0.910	3.630e-01	5.465e-01
	Impairment	0.001	0.002	0.547	5.842e-01	6.407e-01
	Sex	-0.002	0.001	-2.026	4.311e-02	2.388e-01
lingual	Intercept	0.719	0.006	110.870	0.000e+00	0.000e+00
	Age	-0.000	0.000	-0.829	4.076e-01	5.465e-01
	Impairment	0.002	0.003	0.602	5.470e-01	6.199e-01
	Sex	-0.003	0.002	-1.839	6.623e-02	2.388e-01
medial orbitofrontal	Intercept	0.645	0.005	122.861	0.000e+00	0.000e+00
	Age	0.000	0.000	3.801	1.541e-04	8.732e-04
	Impairment	0.004	0.002	1.690	9.147e-02	2.046e-01

ROI	Predictor	Estimate	Std. Error	T-Statistic	pUncorrected	pFDR
	Sex	-0.002	0.001	-1.318	1.879e-01	3.381e-01
middle temporal	Intercept	0.678	0.005	138.249	0.000e+00	0.000e+00
	Age	0.000	0.000	1.483	1.383e-01	3.235e-01
	Impairment	0.006	0.002	2.782	5.526e-03	4.276e-02
	Sex	-0.000	0.001	-0.351	7.258e-01	9.121e-01
paracentral	Intercept	0.753	0.007	112.935	0.000e+00	0.000e+00
	Age	-0.000	0.000	-0.423	6.725e-01	7.691e-01
	Impairment	0.002	0.003	0.673	5.011e-01	5.925e-01
	Sex	0.001	0.002	0.779	4.362e-01	6.448e-01
parahippocampal	Intercept	0.663	0.006	104.666	0.000e+00	0.000e+00
	Age	0.000	0.000	4.614	4.553e-06	3.870e-05
	Impairment	0.010	0.003	3.461	5.644e-04	1.919e-02
	Sex	-0.005	0.002	-2.896	3.879e-03	6.594e-02
pars opercularis	Intercept	0.701	0.005	131.130	0.000e+00	0.000e+00
	Age	0.000	0.000	1.913	5.612e-02	1.735e-01
	Impairment	0.006	0.002	2.739	6.288e-03	4.276e-02
	Sex	-0.002	0.001	-1.673	9.466e-02	2.388e-01
pars orbitalis	Intercept	0.695	0.006	123.499	0.000e+00	0.000e+00
	Age	0.000	0.000	0.419	6.754e-01	7.691e-01
	Impairment	0.003	0.002	1.301	1.935e-01	2.741e-01
	Sex	-0.002	0.001	-1.311	1.902e-01	3.381e-01
pars triangularis	Intercept	0.701	0.006	126.818	0.000e+00	0.000e+00
	Age	0.000	0.000	1.240	2.154e-01	3.860e-01
	Impairment	0.004	0.002	1.751	8.029e-02	2.046e-01
	Sex	-0.002	0.001	-1.722	8.546e-02	2.388e-01
pericalcarine	Intercept	0.736	0.008	92.330	0.000e+00	0.000e+00
	Age	-0.000	0.000	-0.415	6.786e-01	7.691e-01
	Impairment	0.002	0.003	0.666	5.054e-01	5.925e-01
	Sex	-0.006	0.002	-2.958	3.185e-03	6.594e-02
postcentral	Intercept	0.734	0.006	117.397	0.000e+00	0.000e+00
	Age	0.000	0.000	1.239	2.157e-01	3.860e-01

ROI	Predictor	Estimate	Std. Error	T-Statistic	pUncorrected	pFDR
	Impairment	0.004	0.003	1.574	1.158e-01	2.187e-01
	Sex	-0.000	0.002	-0.204	8.380e-01	9.191e-01
posterior cingulate	Intercept	0.704	0.012	58.599	4.349e-298	4.481e-298
	Age	0.001	0.000	2.811	5.050e-03	2.146e-02
	Impairment	0.008	0.005	1.459	1.451e-01	2.450e-01
	Sex	0.000	0.003	0.046	9.630e-01	9.895e-01
precentral	Intercept	0.759	0.007	114.218	0.000e+00	0.000e+00
	Age	-0.000	0.000	-0.100	9.208e-01	9.208e-01
	Impairment	0.005	0.003	1.671	9.518e-02	2.046e-01
	Sex	0.001	0.002	0.781	4.348e-01	6.448e-01
precuneus	Intercept	0.723	0.006	114.787	0.000e+00	0.000e+00
	Age	-0.000	0.000	-1.867	6.226e-02	1.764e-01
	Impairment	0.003	0.003	1.128	2.597e-01	3.532e-01
	Sex	-0.003	0.002	-1.944	5.216e-02	2.388e-01
rostral anterior cingulate	Intercept	0.640	0.007	97.111	0.000e+00	0.000e+00
	Age	0.000	0.000	4.889	1.212e-06	1.374e-05
	Impairment	0.009	0.003	3.240	1.243e-03	2.113e-02
	Sex	0.001	0.002	0.710	4.781e-01	6.773e-01
rostral middle frontal	Intercept	0.702	0.006	122.285	0.000e+00	0.000e+00
	Age	-0.000	0.000	-1.467	1.427e-01	3.235e-01
	Impairment	0.004	0.003	1.491	1.364e-01	2.441e-01
	Sex	-0.002	0.001	-1.554	1.206e-01	2.506e-01
superior frontal	Intercept	0.705	0.006	127.746	0.000e+00	0.000e+00
	Age	-0.000	0.000	-0.836	4.032e-01	5.465e-01
	Impairment	0.004	0.002	1.844	6.546e-02	2.023e-01
	Sex	-0.000	0.001	-0.013	9.895e-01	9.895e-01
superior parietal	Intercept	0.732	0.007	110.349	0.000e+00	0.000e+00
	Age	-0.000	0.000	-1.830	6.755e-02	1.767e-01
	Impairment	0.003	0.003	1.012	3.117e-01	4.076e-01
	Sex	-0.003	0.002	-1.820	6.918e-02	2.388e-01
superior temporal	Intercept	0.697	0.005	128.484	0.000e+00	0.000e+00

ROI	Predictor	Estimate	Std. Error	T-Statistic	pUncorrected	pFDR
	Age	0.000	0.000	3.367	7.951e-04	3.862e-03
	Impairment	0.005	0.002	2.159	3.110e-02	1.175e-01
	Sex	-0.002	0.001	-1.817	6.957e-02	2.388e-01
supramarginal	Intercept	0.706	0.006	123.929	0.000e+00	0.000e+00
	Age	0.000	0.000	0.252	8.014e-01	8.790e-01
	Impairment	0.004	0.002	1.601	1.098e-01	2.187e-01
	Sex	-0.002	0.001	-1.740	8.215e-02	2.388e-01
temporal pole	Intercept	0.648	0.006	102.837	0.000e+00	0.000e+00
	Age	0.001	0.000	5.567	3.467e-08	5.894e-07
	Impairment	0.008	0.003	2.951	3.250e-03	3.683e-02
	Sex	0.001	0.002	0.441	6.591e-01	8.619e-01
transverse temporal	Intercept	0.760	0.007	102.393	0.000e+00	0.000e+00
	Age	0.000	0.000	4.158	3.533e-05	2.402e-04
	Impairment	0.005	0.003	1.665	9.628e-02	2.046e-01
	Sex	-0.003	0.002	-1.534	1.253e-01	2.506e-01

Table A18: Outputs of multiple regression models testing effect of cognitive impairment on regional cortical-adjacent WM R1 in ADCP

ROI	Predictor	Estimate	Std. Error	T-Statistic	pUncorrected	pFDR
bankssts	Intercept	1.212	0.031	38.648	7.734e-81	1.315e-80
	Age	-0.002	0.000	-4.029	8.812e-05	1.198e-04
	Impairment	-0.004	0.008	-0.479	6.324e-01	9.787e-01
	Sex	0.009	0.007	1.195	2.339e-01	4.265e-01
caudal anterior cingulate	Intercept	1.293	0.037	35.164	3.419e-75	4.305e-75
	Age	-0.002	0.001	-4.464	1.553e-05	2.400e-05
	Impairment	0.005	0.009	0.619	5.367e-01	9.787e-01
	Sex	0.006	0.008	0.652	5.157e-01	6.422e-01
caudal middle frontal	Intercept	1.249	0.030	41.449	4.392e-85	1.989e-84
	Age	-0.003	0.000	-6.031	1.177e-08	5.717e-08
	Impairment	0.001	0.007	0.164	8.700e-01	9.787e-01
	Sex	0.010	0.007	1.449	1.495e-01	4.265e-01
cuneus	Intercept	1.120	0.030	37.801	1.670e-79	2.469e-79
	Age	-0.001	0.000	-3.059	2.625e-03	2.879e-03
	Impairment	0.005	0.007	0.662	5.092e-01	9.787e-01
	Sex	-0.014	0.007	-2.015	4.563e-02	3.960e-01
entorhinal	Intercept	1.129	0.036	30.987	8.071e-68	8.071e-68
	Age	-0.002	0.001	-3.832	1.850e-04	2.419e-04
	Impairment	-0.018	0.009	-2.082	3.900e-02	9.633e-01
	Sex	-0.005	0.008	-0.631	5.289e-01	6.422e-01
frontal pole	Intercept	1.162	0.032	35.959	1.615e-76	2.112e-76
	Age	-0.003	0.000	-5.978	1.532e-08	6.511e-08
	Impairment	0.013	0.008	1.734	8.500e-02	9.633e-01
	Sex	0.014	0.007	1.888	6.093e-02	3.960e-01
fusiform	Intercept	1.205	0.031	38.749	5.386e-81	9.638e-81
	Age	-0.002	0.000	-4.473	1.497e-05	2.400e-05
	Impairment	-0.005	0.007	-0.630	5.295e-01	9.787e-01
	Sex	0.005	0.007	0.638	5.243e-01	6.422e-01

ROI	Predictor	Estimate	Std. Error	T-Statistic	pUncorrected	pFDR
inferior parietal	Intercept	1.185	0.032	37.465	5.722e-79	8.106e-79
	Age	-0.002	0.000	-4.262	3.527e-05	4.997e-05
	Impairment	-0.004	0.008	-0.542	5.888e-01	9.787e-01
	Sex	0.003	0.007	0.453	6.511e-01	7.184e-01
inferior temporal	Intercept	1.188	0.030	39.472	4.114e-82	9.325e-82
	Age	-0.002	0.000	-4.705	5.640e-06	1.065e-05
	Impairment	-0.000	0.007	-0.029	9.766e-01	9.787e-01
	Sex	0.008	0.007	1.177	2.411e-01	4.265e-01
insula	Intercept	1.170	0.029	41.003	2.006e-84	6.820e-84
	Age	-0.002	0.000	-4.496	1.358e-05	2.309e-05
	Impairment	0.009	0.007	1.321	1.886e-01	9.787e-01
	Sex	0.007	0.007	1.134	2.587e-01	4.265e-01
isthmus cingulate	Intercept	1.226	0.036	34.172	1.669e-73	1.892e-73
	Age	-0.001	0.001	-2.123	3.540e-02	3.540e-02
	Impairment	0.003	0.009	0.319	7.499e-01	9.787e-01
	Sex	-0.006	0.008	-0.737	4.620e-01	6.283e-01
lateral occipital	Intercept	1.117	0.028	40.474	1.237e-83	3.823e-83
	Age	-0.001	0.000	-2.833	5.230e-03	5.557e-03
	Impairment	-0.000	0.007	-0.041	9.677e-01	9.787e-01
	Sex	-0.005	0.006	-0.819	4.143e-01	5.869e-01
lateral orbitofrontal	Intercept	1.281	0.033	38.749	5.379e-81	9.638e-81
	Age	-0.003	0.000	-6.990	7.949e-11	2.703e-09
	Impairment	0.006	0.008	0.774	4.401e-01	9.787e-01
	Sex	0.009	0.008	1.122	2.634e-01	4.265e-01
lingual	Intercept	1.130	0.027	42.407	1.757e-86	1.493e-85
	Age	-0.001	0.000	-3.533	5.434e-04	6.371e-04
	Impairment	0.001	0.006	0.214	8.306e-01	9.787e-01
	Sex	-0.011	0.006	-1.854	6.562e-02	3.960e-01
medial orbitofrontal	Intercept	1.242	0.033	38.037	7.040e-80	1.088e-79
	Age	-0.003	0.000	-6.789	2.344e-10	3.985e-09
	Impairment	0.008	0.008	0.979	3.293e-01	9.787e-01

ROI	Predictor	Estimate	Std. Error	T-Statistic	pUncorrected	pFDR
	Sex	0.009	0.007	1.208	2.288e-01	4.265e-01
middle temporal	Intercept	1.192	0.030	39.230	9.659e-82	2.053e-81
	Age	-0.002	0.000	-4.805	3.667e-06	7.792e-06
	Impairment	0.001	0.007	0.179	8.580e-01	9.787e-01
	Sex	0.011	0.007	1.576	1.171e-01	4.265e-01
paracentral	Intercept	1.238	0.030	41.430	4.679e-85	1.989e-84
	Age	-0.002	0.000	-5.359	3.018e-07	9.328e-07
	Impairment	0.001	0.007	0.124	9.017e-01	9.787e-01
	Sex	0.008	0.007	1.216	2.257e-01	4.265e-01
parahippocampal	Intercept	1.196	0.034	34.735	1.818e-74	2.131e-74
	Age	-0.002	0.000	-3.466	6.851e-04	7.764e-04
	Impairment	-0.010	0.008	-1.249	2.137e-01	9.787e-01
	Sex	-0.004	0.008	-0.448	6.550e-01	7.184e-01
pars opercularis	Intercept	1.252	0.030	41.551	3.107e-85	1.761e-84
	Age	-0.003	0.000	-6.116	7.661e-09	4.341e-08
	Impairment	0.006	0.007	0.835	4.051e-01	9.787e-01
	Sex	0.014	0.007	2.082	3.905e-02	3.960e-01
pars orbitalis	Intercept	1.178	0.031	38.151	4.653e-80	7.533e-80
	Age	-0.002	0.000	-5.262	4.738e-07	1.342e-06
	Impairment	0.013	0.007	1.746	8.282e-02	9.633e-01
	Sex	0.009	0.007	1.307	1.931e-01	4.265e-01
pars triangularis	Intercept	1.258	0.031	40.099	4.553e-83	1.191e-82
	Age	-0.003	0.000	-6.390	1.899e-09	1.614e-08
	Impairment	0.009	0.008	1.213	2.269e-01	9.787e-01
	Sex	0.013	0.007	1.825	6.989e-02	3.960e-01
pericalcarine	Intercept	1.081	0.033	32.440	1.824e-70	1.938e-70
	Age	-0.001	0.000	-2.271	2.454e-02	2.528e-02
	Impairment	-0.000	0.008	-0.027	9.787e-01	9.787e-01
	Sex	-0.009	0.008	-1.166	2.453e-01	4.265e-01
postcentral	Intercept	1.200	0.028	43.583	3.678e-88	6.253e-87
	Age	-0.002	0.000	-5.202	6.235e-07	1.631e-06

ROI	Predictor	Estimate	Std. Error	T-Statistic	pUncorrected	pFDR
	Impairment	0.005	0.007	0.711	4.783e-01	9.787e-01
	Sex	0.006	0.006	0.921	3.588e-01	5.373e-01
posterior cingulate	Intercept	1.261	0.037	34.118	2.067e-73	2.267e-73
	Age	-0.002	0.001	-3.772	2.312e-04	2.911e-04
	Impairment	0.004	0.009	0.401	6.890e-01	9.787e-01
	Sex	0.004	0.008	0.456	6.487e-01	7.184e-01
precentral	Intercept	1.230	0.028	44.490	1.977e-89	6.722e-88
	Age	-0.002	0.000	-5.733	5.113e-08	1.932e-07
	Impairment	0.003	0.007	0.410	6.827e-01	9.787e-01
	Sex	0.009	0.006	1.421	1.574e-01	4.265e-01
precuneus	Intercept	1.223	0.033	37.434	6.430e-79	8.745e-79
	Age	-0.002	0.000	-4.632	7.690e-06	1.376e-05
	Impairment	-0.003	0.008	-0.414	6.791e-01	9.787e-01
	Sex	-0.000	0.008	-0.052	9.590e-01	9.590e-01
rostral anterior cingulate	Intercept	1.266	0.036	34.881	1.028e-74	1.248e-74
	Age	-0.002	0.001	-4.761	4.436e-06	8.872e-06
	Impairment	0.005	0.009	0.630	5.294e-01	9.787e-01
	Sex	0.012	0.008	1.453	1.483e-01	4.265e-01
rostral middle frontal	Intercept	1.249	0.032	39.104	1.516e-81	3.032e-81
	Age	-0.003	0.000	-6.233	4.246e-09	2.887e-08
	Impairment	0.009	0.008	1.178	2.408e-01	9.787e-01
	Sex	0.016	0.007	2.120	3.564e-02	3.960e-01
superior frontal	Intercept	1.237	0.030	41.857	1.107e-85	7.528e-85
	Age	-0.003	0.000	-6.522	9.551e-10	1.082e-08
	Impairment	0.006	0.007	0.861	3.908e-01	9.787e-01
	Sex	0.011	0.007	1.650	1.010e-01	4.265e-01
superior parietal	Intercept	1.203	0.030	39.940	7.922e-83	1.924e-82
	Age	-0.002	0.000	-4.894	2.486e-06	5.635e-06
	Impairment	-0.002	0.007	-0.276	7.832e-01	9.787e-01
	Sex	0.001	0.007	0.216	8.291e-01	8.542e-01
superior temporal	Intercept	1.208	0.028	42.453	1.507e-86	1.493e-85

ROI	Predictor	Estimate	Std. Error	T-Statistic	pUncorrected	pFDR
	Age	-0.002	0.000	-5.019	1.429e-06	3.470e-06
	Impairment	0.001	0.007	0.150	8.807e-01	9.787e-01
	Sex	0.010	0.007	1.572	1.180e-01	4.265e-01
supramarginal	Intercept	1.231	0.030	41.380	5.539e-85	2.093e-84
	Age	-0.002	0.000	-5.507	1.505e-07	5.117e-07
	Impairment	-0.001	0.007	-0.105	9.161e-01	9.787e-01
	Sex	0.008	0.007	1.203	2.308e-01	4.265e-01
temporal pole	Intercept	1.115	0.036	31.144	4.138e-68	4.263e-68
	Age	-0.002	0.001	-4.359	2.383e-05	3.523e-05
	Impairment	0.003	0.009	0.342	7.328e-01	9.787e-01
	Sex	0.007	0.008	0.911	3.635e-01	5.373e-01
transverse temporal	Intercept	1.211	0.030	40.279	2.436e-83	6.902e-83
	Age	-0.002	0.000	-3.756	2.445e-04	2.969e-04
	Impairment	0.004	0.007	0.501	6.170e-01	9.787e-01
	Sex	0.002	0.007	0.355	7.228e-01	7.680e-01

Table A19: Outputs of regression models testing effects of GM R1 on Dimensional Change Card Sort test performance

ROI	Predictor	Estimate	Std. Error	T-Statistic	pUncorrected	pFDR
antcingulate	Intercept	148.874	17.677	8.422	4.288e-14	2.144e-13
	Age	-0.474	0.119	-3.995	1.049e-04	1.311e-04
	Sex	-1.269	1.972	-0.644	5.209e-01	5.943e-01
	Education	0.496	0.402	1.234	2.193e-01	2.193e-01
	Regional R1	-41.506	21.744	-1.909	5.836e-02	6.089e-02
frontal	Intercept	196.914	40.767	4.830	3.577e-06	3.577e-06
	Age	-0.525	0.117	-4.497	1.449e-05	3.983e-05
	Sex	-1.738	1.980	-0.878	3.816e-01	5.943e-01
	Education	0.536	0.401	1.338	1.830e-01	2.193e-01
	Regional R1	-105.757	55.964	-1.890	6.089e-02	6.089e-02
parietal	Intercept	195.868	37.684	5.198	7.113e-07	8.891e-07
	Age	-0.521	0.116	-4.474	1.593e-05	3.983e-05
	Sex	-1.585	1.970	-0.805	4.224e-01	5.943e-01
	Education	0.555	0.399	1.391	1.665e-01	2.193e-01
	Regional R1	-105.324	51.898	-2.029	4.434e-02	6.089e-02
postcingulate	Intercept	183.290	25.600	7.160	4.374e-11	1.094e-10
	Age	-0.429	0.120	-3.582	4.719e-04	4.719e-04
	Sex	-1.707	1.953	-0.874	3.836e-01	5.943e-01
	Education	0.571	0.395	1.445	1.507e-01	2.193e-01
	Regional R1	-93.163	35.541	-2.621	9.743e-03	2.436e-02
temporal	Intercept	206.157	32.090	6.424	1.992e-09	3.320e-09
	Age	-0.478	0.116	-4.131	6.229e-05	1.038e-04
	Sex	-1.040	1.948	-0.534	5.943e-01	5.943e-01
	Education	0.540	0.395	1.368	1.736e-01	2.193e-01
	Regional R1	-122.692	44.351	-2.766	6.445e-03	2.436e-02

Table A20: Outputs of regression models testing effects of WM R1 on Dimensional Change Card Sort test performance

ROI	Predictor	Estimate	Std. Error	T-Statistic	pUncorrected	pFDR
antcingulate	Intercept	123.119	27.464	4.483	1.534e-05	7.670e-05
	Age	-0.516	0.127	-4.077	7.659e-05	1.915e-04
	Sex	-1.388	2.004	-0.692	4.899e-01	5.108e-01
	Education	0.582	0.405	1.436	1.533e-01	1.544e-01
	Regional R1	-0.187	19.522	-0.010	9.924e-01	9.924e-01
frontal	Intercept	129.338	31.000	4.172	5.308e-05	8.847e-05
	Age	-0.530	0.134	-3.963	1.182e-04	1.970e-04
	Sex	-1.329	2.015	-0.659	5.108e-01	5.108e-01
	Education	0.580	0.405	1.432	1.544e-01	1.544e-01
	Regional R1	-5.169	23.070	-0.224	8.230e-01	9.924e-01
parietal	Intercept	94.267	31.247	3.017	3.042e-03	3.802e-03
	Age	-0.463	0.129	-3.582	4.724e-04	5.905e-04
	Sex	-1.526	1.995	-0.765	4.456e-01	5.108e-01
	Education	0.593	0.404	1.468	1.445e-01	1.544e-01
	Regional R1	23.454	23.855	0.983	3.272e-01	8.180e-01
postcingulate	Intercept	113.560	26.632	4.264	3.701e-05	8.847e-05
	Age	-0.504	0.122	-4.140	6.023e-05	1.915e-04
	Sex	-1.391	1.996	-0.697	4.872e-01	5.108e-01
	Education	0.582	0.405	1.437	1.528e-01	1.544e-01
	Regional R1	7.512	19.394	0.387	6.991e-01	9.924e-01
temporal	Intercept	83.539	30.219	2.764	6.482e-03	6.482e-03
	Age	-0.447	0.127	-3.514	5.966e-04	5.966e-04
	Sex	-1.594	1.988	-0.802	4.241e-01	5.108e-01
	Education	0.579	0.402	1.440	1.521e-01	1.544e-01
	Regional R1	33.266	23.686	1.404	1.624e-01	8.120e-01

Table A21: Outputs of regression models testing effects of GM R1 on List Sorting test performance

ROI	Predictor	Estimate	Std. Error	T-Statistic	pUncorrected	pFDR
antcingulate	Intercept	148.994	21.698	6.867	2.279e-10	1.140e-09
	Age	-0.655	0.146	-4.479	1.599e-05	1.999e-05
	Sex	2.853	2.455	1.162	2.472e-01	3.607e-01
	Education	1.006	0.499	2.017	4.573e-02	4.573e-02
	Regional R1	-42.471	26.658	-1.593	1.135e-01	1.680e-01
frontal	Intercept	196.617	51.205	3.840	1.897e-04	1.897e-04
	Age	-0.707	0.144	-4.912	2.604e-06	6.510e-06
	Sex	2.273	2.478	0.917	3.607e-01	3.607e-01
	Education	1.044	0.498	2.098	3.776e-02	4.573e-02
	Regional R1	-105.860	70.279	-1.506	1.344e-01	1.680e-01
parietal	Intercept	214.738	47.087	4.560	1.145e-05	1.431e-05
	Age	-0.706	0.143	-4.942	2.285e-06	6.510e-06
	Sex	2.345	2.448	0.958	3.397e-01	3.607e-01
	Education	1.056	0.493	2.140	3.416e-02	4.573e-02
	Regional R1	-132.911	64.796	-2.051	4.221e-02	1.055e-01
postcingulate	Intercept	158.335	32.205	4.916	2.552e-06	4.253e-06
	Age	-0.646	0.150	-4.308	3.179e-05	3.179e-05
	Sex	2.546	2.470	1.031	3.044e-01	3.607e-01
	Education	1.081	0.498	2.171	3.169e-02	4.573e-02
	Regional R1	-55.281	44.655	-1.238	2.179e-01	2.179e-01
temporal	Intercept	229.266	40.091	5.719	6.761e-08	1.690e-07
	Age	-0.650	0.142	-4.581	1.053e-05	1.755e-05
	Sex	2.968	2.407	1.233	2.198e-01	3.607e-01
	Education	1.037	0.487	2.131	3.494e-02	4.573e-02
	Regional R1	-157.368	55.537	-2.834	5.321e-03	2.661e-02

Table A22: Outputs of regression models testing effects of WM R1 on List Sorting test performance

ROI	Predictor	Estimate	Std. Error	T-Statistic	pUncorrected	pFDR
antcingulate	Intercept	96.501	28.531	3.382	8.779e-04	1.463e-03
	Age	-0.676	0.131	-5.178	5.854e-07	1.464e-06
	Sex	3.950	2.031	1.945	5.327e-02	5.327e-02
	Education	1.127	0.412	2.737	6.808e-03	6.997e-03
	Regional R1	21.832	19.968	1.093	2.757e-01	4.294e-01
frontal	Intercept	109.515	32.309	3.390	8.562e-04	1.463e-03
	Age	-0.697	0.139	-5.008	1.282e-06	2.137e-06
	Sex	4.044	2.047	1.976	4.966e-02	5.327e-02
	Education	1.127	0.413	2.728	6.997e-03	6.997e-03
	Regional R1	12.117	23.611	0.513	6.084e-01	6.084e-01
parietal	Intercept	83.116	33.193	2.504	1.315e-02	1.357e-02
	Age	-0.651	0.134	-4.855	2.565e-06	2.565e-06
	Sex	4.102	2.015	2.036	4.321e-02	5.327e-02
	Education	1.146	0.412	2.785	5.919e-03	6.997e-03
	Regional R1	33.615	24.965	1.347	1.798e-01	4.294e-01
postcingulate	Intercept	101.481	27.350	3.710	2.739e-04	1.370e-03
	Age	-0.703	0.124	-5.673	5.363e-08	2.681e-07
	Sex	4.173	2.019	2.067	4.014e-02	5.327e-02
	Education	1.130	0.412	2.740	6.746e-03	6.997e-03
	Regional R1	18.587	19.572	0.950	3.435e-01	4.294e-01
temporal	Intercept	79.262	31.800	2.493	1.357e-02	1.357e-02
	Age	-0.647	0.132	-4.908	2.016e-06	2.520e-06
	Sex	3.962	2.017	1.965	5.097e-02	5.327e-02
	Education	1.136	0.411	2.767	6.231e-03	6.997e-03
	Regional R1	37.717	24.424	1.544	1.242e-01	4.294e-01

Table A23: Outputs of regression models testing effects of GM R1 on Pattern Comparison test performance

ROI	Predictor	Estimate	Std. Error	T-Statistic	pUncorrected	pFDR
antcingulate	Intercept	143.340	24.185	5.927	2.349e-08	1.175e-07
	Age	-0.787	0.163	-4.834	3.512e-06	4.390e-06
	Sex	4.268	2.694	1.584	1.154e-01	1.514e-01
	Education	0.937	0.550	1.702	9.105e-02	9.105e-02
	Regional R1	-31.787	29.800	-1.067	2.880e-01	6.155e-01
frontal	Intercept	132.482	55.795	2.374	1.895e-02	1.895e-02
	Age	-0.820	0.161	-5.104	1.083e-06	2.743e-06
	Sex	4.148	2.715	1.528	1.288e-01	1.514e-01
	Education	0.999	0.550	1.817	7.139e-02	9.105e-02
	Regional R1	-12.991	76.813	-0.169	8.659e-01	9.516e-01
parietal	Intercept	126.403	51.547	2.452	1.545e-02	1.895e-02
	Age	-0.819	0.161	-5.101	1.097e-06	2.743e-06
	Sex	4.182	2.707	1.545	1.246e-01	1.514e-01
	Education	1.003	0.549	1.827	6.985e-02	9.105e-02
	Regional R1	-4.330	71.240	-0.061	9.516e-01	9.516e-01
postcingulate	Intercept	171.255	35.397	4.838	3.457e-06	8.643e-06
	Age	-0.750	0.166	-4.529	1.270e-05	1.270e-05
	Sex	3.881	2.691	1.443	1.514e-01	1.514e-01
	Education	0.986	0.545	1.810	7.250e-02	9.105e-02
	Regional R1	-73.537	49.063	-1.499	1.362e-01	6.155e-01
temporal	Intercept	161.359	44.847	3.598	4.459e-04	7.432e-04
	Age	-0.801	0.161	-4.961	2.031e-06	3.385e-06
	Sex	4.330	2.701	1.603	1.112e-01	1.514e-01
	Education	0.982	0.548	1.792	7.538e-02	9.105e-02
	Regional R1	-55.968	62.137	-0.901	3.693e-01	6.155e-01

Table A24: Outputs of regression models testing effects of WM R1 on Pattern Comparison test performance

ROI	Predictor	Estimate	Std. Error	T-Statistic	pUncorrected	pFDR
antcingulate	Intercept	78.216	31.185	2.508	1.297e-02	3.243e-02
	Age	-0.687	0.145	-4.740	4.165e-06	1.041e-05
	Sex	4.811	2.244	2.144	3.327e-02	4.605e-02
	Education	0.596	0.455	1.308	1.923e-01	1.923e-01
	Regional R1	38.939	21.993	1.771	7.823e-02	7.823e-02
frontal	Intercept	49.838	34.342	1.451	1.484e-01	2.473e-01
	Age	-0.604	0.152	-3.978	9.850e-05	9.850e-05
	Sex	4.310	2.246	1.919	5.652e-02	5.652e-02
	Education	0.599	0.452	1.325	1.867e-01	1.923e-01
	Regional R1	62.500	25.321	2.468	1.445e-02	2.408e-02
parietal	Intercept	29.422	34.169	0.861	3.903e-01	3.903e-01
	Age	-0.597	0.145	-4.119	5.671e-05	7.089e-05
	Sex	4.801	2.190	2.192	2.959e-02	4.605e-02
	Education	0.609	0.448	1.359	1.757e-01	1.923e-01
	Regional R1	80.926	25.911	3.123	2.068e-03	5.170e-03
postcingulate	Intercept	75.752	29.864	2.537	1.200e-02	3.243e-02
	Age	-0.720	0.138	-5.223	4.589e-07	2.295e-06
	Sex	5.227	2.216	2.358	1.938e-02	4.605e-02
	Education	0.600	0.455	1.321	1.882e-01	1.923e-01
	Regional R1	42.139	21.530	1.957	5.177e-02	6.471e-02
temporal	Intercept	29.813	33.644	0.886	3.767e-01	3.903e-01
	Age	-0.603	0.144	-4.201	4.072e-05	6.787e-05
	Sex	4.613	2.194	2.102	3.684e-02	4.605e-02
	Education	0.595	0.448	1.329	1.854e-01	1.923e-01
	Regional R1	82.467	26.039	3.167	1.793e-03	5.170e-03

Appendix B

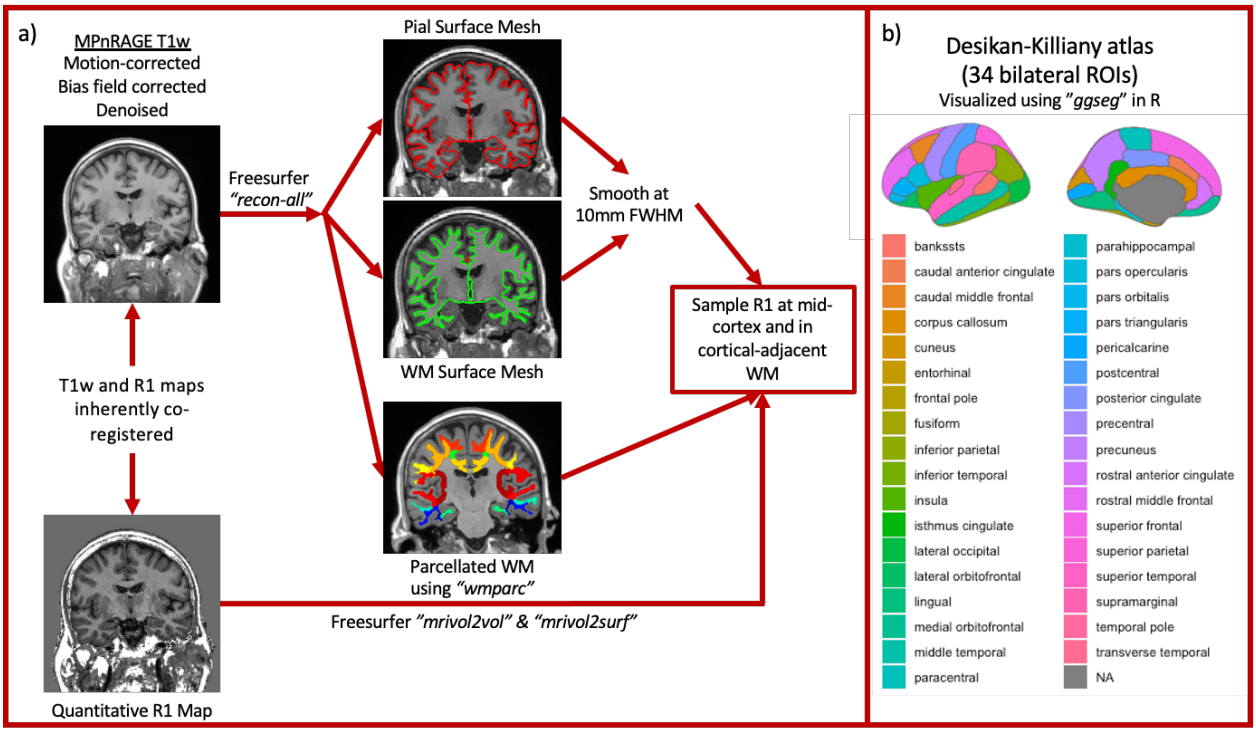

Figure B1: a) Image processing pipeline: T1w images were processed using Advanced Normalization Tools (ANTs) and Freesurfer v6. R1 was sampled at the midpoint of the cortical surface using surface meshes and parcellations produced from Freesurfer for 34 bilaterally-averaged regions of interest (ROI) from the Desikan-Killiany parcellation. b) Regions of interest comprised of bilaterally-averaged regions from the Desikan-Killiany parcellation overlayed onto a brain using the "ggseg" package in R.

Table B1: MPnRAGE acquisition parameters for each protocol used.

Protocol	**N1**	**N2**	**Alpha1**	**Alpha2**	**TD**
A	325/326	111/112	4	6	237/242
B	304	81/82	4	8	505
C	304	81/82	4	8	502/503
D	325	51/61	4	8	505

Table B2: Outputs of multiple regression models testing effect of sex on regional cortical GM R1

ROI	Predictor	Estimate	Std. Error	T-Statistic	pUncorrected	pFDR
bankssts	Intercept	0.712	0.006	114.058	0.000e+00	0.000e+00
	Age	-0.000	0.000	-1.006	3.148e-01	5.097e-01
	Sex	-0.000	0.002	-0.188	8.507e-01	9.163e-01
caudal anterior cingulate	Intercept	0.680	0.010	65.806	1.294e-320	1.375e-320
	Age	0.000	0.000	1.588	1.127e-01	2.936e-01
	Sex	-0.004	0.003	-1.459	1.449e-01	4.810e-01
caudal middle frontal	Intercept	0.720	0.006	114.352	0.000e+00	0.000e+00
	Age	-0.000	0.000	-1.249	2.119e-01	4.414e-01
	Sex	0.000	0.002	0.057	9.549e-01	9.817e-01
cuneus	Intercept	0.739	0.008	91.908	0.000e+00	0.000e+00
	Age	-0.000	0.000	-1.900	5.776e-02	2.020e-01
	Sex	-0.005	0.002	-2.307	2.132e-02	2.416e-01
entorhinal	Intercept	0.778	0.015	51.427	1.005e-253	1.005e-253
	Age	0.000	0.000	0.288	7.733e-01	8.764e-01
	Sex	-0.001	0.004	-0.263	7.927e-01	8.984e-01
frontal pole	Intercept	0.683	0.007	103.883	0.000e+00	0.000e+00
	Age	-0.000	0.000	-1.150	2.507e-01	4.654e-01
	Sex	-0.002	0.002	-1.134	2.571e-01	5.463e-01
fusiform	Intercept	0.684	0.005	125.072	0.000e+00	0.000e+00
	Age	0.000	0.000	0.424	6.715e-01	8.235e-01
	Sex	-0.001	0.001	-0.548	5.837e-01	8.269e-01
inferior parietal	Intercept	0.712	0.007	107.922	0.000e+00	0.000e+00

ROI	Predictor	Estimate	Std. Error	T-Statistic	pUncorrected	pFDR
	Age	-0.000	0.000	-1.553	1.209e-01	2.936e-01
	Sex	-0.002	0.002	-1.347	1.785e-01	4.810e-01
inferior temporal	Intercept	0.669	0.005	127.780	0.000e+00	0.000e+00
	Age	0.000	0.000	1.022	3.070e-01	5.097e-01
	Sex	0.000	0.001	0.023	9.817e-01	9.817e-01
insula	Intercept	0.656	0.006	118.233	0.000e+00	0.000e+00
	Age	0.000	0.000	5.685	1.847e-08	6.280e-07
	Sex	-0.001	0.001	-0.843	3.994e-01	6.466e-01
isthmus cingulate	Intercept	0.728	0.008	87.735	0.000e+00	0.000e+00
	Age	-0.000	0.000	-0.195	8.456e-01	9.070e-01
	Sex	-0.003	0.002	-1.248	2.122e-01	4.810e-01
lateral occipital	Intercept	0.713	0.007	103.380	0.000e+00	0.000e+00
	Age	-0.000	0.000	-0.151	8.803e-01	9.070e-01
	Sex	-0.002	0.002	-1.474	1.410e-01	4.810e-01
lateral orbitofrontal	Intercept	0.679	0.005	131.294	0.000e+00	0.000e+00
	Age	0.000	0.000	0.650	5.159e-01	7.545e-01
	Sex	-0.002	0.001	-1.630	1.034e-01	4.810e-01
lingual	Intercept	0.717	0.007	104.227	0.000e+00	0.000e+00
	Age	-0.000	0.000	-0.946	3.443e-01	5.321e-01
	Sex	-0.003	0.002	-1.720	8.583e-02	4.810e-01
medial orbitofrontal	Intercept	0.645	0.005	117.752	0.000e+00	0.000e+00
	Age	0.000	0.000	3.306	9.897e-04	5.608e-03
	Sex	-0.001	0.001	-1.093	2.749e-01	5.498e-01
middle temporal	Intercept	0.678	0.005	132.673	0.000e+00	0.000e+00
	Age	0.000	0.000	1.127	2.601e-01	4.654e-01
	Sex	-0.000	0.001	-0.371	7.109e-01	8.375e-01
paracentral	Intercept	0.751	0.007	106.899	0.000e+00	0.000e+00
	Age	-0.000	0.000	-0.408	6.835e-01	8.235e-01
	Sex	0.001	0.002	0.775	4.385e-01	6.720e-01
parahippocampal	Intercept	0.663	0.007	98.974	0.000e+00	0.000e+00
	Age	0.000	0.000	4.001	6.894e-05	5.860e-04

ROI	Predictor	Estimate	Std. Error	T-Statistic	pUncorrected	pFDR
	Sex	-0.004	0.002	-2.527	1.171e-02	1.991e-01
pars opercularis	Intercept	0.701	0.006	125.477	0.000e+00	0.000e+00
	Age	0.000	0.000	1.269	2.048e-01	4.414e-01
	Sex	-0.002	0.001	-1.265	2.064e-01	4.810e-01
pars orbitalis	Intercept	0.695	0.006	118.647	0.000e+00	0.000e+00
	Age	0.000	0.000	0.042	9.667e-01	9.667e-01
	Sex	-0.001	0.001	-0.748	4.546e-01	6.720e-01
pars triangularis	Intercept	0.701	0.006	121.611	0.000e+00	0.000e+00
	Age	0.000	0.000	0.543	5.871e-01	7.985e-01
	Sex	-0.001	0.001	-1.015	3.105e-01	5.865e-01
pericalcarine	Intercept	0.732	0.008	86.602	0.000e+00	0.000e+00
	Age	-0.000	0.000	-0.382	7.024e-01	8.235e-01
	Sex	-0.005	0.002	-2.557	1.075e-02	1.991e-01
postcentral	Intercept	0.735	0.007	112.235	0.000e+00	0.000e+00
	Age	0.000	0.000	0.624	5.326e-01	7.545e-01
	Sex	-0.000	0.002	-0.173	8.624e-01	9.163e-01
posterior cingulate	Intercept	0.704	0.013	56.069	1.039e-273	1.070e-273
	Age	*0.000*	*0.000*	*2.398*	*1.670e-02*	*7.097e-02*
	Sex	0.001	0.003	0.366	7.143e-01	8.375e-01
precentral	Intercept	0.759	0.007	108.901	0.000e+00	0.000e+00
	Age	-0.000	0.000	-0.476	6.339e-01	8.235e-01
	Sex	0.002	0.002	0.937	3.492e-01	6.249e-01
precuneus	Intercept	0.720	0.007	108.168	0.000e+00	0.000e+00
	Age	-0.000	0.000	-1.837	6.663e-02	2.020e-01
	Sex	-0.003	0.002	-1.707	8.827e-02	4.810e-01
rostral anterior cingulate	Intercept	0.640	0.007	95.836	0.000e+00	0.000e+00
	Age	0.000	0.000	4.416	1.145e-05	1.298e-04
	Sex	0.001	0.002	0.453	6.510e-01	8.375e-01
rostral middle frontal	Intercept	0.702	0.006	117.016	0.000e+00	0.000e+00
	Age	-0.000	0.000	-1.806	7.129e-02	2.020e-01
	Sex	-0.001	0.001	-0.884	3.771e-01	6.411e-01

ROI	Predictor	Estimate	Std. Error	T-Statistic	pUncorrected	pFDR
superior frontal	Intercept	0.705	0.006	122.628	0.000e+00	0.000e+00
	Age	-0.000	0.000	-1.226	2.207e-01	4.414e-01
	Sex	0.001	0.001	0.379	7.046e-01	8.375e-01
superior parietal	Intercept	0.730	0.007	104.456	0.000e+00	0.000e+00
	Age	-0.000	0.000	-1.863	6.277e-02	2.020e-01
	Sex	-0.003	0.002	-1.631	1.032e-01	4.810e-01
superior temporal	Intercept	0.697	0.006	123.326	0.000e+00	0.000e+00
	Age	0.000	0.000	2.720	6.680e-03	3.245e-02
	Sex	-0.002	0.001	-1.417	1.568e-01	4.810e-01
supramarginal	Intercept	0.706	0.006	118.047	0.000e+00	0.000e+00
	Age	-0.000	0.000	-0.166	8.684e-01	9.070e-01
	Sex	-0.002	0.001	-1.432	1.525e-01	4.810e-01
temporal pole	Intercept	0.650	0.007	99.606	0.000e+00	0.000e+00
	Age	0.000	0.000	4.763	2.267e-06	3.854e-05
	Sex	0.001	0.002	0.499	6.182e-01	8.375e-01
transverse temporal	Intercept	0.760	0.008	97.902	0.000e+00	0.000e+00
	Age	0.000	0.000	3.562	3.909e-04	2.658e-03
	Sex	-0.002	0.002	-1.254	2.102e-01	4.810e-01

Table B3: Outputs of multiple regression models testing effect of sex on regional cortical-adjacent WM R1

ROI	Predictor	Estimate	Std. Error	T-Statistic	pUncorrected	pFDR
bankssts	Intercept	1.098	0.073	15.009	5.774e-45	1.155e-44
	Age	0.004	0.002	1.930	5.401e-02	1.054e-01
	Age^2	-0.000	0.000	-3.001	2.775e-03	4.946e-03
	Sex	-0.013	0.003	-4.315	1.802e-05	4.376e-05
caudal anterior cingulate	Intercept	1.072	0.078	13.672	2.471e-38	3.000e-38
	Age	0.007	0.002	2.757	5.973e-03	3.385e-02
	Age^2	-0.000	0.000	-3.836	1.352e-04	6.742e-04
	Sex	-0.016	0.003	-5.278	1.688e-07	5.739e-07
caudal middle frontal	Intercept	1.107	0.069	16.075	1.721e-50	1.170e-49
	Age	0.003	0.002	1.624	1.048e-01	1.423e-01
	Age^2	-0.000	0.000	-2.937	3.416e-03	5.138e-03
	Sex	-0.007	0.003	-2.426	1.549e-02	1.816e-02
cuneus	Intercept	1.104	0.073	15.036	4.176e-45	8.874e-45
	Age	0.001	0.002	0.304	7.609e-01	8.085e-01
	Age^2	-0.000	0.000	-0.987	3.240e-01	3.338e-01
	Sex	-0.022	0.003	-7.560	1.125e-13	3.825e-12
entorhinal	Intercept	0.743	0.078	9.507	2.315e-20	2.315e-20
	Age	0.011	0.002	4.607	4.759e-06	1.618e-04
	Age^2	-0.000	0.000	-5.546	3.992e-08	1.357e-06
	Sex	-0.009	0.003	-2.923	3.565e-03	4.662e-03
frontal pole	Intercept	0.951	0.076	12.447	1.355e-32	1.486e-32
	Age	0.005	0.002	2.217	2.691e-02	7.290e-02
	Age^2	-0.000	0.000	-3.376	7.719e-04	2.242e-03
	Sex	-0.000	0.003	-0.105	9.166e-01	9.166e-01
fusiform	Intercept	1.077	0.073	14.783	8.051e-44	1.244e-43
	Age	0.004	0.002	1.786	7.455e-02	1.207e-01
	Age^2	-0.000	0.000	-2.975	3.024e-03	4.946e-03
	Sex	-0.009	0.003	-3.260	1.164e-03	1.885e-03

ROI	Predictor	Estimate	Std. Error	T-Statistic	pUncorrected	pFDR
inferior parietal	Intercept	1.089	0.073	14.820	5.226e-44	8.461e-44
	Age	0.004	0.002	1.605	1.088e-01	1.423e-01
	Age^2	-0.000	0.000	-2.744	6.213e-03	8.450e-03
	Sex	-0.018	0.003	-6.285	5.417e-10	3.684e-09
inferior temporal	Intercept	1.073	0.071	15.143	1.191e-45	2.892e-45
	Age	0.004	0.002	1.710	8.773e-02	1.297e-01
	Age^2	-0.000	0.000	-2.910	3.714e-03	5.261e-03
	Sex	-0.011	0.003	-3.770	1.757e-04	3.514e-04
insula	Intercept	0.995	0.064	15.546	9.966e-48	4.061e-47
	Age	0.005	0.002	2.502	1.257e-02	5.040e-02
	Age^2	-0.000	0.000	-3.390	7.325e-04	2.242e-03
	Sex	-0.010	0.003	-3.869	1.181e-04	2.510e-04
isthmus cingulate	Intercept	1.110	0.074	14.945	1.215e-44	2.174e-44
	Age	0.005	0.002	2.150	3.185e-02	7.290e-02
	Age^2	-0.000	0.000	-2.971	3.055e-03	4.946e-03
	Sex	-0.018	0.003	-6.082	1.848e-09	1.047e-08
lateral occipital	Intercept	1.141	0.069	16.463	1.485e-52	1.683e-51
	Age	0.001	0.002	0.255	7.990e-01	8.232e-01
	Age^2	-0.000	0.000	-1.135	2.568e-01	2.728e-01
	Sex	-0.018	0.003	-6.565	9.465e-11	1.609e-09
lateral orbitofrontal	Intercept	0.961	0.071	13.451	2.843e-37	3.333e-37
	Age	0.008	0.002	3.529	4.413e-04	7.502e-03
	Age^2	-0.000	0.000	-4.905	1.134e-06	1.928e-05
	Sex	-0.006	0.003	-2.282	2.275e-02	2.495e-02
lingual	Intercept	1.073	0.069	15.540	1.075e-47	4.061e-47
	Age	0.002	0.002	1.015	3.104e-01	3.643e-01
	Age^2	-0.000	0.000	-1.860	6.331e-02	6.944e-02
	Sex	-0.018	0.003	-6.465	1.777e-10	2.014e-09
medial orbitofrontal	Intercept	0.954	0.072	13.199	4.454e-36	5.048e-36
	Age	0.007	0.002	3.115	1.906e-03	1.296e-02
	Age^2	-0.000	0.000	-4.471	8.914e-06	1.010e-04

ROI	Predictor	Estimate	Std. Error	T-Statistic	pUncorrected	pFDR
	Sex	-0.008	0.003	-2.659	8.003e-03	1.008e-02
middle temporal	Intercept	1.086	0.070	15.559	8.557e-48	4.061e-47
	Age	0.004	0.002	1.728	8.431e-02	1.297e-01
	Age^2	-0.000	0.000	-3.012	2.675e-03	4.946e-03
	Sex	-0.012	0.003	-4.426	1.096e-05	2.866e-05
paracentral	Intercept	1.145	0.071	16.132	8.584e-51	7.296e-50
	Age	0.002	0.002	0.992	3.214e-01	3.643e-01
	Age^2	-0.000	0.000	-2.100	3.608e-02	4.381e-02
	Sex	-0.010	0.003	-3.669	2.595e-04	4.902e-04
parahippocampal	Intercept	0.933	0.078	11.897	3.927e-30	4.172e-30
	Age	0.008	0.002	3.287	1.057e-03	8.984e-03
	Age^2	-0.000	0.000	-4.080	4.955e-05	3.369e-04
	Sex	-0.017	0.003	-5.546	3.987e-08	1.506e-07
pars opercularis	Intercept	1.083	0.069	15.693	1.723e-48	9.764e-48
	Age	0.004	0.002	2.081	3.775e-02	8.022e-02
	Age^2	-0.000	0.000	-3.357	8.248e-04	2.242e-03
	Sex	-0.009	0.003	-3.151	1.690e-03	2.498e-03
pars orbitalis	Intercept	1.014	0.070	14.487	2.469e-42	3.358e-42
	Age	0.005	0.002	2.216	2.700e-02	7.290e-02
	Age^2	-0.000	0.000	-3.476	5.367e-04	2.028e-03
	Sex	-0.006	0.003	-2.076	3.822e-02	4.061e-02
pars triangularis	Intercept	1.051	0.070	15.100	1.977e-45	4.481e-45
	Age	0.005	0.002	2.480	1.334e-02	5.040e-02
	Age^2	-0.000	0.000	-3.829	1.388e-04	6.742e-04
	Sex	-0.007	0.003	-2.537	1.139e-02	1.383e-02
pericalcarine	Intercept	1.105	0.078	14.101	2.007e-40	2.527e-40
	Age	-0.000	0.002	-0.030	9.760e-01	9.760e-01
	Age^2	-0.000	0.000	-0.584	5.596e-01	5.596e-01
	Sex	-0.020	0.003	-6.300	4.948e-10	3.684e-09
postcentral	Intercept	1.114	0.067	16.583	3.405e-53	5.789e-52
	Age	0.002	0.002	1.006	3.147e-01	3.643e-01

ROI	Predictor	Estimate	Std. Error	T-Statistic	pUncorrected	pFDR
	Age^2	-0.000	0.000	-2.023	4.341e-02	5.089e-02
	Sex	-0.011	0.003	-4.006	6.764e-05	1.533e-04
posterior cingulate	Intercept	1.107	0.074	14.902	2.017e-44	3.429e-44
	Age	0.005	0.002	2.146	3.216e-02	7.290e-02
	Age^2	-0.000	0.000	-3.162	1.628e-03	3.460e-03
	Sex	-0.015	0.003	-5.123	3.784e-07	1.170e-06
precentral	Intercept	1.154	0.067	17.178	2.088e-56	7.099e-55
	Age	0.002	0.002	0.822	4.115e-01	4.513e-01
	Age^2	-0.000	0.000	-1.980	4.808e-02	5.449e-02
	Sex	-0.008	0.003	-2.997	2.811e-03	3.982e-03
precuneus	Intercept	1.085	0.075	14.452	3.678e-42	4.810e-42
	Age	0.004	0.002	1.892	5.892e-02	1.054e-01
	Age^2	-0.000	0.000	-3.099	2.009e-03	4.018e-03
	Sex	-0.018	0.003	-5.948	4.079e-09	1.734e-08
rostral anterior cingulate	Intercept	1.110	0.076	14.515	1.781e-42	2.523e-42
	Age	0.004	0.002	1.684	9.267e-02	1.313e-01
	Age^2	-0.000	0.000	-2.714	6.794e-03	8.884e-03
	Sex	-0.005	0.003	-1.684	9.255e-02	9.535e-02
rostral middle frontal	Intercept	1.082	0.072	14.953	1.113e-44	2.102e-44
	Age	0.004	0.002	1.855	6.397e-02	1.087e-01
	Age^2	-0.000	0.000	-3.173	1.568e-03	3.460e-03
	Sex	-0.008	0.003	-2.934	3.442e-03	4.662e-03
superior frontal	Intercept	1.072	0.070	15.315	1.569e-46	4.342e-46
	Age	0.004	0.002	1.902	5.759e-02	1.054e-01
	Age^2	-0.000	0.000	-3.326	9.232e-04	2.242e-03
	Sex	-0.009	0.003	-3.238	1.256e-03	1.941e-03
superior parietal	Intercept	1.125	0.074	15.310	1.660e-46	4.342e-46
	Age	0.002	0.002	1.105	2.694e-01	3.392e-01
	Age^2	-0.000	0.000	-2.243	2.515e-02	3.167e-02
	Sex	-0.018	0.003	-6.035	2.446e-09	1.188e-08
superior temporal	Intercept	1.036	0.067	15.514	1.474e-47	5.012e-47

ROI	Predictor	Estimate	Std. Error	T-Statistic	pUncorrected	pFDR
	Age	0.005	0.002	2.522	1.186e-02	5.040e-02
	Age^2	-0.000	0.000	-3.639	2.917e-04	1.240e-03
	Sex	-0.010	0.003	-3.602	3.359e-04	6.011e-04
supramarginal	Intercept	1.064	0.073	14.630	4.758e-43	7.034e-43
	Age	0.005	0.002	2.165	3.073e-02	7.290e-02
	Age^2	-0.000	0.000	-3.328	9.162e-04	2.242e-03
	Sex	-0.014	0.003	-4.909	1.111e-06	3.148e-06
temporal pole	Intercept	0.833	0.074	11.201	4.019e-27	4.141e-27
	Age	0.008	0.002	3.412	6.767e-04	7.669e-03
	Age^2	-0.000	0.000	-4.280	2.102e-05	1.787e-04
	Sex	-0.007	0.003	-2.393	1.694e-02	1.920e-02
transverse temporal	Intercept	1.055	0.068	15.434	3.784e-47	1.170e-46
	Age	0.005	0.002	2.269	2.353e-02	7.290e-02
	Age^2	-0.000	0.000	-2.931	3.476e-03	5.138e-03
	Sex	-0.009	0.003	-3.456	5.774e-04	9.816e-04

Table B4: Outputs of multiple regression models testing effect of APOE Status on regional cortical GM R1

ROI	Predictor	Estimate	Std. Error	T-Statistic	pUncorrected	pFDR
bankssts	Intercept	0.712	0.006	112.903	0.000e+00	0.000e+00
	Age	-0.000	0.000	-0.910	3.634e-01	5.616e-01
	APOE Status	0.000	0.001	0.316	7.523e-01	9.041e-01
	Sex	-0.000	0.002	-0.153	8.780e-01	9.329e-01
caudal anterior cingulate	Intercept	0.677	0.010	65.201	2.058e-318	2.187e-318
	Age	0.000	0.000	1.665	9.635e-02	2.520e-01
	APOE Status	0.003	0.002	1.330	1.841e-01	9.041e-01
	Sex	-0.004	0.003	-1.532	1.260e-01	4.902e-01
caudal middle frontal	Intercept	0.720	0.006	113.623	0.000e+00	0.000e+00
	Age	-0.000	0.000	-1.260	2.080e-01	4.160e-01
	APOE Status	0.000	0.002	0.271	7.863e-01	9.041e-01
	Sex	-0.000	0.002	-0.015	9.880e-01	9.880e-01
cuneus	Intercept	0.740	0.008	91.148	0.000e+00	0.000e+00
	Age	-0.000	0.000	-1.972	4.899e-02	1.851e-01
	APOE Status	-0.002	0.002	-0.961	3.368e-01	9.041e-01
	Sex	-0.004	0.002	-2.228	2.614e-02	2.963e-01
entorhinal	Intercept	0.772	0.015	50.023	6.415e-247	6.415e-247
	Age	0.000	0.000	0.486	6.270e-01	7.520e-01
	APOE Status	0.004	0.004	1.203	2.294e-01	9.041e-01
	Sex	-0.001	0.004	-0.165	8.688e-01	9.329e-01
frontal pole	Intercept	0.683	0.007	103.292	0.000e+00	0.000e+00
	Age	-0.000	0.000	-1.208	2.275e-01	4.297e-01
	APOE Status	0.001	0.002	0.751	4.528e-01	9.041e-01
	Sex	-0.002	0.002	-1.219	2.234e-01	5.102e-01
fusiform	Intercept	0.684	0.006	124.153	0.000e+00	0.000e+00
	Age	0.000	0.000	0.435	6.635e-01	7.520e-01
	APOE Status	-0.000	0.001	-0.003	9.975e-01	9.975e-01
	Sex	-0.001	0.001	-0.550	5.822e-01	8.248e-01

ROI	Predictor	Estimate	Std. Error	T-Statistic	pUncorrected	pFDR
inferior parietal	Intercept	0.711	0.007	106.996	0.000e+00	0.000e+00
	Age	-0.000	0.000	-1.443	1.494e-01	3.628e-01
	APOE Status	0.001	0.002	0.742	4.583e-01	9.041e-01
	Sex	-0.002	0.002	-1.364	1.730e-01	4.902e-01
inferior temporal	Intercept	0.669	0.005	126.478	0.000e+00	0.000e+00
	Age	0.000	0.000	1.056	2.911e-01	4.949e-01
	APOE Status	0.001	0.001	0.698	4.855e-01	9.041e-01
	Sex	-0.000	0.001	-0.048	9.617e-01	9.880e-01
insula	Intercept	0.657	0.006	117.908	0.000e+00	0.000e+00
	Age	0.000	0.000	5.697	1.723e-08	5.858e-07
	APOE Status	-0.000	0.001	-0.340	7.336e-01	9.041e-01
	Sex	-0.001	0.001	-0.837	4.027e-01	6.588e-01
isthmus cingulate	Intercept	0.726	0.008	86.056	0.000e+00	0.000e+00
	Age	-0.000	0.000	-0.043	9.654e-01	9.654e-01
	APOE Status	0.001	0.002	0.624	5.327e-01	9.041e-01
	Sex	-0.002	0.002	-1.214	2.251e-01	5.102e-01
lateral occipital	Intercept	0.713	0.007	101.900	0.000e+00	0.000e+00
	Age	-0.000	0.000	-0.129	8.977e-01	9.538e-01
	APOE Status	-0.001	0.002	-0.320	7.491e-01	9.041e-01
	Sex	-0.002	0.002	-1.466	1.432e-01	4.902e-01
lateral orbitofrontal	Intercept	0.678	0.006	120.847	0.000e+00	0.000e+00
	Age	0.000	0.000	0.864	3.879e-01	5.734e-01
	APOE Status	-0.001	0.001	-0.649	5.163e-01	9.041e-01
	Sex	-0.003	0.001	-2.024	4.329e-02	3.680e-01
lingual	Intercept	0.717	0.007	102.914	0.000e+00	0.000e+00
	Age	-0.000	0.000	-0.986	3.246e-01	5.255e-01
	APOE Status	-0.001	0.002	-0.448	6.541e-01	9.041e-01
	Sex	-0.003	0.002	-1.625	1.046e-01	4.902e-01
medial orbitofrontal	Intercept	0.646	0.005	117.497	0.000e+00	0.000e+00
	Age	0.000	0.000	3.099	2.010e-03	1.139e-02
	APOE Status	-0.001	0.001	-0.561	5.752e-01	9.041e-01

ROI	Predictor	Estimate	Std. Error	T-Statistic	pUncorrected	pFDR
	Sex	-0.002	0.001	-1.148	2.512e-01	5.268e-01
middle temporal	Intercept	0.677	0.005	131.402	0.000e+00	0.000e+00
	Age	0.000	0.000	1.162	2.457e-01	4.397e-01
	APOE Status	0.000	0.001	0.274	7.839e-01	9.041e-01
	Sex	-0.001	0.001	-0.417	6.768e-01	8.523e-01
paracentral	Intercept	0.751	0.007	106.507	0.000e+00	0.000e+00
	Age	-0.000	0.000	-0.511	6.092e-01	7.520e-01
	APOE Status	-0.000	0.002	-0.255	7.988e-01	9.041e-01
	Sex	0.001	0.002	0.724	4.694e-01	6.939e-01
parahippocampal	Intercept	0.663	0.007	98.323	0.000e+00	0.000e+00
	Age	0.000	0.000	3.961	8.134e-05	6.914e-04
	APOE Status	-0.001	0.002	-0.360	7.188e-01	9.041e-01
	Sex	-0.004	0.002	-2.518	1.200e-02	2.156e-01
pars opercularis	Intercept	0.701	0.006	125.038	0.000e+00	0.000e+00
	Age	0.000	0.000	1.284	1.996e-01	4.160e-01
	APOE Status	-0.000	0.001	-0.188	8.509e-01	9.041e-01
	Sex	-0.002	0.001	-1.257	2.091e-01	5.102e-01
pars orbitalis	Intercept	0.696	0.006	118.007	0.000e+00	0.000e+00
	Age	-0.000	0.000	-0.142	8.869e-01	9.538e-01
	APOE Status	-0.001	0.001	-0.514	6.075e-01	9.041e-01
	Sex	-0.001	0.001	-0.785	4.325e-01	6.684e-01
pars triangularis	Intercept	0.702	0.006	121.083	0.000e+00	0.000e+00
	Age	0.000	0.000	0.455	6.490e-01	7.520e-01
	APOE Status	-0.000	0.001	-0.192	8.477e-01	9.041e-01
	Sex	-0.001	0.001	-1.041	2.984e-01	5.636e-01
pericalcarine	Intercept	0.733	0.009	85.828	0.000e+00	0.000e+00
	Age	-0.000	0.000	-0.443	6.580e-01	7.520e-01
	APOE Status	-0.001	0.002	-0.531	5.956e-01	9.041e-01
	Sex	-0.005	0.002	-2.498	1.268e-02	2.156e-01
postcentral	Intercept	0.735	0.007	111.612	0.000e+00	0.000e+00
	Age	0.000	0.000	0.579	5.624e-01	7.520e-01

ROI	Predictor	Estimate	Std. Error	T-Statistic	pUncorrected	pFDR
	APOE Status	0.000	0.002	0.213	8.313e-01	9.041e-01
	Sex	-0.000	0.002	-0.264	7.916e-01	8.971e-01
posterior cingulate	Intercept	0.702	0.013	55.508	2.266e-271	2.335e-271
	Age	0.000	0.000	2.500	1.263e-02	5.368e-02
	APOE Status	0.002	0.003	0.817	4.140e-01	9.041e-01
	Sex	0.001	0.003	0.328	7.431e-01	8.749e-01
precentral	Intercept	0.759	0.007	108.320	0.000e+00	0.000e+00
	Age	-0.000	0.000	-0.548	5.841e-01	7.520e-01
	APOE Status	0.000	0.002	0.190	8.495e-01	9.041e-01
	Sex	0.001	0.002	0.830	4.069e-01	6.588e-01
precuneus	Intercept	0.720	0.007	107.316	0.000e+00	0.000e+00
	Age	-0.000	0.000	-1.819	6.931e-02	2.080e-01
	APOE Status	-0.000	0.002	-0.109	9.135e-01	9.412e-01
	Sex	-0.003	0.002	-1.654	9.849e-02	4.902e-01
rostral anterior cingulate	Intercept	0.639	0.007	95.044	0.000e+00	0.000e+00
	Age	0.000	0.000	4.518	7.184e-06	1.221e-04
	APOE Status	0.001	0.002	0.601	5.483e-01	9.041e-01
	Sex	0.001	0.002	0.515	6.067e-01	8.251e-01
rostral middle frontal	Intercept	0.701	0.006	116.487	0.000e+00	0.000e+00
	Age	-0.000	0.000	-1.793	7.342e-02	2.080e-01
	APOE Status	0.001	0.001	0.647	5.176e-01	9.041e-01
	Sex	-0.001	0.001	-0.923	3.565e-01	6.379e-01
superior frontal	Intercept	0.705	0.006	121.933	0.000e+00	0.000e+00
	Age	-0.000	0.000	-1.262	2.072e-01	4.160e-01
	APOE Status	0.000	0.001	0.261	7.940e-01	9.041e-01
	Sex	0.000	0.001	0.324	7.462e-01	8.749e-01
superior parietal	Intercept	0.729	0.007	103.725	0.000e+00	0.000e+00
	Age	-0.000	0.000	-1.844	6.553e-02	2.080e-01
	APOE Status	0.000	0.002	0.273	7.849e-01	9.041e-01
	Sex	-0.003	0.002	-1.634	1.028e-01	4.902e-01
superior temporal	Intercept	0.697	0.006	122.668	0.000e+00	0.000e+00

ROI	Predictor	Estimate	Std. Error	T-Statistic	pUncorrected	pFDR
	Age	0.000	0.000	2.697	7.156e-03	3.476e-02
	APOE Status	-0.001	0.001	-0.845	3.985e-01	9.041e-01
	Sex	-0.002	0.001	-1.364	1.730e-01	4.902e-01
supramarginal	Intercept	0.705	0.006	117.331	0.000e+00	0.000e+00
	Age	-0.000	0.000	-0.088	9.298e-01	9.580e-01
	APOE Status	0.000	0.001	0.284	7.766e-01	9.041e-01
	Sex	-0.002	0.001	-1.431	1.529e-01	4.902e-01
temporal pole	Intercept	0.653	0.007	98.665	0.000e+00	0.000e+00
	Age	0.000	0.000	4.413	1.163e-05	1.318e-04
	APOE Status	-0.002	0.002	-1.510	1.315e-01	9.041e-01
	Sex	0.001	0.002	0.455	6.494e-01	8.492e-01
transverse temporal	Intercept	0.760	0.008	97.260	0.000e+00	0.000e+00
	Age	0.000	0.000	3.587	3.546e-04	2.411e-03
	APOE Status	-0.002	0.002	-1.199	2.308e-01	9.041e-01
	Sex	-0.002	0.002	-1.119	2.634e-01	5.268e-01

Table B5: Outputs of multiple regression models testing effect of APOE Status on regional cortical-adjacent WM R1

ROI	Predictor	Estimate	Std. Error	T-Statistic	pUncorrected	pFDR
bankssts	Intercept	1.085	0.073	14.814	5.436e-44	1.155e-43
	Age	0.005	0.002	2.143	3.238e-02	6.154e-02
	Age^2	-0.000	0.000	-3.230	1.291e-03	2.335e-03
	APOE Status	-0.003	0.003	-1.191	2.340e-01	9.233e-01
	Sex	-0.012	0.003	-4.276	2.140e-05	5.197e-05
caudal anterior cingulate	Intercept	1.067	0.079	13.569	7.591e-38	9.218e-38
	Age	0.007	0.002	2.800	5.239e-03	2.590e-02
	Age^2	-0.000	0.000	-3.885	1.111e-04	4.841e-04
	APOE Status	0.002	0.003	0.782	4.347e-01	9.233e-01
	Sex	-0.016	0.003	-5.247	1.986e-07	6.752e-07
caudal middle frontal	Intercept	1.100	0.069	15.955	7.096e-50	4.825e-49
	Age	0.004	0.002	1.740	8.220e-02	1.075e-01
	Age^2	-0.000	0.000	-3.069	2.218e-03	3.142e-03
	APOE Status	-0.001	0.003	-0.455	6.489e-01	9.233e-01
	Sex	-0.007	0.003	-2.495	1.280e-02	1.501e-02
cuneus	Intercept	1.081	0.074	14.610	5.791e-43	9.845e-43
	Age	0.001	0.002	0.625	5.322e-01	5.655e-01
	Age^2	-0.000	0.000	-1.319	1.875e-01	1.932e-01
	APOE Status	-0.001	0.003	-0.367	7.139e-01	9.233e-01
	Sex	-0.022	0.003	-7.357	4.727e-13	1.607e-11
entorhinal	Intercept	0.739	0.078	9.421	4.821e-20	4.821e-20
	Age	0.011	0.002	4.666	3.608e-06	1.227e-04
	Age^2	-0.000	0.000	-5.628	2.531e-08	8.605e-07
	APOE Status	-0.001	0.003	-0.456	6.484e-01	9.233e-01
	Sex	-0.009	0.003	-2.922	3.573e-03	4.672e-03
frontal pole	Intercept	0.953	0.077	12.430	1.605e-32	1.760e-32
	Age	0.005	0.002	2.205	2.776e-02	5.899e-02
	Age^2	-0.000	0.000	-3.392	7.282e-04	1.768e-03

ROI	Predictor	Estimate	Std. Error	T-Statistic	pUncorrected	pFDR
	APOE Status	0.001	0.003	0.210	8.337e-01	9.622e-01
	Sex	-0.001	0.003	-0.258	7.963e-01	7.963e-01
fusiform	Intercept	1.060	0.073	14.524	1.561e-42	2.412e-42
	Age	0.005	0.002	2.028	4.286e-02	7.301e-02
	Age^2	-0.000	0.000	-3.226	1.306e-03	2.335e-03
	APOE Status	-0.002	0.003	-0.737	4.611e-01	9.233e-01
	Sex	-0.009	0.003	-3.144	1.728e-03	2.671e-03
inferior parietal	Intercept	1.071	0.074	14.544	1.251e-42	2.025e-42
	Age	0.004	0.002	1.865	6.258e-02	8.865e-02
	Age^2	-0.000	0.000	-3.013	2.668e-03	3.628e-03
	APOE Status	-0.001	0.003	-0.417	6.768e-01	9.233e-01
	Sex	-0.018	0.003	-6.239	7.185e-10	6.107e-09
inferior temporal	Intercept	1.061	0.071	14.939	1.275e-44	3.096e-44
	Age	0.004	0.002	1.899	5.796e-02	8.568e-02
	Age^2	-0.000	0.000	-3.111	1.932e-03	2.856e-03
	APOE Status	-0.002	0.003	-0.727	4.674e-01	9.233e-01
	Sex	-0.010	0.003	-3.722	2.119e-04	4.238e-04
insula	Intercept	0.978	0.064	15.277	2.373e-46	7.335e-46
	Age	0.005	0.002	2.768	5.778e-03	2.590e-02
	Age^2	-0.000	0.000	-3.662	2.664e-04	1.006e-03
	APOE Status	-0.001	0.002	-0.368	7.128e-01	9.233e-01
	Sex	-0.010	0.003	-3.857	1.240e-04	2.635e-04
isthmus cingulate	Intercept	1.100	0.074	14.762	1.003e-43	1.795e-43
	Age	0.005	0.002	2.309	2.122e-02	5.166e-02
	Age^2	-0.000	0.000	-3.145	1.721e-03	2.660e-03
	APOE Status	-0.002	0.003	-0.611	5.416e-01	9.233e-01
	Sex	-0.018	0.003	-6.061	2.089e-09	1.184e-08
lateral occipital	Intercept	1.126	0.069	16.209	3.228e-51	3.658e-50
	Age	0.001	0.002	0.510	6.100e-01	6.285e-01
	Age^2	-0.000	0.000	-1.413	1.581e-01	1.680e-01
	APOE Status	-0.004	0.003	-1.404	1.608e-01	9.233e-01

ROI	Predictor	Estimate	Std. Error	T-Statistic	pUncorrected	pFDR
	Sex	-0.018	0.003	-6.496	1.458e-10	2.479e-09
lateral orbitofrontal	Intercept	0.950	0.072	13.263	2.174e-36	2.549e-36
	Age	0.008	0.002	3.673	2.557e-04	4.347e-03
	Age^2	-0.000	0.000	-5.059	5.255e-07	8.934e-06
	APOE Status	-0.000	0.003	-0.047	9.622e-01	9.622e-01
	Sex	-0.007	0.003	-2.290	2.228e-02	2.444e-02
lingual	Intercept	1.058	0.069	15.319	1.451e-46	5.848e-46
	Age	0.003	0.002	1.279	2.013e-01	2.444e-01
	Age^2	-0.000	0.000	-2.148	3.204e-02	3.514e-02
	APOE Status	-0.003	0.003	-1.225	2.208e-01	9.233e-01
	Sex	-0.017	0.003	-6.354	3.554e-10	4.028e-09
medial orbitofrontal	Intercept	0.952	0.072	13.135	8.774e-36	9.944e-36
	Age	0.007	0.002	3.155	1.665e-03	1.132e-02
	Age^2	-0.000	0.000	-4.532	6.749e-06	7.649e-05
	APOE Status	0.000	0.003	0.054	9.571e-01	9.622e-01
	Sex	-0.008	0.003	-2.709	6.890e-03	8.676e-03
middle temporal	Intercept	1.075	0.070	15.403	5.340e-47	2.594e-46
	Age	0.004	0.002	1.913	5.616e-02	8.568e-02
	Age^2	-0.000	0.000	-3.210	1.383e-03	2.335e-03
	APOE Status	-0.002	0.003	-0.907	3.645e-01	9.233e-01
	Sex	-0.012	0.003	-4.375	1.376e-05	3.599e-05
paracentral	Intercept	1.141	0.071	16.099	1.226e-50	1.042e-49
	Age	0.002	0.002	1.065	2.872e-01	3.255e-01
	Age^2	-0.000	0.000	-2.192	2.870e-02	3.485e-02
	APOE Status	-0.001	0.003	-0.294	7.690e-01	9.338e-01
	Sex	-0.010	0.003	-3.666	2.631e-04	4.970e-04
parahippocampal	Intercept	0.929	0.079	11.819	8.569e-30	9.105e-30
	Age	0.008	0.002	3.354	8.347e-04	7.604e-03
	Age^2	-0.000	0.000	-4.172	3.359e-05	2.284e-04
	APOE Status	-0.003	0.003	-1.101	2.714e-01	9.233e-01
	Sex	-0.017	0.003	-5.490	5.408e-08	2.043e-07

ROI	Predictor	Estimate	Std. Error	T-Statistic	pUncorrected	pFDR
pars opercularis	Intercept	1.068	0.069	15.439	3.476e-47	1.970e-46
	Age	0.005	0.002	2.308	2.127e-02	5.166e-02
	Age^2	-0.000	0.000	-3.591	3.497e-04	1.081e-03
	APOE Status	-0.001	0.003	-0.526	5.988e-01	9.233e-01
	Sex	-0.009	0.003	-3.112	1.924e-03	2.844e-03
pars orbitalis	Intercept	1.006	0.070	14.318	1.658e-41	2.349e-41
	Age	0.005	0.002	2.347	1.917e-02	5.166e-02
	Age^2	-0.000	0.000	-3.624	3.084e-04	1.049e-03
	APOE Status	-0.001	0.003	-0.441	6.592e-01	9.233e-01
	Sex	-0.006	0.003	-2.114	3.485e-02	3.703e-02
pars triangularis	Intercept	1.039	0.070	14.890	2.247e-44	5.093e-44
	Age	0.006	0.002	2.663	7.906e-03	2.987e-02
	Age^2	-0.000	0.000	-4.018	6.437e-05	3.648e-04
	APOE Status	-0.001	0.003	-0.345	7.301e-01	9.233e-01
	Sex	-0.007	0.003	-2.536	1.139e-02	1.383e-02
pericalcarine	Intercept	1.090	0.079	13.838	3.769e-39	4.746e-39
	Age	0.000	0.002	0.189	8.500e-01	8.500e-01
	Age^2	-0.000	0.000	-0.822	4.114e-01	4.114e-01
	APOE Status	-0.004	0.003	-1.334	1.826e-01	9.233e-01
	Sex	-0.019	0.003	-6.065	2.047e-09	1.184e-08
postcentral	Intercept	1.107	0.067	16.498	9.368e-53	1.593e-51
	Age	0.002	0.002	1.129	2.594e-01	3.041e-01
	Age^2	-0.000	0.000	-2.163	3.084e-02	3.495e-02
	APOE Status	-0.000	0.003	-0.096	9.238e-01	9.622e-01
	Sex	-0.011	0.003	-4.029	6.144e-05	1.393e-04
posterior cingulate	Intercept	1.098	0.074	14.770	9.134e-44	1.725e-43
	Age	0.005	0.002	2.274	2.324e-02	5.268e-02
	Age^2	-0.000	0.000	-3.303	9.988e-04	2.122e-03
	APOE Status	-0.001	0.003	-0.396	6.922e-01	9.233e-01
	Sex	-0.015	0.003	-5.087	4.557e-07	1.409e-06
precentral	Intercept	1.144	0.067	17.029	1.292e-55	4.393e-54

ROI	Predictor	Estimate	Std. Error	T-Statistic	pUncorrected	pFDR
	Age	0.002	0.002	0.994	3.207e-01	3.517e-01
	Age^2	-0.000	0.000	-2.169	3.035e-02	3.495e-02
	APOE Status	-0.001	0.003	-0.532	5.946e-01	9.233e-01
	Sex	-0.008	0.003	-2.992	2.856e-03	4.046e-03
precuneus	Intercept	1.067	0.075	14.196	6.663e-41	8.713e-41
	Age	0.005	0.002	2.141	3.258e-02	6.154e-02
	Age^2	-0.000	0.000	-3.361	8.127e-04	1.842e-03
	APOE Status	-0.001	0.003	-0.474	6.354e-01	9.233e-01
	Sex	-0.017	0.003	-5.863	6.698e-09	2.847e-08
rostral anterior cingulate	Intercept	1.097	0.077	14.247	3.736e-41	5.081e-41
	Age	0.004	0.002	1.837	6.654e-02	9.049e-02
	Age^2	-0.000	0.000	-2.874	4.164e-03	5.445e-03
	APOE Status	0.001	0.003	0.408	6.833e-01	9.233e-01
	Sex	-0.005	0.003	-1.686	9.213e-02	9.492e-02
rostral middle frontal	Intercept	1.074	0.073	14.799	6.472e-44	1.294e-43
	Age	0.004	0.002	1.960	5.040e-02	8.160e-02
	Age^2	-0.000	0.000	-3.285	1.064e-03	2.128e-03
	APOE Status	0.000	0.003	0.093	9.259e-01	9.622e-01
	Sex	-0.009	0.003	-2.977	2.996e-03	4.075e-03
superior frontal	Intercept	1.064	0.070	15.172	8.224e-46	2.330e-45
	Age	0.004	0.002	2.027	4.295e-02	7.301e-02
	Age^2	-0.000	0.000	-3.466	5.576e-04	1.458e-03
	APOE Status	-0.000	0.003	-0.158	8.746e-01	9.622e-01
	Sex	-0.009	0.003	-3.273	1.110e-03	1.797e-03
superior parietal	Intercept	1.110	0.074	15.053	3.338e-45	8.730e-45
	Age	0.003	0.002	1.337	1.816e-01	2.287e-01
	Age^2	-0.000	0.000	-2.489	1.303e-02	1.641e-02
	APOE Status	-0.002	0.003	-0.533	5.940e-01	9.233e-01
	Sex	-0.017	0.003	-5.950	4.020e-09	1.953e-08
superior temporal	Intercept	1.022	0.067	15.313	1.548e-46	5.848e-46
	Age	0.006	0.002	2.750	6.094e-03	2.590e-02

ROI	Predictor	Estimate	Std. Error	T-Statistic	pUncorrected	pFDR
	Age^2	-0.000	0.000	-3.878	1.139e-04	4.841e-04
	APOE Status	-0.003	0.003	-1.013	3.114e-01	9.233e-01
	Sex	-0.009	0.003	-3.549	4.092e-04	7.323e-04
supramarginal	Intercept	1.052	0.073	14.478	2.659e-42	3.931e-42
	Age	0.005	0.002	2.350	1.903e-02	5.166e-02
	Age^2	-0.000	0.000	-3.526	4.456e-04	1.263e-03
	APOE Status	-0.001	0.003	-0.341	7.332e-01	9.233e-01
	Sex	-0.014	0.003	-4.892	1.212e-06	3.434e-06
temporal pole	Intercept	0.842	0.074	11.303	1.469e-27	1.514e-27
	Age	0.008	0.002	3.334	8.946e-04	7.604e-03
	Age^2	-0.000	0.000	-4.235	2.560e-05	2.176e-04
	APOE Status	-0.004	0.003	-1.399	1.622e-01	9.233e-01
	Sex	-0.007	0.003	-2.365	1.828e-02	2.072e-02
transverse temporal	Intercept	1.042	0.068	15.277	2.372e-46	7.335e-46
	Age	0.005	0.002	2.513	1.216e-02	4.134e-02
	Age^2	-0.000	0.000	-3.197	1.442e-03	2.335e-03
	APOE Status	-0.006	0.003	-2.426	1.549e-02	5.267e-01
	Sex	-0.009	0.003	-3.295	1.028e-03	1.748e-03

Table B6: Outputs of multiple regression models testing interaction effect of sex and APOE Status on regional cortical GM R1

ROI	Predictor	Estimate	Std. Error	T-Statistic	pUncorrected	pFDR
bankssts	Intercept	0.711	0.006	111.766	0.000e+00	0.000e+00
	Age	-0.000	0.000	-0.901	3.680e-01	5.687e-01
	APOE Status	0.001	0.003	0.481	6.307e-01	8.935e-01
	Sex	0.000	0.002	0.096	9.233e-01	9.966e-01
	APOE Status*Sex	-0.001	0.003	-0.367	7.138e-01	7.829e-01
caudal anterior cingulate	Intercept	0.678	0.010	64.683	6.637e-316	7.052e-316
	Age	0.000	0.000	1.658	9.781e-02	2.558e-01
	APOE Status	0.001	0.004	0.155	8.767e-01	9.775e-01
	Sex	-0.005	0.003	-1.672	9.490e-02	8.976e-01
	APOE Status*Sex	0.004	0.005	0.747	4.550e-01	7.829e-01
caudal middle frontal	Intercept	0.719	0.006	112.461	0.000e+00	0.000e+00
	Age	-0.000	0.000	-1.249	2.122e-01	4.244e-01
	APOE Status	0.002	0.003	0.825	4.095e-01	8.792e-01
	Sex	0.001	0.002	0.480	6.314e-01	9.966e-01
	APOE Status*Sex	-0.003	0.003	-0.818	4.137e-01	7.829e-01
cuneus	Intercept	0.739	0.008	90.193	0.000e+00	0.000e+00
	Age	-0.000	0.000	-1.956	5.087e-02	1.922e-01
	APOE Status	0.000	0.003	0.059	9.528e-01	9.775e-01
	Sex	-0.003	0.002	-1.327	1.848e-01	8.976e-01
	APOE Status*Sex	-0.003	0.004	-0.752	4.525e-01	7.829e-01
entorhinal	Intercept	0.769	0.016	49.407	1.477e-243	1.477e-243
	Age	0.000	0.000	0.509	6.111e-01	7.536e-01
	APOE Status	0.012	0.006	1.881	6.028e-02	8.792e-01
	Sex	0.003	0.005	0.743	4.575e-01	9.966e-01
	APOE Status*Sex	-0.011	0.008	-1.449	1.478e-01	7.829e-01
frontal pole	Intercept	0.683	0.007	102.245	0.000e+00	0.000e+00
	Age	-0.000	0.000	-1.200	2.307e-01	4.318e-01
	APOE Status	0.002	0.003	0.733	4.640e-01	8.792e-01

ROI	Predictor	Estimate	Std. Error	T-Statistic	pUncorrected	pFDR
	Sex	-0.002	0.002	-0.751	4.526e-01	9.966e-01
	APOE Status*Sex	-0.001	0.003	-0.368	7.131e-01	7.829e-01
fusiform	Intercept	0.684	0.006	122.889	0.000e+00	0.000e+00
	Age	0.000	0.000	0.457	6.481e-01	7.536e-01
	APOE Status	0.002	0.002	0.902	3.671e-01	8.792e-01
	Sex	0.000	0.002	0.225	8.220e-01	9.966e-01
	APOE Status*Sex	-0.003	0.003	-1.108	2.682e-01	7.829e-01
inferior parietal	Intercept	0.710	0.007	105.892	0.000e+00	0.000e+00
	Age	-0.000	0.000	-1.429	1.534e-01	3.725e-01
	APOE Status	0.003	0.003	1.002	3.168e-01	8.792e-01
	Sex	-0.001	0.002	-0.665	5.062e-01	9.966e-01
	APOE Status*Sex	-0.002	0.003	-0.704	4.819e-01	7.829e-01
inferior temporal	Intercept	0.669	0.005	125.218	0.000e+00	0.000e+00
	Age	0.000	0.000	1.060	2.896e-01	4.923e-01
	APOE Status	0.001	0.002	0.587	5.572e-01	8.792e-01
	Sex	0.000	0.002	0.097	9.224e-01	9.966e-01
	APOE Status*Sex	-0.001	0.003	-0.227	8.207e-01	8.207e-01
insula	Intercept	0.656	0.006	116.693	0.000e+00	0.000e+00
	Age	0.000	0.000	5.715	1.557e-08	5.294e-07
	APOE Status	0.002	0.002	0.662	5.079e-01	8.792e-01
	Sex	-0.000	0.002	-0.034	9.726e-01	9.966e-01
	APOE Status*Sex	-0.003	0.003	-1.053	2.928e-01	7.829e-01
isthmus cingulate	Intercept	0.725	0.009	85.174	0.000e+00	0.000e+00
	Age	-0.000	0.000	-0.036	9.712e-01	9.712e-01
	APOE Status	0.002	0.003	0.674	5.008e-01	8.792e-01
	Sex	-0.002	0.003	-0.735	4.627e-01	9.966e-01
	APOE Status*Sex	-0.002	0.004	-0.384	7.008e-01	7.829e-01
lateral occipital	Intercept	0.713	0.007	100.847	0.000e+00	0.000e+00
	Age	-0.000	0.000	-0.116	9.076e-01	9.643e-01
	APOE Status	0.001	0.003	0.264	7.921e-01	9.775e-01
	Sex	-0.002	0.002	-0.840	4.010e-01	9.966e-01

ROI	Predictor	Estimate	Std. Error	T-Statistic	pUncorrected	pFDR
	APOE Status*Sex	-0.002	0.004	-0.549	5.830e-01	7.829e-01
lateral orbitofrontal	Intercept	0.678	0.006	119.628	0.000e+00	0.000e+00
	Age	0.000	0.000	0.869	3.854e-01	5.697e-01
	APOE Status	-0.000	0.002	-0.028	9.775e-01	9.775e-01
	Sex	-0.002	0.002	-1.358	1.748e-01	8.976e-01
	APOE Status*Sex	-0.001	0.003	-0.423	6.726e-01	7.829e-01
lingual	Intercept	0.716	0.007	101.831	0.000e+00	0.000e+00
	Age	-0.000	0.000	-0.954	3.402e-01	5.508e-01
	APOE Status	0.003	0.003	0.945	3.449e-01	8.792e-01
	Sex	-0.001	0.002	-0.409	6.827e-01	9.966e-01
	APOE Status*Sex	-0.005	0.003	-1.480	1.392e-01	7.829e-01
medial orbitofrontal	Intercept	0.646	0.006	116.332	0.000e+00	0.000e+00
	Age	0.000	0.000	3.101	2.000e-03	1.133e-02
	APOE Status	-0.000	0.002	-0.105	9.162e-01	9.775e-01
	Sex	-0.001	0.002	-0.754	4.513e-01	9.966e-01
	APOE Status*Sex	-0.001	0.003	-0.266	7.902e-01	8.183e-01
middle temporal	Intercept	0.677	0.005	130.072	0.000e+00	0.000e+00
	Age	0.000	0.000	1.173	2.413e-01	4.318e-01
	APOE Status	0.001	0.002	0.606	5.448e-01	8.792e-01
	Sex	-0.000	0.002	-0.004	9.966e-01	9.966e-01
	APOE Status*Sex	-0.001	0.003	-0.548	5.836e-01	7.829e-01
paracentral	Intercept	0.750	0.007	105.426	0.000e+00	0.000e+00
	Age	-0.000	0.000	-0.493	6.220e-01	7.536e-01
	APOE Status	0.003	0.003	0.889	3.744e-01	8.792e-01
	Sex	0.003	0.002	1.335	1.822e-01	8.976e-01
	APOE Status*Sex	-0.004	0.004	-1.268	2.050e-01	7.829e-01
parahippocampal	Intercept	0.662	0.007	97.273	0.000e+00	0.000e+00
	Age	0.000	0.000	3.982	7.470e-05	6.350e-04
	APOE Status	0.002	0.003	0.570	5.689e-01	8.792e-01
	Sex	-0.003	0.002	-1.436	1.513e-01	8.976e-01
	APOE Status*Sex	-0.003	0.003	-0.952	3.412e-01	7.829e-01

ROI	Predictor	Estimate	Std. Error	T-Statistic	pUncorrected	pFDR
pars opercularis	Intercept	0.700	0.006	123.791	0.000e+00	0.000e+00
	Age	0.000	0.000	1.307	1.917e-01	4.244e-01
	APOE Status	0.002	0.002	1.053	2.927e-01	8.792e-01
	Sex	-0.000	0.002	-0.148	8.828e-01	9.966e-01
	APOE Status*Sex	-0.004	0.003	-1.424	1.549e-01	7.829e-01
pars orbitalis	Intercept	0.696	0.006	116.824	0.000e+00	0.000e+00
	Age	-0.000	0.000	-0.137	8.913e-01	9.643e-01
	APOE Status	-0.000	0.002	-0.083	9.342e-01	9.775e-01
	Sex	-0.001	0.002	-0.469	6.395e-01	9.966e-01
	APOE Status*Sex	-0.001	0.003	-0.261	7.942e-01	8.183e-01
pars triangularis	Intercept	0.701	0.006	119.854	0.000e+00	0.000e+00
	Age	0.000	0.000	0.481	6.305e-01	7.536e-01
	APOE Status	0.002	0.002	1.002	3.165e-01	8.792e-01
	Sex	-0.000	0.002	-0.009	9.926e-01	9.966e-01
	APOE Status*Sex	-0.004	0.003	-1.362	1.736e-01	7.829e-01
pericalcarine	Intercept	0.732	0.009	84.938	0.000e+00	0.000e+00
	Age	-0.000	0.000	-0.433	6.649e-01	7.536e-01
	APOE Status	0.000	0.004	0.086	9.313e-01	9.775e-01
	Sex	-0.004	0.003	-1.703	8.904e-02	8.976e-01
	APOE Status*Sex	-0.002	0.004	-0.481	6.308e-01	7.829e-01
postcentral	Intercept	0.734	0.007	110.469	0.000e+00	0.000e+00
	Age	0.000	0.000	0.591	5.545e-01	7.536e-01
	APOE Status	0.002	0.003	0.810	4.183e-01	8.792e-01
	Sex	0.001	0.002	0.294	7.686e-01	9.966e-01
	APOE Status*Sex	-0.003	0.003	-0.841	4.008e-01	7.829e-01
posterior cingulate	Intercept	0.702	0.013	55.003	9.349e-269	9.632e-269
	Age	0.000	0.000	2.492	1.292e-02	5.491e-02
	APOE Status	0.000	0.005	0.088	9.300e-01	9.775e-01
	Sex	-0.000	0.004	-0.024	9.809e-01	9.966e-01
	APOE Status*Sex	0.003	0.006	0.471	6.380e-01	7.829e-01
precentral	Intercept	0.758	0.007	107.247	0.000e+00	0.000e+00

ROI	Predictor	Estimate	Std. Error	T-Statistic	pUncorrected	pFDR
	Age	-0.000	0.000	-0.528	5.978e-01	7.536e-01
	APOE Status	0.004	0.003	1.467	1.429e-01	8.792e-01
	Sex	0.004	0.002	1.663	9.674e-02	8.976e-01
	APOE Status*Sex	-0.006	0.004	-1.662	9.694e-02	7.829e-01
precuneus	Intercept	0.719	0.007	106.206	0.000e+00	0.000e+00
	Age	-0.000	0.000	-1.793	7.342e-02	2.142e-01
	APOE Status	0.003	0.003	1.078	2.815e-01	8.792e-01
	Sex	-0.001	0.002	-0.480	6.312e-01	9.966e-01
	APOE Status*Sex	-0.005	0.003	-1.400	1.620e-01	7.829e-01
rostral anterior cingulate	Intercept	0.640	0.007	94.232	0.000e+00	0.000e+00
	Age	0.000	0.000	4.506	7.619e-06	1.295e-04
	APOE Status	-0.000	0.003	-0.160	8.730e-01	9.775e-01
	Sex	0.000	0.002	0.039	9.687e-01	9.966e-01
	APOE Status*Sex	0.002	0.003	0.618	5.366e-01	7.829e-01
rostral middle frontal	Intercept	0.701	0.006	115.295	0.000e+00	0.000e+00
	Age	-0.000	0.000	-1.779	7.559e-02	2.142e-01
	APOE Status	0.003	0.002	1.036	3.003e-01	8.792e-01
	Sex	-0.000	0.002	-0.248	8.042e-01	9.966e-01
	APOE Status*Sex	-0.002	0.003	-0.811	4.179e-01	7.829e-01
superior frontal	Intercept	0.705	0.006	120.719	0.000e+00	0.000e+00
	Age	-0.000	0.000	-1.257	2.092e-01	4.244e-01
	APOE Status	0.001	0.002	0.496	6.201e-01	8.935e-01
	Sex	0.001	0.002	0.512	6.091e-01	9.966e-01
	APOE Status*Sex	-0.001	0.003	-0.423	6.725e-01	7.829e-01
superior parietal	Intercept	0.728	0.007	102.647	0.000e+00	0.000e+00
	Age	-0.000	0.000	-1.822	6.883e-02	2.142e-01
	APOE Status	0.003	0.003	1.103	2.703e-01	8.792e-01
	Sex	-0.001	0.002	-0.607	5.438e-01	9.966e-01
	APOE Status*Sex	-0.004	0.004	-1.160	2.464e-01	7.829e-01
superior temporal	Intercept	0.697	0.006	121.416	0.000e+00	0.000e+00
	Age	0.000	0.000	2.708	6.921e-03	3.362e-02

ROI	Predictor	Estimate	Std. Error	T-Statistic	pUncorrected	pFDR
	APOE Status	0.000	0.002	0.029	9.768e-01	9.775e-01
	Sex	-0.001	0.002	-0.708	4.792e-01	9.966e-01
	APOE Status*Sex	-0.002	0.003	-0.632	5.278e-01	7.829e-01
supramarginal	Intercept	0.705	0.006	116.126	0.000e+00	0.000e+00
	Age	-0.000	0.000	-0.075	9.401e-01	9.686e-01
	APOE Status	0.002	0.002	0.728	4.667e-01	8.792e-01
	Sex	-0.001	0.002	-0.724	4.695e-01	9.966e-01
	APOE Status*Sex	-0.002	0.003	-0.692	4.891e-01	7.829e-01
temporal pole	Intercept	0.653	0.007	97.808	0.000e+00	0.000e+00
	Age	0.000	0.000	4.396	1.254e-05	1.421e-04
	APOE Status	-0.004	0.003	-1.319	1.876e-01	8.792e-01
	Sex	0.000	0.002	0.034	9.725e-01	9.966e-01
	APOE Status*Sex	0.002	0.003	0.549	5.829e-01	7.829e-01
transverse temporal	Intercept	0.758	0.008	96.300	0.000e+00	0.000e+00
	Age	0.000	0.000	3.624	3.086e-04	2.098e-03
	APOE Status	0.003	0.003	0.991	3.222e-01	8.792e-01
	Sex	0.001	0.002	0.356	7.220e-01	9.966e-01
	APOE Status*Sex	-0.008	0.004	-2.062	3.953e-02	7.829e-01

Table B7: Outputs of linear regression models assessing interaction effect of sex and APOE status on cortical-adjacent WM R1

ROI	Predictor	Estimate	Std. Error	T-Statistic	pUncorrected	pFDR
bankssts	Intercept	1.085	0.073	14.840	4.108e-44	8.730e-44
	Age	0.005	0.002	2.106	3.551e-02	6.940e-02
	Age^2	-0.000	0.000	-3.192	1.470e-03	2.630e-03
	APOE Status	0.005	0.005	0.931	3.523e-01	3.864e-01
	Sex	-0.008	0.004	-2.229	2.606e-02	6.329e-02
	APOE Status*Sex	-0.012	0.006	-1.979	4.821e-02	8.792e-02
caudal anterior cingulate	Intercept	1.067	0.079	13.587	6.237e-38	7.573e-38
	Age	0.007	0.002	2.764	5.843e-03	2.934e-02
	Age^2	-0.000	0.000	-3.848	1.286e-04	5.708e-04
	APOE Status	0.010	0.005	1.867	6.231e-02	3.549e-01
	Sex	-0.012	0.004	-3.147	1.709e-03	6.247e-03
	APOE Status*Sex	-0.011	0.006	-1.733	8.355e-02	1.066e-01
caudal middle frontal	Intercept	1.100	0.069	15.967	6.238e-50	4.242e-49
	Age	0.004	0.002	1.709	8.779e-02	1.148e-01
	Age^2	-0.000	0.000	-3.038	2.460e-03	3.485e-03
	APOE Status	0.004	0.005	0.932	3.516e-01	3.864e-01
	Sex	-0.004	0.003	-1.110	2.673e-01	3.246e-01
	APOE Status*Sex	-0.008	0.006	-1.460	1.448e-01	1.539e-01
cuneus	Intercept	1.081	0.074	14.641	4.123e-43	7.009e-43
	Age	0.001	0.002	0.583	5.604e-01	5.954e-01
	Age^2	-0.000	0.000	-1.276	2.023e-01	2.084e-01
	APOE Status	0.007	0.005	1.421	1.557e-01	3.549e-01
	Sex	-0.017	0.004	-4.679	3.394e-06	1.154e-04
	APOE Status*Sex	-0.012	0.006	-2.000	4.590e-02	8.792e-02
entorhinal	Intercept	0.739	0.078	9.434	4.331e-20	4.331e-20
	Age	0.011	0.002	4.633	4.207e-06	1.430e-04
	Age^2	-0.000	0.000	-5.595	3.046e-08	1.036e-06
	APOE Status	0.006	0.005	1.185	2.363e-01	3.549e-01

ROI	Predictor	Estimate	Std. Error	T-Statistic	pUncorrected	pFDR
	Sex	-0.005	0.004	-1.269	2.047e-01	2.900e-01
	APOE Status*Sex	-0.011	0.006	-1.772	7.685e-02	1.066e-01
frontal pole	Intercept	0.953	0.077	12.437	1.503e-32	1.648e-32
	Age	0.005	0.002	2.175	2.990e-02	6.354e-02
	Age^2	-0.000	0.000	-3.362	8.102e-04	1.968e-03
	APOE Status	0.006	0.005	1.206	2.283e-01	3.549e-01
	Sex	0.002	0.004	0.596	5.514e-01	5.514e-01
	APOE Status*Sex	-0.008	0.006	-1.327	1.848e-01	1.904e-01
fusiform	Intercept	1.060	0.073	14.552	1.144e-42	1.768e-42
	Age	0.004	0.002	1.989	4.701e-02	7.992e-02
	Age^2	-0.000	0.000	-3.188	1.491e-03	2.630e-03
	APOE Status	0.006	0.005	1.214	2.253e-01	3.549e-01
	Sex	-0.005	0.004	-1.314	1.891e-01	2.795e-01
	APOE Status*Sex	-0.012	0.006	-2.005	4.528e-02	8.792e-02
inferior parietal	Intercept	1.071	0.073	14.575	8.809e-43	1.426e-42
	Age	0.004	0.002	1.824	6.859e-02	9.506e-02
	Age^2	-0.000	0.000	-2.972	3.046e-03	4.143e-03
	APOE Status	0.007	0.005	1.484	1.382e-01	3.549e-01
	Sex	-0.014	0.004	-3.724	2.097e-04	2.377e-03
	APOE Status*Sex	-0.013	0.006	-2.108	3.531e-02	8.792e-02
inferior temporal	Intercept	1.061	0.071	14.965	9.502e-45	2.308e-44
	Age	0.004	0.002	1.860	6.330e-02	9.357e-02
	Age^2	-0.000	0.000	-3.072	2.199e-03	3.251e-03
	APOE Status	0.006	0.005	1.176	2.401e-01	3.549e-01
	Sex	-0.006	0.004	-1.805	7.151e-02	1.430e-01
	APOE Status*Sex	-0.011	0.006	-1.951	5.143e-02	8.792e-02
insula	Intercept	0.978	0.064	15.304	1.756e-46	5.539e-46
	Age	0.005	0.002	2.733	6.419e-03	2.934e-02
	Age^2	-0.000	0.000	-3.628	3.041e-04	1.149e-03
	APOE Status	0.006	0.004	1.499	1.343e-01	3.549e-01
	Sex	-0.006	0.003	-1.820	6.918e-02	1.430e-01

ROI	Predictor	Estimate	Std. Error	T-Statistic	pUncorrected	pFDR
	APOE Status*Sex	-0.011	0.005	-2.093	3.667e-02	8.792e-02
isthmus cingulate	Intercept	1.100	0.074	14.795	6.925e-44	1.308e-43
	Age	0.005	0.002	2.270	2.346e-02	5.731e-02
	Age^2	-0.000	0.000	-3.106	1.961e-03	3.031e-03
	APOE Status	0.007	0.005	1.465	1.432e-01	3.549e-01
	Sex	-0.013	0.004	-3.505	4.816e-04	2.729e-03
	APOE Status*Sex	-0.014	0.006	-2.224	2.644e-02	8.792e-02
lateral occipital	Intercept	1.126	0.069	16.249	2.020e-51	2.289e-50
	Age	0.001	0.002	0.466	6.416e-01	6.610e-01
	Age^2	-0.000	0.000	-1.368	1.717e-01	1.824e-01
	APOE Status	0.005	0.005	0.988	3.232e-01	3.864e-01
	Sex	-0.013	0.003	-3.871	1.174e-04	1.996e-03
	APOE Status*Sex	-0.013	0.006	-2.201	2.805e-02	8.792e-02
lateral orbitofrontal	Intercept	0.951	0.072	13.287	1.685e-36	1.976e-36
	Age	0.008	0.002	3.636	2.952e-04	5.018e-03
	Age^2	-0.000	0.000	-5.022	6.344e-07	1.078e-05
	APOE Status	0.008	0.005	1.565	1.180e-01	3.549e-01
	Sex	-0.002	0.004	-0.659	5.100e-01	5.255e-01
	APOE Status*Sex	-0.011	0.006	-1.948	5.172e-02	8.792e-02
lingual	Intercept	1.058	0.069	15.369	8.147e-47	3.462e-46
	Age	0.003	0.002	1.231	2.187e-01	2.656e-01
	Age^2	-0.000	0.000	-2.100	3.606e-02	3.955e-02
	APOE Status	0.006	0.005	1.315	1.890e-01	3.549e-01
	Sex	-0.012	0.003	-3.594	3.456e-04	2.729e-03
	APOE Status*Sex	-0.014	0.006	-2.477	1.347e-02	8.792e-02
medial orbitofrontal	Intercept	0.952	0.072	13.153	7.283e-36	8.254e-36
	Age	0.007	0.002	3.119	1.884e-03	1.281e-02
	Age^2	-0.000	0.000	-4.495	8.004e-06	9.071e-05
	APOE Status	0.007	0.005	1.442	1.497e-01	3.549e-01
	Sex	-0.004	0.004	-1.124	2.614e-01	3.246e-01
	APOE Status*Sex	-0.010	0.006	-1.726	8.467e-02	1.066e-01

ROI	Predictor	Estimate	Std. Error	T-Statistic	pUncorrected	pFDR
middle temporal	Intercept	1.075	0.070	15.417	4.590e-47	2.229e-46
	Age	0.004	0.002	1.880	6.044e-02	9.341e-02
	Age^2	-0.000	0.000	-3.177	1.547e-03	2.630e-03
	APOE Status	0.004	0.005	0.745	4.565e-01	4.850e-01
	Sex	-0.009	0.003	-2.563	1.056e-02	2.762e-02
	APOE Status*Sex	-0.009	0.006	-1.550	1.216e-01	1.378e-01
paracentral	Intercept	1.141	0.071	16.130	8.557e-51	7.273e-50
	Age	0.002	0.002	1.024	3.061e-01	3.469e-01
	Age^2	-0.000	0.000	-2.151	3.177e-02	3.858e-02
	APOE Status	0.007	0.005	1.482	1.386e-01	3.549e-01
	Sex	-0.006	0.004	-1.715	8.680e-02	1.640e-01
	APOE Status*Sex	-0.012	0.006	-2.020	4.370e-02	8.792e-02
parahippocampal	Intercept	0.929	0.078	11.845	6.656e-30	7.072e-30
	Age	0.008	0.002	3.315	9.588e-04	8.542e-03
	Age^2	-0.000	0.000	-4.132	3.979e-05	2.706e-04
	APOE Status	0.006	0.005	1.086	2.778e-01	3.659e-01
	Sex	-0.012	0.004	-3.122	1.860e-03	6.247e-03
	APOE Status*Sex	-0.014	0.006	-2.107	3.540e-02	8.792e-02
pars opercularis	Intercept	1.068	0.069	15.472	2.380e-47	1.349e-46
	Age	0.005	0.002	2.268	2.360e-02	5.731e-02
	Age^2	-0.000	0.000	-3.552	4.052e-04	1.252e-03
	APOE Status	0.007	0.005	1.426	1.544e-01	3.549e-01
	Sex	-0.004	0.003	-1.214	2.250e-01	3.060e-01
	APOE Status*Sex	-0.012	0.006	-2.116	3.469e-02	8.792e-02
pars orbitalis	Intercept	1.006	0.070	14.329	1.479e-41	2.095e-41
	Age	0.005	0.002	2.318	2.073e-02	5.731e-02
	Age^2	-0.000	0.000	-3.595	3.452e-04	1.174e-03
	APOE Status	0.005	0.005	0.962	3.362e-01	3.864e-01
	Sex	-0.003	0.003	-0.789	4.302e-01	4.718e-01
	APOE Status*Sex	-0.009	0.006	-1.488	1.372e-01	1.505e-01
pars triangularis	Intercept	1.039	0.070	14.909	1.825e-44	4.137e-44

ROI	Predictor	Estimate	Std. Error	T-Statistic	pUncorrected	pFDR
	Age	0.006	0.002	2.630	8.707e-03	3.289e-02
	Age^2	-0.000	0.000	-3.985	7.364e-05	4.173e-04
	APOE Status	0.006	0.005	1.291	1.969e-01	3.549e-01
	Sex	-0.003	0.003	-0.924	3.558e-01	4.032e-01
	APOE Status*Sex	-0.010	0.006	-1.823	6.864e-02	1.061e-01
pericalcarine	Intercept	1.090	0.079	13.879	2.429e-39	3.059e-39
	Age	0.000	0.002	0.140	8.886e-01	8.886e-01
	Age^2	-0.000	0.000	-0.772	4.404e-01	4.404e-01
	APOE Status	0.006	0.005	1.058	2.906e-01	3.659e-01
	Sex	-0.014	0.004	-3.511	4.714e-04	2.729e-03
	APOE Status*Sex	-0.014	0.006	-2.237	2.560e-02	8.792e-02
postcentral	Intercept	1.107	0.067	16.537	5.916e-53	1.006e-51
	Age	0.002	0.002	1.085	2.782e-01	3.262e-01
	Age^2	-0.000	0.000	-2.120	3.430e-02	3.887e-02
	APOE Status	0.008	0.005	1.738	8.252e-02	3.549e-01
	Sex	-0.006	0.003	-1.900	5.774e-02	1.309e-01
	APOE Status*Sex	-0.012	0.006	-2.194	2.852e-02	8.792e-02
posterior cingulate	Intercept	1.098	0.074	14.785	7.783e-44	1.393e-43
	Age	0.005	0.002	2.241	2.529e-02	5.732e-02
	Age^2	-0.000	0.000	-3.270	1.123e-03	2.386e-03
	APOE Status	0.005	0.005	1.081	2.801e-01	3.659e-01
	Sex	-0.011	0.004	-3.097	2.021e-03	6.247e-03
	APOE Status*Sex	-0.010	0.006	-1.601	1.099e-01	1.312e-01
precentral	Intercept	1.144	0.067	17.063	8.644e-56	2.939e-54
	Age	0.002	0.002	0.952	3.413e-01	3.743e-01
	Age^2	-0.000	0.000	-2.128	3.361e-02	3.887e-02
	APOE Status	0.006	0.005	1.358	1.750e-01	3.549e-01
	Sex	-0.004	0.003	-1.162	2.456e-01	3.212e-01
	APOE Status*Sex	-0.011	0.006	-2.036	4.212e-02	8.792e-02
precuneus	Intercept	1.067	0.075	14.245	3.884e-41	5.079e-41
	Age	0.005	0.002	2.092	3.674e-02	6.940e-02

ROI	Predictor	Estimate	Std. Error	T-Statistic	pUncorrected	pFDR
	Age^2	-0.000	0.000	-3.314	9.633e-04	2.183e-03
	APOE Status	0.009	0.005	1.745	8.138e-02	3.549e-01
	Sex	-0.012	0.004	-3.212	1.370e-03	5.822e-03
	APOE Status*Sex	-0.015	0.006	-2.469	1.377e-02	8.792e-02
rostral anterior cingulate	Intercept	1.098	0.077	14.246	3.807e-41	5.079e-41
	Age	0.004	0.002	1.815	6.990e-02	9.506e-02
	Age^2	-0.000	0.000	-2.850	4.482e-03	5.861e-03
	APOE Status	0.006	0.005	1.063	2.880e-01	3.659e-01
	Sex	-0.003	0.004	-0.735	4.627e-01	4.916e-01
	APOE Status*Sex	-0.006	0.006	-1.013	3.112e-01	3.112e-01
rostral middle frontal	Intercept	1.074	0.072	14.819	5.244e-44	1.049e-43
	Age	0.004	0.002	1.924	5.473e-02	8.861e-02
	Age^2	-0.000	0.000	-3.250	1.205e-03	2.410e-03
	APOE Status	0.007	0.005	1.483	1.384e-01	3.549e-01
	Sex	-0.005	0.004	-1.324	1.859e-01	2.795e-01
	APOE Status*Sex	-0.010	0.006	-1.748	8.081e-02	1.066e-01
superior frontal	Intercept	1.064	0.070	15.192	6.588e-46	1.867e-45
	Age	0.004	0.002	1.991	4.680e-02	7.992e-02
	Age^2	-0.000	0.000	-3.430	6.356e-04	1.662e-03
	APOE Status	0.006	0.005	1.333	1.828e-01	3.549e-01
	Sex	-0.005	0.003	-1.564	1.182e-01	2.115e-01
	APOE Status*Sex	-0.010	0.006	-1.741	8.202e-02	1.066e-01
superior parietal	Intercept	1.110	0.073	15.107	1.787e-45	4.674e-45
	Age	0.003	0.002	1.287	1.986e-01	2.501e-01
	Age^2	-0.000	0.000	-2.439	1.493e-02	1.880e-02
	APOE Status	0.009	0.005	1.791	7.365e-02	3.549e-01
	Sex	-0.012	0.004	-3.224	1.317e-03	5.822e-03
	APOE Status*Sex	-0.015	0.006	-2.567	1.044e-02	8.792e-02
superior temporal	Intercept	1.022	0.067	15.350	1.016e-46	3.838e-46
	Age	0.006	0.002	2.709	6.904e-03	2.934e-02
	Age^2	-0.000	0.000	-3.837	1.343e-04	5.708e-04

ROI	Predictor	Estimate	Std. Error	T-Statistic	pUncorrected	pFDR
	APOE Status	0.005	0.004	1.195	2.326e-01	3.549e-01
	Sex	-0.005	0.003	-1.531	1.262e-01	2.145e-01
	APOE Status*Sex	-0.012	0.005	-2.176	2.988e-02	8.792e-02
supramarginal	Intercept	1.052	0.072	14.512	1.829e-42	2.704e-42
	Age	0.005	0.002	2.309	2.123e-02	5.731e-02
	Age^2	-0.000	0.000	-3.486	5.179e-04	1.467e-03
	APOE Status	0.008	0.005	1.571	1.166e-01	3.549e-01
	Sex	-0.009	0.004	-2.611	9.200e-03	2.607e-02
	APOE Status*Sex	-0.013	0.006	-2.162	3.091e-02	8.792e-02
temporal pole	Intercept	0.842	0.074	11.316	1.294e-27	1.333e-27
	Age	0.008	0.002	3.302	1.005e-03	8.542e-03
	Age^2	-0.000	0.000	-4.201	2.961e-05	2.517e-04
	APOE Status	0.002	0.005	0.493	6.219e-01	6.407e-01
	Sex	-0.003	0.004	-0.938	3.485e-01	4.032e-01
	APOE Status*Sex	-0.010	0.006	-1.591	1.119e-01	1.312e-01
transverse temporal	Intercept	1.042	0.068	15.302	1.792e-46	5.539e-46
	Age	0.005	0.002	2.478	1.343e-02	4.566e-02
	Age^2	-0.000	0.000	-3.161	1.633e-03	2.644e-03
	APOE Status	0.001	0.005	0.159	8.734e-01	8.734e-01
	Sex	-0.005	0.003	-1.482	1.387e-01	2.246e-01
	APOE Status*Sex	-0.011	0.006	-1.906	5.707e-02	9.240e-02

Appendix C

Overview of ADRC and WRAP studies and visit procedures:

The ADRC clinical core is an ongoing longitudinal study that recruits individuals who are cognitively unimpaired (CU) or are diagnosed with mild cognitive impairment (MCI) or dementia. These individuals undergo annual medical assessment, laboratory testing, and cognitive testing. A subset of ADRC participants undergo biannual MRI with an additional subset undergoing lumbar puncture for cerebrospinal fluid (CSF) biomarker analysis. The WRAP study is an ongoing (~20 years) longitudinal investigation of participants who were CU at enrollment. The cohort is enriched for family history of Alzheimer's disease, and participants undergo biannual medical assessment, laboratory testing, cognitive evaluation, and extensive characterization of medical history, physical activity, caregiver and other stress, social support, diet, sleep quality, and mood. A subset of participants in WRAP are also enrolled in biomarker studies that include biannual MRI, amyloid and tau PET imaging, and lumbar puncture for CSF biomarker analysis.

Affiliated studies with MPnRAGE MRI:

The Longitudinal Early Alzheimer's Disease study [LEAD, n = 8]; the Synapse study [n = 2]; and the Longitudinal Impact of Fitness and Exercise study [LIFE, n = 3].

Table C1: MPnRAGE acquisition parameters for each protocol used.

Protocol	N1	N2	Alpha1	Alpha2	TD
A	325/326	111/112	4	6	237/242
B	304	81/82	4	8	505
C	304	81/82	4	8	502/503
D	325	51/61	4	8	505

Figure C1: Outline of image processing steps conducted using FSL and Freesurfer and resulting WM parcellation maps and surface meshes.

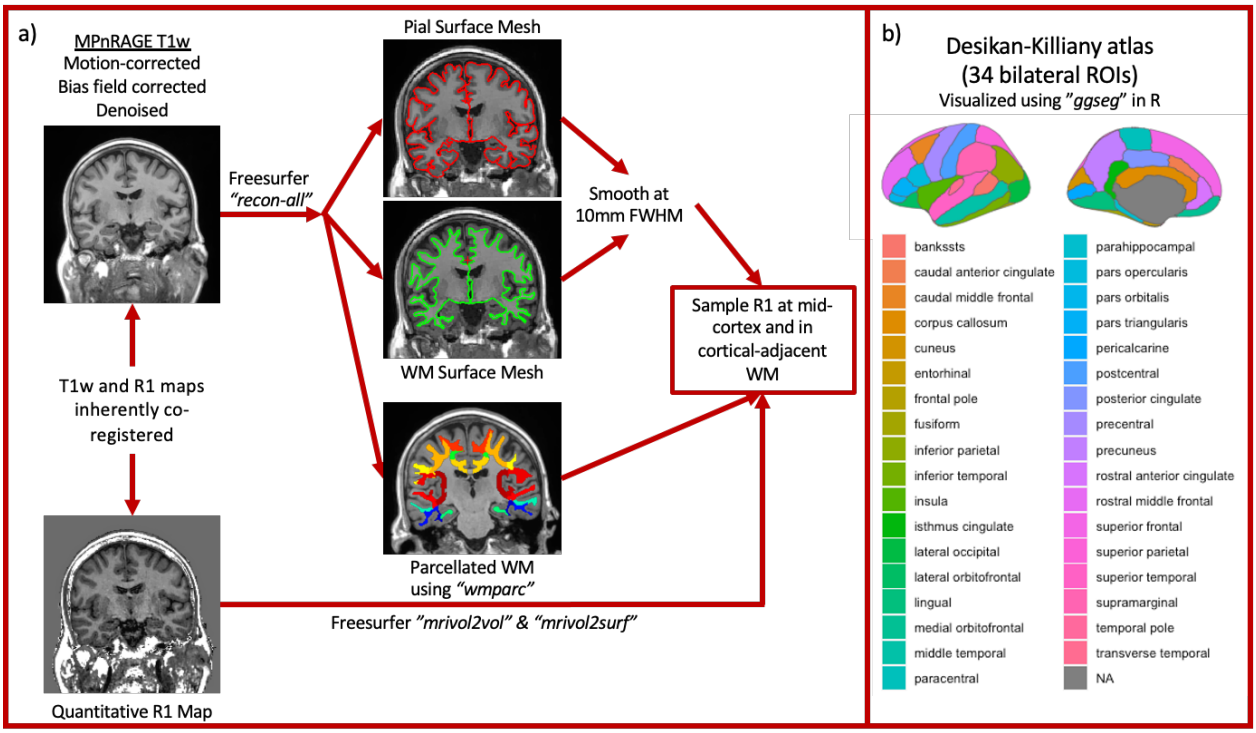

Figure C1: a) Image processing pipeline: T1w images were processed using Advanced Normalization Tools (ANTs) and Freesurfer v6. R1 was sampled at the midpoint of the cortical surface using surface meshes and parcellations produced from Freesurfer for 34 bilaterally-averaged regions of interest (ROI) from the Desikan-Killiany parcellation. b) Regions of interest comprised of bilaterally-averaged regions from the Desikan-Killiany parcellation overlayed onto a brain using the "ggseg" package in R.

Table C2: Outputs of linear regression models assessing effects of CSF Aβ42/40 on cortical GM

R1

ROI	Predictor	Estimate	Std. Error	T-Statistic	pUncorrected	pFDR
bankssts	Intercept	0.701	0.012	59.879	1.201e-199	2.722e-199
	Age	-0.000	0.000	-0.358	7.203e-01	8.713e-01
	AB_42_40	0.160	0.065	2.447	1.485e-02	8.593e-02
	Sex	0.002	0.002	1.069	2.857e-01	9.895e-01
	APOE4 Status	0.004	0.002	1.632	1.035e-01	8.998e-01
	Time b/w LP and MRI	0.001	0.000	1.582	1.144e-01	1.441e-01
caudal anterior cingulate	Intercept	0.686	0.018	37.734	6.534e-132	6.942e-132
	Age	0.000	0.000	1.230	2.194e-01	5.738e-01
	AB_42_40	-0.098	0.102	-0.963	3.361e-01	4.416e-01
	Sex	-0.006	0.003	-1.798	7.297e-02	9.180e-01
	APOE4 Status	-0.001	0.004	-0.242	8.088e-01	9.383e-01
	Time b/w LP and MRI	0.001	0.001	1.689	9.210e-02	1.204e-01
caudal middle frontal	Intercept	0.713	0.012	61.695	2.947e-204	7.708e-204
	Age	-0.000	0.000	-0.523	6.016e-01	8.286e-01
	AB_42_40	0.091	0.065	1.405	1.608e-01	2.790e-01
	Sex	0.000	0.002	0.192	8.479e-01	9.895e-01
	APOE4 Status	0.003	0.002	1.171	2.424e-01	8.998e-01
	Time b/w LP and MRI	0.001	0.000	2.040	4.207e-02	7.528e-02
cuneus	Intercept	0.726	0.015	48.534	4.489e-168	5.263e-168
	Age	-0.000	0.000	-1.105	2.697e-01	6.550e-01
	AB_42_40	0.198	0.084	2.370	1.826e-02	8.593e-02
	Sex	-0.004	0.003	-1.612	1.077e-01	9.180e-01
	APOE4 Status	-0.000	0.003	-0.025	9.804e-01	9.804e-01
	Time b/w LP and MRI	0.001	0.001	2.634	8.765e-03	3.725e-02
entorhinal	Intercept	0.828	0.029	28.939	1.930e-99	1.930e-99
	Age	-0.001	0.000	-1.614	1.072e-01	4.027e-01
	AB_42_40	-0.148	0.160	-0.926	3.549e-01	4.469e-01
	Sex	0.002	0.005	0.374	7.084e-01	9.895e-01

ROI	Predictor	Estimate	Std. Error	T-Statistic	pUncorrected	pFDR
	APOE4 Status	0.001	0.006	0.122	9.033e-01	9.383e-01
	Time b/w LP and MRI	0.001	0.001	1.129	2.594e-01	2.756e-01
frontal pole	Intercept	0.674	0.013	53.285	6.469e-182	9.563e-182
	Age	-0.000	0.000	-0.481	6.305e-01	8.286e-01
	AB_42_40	0.098	0.071	1.394	1.641e-01	2.790e-01
	Sex	-0.004	0.002	-1.526	1.278e-01	9.180e-01
	APOE4 Status	0.002	0.002	0.879	3.797e-01	8.998e-01
	Time b/w LP and MRI	0.001	0.000	3.218	1.400e-03	2.772e-02
fusiform	Intercept	0.686	0.010	67.754	7.137e-219	1.213e-217
	Age	0.000	0.000	0.443	6.580e-01	8.286e-01
	AB_42_40	-0.000	0.057	-0.000	9.998e-01	9.998e-01
	Sex	0.001	0.002	0.557	5.776e-01	9.895e-01
	APOE4 Status	-0.001	0.002	-0.301	7.632e-01	9.383e-01
	Time b/w LP and MRI	0.001	0.000	2.062	3.991e-02	7.528e-02
inferior parietal	Intercept	0.692	0.012	56.115	1.010e-189	1.717e-189
	Age	-0.000	0.000	-0.276	7.825e-01	8.805e-01
	AB_42_40	0.215	0.069	3.117	1.959e-03	3.330e-02
	Sex	-0.001	0.002	-0.481	6.308e-01	9.895e-01
	APOE4 Status	0.005	0.002	1.919	5.569e-02	8.998e-01
	Time b/w LP and MRI	0.001	0.000	2.322	2.075e-02	5.490e-02
inferior temporal	Intercept	0.670	0.010	65.916	1.475e-214	7.164e-214
	Age	0.000	0.000	0.935	3.503e-01	7.394e-01
	AB_42_40	-0.003	0.057	-0.049	9.612e-01	9.903e-01
	Sex	0.000	0.002	0.207	8.365e-01	9.895e-01
	APOE4 Status	-0.000	0.002	-0.199	8.421e-01	9.383e-01
	Time b/w LP and MRI	0.001	0.000	2.317	2.099e-02	5.490e-02
insula	Intercept	0.656	0.010	66.792	1.255e-216	1.067e-215
	Age	0.000	0.000	4.208	3.196e-05	1.087e-03
	AB_42_40	0.009	0.055	0.155	8.765e-01	9.313e-01
	Sex	0.001	0.002	0.301	7.636e-01	9.895e-01
	APOE4 Status	-0.000	0.002	-0.198	8.432e-01	9.383e-01

ROI	Predictor	Estimate	Std. Error	T-Statistic	pUncorrected	pFDR
	Time b/w LP and MRI	0.001	0.000	2.276	2.337e-02	5.676e-02
isthmus cingulate	Intercept	0.710	0.015	46.476	2.516e-161	2.851e-161
	Age	0.000	0.000	0.726	4.685e-01	8.286e-01
	AB_42_40	0.153	0.085	1.792	7.395e-02	1.701e-01
	Sex	-0.000	0.003	-0.156	8.763e-01	9.895e-01
	APOE4 Status	0.002	0.003	0.764	4.456e-01	8.998e-01
	Time b/w LP and MRI	0.001	0.001	1.192	2.338e-01	2.564e-01
lateral occipital	Intercept	0.693	0.013	52.700	2.927e-180	3.981e-180
	Age	0.000	0.000	0.898	3.697e-01	7.394e-01
	AB_42_40	0.171	0.074	2.332	2.022e-02	8.593e-02
	Sex	-0.002	0.002	-1.009	3.137e-01	9.895e-01
	APOE4 Status	0.002	0.003	0.634	5.267e-01	8.998e-01
	Time b/w LP and MRI	0.001	0.000	2.488	1.327e-02	4.460e-02
lateral orbitofrontal	Intercept	0.691	0.011	63.311	2.886e-208	9.812e-208
	Age	-0.000	0.000	-0.462	6.441e-01	8.286e-01
	AB_42_40	-0.045	0.061	-0.744	4.575e-01	5.185e-01
	Sex	-0.003	0.002	-1.455	1.464e-01	9.180e-01
	APOE4 Status	-0.003	0.002	-1.185	2.368e-01	8.998e-01
	Time b/w LP and MRI	0.001	0.000	2.824	4.990e-03	2.772e-02
lingual	Intercept	0.706	0.013	54.160	2.317e-184	3.581e-184
	Age	-0.000	0.000	-0.140	8.889e-01	9.158e-01
	AB_42_40	0.110	0.073	1.515	1.306e-01	2.612e-01
	Sex	-0.000	0.002	-0.100	9.207e-01	9.895e-01
	APOE4 Status	0.001	0.003	0.444	6.570e-01	9.383e-01
	Time b/w LP and MRI	0.001	0.000	2.207	2.789e-02	5.927e-02
medial orbitofrontal	Intercept	0.655	0.010	65.104	2.787e-212	1.053e-211
	Age	0.000	0.000	1.524	1.284e-01	4.027e-01
	AB_42_40	-0.051	0.056	-0.897	3.704e-01	4.498e-01
	Sex	-0.003	0.002	-1.401	1.620e-01	9.180e-01
	APOE4 Status	-0.002	0.002	-0.994	3.209e-01	8.998e-01
	Time b/w LP and MRI	0.001	0.000	2.591	9.929e-03	3.751e-02

ROI	Predictor	Estimate	Std. Error	T-Statistic	pUncorrected	pFDR
middle temporal	Intercept	0.673	0.009	71.651	1.049e-227	3.567e-226
	Age	0.000	0.000	1.236	2.174e-01	5.738e-01
	AB_42_40	0.050	0.052	0.960	3.377e-01	4.416e-01
	Sex	0.000	0.002	0.061	9.512e-01	9.895e-01
	APOE4 Status	0.001	0.002	0.372	7.100e-01	9.383e-01
	Time b/w LP and MRI	0.001	0.000	2.808	5.226e-03	2.772e-02
paracentral	Intercept	0.743	0.013	57.931	2.806e-194	5.612e-194
	Age	0.000	0.000	0.068	9.455e-01	9.455e-01
	AB_42_40	0.142	0.072	1.971	4.940e-02	1.527e-01
	Sex	0.002	0.002	0.792	4.287e-01	9.895e-01
	APOE4 Status	0.002	0.002	0.630	5.293e-01	8.998e-01
	Time b/w LP and MRI	0.000	0.000	0.346	7.296e-01	7.296e-01
parahippocampal	Intercept	0.668	0.013	52.363	2.662e-179	3.481e-179
	Age	0.000	0.000	2.566	1.066e-02	7.936e-02
	AB_42_40	-0.070	0.071	-0.986	3.248e-01	4.416e-01
	Sex	0.001	0.002	0.442	6.589e-01	9.895e-01
	APOE4 Status	-0.003	0.002	-1.168	2.436e-01	8.998e-01
	Time b/w LP and MRI	0.001	0.000	1.911	5.675e-02	8.364e-02
pars opercularis	Intercept	0.689	0.010	66.601	3.526e-216	1.998e-215
	Age	0.000	0.000	1.611	1.080e-01	4.027e-01
	AB_42_40	0.117	0.058	2.016	4.446e-02	1.527e-01
	Sex	-0.001	0.002	-0.514	6.073e-01	9.895e-01
	APOE4 Status	0.002	0.002	0.768	4.428e-01	8.998e-01
	Time b/w LP and MRI	0.001	0.000	1.893	5.904e-02	8.364e-02
pars orbitalis	Intercept	0.686	0.011	61.755	2.083e-204	5.902e-204
	Age	0.000	0.000	0.558	5.773e-01	8.286e-01
	AB_42_40	0.082	0.062	1.327	1.853e-01	3.000e-01
	Sex	-0.002	0.002	-0.961	3.370e-01	9.895e-01
	APOE4 Status	0.000	0.002	0.122	9.031e-01	9.383e-01
	Time b/w LP and MRI	0.001	0.000	2.887	4.104e-03	2.772e-02
pars triangularis	Intercept	0.694	0.011	65.866	1.940e-214	8.245e-214

ROI	Predictor	Estimate	Std. Error	T-Statistic	pUncorrected	pFDR
	Age	0.000	0.000	0.621	5.353e-01	8.286e-01
	AB_42_40	0.106	0.059	1.792	7.385e-02	1.701e-01
	Sex	-0.002	0.002	-1.097	2.735e-01	9.895e-01
	APOE4 Status	0.001	0.002	0.640	5.227e-01	8.998e-01
	Time b/w LP and MRI	0.001	0.000	2.931	3.576e-03	2.772e-02
pericalcarine	Intercept	0.720	0.016	44.830	1.354e-156	1.485e-156
	Age	0.000	0.000	0.328	7.432e-01	8.713e-01
	AB_42_40	0.106	0.090	1.177	2.399e-01	3.546e-01
	Sex	-0.005	0.003	-1.729	8.463e-02	9.180e-01
	APOE4 Status	0.000	0.003	0.123	9.022e-01	9.383e-01
	Time b/w LP and MRI	0.001	0.001	2.457	1.443e-02	4.460e-02
postcentral	Intercept	0.715	0.012	57.918	1.535e-194	3.262e-194
	Age	0.000	0.000	1.516	1.303e-01	4.027e-01
	AB_42_40	0.164	0.069	2.383	1.764e-02	8.593e-02
	Sex	0.001	0.002	0.391	6.959e-01	9.895e-01
	APOE4 Status	0.002	0.002	0.799	4.246e-01	8.998e-01
	Time b/w LP and MRI	0.001	0.000	1.528	1.272e-01	1.545e-01
posterior cingulate	Intercept	0.710	0.022	32.088	1.799e-110	1.854e-110
	Age	0.000	0.000	1.543	1.237e-01	4.027e-01
	AB_42_40	0.020	0.124	0.163	8.702e-01	9.313e-01
	Sex	-0.001	0.004	-0.153	8.784e-01	9.895e-01
	APOE4 Status	0.001	0.004	0.194	8.465e-01	9.383e-01
	Time b/w LP and MRI	0.001	0.001	0.945	3.453e-01	3.558e-01
precentral	Intercept	0.748	0.013	57.419	3.220e-193	6.082e-193
	Age	0.000	0.000	0.173	8.628e-01	9.158e-01
	AB_42_40	0.130	0.073	1.787	7.476e-02	1.701e-01
	Sex	0.002	0.002	0.803	4.224e-01	9.895e-01
	APOE4 Status	0.002	0.003	0.944	3.455e-01	8.998e-01
	Time b/w LP and MRI	0.001	0.000	1.693	9.133e-02	1.204e-01
precuneus	Intercept	0.702	0.012	56.371	2.050e-190	3.668e-190
	Age	-0.000	0.000	-0.661	5.088e-01	8.286e-01

ROI	Predictor	Estimate	Std. Error	T-Statistic	pUncorrected	pFDR
	AB_42_40	0.200	0.070	2.875	4.256e-03	3.618e-02
	Sex	-0.000	0.002	-0.013	9.895e-01	9.895e-01
	APOE4 Status	0.003	0.002	1.059	2.904e-01	8.998e-01
	Time b/w LP and MRI	0.001	0.000	2.220	2.702e-02	5.927e-02
rostral anterior cingulate	Intercept	0.649	0.012	53.193	2.178e-181	3.086e-181
	Age	0.000	0.000	2.912	3.797e-03	4.303e-02
	AB_42_40	-0.096	0.068	-1.400	1.622e-01	2.790e-01
	Sex	-0.000	0.002	-0.013	9.893e-01	9.895e-01
	APOE4 Status	0.000	0.002	0.112	9.107e-01	9.383e-01
	Time b/w LP and MRI	0.001	0.000	1.418	1.571e-01	1.828e-01
rostral middle frontal	Intercept	0.693	0.011	61.555	6.637e-204	1.612e-203
	Age	-0.000	0.000	-1.026	3.053e-01	6.920e-01
	AB_42_40	0.126	0.063	2.011	4.498e-02	1.527e-01
	Sex	-0.003	0.002	-1.296	1.958e-01	9.510e-01
	APOE4 Status	0.003	0.002	1.481	1.393e-01	8.998e-01
	Time b/w LP and MRI	0.001	0.000	3.080	2.218e-03	2.772e-02
superior frontal	Intercept	0.704	0.010	67.238	2.535e-217	2.873e-216
	Age	-0.000	0.000	-0.747	4.554e-01	8.286e-01
	AB_42_40	0.050	0.059	0.855	3.933e-01	4.611e-01
	Sex	0.000	0.002	0.235	8.143e-01	9.895e-01
	APOE4 Status	0.001	0.002	0.638	5.241e-01	8.998e-01
	Time b/w LP and MRI	0.001	0.000	1.964	5.021e-02	8.364e-02
superior parietal	Intercept	0.705	0.013	55.615	2.295e-188	3.716e-188
	Age	-0.000	0.000	-0.250	8.028e-01	8.805e-01
	AB_42_40	0.233	0.071	3.295	1.075e-03	3.330e-02
	Sex	-0.001	0.002	-0.329	7.426e-01	9.895e-01
	APOE4 Status	0.004	0.002	1.422	1.558e-01	8.998e-01
	Time b/w LP and MRI	0.001	0.000	1.915	5.628e-02	8.364e-02
superior temporal	Intercept	0.689	0.010	66.695	2.122e-216	1.443e-215
	Age	0.000	0.000	2.307	2.155e-02	1.221e-01
	AB_42_40	0.103	0.058	1.785	7.503e-02	1.701e-01

ROI	Predictor	Estimate	Std. Error	T-Statistic	pUncorrected	pFDR
	Sex	-0.000	0.002	-0.031	9.755e-01	9.895e-01
	APOE4 Status	0.000	0.002	0.211	8.333e-01	9.383e-01
	Time b/w LP and MRI	0.001	0.000	2.181	2.981e-02	5.962e-02
supramarginal	Intercept	0.690	0.011	62.943	2.325e-207	7.186e-207
	Age	0.000	0.000	0.606	5.451e-01	8.286e-01
	AB_42_40	0.178	0.061	2.904	3.894e-03	3.618e-02
	Sex	-0.001	0.002	-0.540	5.895e-01	9.895e-01
	APOE4 Status	0.003	0.002	1.406	1.606e-01	8.998e-01
	Time b/w LP and MRI	0.001	0.000	1.900	5.822e-02	8.364e-02
temporal pole	Intercept	0.656	0.013	50.742	1.264e-174	1.535e-174
	Age	0.001	0.000	3.719	2.294e-04	3.900e-03
	AB_42_40	-0.125	0.072	-1.726	8.516e-02	1.810e-01
	Sex	0.001	0.002	0.613	5.404e-01	9.895e-01
	APOE4 Status	-0.004	0.003	-1.635	1.029e-01	8.998e-01
	Time b/w LP and MRI	0.001	0.000	1.403	1.613e-01	1.828e-01
transverse temporal	Intercept	0.755	0.015	51.878	6.498e-178	8.183e-178
	Age	0.000	0.000	2.534	1.167e-02	7.936e-02
	AB_42_40	0.096	0.081	1.180	2.388e-01	3.546e-01
	Sex	-0.001	0.003	-0.233	8.160e-01	9.895e-01
	APOE4 Status	-0.001	0.003	-0.450	6.532e-01	9.383e-01
	Time b/w LP and MRI	0.001	0.001	2.779	5.708e-03	2.772e-02

Table C2: Estimated outputs of each linear regression model assessing the effects of CSF Aβ42/40 ratio on cortical GM R1. Covariates in each model included age, sex, APOE4 status, and time between lumbar puncture and MRI. Abbreviations: AB_42_40, CSF Aβ42/40 ratio; LP, lumbar puncture; MRI, magnetic resonance imaging; pUncorrected, *p*-value uncorrected for multiple comparisons; pFDR, Benjamini-Hochberg FDR-corrected *p*-value.

Table C3: Outputs of linear regression models assessing effects of CSF Aβ42/40 on cortical-adjacent WM R1

ROI	Predictor	Estimate	Std. Error	T-Statistic	pUncorrected	pFDR
bankssts	Intercept	1.019	0.119	8.528	3.241e-16	5.009e-16
	Age	0.007	0.004	1.860	6.362e-02	1.627e-01
	Age^2	-0.000	0.000	-2.579	1.026e-02	2.133e-02
	AB_42_40	0.290	0.136	2.127	3.406e-02	1.564e-01
	Sex	-0.012	0.004	-2.622	9.073e-03	2.203e-02
	APOE4 Status	0.003	0.005	0.633	5.268e-01	9.748e-01
	Time b/w LP and MRI	-0.000	0.001	-0.485	6.282e-01	9.971e-01
caudal anterior cingulate	Intercept	1.003	0.112	8.976	1.182e-17	2.871e-17
	Age	0.009	0.003	2.714	6.942e-03	5.901e-02
	Age^2	-0.000	0.000	-3.631	3.203e-04	4.196e-03
	AB_42_40	0.146	0.128	1.142	2.541e-01	3.456e-01
	Sex	-0.017	0.004	-4.038	6.493e-05	4.051e-04
	APOE4 Status	0.007	0.004	1.633	1.034e-01	9.748e-01
	Time b/w LP and MRI	-0.000	0.001	-0.345	7.299e-01	9.971e-01
caudal middle frontal	Intercept	1.124	0.123	9.149	3.166e-18	1.076e-17
	Age	0.003	0.004	0.800	4.244e-01	4.810e-01
	Age^2	-0.000	0.000	-1.634	1.030e-01	1.208e-01
	AB_42_40	0.203	0.140	1.447	1.487e-01	2.661e-01
	Sex	-0.005	0.005	-1.024	3.064e-01	3.157e-01
	APOE4 Status	0.001	0.005	0.148	8.822e-01	9.748e-01
	Time b/w LP and MRI	0.000	0.001	0.520	6.034e-01	9.971e-01
cuneus	Intercept	1.080	0.117	9.234	1.649e-18	7.008e-18
	Age	0.002	0.003	0.505	6.141e-01	6.304e-01
	Age^2	-0.000	0.000	-1.037	3.004e-01	3.004e-01
	AB_42_40	0.131	0.133	0.984	3.256e-01	4.037e-01
	Sex	-0.023	0.004	-5.366	1.378e-07	4.685e-06
	APOE4 Status	-0.001	0.005	-0.251	8.016e-01	9.748e-01
	Time b/w LP and MRI	0.000	0.001	0.308	7.585e-01	9.971e-01

ROI	Predictor	Estimate	Std. Error	T-Statistic	pUncorrected	pFDR
entorhinal	Intercept	0.606	0.123	4.929	1.221e-06	1.221e-06
	Age	0.016	0.004	4.267	2.490e-05	8.466e-04
	Age^2	-0.000	0.000	-5.142	4.302e-07	1.463e-05
	AB_42_40	0.252	0.140	1.797	7.312e-02	1.673e-01
	Sex	-0.009	0.005	-2.003	4.585e-02	7.795e-02
	APOE4 Status	0.002	0.005	0.365	7.156e-01	9.748e-01
	Time b/w LP and MRI	-0.000	0.001	-0.567	5.709e-01	9.971e-01
frontal pole	Intercept	0.925	0.122	7.564	2.796e-13	3.067e-13
	Age	0.006	0.004	1.691	9.168e-02	1.627e-01
	Age^2	-0.000	0.000	-2.546	1.129e-02	2.133e-02
	AB_42_40	0.130	0.140	0.931	3.527e-01	4.037e-01
	Sex	-0.002	0.005	-0.365	7.155e-01	7.155e-01
	APOE4 Status	-0.002	0.005	-0.476	6.345e-01	9.748e-01
	Time b/w LP and MRI	0.000	0.001	0.184	8.539e-01	9.971e-01
fusiform	Intercept	0.968	0.113	8.600	1.925e-16	3.117e-16
	Age	0.007	0.003	2.237	2.585e-02	1.256e-01
	Age^2	-0.000	0.000	-3.180	1.591e-03	9.016e-03
	AB_42_40	0.265	0.128	2.066	3.944e-02	1.564e-01
	Sex	-0.008	0.004	-1.947	5.221e-02	8.069e-02
	APOE4 Status	0.002	0.004	0.388	6.982e-01	9.748e-01
	Time b/w LP and MRI	-0.001	0.001	-0.858	3.912e-01	9.971e-01
inferior parietal	Intercept	1.000	0.123	8.103	6.842e-15	8.616e-15
	Age	0.006	0.004	1.670	9.566e-02	1.627e-01
	Age^2	-0.000	0.000	-2.435	1.533e-02	2.482e-02
	AB_42_40	0.340	0.141	2.417	1.609e-02	1.564e-01
	Sex	-0.019	0.005	-4.014	7.148e-05	4.051e-04
	APOE4 Status	0.004	0.005	0.794	4.277e-01	9.748e-01
	Time b/w LP and MRI	-0.000	0.001	-0.070	9.442e-01	9.971e-01
inferior temporal	Intercept	0.985	0.105	9.370	5.773e-19	3.271e-18
	Age	0.006	0.003	2.070	3.911e-02	1.417e-01
	Age^2	-0.000	0.000	-3.020	2.692e-03	1.144e-02

ROI	Predictor	Estimate	Std. Error	T-Statistic	pUncorrected	pFDR
	AB_42_40	0.262	0.120	2.187	2.930e-02	1.564e-01
	Sex	-0.010	0.004	-2.550	1.115e-02	2.527e-02
	APOE4 Status	0.003	0.004	0.754	4.512e-01	9.748e-01
	Time b/w LP and MRI	-0.001	0.001	-1.030	3.036e-01	9.971e-01
insula	Intercept	0.996	0.107	9.280	1.154e-18	5.605e-18
	Age	0.005	0.003	1.623	1.053e-01	1.627e-01
	Age^2	-0.000	0.000	-2.272	2.365e-02	3.350e-02
	AB_42_40	0.089	0.123	0.730	4.657e-01	4.766e-01
	Sex	-0.009	0.004	-2.315	2.114e-02	4.228e-02
	APOE4 Status	0.001	0.004	0.311	7.556e-01	9.748e-01
	Time b/w LP and MRI	-0.000	0.001	-0.039	9.687e-01	9.971e-01
isthmus cingulate	Intercept	1.036	0.129	8.026	1.174e-14	1.426e-14
	Age	0.008	0.004	2.003	4.583e-02	1.417e-01
	Age^2	-0.000	0.000	-2.616	9.250e-03	2.133e-02
	AB_42_40	0.105	0.147	0.713	4.766e-01	4.766e-01
	Sex	-0.017	0.005	-3.539	4.498e-04	2.185e-03
	APOE4 Status	-0.000	0.005	-0.027	9.783e-01	9.783e-01
	Time b/w LP and MRI	-0.000	0.001	-0.280	7.798e-01	9.971e-01
lateral occipital	Intercept	1.032	0.109	9.429	3.643e-19	2.477e-18
	Age	0.004	0.003	1.144	2.533e-01	3.312e-01
	Age^2	-0.000	0.000	-1.778	7.617e-02	9.249e-02
	AB_42_40	0.343	0.125	2.749	6.263e-03	1.564e-01
	Sex	-0.021	0.004	-5.101	5.266e-07	8.952e-06
	APOE4 Status	0.001	0.004	0.250	8.026e-01	9.748e-01
	Time b/w LP and MRI	-0.000	0.001	-0.128	8.984e-01	9.971e-01
lateral orbitofrontal	Intercept	0.957	0.118	8.123	5.944e-15	7.773e-15
	Age	0.008	0.003	2.339	1.985e-02	1.256e-01
	Age^2	-0.000	0.000	-3.360	8.552e-04	5.815e-03
	AB_42_40	0.126	0.134	0.936	3.498e-01	4.037e-01
	Sex	-0.006	0.004	-1.305	1.927e-01	2.134e-01
	APOE4 Status	0.002	0.005	0.327	7.437e-01	9.748e-01

ROI	Predictor	Estimate	Std. Error	T-Statistic	pUncorrected	pFDR
	Time b/w LP and MRI	0.000	0.001	0.207	8.363e-01	9.971e-01
lingual	Intercept	1.016	0.115	8.812	4.016e-17	8.534e-17
	Age	0.004	0.003	1.205	2.287e-01	3.110e-01
	Age^2	-0.000	0.000	-1.837	6.689e-02	8.724e-02
	AB_42_40	0.211	0.132	1.603	1.097e-01	2.072e-01
	Sex	-0.017	0.004	-4.027	6.787e-05	4.051e-04
	APOE4 Status	-0.002	0.005	-0.345	7.303e-01	9.748e-01
	Time b/w LP and MRI	0.000	0.001	0.011	9.915e-01	9.971e-01
medial orbitofrontal	Intercept	0.996	0.118	8.443	6.042e-16	8.560e-16
	Age	0.006	0.003	1.687	9.249e-02	1.627e-01
	Age^2	-0.000	0.000	-2.678	7.714e-03	2.133e-02
	AB_42_40	0.124	0.135	0.923	3.565e-01	4.037e-01
	Sex	-0.009	0.004	-1.953	5.153e-02	8.069e-02
	APOE4 Status	0.000	0.005	0.043	9.657e-01	9.783e-01
	Time b/w LP and MRI	0.000	0.001	0.262	7.938e-01	9.971e-01
middle temporal	Intercept	1.036	0.109	9.508	1.967e-19	1.672e-18
	Age	0.005	0.003	1.644	1.011e-01	1.627e-01
	Age^2	-0.000	0.000	-2.601	9.637e-03	2.133e-02
	AB_42_40	0.250	0.124	2.014	4.470e-02	1.564e-01
	Sex	-0.013	0.004	-3.150	1.760e-03	6.103e-03
	APOE4 Status	0.001	0.004	0.321	7.483e-01	9.748e-01
	Time b/w LP and MRI	-0.000	0.001	-0.385	7.003e-01	9.971e-01
paracentral	Intercept	1.125	0.124	9.096	4.737e-18	1.342e-17
	Age	0.003	0.004	0.730	4.658e-01	5.109e-01
	Age^2	-0.000	0.000	-1.444	1.495e-01	1.694e-01
	AB_42_40	0.282	0.141	2.002	4.599e-02	1.564e-01
	Sex	-0.007	0.005	-1.523	1.284e-01	1.559e-01
	APOE4 Status	0.002	0.005	0.427	6.695e-01	9.748e-01
	Time b/w LP and MRI	-0.000	0.001	-0.533	5.944e-01	9.971e-01
parahippocampal	Intercept	0.852	0.127	6.696	7.441e-11	7.666e-11
	Age	0.011	0.004	2.837	4.787e-03	5.901e-02

ROI	Predictor	Estimate	Std. Error	T-Statistic	pUncorrected	pFDR
	Age^2	-0.000	0.000	-3.542	4.455e-04	4.196e-03
	AB_42_40	0.295	0.145	2.029	4.313e-02	1.564e-01
	Sex	-0.015	0.005	-3.144	1.795e-03	6.103e-03
	APOE4 Status	-0.001	0.005	-0.257	7.975e-01	9.748e-01
	Time b/w LP and MRI	-0.001	0.001	-1.250	2.121e-01	9.971e-01
pars opercularis	Intercept	1.036	0.118	8.778	5.181e-17	1.036e-16
	Age	0.006	0.003	1.629	1.042e-01	1.627e-01
	Age^2	-0.000	0.000	-2.446	1.490e-02	2.482e-02
	AB_42_40	0.223	0.135	1.655	9.878e-02	1.976e-01
	Sex	-0.008	0.004	-1.853	6.457e-02	8.782e-02
	APOE4 Status	0.002	0.005	0.463	6.438e-01	9.748e-01
	Time b/w LP and MRI	0.000	0.001	0.017	9.866e-01	9.971e-01
pars orbitalis	Intercept	1.023	0.112	9.103	4.496e-18	1.342e-17
	Age	0.005	0.003	1.385	1.668e-01	2.363e-01
	Age^2	-0.000	0.000	-2.297	2.213e-02	3.271e-02
	AB_42_40	0.167	0.128	1.299	1.948e-01	3.011e-01
	Sex	-0.005	0.004	-1.296	1.958e-01	2.134e-01
	APOE4 Status	-0.000	0.004	-0.100	9.206e-01	9.781e-01
	Time b/w LP and MRI	-0.000	0.001	-0.014	9.891e-01	9.971e-01
pars triangularis	Intercept	1.014	0.117	8.690	9.898e-17	1.870e-16
	Age	0.007	0.003	1.916	5.609e-02	1.589e-01
	Age^2	-0.000	0.000	-2.867	4.364e-03	1.642e-02
	AB_42_40	0.158	0.133	1.185	2.368e-01	3.355e-01
	Sex	-0.006	0.004	-1.281	2.008e-01	2.134e-01
	APOE4 Status	0.001	0.005	0.260	7.947e-01	9.748e-01
	Time b/w LP and MRI	0.000	0.001	0.071	9.438e-01	9.971e-01
pericalcarine	Intercept	0.990	0.128	7.766	7.109e-14	8.057e-14
	Age	0.003	0.004	0.918	3.591e-01	4.210e-01
	Age^2	-0.000	0.000	-1.353	1.768e-01	1.939e-01
	AB_42_40	0.189	0.146	1.301	1.940e-01	3.011e-01
	Sex	-0.019	0.005	-4.041	6.405e-05	4.051e-04

ROI	Predictor	Estimate	Std. Error	T-Statistic	pUncorrected	pFDR
	APOE4 Status	-0.002	0.005	-0.329	7.420e-01	9.748e-01
	Time b/w LP and MRI	0.001	0.001	0.579	5.627e-01	9.971e-01
postcentral	Intercept	1.129	0.115	9.834	1.511e-20	2.569e-19
	Age	0.002	0.003	0.498	6.189e-01	6.304e-01
	Age^2	-0.000	0.000	-1.186	2.365e-01	2.437e-01
	AB_42_40	0.179	0.131	1.366	1.727e-01	2.936e-01
	Sex	-0.008	0.004	-1.893	5.907e-02	8.368e-02
	APOE4 Status	0.001	0.005	0.208	8.352e-01	9.748e-01
	Time b/w LP and MRI	-0.000	0.001	-0.017	9.864e-01	9.971e-01
posterior cingulate	Intercept	1.068	0.126	8.501	3.952e-16	5.842e-16
	Age	0.006	0.004	1.636	1.026e-01	1.627e-01
	Age^2	-0.000	0.000	-2.350	1.928e-02	2.980e-02
	AB_42_40	0.260	0.143	1.815	7.031e-02	1.673e-01
	Sex	-0.013	0.005	-2.704	7.139e-03	1.867e-02
	APOE4 Status	0.002	0.005	0.346	7.295e-01	9.748e-01
	Time b/w LP and MRI	-0.001	0.001	-0.714	4.756e-01	9.971e-01
precentral	Intercept	1.153	0.119	9.718	3.787e-20	4.292e-19
	Age	0.002	0.004	0.482	6.304e-01	6.304e-01
	Age^2	-0.000	0.000	-1.225	2.213e-01	2.351e-01
	AB_42_40	0.239	0.135	1.764	7.849e-02	1.673e-01
	Sex	-0.007	0.004	-1.538	1.250e-01	1.559e-01
	APOE4 Status	0.001	0.005	0.232	8.164e-01	9.748e-01
	Time b/w LP and MRI	0.000	0.001	0.231	8.173e-01	9.971e-01
precuneus	Intercept	1.003	0.129	7.777	6.578e-14	7.712e-14
	Age	0.007	0.004	1.774	7.689e-02	1.627e-01
	Age^2	-0.000	0.000	-2.590	9.958e-03	2.133e-02
	AB_42_40	0.274	0.147	1.860	6.366e-02	1.673e-01
	Sex	-0.014	0.005	-2.998	2.894e-03	8.945e-03
	APOE4 Status	0.002	0.005	0.328	7.430e-01	9.748e-01
	Time b/w LP and MRI	-0.000	0.001	-0.410	6.819e-01	9.971e-01
rostral anterior cingulate	Intercept	1.000	0.111	9.020	8.498e-18	2.223e-17

ROI	Predictor	Estimate	Std. Error	T-Statistic	pUncorrected	pFDR
	Age	0.008	0.003	2.295	2.229e-02	1.256e-01
	Age^2	-0.000	0.000	-3.129	1.886e-03	9.161e-03
	AB_42_40	0.130	0.127	1.028	3.047e-01	3.985e-01
	Sex	-0.007	0.004	-1.664	9.685e-02	1.267e-01
	APOE4 Status	0.004	0.004	1.001	3.173e-01	9.748e-01
	Time b/w LP and MRI	0.000	0.001	0.004	9.971e-01	9.971e-01
rostral middle frontal	Intercept	1.107	0.125	8.847	3.077e-17	6.975e-17
	Age	0.003	0.004	0.937	3.496e-01	4.210e-01
	Age^2	-0.000	0.000	-1.822	6.928e-02	8.724e-02
	AB_42_40	0.174	0.143	1.215	2.250e-01	3.326e-01
	Sex	-0.009	0.005	-1.926	5.482e-02	8.104e-02
	APOE4 Status	0.001	0.005	0.144	8.857e-01	9.748e-01
	Time b/w LP and MRI	0.000	0.001	0.557	5.776e-01	9.971e-01
superior frontal	Intercept	1.055	0.102	10.309	3.282e-22	1.116e-20
	Age	0.005	0.003	1.567	1.179e-01	1.743e-01
	Age^2	-0.000	0.000	-2.645	8.487e-03	2.133e-02
	AB_42_40	0.103	0.117	0.878	3.805e-01	4.043e-01
	Sex	-0.010	0.004	-2.495	1.301e-02	2.765e-02
	APOE4 Status	0.003	0.004	0.672	5.017e-01	9.748e-01
	Time b/w LP and MRI	0.000	0.001	0.106	9.160e-01	9.971e-01
superior parietal	Intercept	1.067	0.124	8.632	1.523e-16	2.589e-16
	Age	0.004	0.004	1.114	2.660e-01	3.350e-01
	Age^2	-0.000	0.000	-1.867	6.260e-02	8.514e-02
	AB_42_40	0.308	0.141	2.181	2.978e-02	1.564e-01
	Sex	-0.016	0.005	-3.379	8.005e-04	3.402e-03
	APOE4 Status	0.002	0.005	0.431	6.667e-01	9.748e-01
	Time b/w LP and MRI	-0.000	0.001	-0.265	7.908e-01	9.971e-01
superior temporal	Intercept	0.995	0.108	9.178	2.532e-18	9.565e-18
	Age	0.006	0.003	2.019	4.421e-02	1.417e-01
	Age^2	-0.000	0.000	-2.834	4.829e-03	1.642e-02
	AB_42_40	0.218	0.124	1.763	7.873e-02	1.673e-01

ROI	Predictor	Estimate	Std. Error	T-Statistic	pUncorrected	pFDR
	Sex	-0.009	0.004	-2.224	2.670e-02	5.043e-02
	APOE4 Status	0.001	0.004	0.140	8.888e-01	9.748e-01
	Time b/w LP and MRI	-0.000	0.001	-0.191	8.483e-01	9.971e-01
supramarginal	Intercept	1.015	0.122	8.317	1.498e-15	2.037e-15
	Age	0.006	0.004	1.716	8.702e-02	1.627e-01
	Age^2	-0.000	0.000	-2.508	1.254e-02	2.244e-02
	AB_42_40	0.282	0.139	2.023	4.371e-02	1.564e-01
	Sex	-0.013	0.005	-2.863	4.428e-03	1.255e-02
	APOE4 Status	0.002	0.005	0.507	6.126e-01	9.748e-01
	Time b/w LP and MRI	-0.000	0.001	-0.156	8.760e-01	9.971e-01
temporal pole	Intercept	0.794	0.117	6.815	3.553e-11	3.775e-11
	Age	0.010	0.003	2.755	6.143e-03	5.901e-02
	Age^2	-0.000	0.000	-3.514	4.936e-04	4.196e-03
	AB_42_40	0.120	0.133	0.901	3.681e-01	4.037e-01
	Sex	-0.006	0.004	-1.472	1.419e-01	1.664e-01
	APOE4 Status	-0.002	0.005	-0.349	7.270e-01	9.748e-01
	Time b/w LP and MRI	-0.001	0.001	-0.838	4.027e-01	9.971e-01
transverse temporal	Intercept	0.980	0.113	8.672	1.131e-16	2.024e-16
	Age	0.007	0.003	2.090	3.723e-02	1.417e-01
	Age^2	-0.000	0.000	-2.561	1.080e-02	2.133e-02
	AB_42_40	0.234	0.129	1.813	7.056e-02	1.673e-01
	Sex	-0.009	0.004	-2.086	3.766e-02	6.739e-02
	APOE4 Status	-0.002	0.004	-0.552	5.815e-01	9.748e-01
	Time b/w LP and MRI	0.000	0.001	0.516	6.065e-01	9.971e-01

Table C3: Estimated outputs of each linear regression model assessing the effects of CSF Aβ42/40 ratio on cortical-adjacent WM R1. Covariates in each model included age, age^2, sex, APOE4 status, and time between lumbar puncture and MRI. Abbreviations: AB_42_40, CSF Aβ42/40 ratio; LP, lumbar puncture; MRI, magnetic resonance imaging; pUncorrected, *p*-value uncorrected for multiple comparisons; pFDR, Benjamini-Hochberg FDR-corrected *p*-value.

Table C4: Outputs of linear regression models assessing effects of CSF $pTau_{181}$ on cortical GM R1

ROI	Predictor	Estimate	Std. Error	T-Statistic	pUncorrected	pFDR
bankssts	Intercept	0.729	0.010	71.613	1.276e-227	2.892e-227
	Age	-0.000	0.000	-0.324	7.458e-01	8.744e-01
	pTau_transformed	-0.006	0.003	-2.210	2.769e-02	6.725e-02
	Sex	0.002	0.002	1.090	2.764e-01	9.910e-01
	APOE4 Status	0.003	0.002	1.176	2.401e-01	9.897e-01
	Time b/w LP and MRI	0.001	0.000	1.797	7.314e-02	9.605e-02
caudal anterior cingulate	Intercept	0.686	0.016	43.436	4.333e-151	4.604e-151
	Age	0.000	0.000	2.072	3.895e-02	1.734e-01
	pTau_transformed	-0.007	0.004	-1.490	1.370e-01	2.025e-01
	Sex	-0.006	0.003	-1.724	8.553e-02	9.764e-01
	APOE4 Status	0.001	0.003	0.421	6.737e-01	9.897e-01
	Time b/w LP and MRI	0.001	0.001	1.428	1.542e-01	1.872e-01
caudal middle frontal	Intercept	0.730	0.010	72.813	2.939e-230	7.687e-230
	Age	-0.000	0.000	-0.355	7.228e-01	8.744e-01
	pTau_transformed	-0.005	0.003	-1.686	9.266e-02	1.650e-01
	Sex	0.001	0.002	0.240	8.105e-01	9.910e-01
	APOE4 Status	0.002	0.002	0.994	3.209e-01	9.897e-01
	Time b/w LP and MRI	0.001	0.000	2.168	3.079e-02	5.510e-02
cuneus	Intercept	0.762	0.013	58.748	1.018e-196	1.236e-196
	Age	-0.000	0.000	-0.958	3.389e-01	6.198e-01
	pTau_transformed	-0.009	0.004	-2.433	1.542e-02	5.692e-02
	Sex	-0.004	0.003	-1.564	1.186e-01	9.764e-01
	APOE4 Status	-0.001	0.003	-0.519	6.043e-01	9.897e-01
	Time b/w LP and MRI	0.001	0.001	2.813	5.162e-03	2.539e-02
entorhinal	Intercept	0.816	0.025	32.753	2.175e-114	2.175e-114
	Age	-0.000	0.000	-1.157	2.482e-01	5.626e-01
	pTau_transformed	-0.003	0.007	-0.381	7.034e-01	7.715e-01
	Sex	0.002	0.005	0.385	7.002e-01	9.910e-01
	APOE4 Status	0.003	0.005	0.586	5.583e-01	9.897e-01
	Time b/w LP and MRI	0.001	0.001	0.960	3.379e-01	3.590e-01

ROI	Predictor	Estimate	Std. Error	T-Statistic	pUncorrected	pFDR
frontal pole	Intercept	0.696	0.011	63.614	5.211e-209	7.382e-209
	Age	-0.000	0.000	-0.072	9.429e-01	9.671e-01
	pTau_transformed	-0.007	0.003	-2.334	2.009e-02	5.692e-02
	Sex	-0.003	0.002	-1.466	1.434e-01	9.764e-01
	APOE4 Status	0.002	0.002	0.812	4.172e-01	9.897e-01
	Time b/w LP and MRI	0.001	0.000	3.293	1.082e-03	1.924e-02
fusiform	Intercept	0.688	0.009	78.179	1.299e-241	8.833e-241
	Age	0.000	0.000	0.628	5.303e-01	7.212e-01
	pTau_transformed	-0.001	0.002	-0.525	5.998e-01	7.163e-01
	Sex	0.001	0.002	0.578	5.637e-01	9.910e-01
	APOE4 Status	-0.000	0.002	-0.221	8.250e-01	9.897e-01
	Time b/w LP and MRI	0.001	0.000	2.040	4.199e-02	6.207e-02
inferior parietal	Intercept	0.732	0.011	68.535	1.119e-220	2.238e-220
	Age	-0.000	0.000	-0.041	9.671e-01	9.671e-01
	pTau_transformed	-0.010	0.003	-3.356	8.669e-04	2.947e-02
	Sex	-0.001	0.002	-0.411	6.811e-01	9.910e-01
	APOE4 Status	0.003	0.002	1.422	1.559e-01	9.897e-01
	Time b/w LP and MRI	0.001	0.000	2.551	1.111e-02	3.777e-02
inferior temporal	Intercept	0.672	0.009	76.109	2.576e-237	1.095e-236
	Age	0.000	0.000	1.174	2.412e-01	5.626e-01
	pTau_transformed	-0.002	0.003	-0.649	5.170e-01	6.510e-01
	Sex	0.000	0.002	0.228	8.195e-01	9.910e-01
	APOE4 Status	-0.000	0.002	-0.070	9.445e-01	9.897e-01
	Time b/w LP and MRI	0.001	0.000	2.285	2.284e-02	5.156e-02
insula	Intercept	0.663	0.009	77.879	5.375e-241	2.611e-240
	Age	0.001	0.000	4.735	3.069e-06	1.043e-04
	pTau_transformed	-0.004	0.002	-1.663	9.705e-02	1.650e-01
	Sex	0.001	0.002	0.368	7.130e-01	9.910e-01
	APOE4 Status	0.000	0.002	0.040	9.683e-01	9.897e-01
	Time b/w LP and MRI	0.001	0.000	2.180	2.988e-02	5.510e-02
isthmus cingulate	Intercept	0.741	0.013	55.850	1.947e-188	2.207e-188

ROI	Predictor	Estimate	Std. Error	T-Statistic	pUncorrected	pFDR
	Age	0.000	0.000	1.016	3.102e-01	6.198e-01
	pTau_transformed	-0.009	0.004	-2.347	1.941e-02	5.692e-02
	Sex	-0.000	0.003	-0.094	9.253e-01	9.910e-01
	APOE4 Status	0.001	0.003	0.514	6.075e-01	9.897e-01
	Time b/w LP and MRI	0.001	0.001	1.316	1.888e-01	2.214e-01
lateral occipital	Intercept	0.728	0.011	64.048	4.556e-210	6.735e-210
	Age	0.000	0.000	1.229	2.199e-01	5.626e-01
	pTau_transformed	-0.010	0.003	-2.962	3.240e-03	3.672e-02
	Sex	-0.002	0.002	-0.935	3.504e-01	9.910e-01
	APOE4 Status	0.001	0.002	0.305	7.603e-01	9.897e-01
	Time b/w LP and MRI	0.001	0.000	2.599	9.709e-03	3.668e-02
lateral orbitofrontal	Intercept	0.687	0.010	72.246	5.118e-229	1.243e-228
	Age	-0.000	0.000	-0.192	8.479e-01	9.300e-01
	pTau_transformed	-0.000	0.003	-0.070	9.439e-01	9.680e-01
	Sex	-0.003	0.002	-1.449	1.481e-01	9.764e-01
	APOE4 Status	-0.002	0.002	-0.944	3.456e-01	9.897e-01
	Time b/w LP and MRI	0.001	0.000	2.724	6.731e-03	2.861e-02
lingual	Intercept	0.730	0.011	64.675	1.375e-211	2.125e-211
	Age	0.000	0.000	0.199	8.420e-01	9.300e-01
	pTau_transformed	-0.007	0.003	-2.218	2.710e-02	6.725e-02
	Sex	-0.000	0.002	-0.045	9.640e-01	9.910e-01
	APOE4 Status	0.001	0.002	0.298	7.658e-01	9.897e-01
	Time b/w LP and MRI	0.001	0.000	2.242	2.549e-02	5.156e-02
medial orbitofrontal	Intercept	0.651	0.009	74.199	7.133e-233	2.425e-232
	Age	0.000	0.000	1.895	5.887e-02	2.224e-01
	pTau_transformed	-0.001	0.002	-0.294	7.690e-01	8.171e-01
	Sex	-0.003	0.002	-1.367	1.723e-01	9.764e-01
	APOE4 Status	-0.001	0.002	-0.635	5.260e-01	9.897e-01
	Time b/w LP and MRI	0.001	0.000	2.442	1.503e-02	3.931e-02
middle temporal	Intercept	0.684	0.008	83.954	4.330e-253	1.472e-251
	Age	0.000	0.000	1.478	1.402e-01	4.333e-01

ROI	Predictor	Estimate	Std. Error	T-Statistic	pUncorrected	pFDR
	pTau_transformed	-0.004	0.002	-1.543	1.236e-01	1.910e-01
	Sex	0.000	0.002	0.112	9.107e-01	9.910e-01
	APOE4 Status	0.001	0.002	0.298	7.662e-01	9.897e-01
	Time b/w LP and MRI	0.001	0.000	2.866	4.375e-03	2.539e-02
paracentral	Intercept	0.761	0.011	67.989	4.592e-219	8.217e-219
	Age	-0.000	0.000	-0.382	7.029e-01	8.744e-01
	pTau_transformed	-0.002	0.003	-0.509	6.110e-01	7.163e-01
	Sex	0.002	0.002	0.771	4.414e-01	9.910e-01
	APOE4 Status	-0.000	0.002	-0.040	9.685e-01	9.897e-01
	Time b/w LP and MRI	0.000	0.000	0.644	5.198e-01	5.198e-01
parahippocampal	Intercept	0.661	0.011	59.450	1.531e-198	1.928e-198
	Age	0.000	0.000	2.863	4.415e-03	3.002e-02
	pTau_transformed	-0.000	0.003	-0.040	9.680e-01	9.680e-01
	Sex	0.001	0.002	0.446	6.557e-01	9.910e-01
	APOE4 Status	-0.002	0.002	-0.830	4.069e-01	9.897e-01
	Time b/w LP and MRI	0.001	0.000	1.763	7.875e-02	9.917e-02
pars opercularis	Intercept	0.711	0.009	79.007	2.650e-243	3.003e-242
	Age	0.000	0.000	1.694	9.097e-02	3.093e-01
	pTau_transformed	-0.005	0.003	-2.059	4.017e-02	8.536e-02
	Sex	-0.001	0.002	-0.453	6.508e-01	9.910e-01
	APOE4 Status	0.001	0.002	0.380	7.044e-01	9.897e-01
	Time b/w LP and MRI	0.001	0.000	2.087	3.751e-02	6.073e-02
pars orbitalis	Intercept	0.707	0.010	73.670	4.049e-232	1.252e-231
	Age	0.000	0.000	1.115	2.657e-01	5.646e-01
	pTau_transformed	-0.007	0.003	-2.692	7.405e-03	5.035e-02
	Sex	-0.002	0.002	-0.872	3.838e-01	9.910e-01
	APOE4 Status	0.000	0.002	0.085	9.320e-01	9.897e-01
	Time b/w LP and MRI	0.001	0.000	2.911	3.807e-03	2.539e-02
pars triangularis	Intercept	0.716	0.009	78.370	5.274e-242	4.483e-241
	Age	0.000	0.000	0.913	3.616e-01	6.198e-01
	pTau_transformed	-0.006	0.003	-2.398	1.695e-02	5.692e-02

ROI	Predictor	Estimate	Std. Error	T-Statistic	pUncorrected	pFDR
	Sex	-0.002	0.002	-1.015	3.105e-01	9.910e-01
	APOE4 Status	0.001	0.002	0.394	6.938e-01	9.897e-01
	Time b/w LP and MRI	0.001	0.000	3.075	2.256e-03	2.539e-02
pericalcarine	Intercept	0.744	0.014	53.463	2.047e-182	2.245e-182
	Age	0.000	0.000	0.638	5.240e-01	7.212e-01
	pTau_transformed	-0.007	0.004	-1.863	6.323e-02	1.194e-01
	Sex	-0.005	0.003	-1.684	9.298e-02	9.764e-01
	APOE4 Status	0.000	0.003	0.013	9.897e-01	9.897e-01
	Time b/w LP and MRI	0.001	0.001	2.474	1.379e-02	3.907e-02
postcentral	Intercept	0.743	0.011	69.074	6.516e-222	1.385e-221
	Age	0.000	0.000	1.412	1.588e-01	4.499e-01
	pTau_transformed	-0.006	0.003	-1.908	5.712e-02	1.142e-01
	Sex	0.001	0.002	0.422	6.734e-01	9.910e-01
	APOE4 Status	0.001	0.002	0.242	8.090e-01	9.897e-01
	Time b/w LP and MRI	0.001	0.000	1.795	7.345e-02	9.605e-02
posterior cingulate	Intercept	0.726	0.019	37.713	7.618e-131	7.849e-131
	Age	0.001	0.000	2.052	4.080e-02	1.734e-01
	pTau_transformed	-0.009	0.005	-1.589	1.130e-01	1.830e-01
	Sex	-0.000	0.004	-0.086	9.316e-01	9.910e-01
	APOE4 Status	0.002	0.004	0.435	6.640e-01	9.897e-01
	Time b/w LP and MRI	0.001	0.001	0.872	3.839e-01	3.955e-01
precentral	Intercept	0.769	0.011	67.787	5.984e-219	1.017e-218
	Age	0.000	0.000	0.050	9.605e-01	9.671e-01
	pTau_transformed	-0.004	0.003	-1.269	2.050e-01	2.904e-01
	Sex	0.002	0.002	0.824	4.105e-01	9.910e-01
	APOE4 Status	0.001	0.002	0.518	6.049e-01	9.897e-01
	Time b/w LP and MRI	0.001	0.000	1.918	5.584e-02	7.911e-02
precuneus	Intercept	0.737	0.011	68.000	1.922e-219	3.630e-219
	Age	-0.000	0.000	-0.648	5.175e-01	7.212e-01
	pTau_transformed	-0.008	0.003	-2.495	1.301e-02	5.692e-02
	Sex	0.000	0.002	0.020	9.844e-01	9.910e-01

ROI	Predictor	Estimate	Std. Error	T-Statistic	pUncorrected	pFDR
	APOE4 Status	0.001	0.002	0.441	6.598e-01	9.897e-01
	Time b/w LP and MRI	0.001	0.000	2.480	1.354e-02	3.907e-02
rostral anterior cingulate	Intercept	0.637	0.011	59.787	4.215e-199	5.512e-199
	Age	0.000	0.000	3.162	1.690e-03	1.915e-02
	pTau_transformed	0.001	0.003	0.396	6.925e-01	7.715e-01
	Sex	-0.000	0.002	-0.011	9.910e-01	9.910e-01
	APOE4 Status	0.001	0.002	0.623	5.333e-01	9.897e-01
	Time b/w LP and MRI	0.001	0.000	1.222	2.225e-01	2.522e-01
rostral middle frontal	Intercept	0.716	0.010	73.195	4.311e-231	1.221e-230
	Age	-0.000	0.000	-0.908	3.646e-01	6.198e-01
	pTau_transformed	-0.006	0.003	-2.059	4.012e-02	8.536e-02
	Sex	-0.003	0.002	-1.232	2.185e-01	9.910e-01
	APOE4 Status	0.002	0.002	1.144	2.531e-01	9.897e-01
	Time b/w LP and MRI	0.001	0.000	3.280	1.132e-03	1.924e-02
superior frontal	Intercept	0.713	0.009	78.260	2.262e-241	1.282e-240
	Age	-0.000	0.000	-0.701	4.839e-01	7.212e-01
	pTau_transformed	-0.002	0.003	-0.856	3.925e-01	5.338e-01
	Sex	0.000	0.002	0.261	7.944e-01	9.910e-01
	APOE4 Status	0.001	0.002	0.490	6.241e-01	9.897e-01
	Time b/w LP and MRI	0.001	0.000	2.064	3.970e-02	6.135e-02
superior parietal	Intercept	0.745	0.011	67.372	5.517e-218	8.932e-218
	Age	-0.000	0.000	-0.343	7.319e-01	8.744e-01
	pTau_transformed	-0.008	0.003	-2.627	8.948e-03	5.071e-02
	Sex	-0.001	0.002	-0.296	7.674e-01	9.910e-01
	APOE4 Status	0.002	0.002	0.684	4.944e-01	9.897e-01
	Time b/w LP and MRI	0.001	0.000	2.238	2.578e-02	5.156e-02
superior temporal	Intercept	0.712	0.009	79.731	9.048e-245	1.538e-243
	Age	0.000	0.000	2.756	6.128e-03	3.473e-02
	pTau_transformed	-0.007	0.003	-2.827	4.934e-03	4.194e-02
	Sex	0.000	0.002	0.057	9.548e-01	9.910e-01
	APOE4 Status	0.000	0.002	0.030	9.761e-01	9.897e-01

ROI	Predictor	Estimate	Std. Error	T-Statistic	pUncorrected	pFDR
	Time b/w LP and MRI	0.001	0.000	2.254	2.473e-02	5.156e-02
supramarginal	Intercept	0.723	0.010	76.045	3.513e-237	1.327e-236
	Age	0.000	0.000	0.792	4.291e-01	6.947e-01
	pTau_transformed	-0.008	0.003	-3.074	2.263e-03	3.672e-02
	Sex	-0.001	0.002	-0.473	6.366e-01	9.910e-01
	APOE4 Status	0.002	0.002	0.901	3.683e-01	9.897e-01
	Time b/w LP and MRI	0.001	0.000	2.128	3.393e-02	5.768e-02
temporal pole	Intercept	0.646	0.011	57.324	5.740e-193	6.730e-193
	Age	0.001	0.000	4.438	1.183e-05	2.011e-04
	pTau_transformed	-0.002	0.003	-0.702	4.833e-01	6.320e-01
	Sex	0.002	0.002	0.640	5.222e-01	9.910e-01
	APOE4 Status	-0.002	0.002	-0.873	3.832e-01	9.897e-01
	Time b/w LP and MRI	0.000	0.000	1.088	2.771e-01	3.039e-01
transverse temporal	Intercept	0.779	0.013	61.941	7.127e-205	9.693e-205
	Age	0.001	0.000	3.039	2.529e-03	2.150e-02
	pTau_transformed	-0.009	0.004	-2.451	1.467e-02	5.692e-02
	Sex	-0.000	0.003	-0.146	8.840e-01	9.910e-01
	APOE4 Status	-0.001	0.003	-0.517	6.055e-01	9.897e-01
	Time b/w LP and MRI	0.001	0.000	2.808	5.227e-03	2.539e-02

Table C4: Estimated outputs of each linear regression model assessing the effects of CSF $pTau_{181}$ on cortical GM R1. Covariates in each model included age, sex, APOE4 status, and time between lumbar puncture and MRI. Abbreviations: pTau_transformed, CSF tau phosphorylated at threonine 181 (log-transformed); LP, lumbar puncture; MRI, magnetic resonance imaging; pUncorrected, *p*-value uncorrected for multiple comparisons; pFDR, Benjamini-Hochberg FDR-corrected *p*-value.

Table C5: Outputs of linear regression models assessing effects of CSF $pTau_{181}$ on cortical-adjacent WM R1

ROI	Predictor	Estimate	Std. Error	T-Statistic	pUncorrected	pFDR
bankssts	Intercept	1.108	0.117	9.439	3.370e-19	5.729e-19
	Age	0.006	0.003	1.723	8.575e-02	1.973e-01
	Age^2	-0.000	0.000	-2.396	1.705e-02	3.287e-02
	pTau_transformed	-0.020	0.006	-3.418	6.971e-04	5.925e-03
	Sex	-0.011	0.004	-2.526	1.193e-02	2.897e-02
	APOE4 Status	0.002	0.004	0.426	6.701e-01	9.927e-01
	Time b/w LP and MRI	-0.000	0.001	-0.365	7.153e-01	9.968e-01
caudal anterior cingulate	Intercept	1.049	0.111	9.488	2.329e-19	4.658e-19
	Age	0.009	0.003	2.635	8.739e-03	7.428e-02
	Age^2	-0.000	0.000	-3.523	4.777e-04	6.854e-03
	pTau_transformed	-0.010	0.006	-1.826	6.862e-02	8.045e-02
	Sex	-0.017	0.004	-3.987	7.991e-05	5.865e-04
	APOE4 Status	0.007	0.004	1.610	1.081e-01	9.927e-01
	Time b/w LP and MRI	-0.000	0.001	-0.297	7.664e-01	9.968e-01
caudal middle frontal	Intercept	1.195	0.121	9.885	1.006e-20	4.276e-20
	Age	0.003	0.004	0.695	4.877e-01	5.527e-01
	Age^2	-0.000	0.000	-1.484	1.386e-01	1.625e-01
	pTau_transformed	-0.018	0.006	-2.900	3.944e-03	9.578e-03
	Sex	-0.004	0.005	-0.951	3.422e-01	3.526e-01
	APOE4 Status	0.000	0.005	0.091	9.276e-01	9.927e-01
	Time b/w LP and MRI	0.001	0.001	0.605	5.458e-01	9.968e-01
cuneus	Intercept	1.123	0.116	9.723	3.643e-20	1.126e-19
	Age	0.002	0.003	0.436	6.631e-01	7.045e-01
	Age^2	-0.000	0.000	-0.939	3.483e-01	3.483e-01
	pTau_transformed	-0.011	0.006	-1.827	6.851e-02	8.045e-02
	Sex	-0.023	0.004	-5.316	1.786e-07	6.072e-06
	APOE4 Status	-0.001	0.004	-0.338	7.357e-01	9.927e-01
	Time b/w LP and MRI	0.000	0.001	0.328	7.431e-01	9.968e-01

ROI	Predictor	Estimate	Std. Error	T-Statistic	pUncorrected	pFDR
entorhinal	Intercept	0.659	0.122	5.395	1.187e-07	1.187e-07
	Age	0.015	0.004	4.151	4.061e-05	1.381e-03
	Age^2	-0.000	0.000	-5.027	7.598e-07	2.583e-05
	pTau_transformed	-0.007	0.006	-1.189	2.350e-01	2.421e-01
	Sex	-0.009	0.005	-1.951	5.181e-02	8.808e-02
	APOE4 Status	-0.001	0.005	-0.136	8.916e-01	9.927e-01
	Time b/w LP and MRI	-0.000	0.001	-0.367	7.140e-01	9.968e-01
frontal pole	Intercept	0.998	0.119	8.391	8.795e-16	9.968e-16
	Age	0.006	0.004	1.655	9.864e-02	1.973e-01
	Age^2	-0.000	0.000	-2.426	1.573e-02	3.287e-02
	pTau_transformed	-0.024	0.006	-3.974	8.403e-05	1.429e-03
	Sex	-0.001	0.004	-0.235	8.147e-01	8.147e-01
	APOE4 Status	-0.001	0.004	-0.185	8.533e-01	9.927e-01
	Time b/w LP and MRI	0.000	0.001	0.072	9.427e-01	9.968e-01
fusiform	Intercept	1.045	0.111	9.428	3.676e-19	5.952e-19
	Age	0.007	0.003	2.112	3.530e-02	1.715e-01
	Age^2	-0.000	0.000	-3.017	2.718e-03	1.341e-02
	pTau_transformed	-0.017	0.006	-3.062	2.351e-03	8.350e-03
	Sex	-0.008	0.004	-1.849	6.514e-02	9.585e-02
	APOE4 Status	0.001	0.004	0.130	8.968e-01	9.927e-01
	Time b/w LP and MRI	-0.001	0.001	-0.754	4.515e-01	9.968e-01
inferior parietal	Intercept	1.099	0.121	9.064	6.016e-18	8.182e-18
	Age	0.006	0.004	1.523	1.286e-01	1.973e-01
	Age^2	-0.000	0.000	-2.244	2.537e-02	4.108e-02
	pTau_transformed	-0.022	0.006	-3.630	3.204e-04	3.631e-03
	Sex	-0.018	0.005	-3.922	1.035e-04	5.865e-04
	APOE4 Status	0.002	0.005	0.523	6.014e-01	9.927e-01
	Time b/w LP and MRI	0.000	0.001	0.096	9.233e-01	9.968e-01
inferior temporal	Intercept	1.060	0.104	10.238	5.793e-22	3.283e-21
	Age	0.006	0.003	1.924	5.504e-02	1.808e-01
	Age^2	-0.000	0.000	-2.840	4.740e-03	2.014e-02

ROI	Predictor	Estimate	Std. Error	T-Statistic	pUncorrected	pFDR
	pTau_transformed	-0.016	0.005	-3.058	2.383e-03	8.350e-03
	Sex	-0.010	0.004	-2.458	1.440e-02	3.264e-02
	APOE4 Status	0.002	0.004	0.466	6.415e-01	9.927e-01
	Time b/w LP and MRI	-0.001	0.001	-0.917	3.595e-01	9.968e-01
insula	Intercept	1.030	0.106	9.704	4.218e-20	1.195e-19
	Age	0.005	0.003	1.575	1.160e-01	1.973e-01
	Age^2	-0.000	0.000	-2.191	2.906e-02	4.334e-02
	pTau_transformed	-0.009	0.005	-1.637	1.025e-01	1.124e-01
	Sex	-0.009	0.004	-2.262	2.425e-02	4.850e-02
	APOE4 Status	0.001	0.004	0.330	7.414e-01	9.927e-01
	Time b/w LP and MRI	-0.000	0.001	-0.023	9.820e-01	9.968e-01
isthmus cingulate	Intercept	1.077	0.127	8.451	5.714e-16	6.699e-16
	Age	0.007	0.004	1.965	5.011e-02	1.808e-01
	Age^2	-0.000	0.000	-2.538	1.154e-02	3.094e-02
	pTau_transformed	-0.012	0.006	-1.808	7.135e-02	8.086e-02
	Sex	-0.017	0.005	-3.495	5.286e-04	2.567e-03
	APOE4 Status	0.000	0.005	0.009	9.927e-01	9.927e-01
	Time b/w LP and MRI	-0.000	0.001	-0.265	7.908e-01	9.968e-01
lateral occipital	Intercept	1.137	0.107	10.647	1.984e-23	3.373e-22
	Age	0.003	0.003	0.970	3.328e-01	4.200e-01
	Age^2	-0.000	0.000	-1.548	1.225e-01	1.487e-01
	pTau_transformed	-0.024	0.005	-4.501	8.915e-06	3.031e-04
	Sex	-0.020	0.004	-5.012	8.170e-07	1.389e-05
	APOE4 Status	-0.000	0.004	-0.050	9.603e-01	9.927e-01
	Time b/w LP and MRI	-0.000	0.001	-0.004	9.968e-01	9.968e-01
lateral orbitofrontal	Intercept	1.008	0.116	8.694	9.621e-17	1.212e-16
	Age	0.008	0.003	2.289	2.261e-02	1.495e-01
	Age^2	-0.000	0.000	-3.261	1.207e-03	8.208e-03
	pTau_transformed	-0.015	0.006	-2.466	1.408e-02	2.176e-02
	Sex	-0.005	0.004	-1.238	2.165e-01	2.420e-01
	APOE4 Status	0.002	0.004	0.423	6.729e-01	9.927e-01

ROI	Predictor	Estimate	Std. Error	T-Statistic	pUncorrected	pFDR
	Time b/w LP and MRI	0.000	0.001	0.199	8.427e-01	9.968e-01
lingual	Intercept	1.076	0.114	9.442	3.301e-19	5.729e-19
	Age	0.004	0.003	1.095	2.741e-01	3.728e-01
	Age^2	-0.000	0.000	-1.702	8.961e-02	1.174e-01
	pTau_transformed	-0.013	0.006	-2.204	2.812e-02	3.860e-02
	Sex	-0.017	0.004	-3.955	9.084e-05	5.865e-04
	APOE4 Status	-0.003	0.004	-0.632	5.279e-01	9.927e-01
	Time b/w LP and MRI	0.000	0.001	0.132	8.954e-01	9.968e-01
medial orbitofrontal	Intercept	1.043	0.116	8.970	1.225e-17	1.602e-17
	Age	0.006	0.003	1.631	1.037e-01	1.973e-01
	Age^2	-0.000	0.000	-2.582	1.019e-02	3.094e-02
	pTau_transformed	-0.013	0.006	-2.187	2.936e-02	3.860e-02
	Sex	-0.008	0.004	-1.883	6.044e-02	9.585e-02
	APOE4 Status	0.000	0.004	0.057	9.546e-01	9.927e-01
	Time b/w LP and MRI	0.000	0.001	0.267	7.895e-01	9.968e-01
middle temporal	Intercept	1.111	0.107	10.361	2.116e-22	1.439e-21
	Age	0.005	0.003	1.516	1.302e-01	1.973e-01
	Age^2	-0.000	0.000	-2.435	1.534e-02	3.287e-02
	pTau_transformed	-0.017	0.005	-3.153	1.737e-03	8.350e-03
	Sex	-0.012	0.004	-3.066	2.318e-03	7.881e-03
	APOE4 Status	0.000	0.004	0.097	9.224e-01	9.927e-01
	Time b/w LP and MRI	-0.000	0.001	-0.282	7.783e-01	9.968e-01
paracentral	Intercept	1.199	0.123	9.784	2.234e-20	7.596e-20
	Age	0.002	0.004	0.579	5.628e-01	6.173e-01
	Age^2	-0.000	0.000	-1.278	2.020e-01	2.215e-01
	pTau_transformed	-0.014	0.006	-2.232	2.617e-02	3.860e-02
	Sex	-0.007	0.005	-1.452	1.472e-01	1.787e-01
	APOE4 Status	0.000	0.005	0.043	9.655e-01	9.927e-01
	Time b/w LP and MRI	-0.000	0.001	-0.352	7.252e-01	9.968e-01
parahippocampal	Intercept	0.927	0.126	7.351	1.151e-12	1.223e-12
	Age	0.010	0.004	2.690	7.444e-03	7.428e-02

ROI	Predictor	Estimate	Std. Error	T-Statistic	pUncorrected	pFDR
	Age^2	-0.000	0.000	-3.377	8.063e-04	6.854e-03
	pTau_transformed	-0.014	0.006	-2.111	3.544e-02	4.463e-02
	Sex	-0.015	0.005	-3.077	2.234e-03	7.881e-03
	APOE4 Status	-0.003	0.005	-0.714	4.758e-01	9.927e-01
	Time b/w LP and MRI	-0.001	0.001	-1.064	2.881e-01	9.968e-01
pars opercularis	Intercept	1.110	0.116	9.550	1.417e-19	3.237e-19
	Age	0.005	0.003	1.516	1.302e-01	1.973e-01
	Age^2	-0.000	0.000	-2.287	2.270e-02	3.859e-02
	pTau_transformed	-0.018	0.006	-2.993	2.937e-03	8.350e-03
	Sex	-0.008	0.004	-1.779	7.597e-02	1.033e-01
	APOE4 Status	0.002	0.004	0.379	7.051e-01	9.927e-01
	Time b/w LP and MRI	0.000	0.001	0.100	9.201e-01	9.968e-01
pars orbitalis	Intercept	1.087	0.110	9.858	1.245e-20	4.703e-20
	Age	0.004	0.003	1.300	1.943e-01	2.753e-01
	Age^2	-0.000	0.000	-2.159	3.148e-02	4.460e-02
	pTau_transformed	-0.017	0.006	-3.088	2.161e-03	8.350e-03
	Sex	-0.005	0.004	-1.215	2.252e-01	2.420e-01
	APOE4 Status	-0.000	0.004	-0.077	9.385e-01	9.927e-01
	Time b/w LP and MRI	-0.000	0.001	-0.019	9.846e-01	9.968e-01
pars triangularis	Intercept	1.071	0.115	9.314	8.902e-19	1.376e-18
	Age	0.006	0.003	1.841	6.638e-02	1.881e-01
	Age^2	-0.000	0.000	-2.748	6.279e-03	2.372e-02
	pTau_transformed	-0.015	0.006	-2.521	1.211e-02	2.142e-02
	Sex	-0.005	0.004	-1.208	2.278e-01	2.420e-01
	APOE4 Status	0.001	0.004	0.256	7.981e-01	9.927e-01
	Time b/w LP and MRI	0.000	0.001	0.110	9.126e-01	9.968e-01
pericalcarine	Intercept	1.026	0.127	8.103	6.846e-15	7.509e-15
	Age	0.003	0.004	0.835	4.042e-01	4.739e-01
	Age^2	-0.000	0.000	-1.285	1.996e-01	2.215e-01
	pTau_transformed	-0.004	0.006	-0.574	5.666e-01	5.666e-01
	Sex	-0.019	0.005	-4.007	7.370e-05	5.865e-04

ROI	Predictor	Estimate	Std. Error	T-Statistic	pUncorrected	pFDR
	APOE4 Status	-0.004	0.005	-0.784	4.333e-01	9.927e-01
	Time b/w LP and MRI	0.001	0.001	0.763	4.459e-01	9.968e-01
postcentral	Intercept	1.185	0.114	10.438	1.126e-22	1.084e-21
	Age	0.001	0.003	0.396	6.920e-01	7.130e-01
	Age^2	-0.000	0.000	-1.056	2.918e-01	3.006e-01
	pTau_transformed	-0.013	0.006	-2.184	2.952e-02	3.860e-02
	Sex	-0.008	0.004	-1.832	6.766e-02	9.585e-02
	APOE4 Status	0.000	0.004	0.055	9.561e-01	9.927e-01
	Time b/w LP and MRI	0.000	0.001	0.068	9.459e-01	9.968e-01
posterior cingulate	Intercept	1.143	0.124	9.205	2.055e-18	3.038e-18
	Age	0.006	0.004	1.504	1.335e-01	1.973e-01
	Age^2	-0.000	0.000	-2.187	2.932e-02	4.334e-02
	pTau_transformed	-0.016	0.006	-2.496	1.296e-02	2.142e-02
	Sex	-0.012	0.005	-2.637	8.687e-03	2.272e-02
	APOE4 Status	0.000	0.005	0.084	9.327e-01	9.927e-01
	Time b/w LP and MRI	-0.001	0.001	-0.572	5.673e-01	9.968e-01
precentral	Intercept	1.222	0.117	10.423	1.275e-22	1.084e-21
	Age	0.001	0.003	0.353	7.246e-01	7.246e-01
	Age^2	-0.000	0.000	-1.069	2.856e-01	3.006e-01
	pTau_transformed	-0.015	0.006	-2.489	1.323e-02	2.142e-02
	Sex	-0.007	0.004	-1.469	1.426e-01	1.787e-01
	APOE4 Status	-0.000	0.004	-0.031	9.755e-01	9.927e-01
	Time b/w LP and MRI	0.000	0.001	0.371	7.110e-01	9.968e-01
precuneus	Intercept	1.085	0.127	8.524	3.351e-16	4.069e-16
	Age	0.006	0.004	1.650	9.979e-02	1.973e-01
	Age^2	-0.000	0.000	-2.429	1.557e-02	3.287e-02
	pTau_transformed	-0.018	0.006	-2.800	5.359e-03	1.215e-02
	Sex	-0.014	0.005	-2.925	3.648e-03	1.128e-02
	APOE4 Status	0.000	0.005	0.098	9.217e-01	9.927e-01
	Time b/w LP and MRI	-0.000	0.001	-0.290	7.719e-01	9.968e-01
rostral anterior cingulate	Intercept	1.052	0.109	9.643	6.923e-20	1.811e-19

ROI	Predictor	Estimate	Std. Error	T-Statistic	pUncorrected	pFDR
	Age	0.007	0.003	2.229	2.638e-02	1.495e-01
	Age^2	-0.000	0.000	-3.012	2.760e-03	1.341e-02
	pTau_transformed	-0.014	0.006	-2.577	1.034e-02	1.953e-02
	Sex	-0.007	0.004	-1.577	1.156e-01	1.512e-01
	APOE4 Status	0.005	0.004	1.117	2.646e-01	9.927e-01
	Time b/w LP and MRI	-0.000	0.001	-0.024	9.806e-01	9.968e-01
rostral middle frontal	Intercept	1.175	0.123	9.549	1.428e-19	3.237e-19
	Age	0.003	0.004	0.849	3.962e-01	4.739e-01
	Age^2	-0.000	0.000	-1.683	9.321e-02	1.174e-01
	pTau_transformed	-0.018	0.006	-2.927	3.621e-03	9.470e-03
	Sex	-0.009	0.005	-1.865	6.287e-02	9.585e-02
	APOE4 Status	0.001	0.005	0.194	8.465e-01	9.927e-01
	Time b/w LP and MRI	0.001	0.001	0.599	5.492e-01	9.968e-01
superior frontal	Intercept	1.102	0.101	10.944	1.672e-24	5.685e-23
	Age	0.005	0.003	1.504	1.335e-01	1.973e-01
	Age^2	-0.000	0.000	-2.529	1.183e-02	3.094e-02
	pTau_transformed	-0.014	0.005	-2.645	8.508e-03	1.702e-02
	Sex	-0.009	0.004	-2.417	1.611e-02	3.423e-02
	APOE4 Status	0.003	0.004	0.842	4.005e-01	9.927e-01
	Time b/w LP and MRI	0.000	0.001	0.049	9.607e-01	9.968e-01
superior parietal	Intercept	1.154	0.122	9.461	2.849e-19	5.381e-19
	Age	0.004	0.004	0.968	3.335e-01	4.200e-01
	Age^2	-0.000	0.000	-1.690	9.178e-02	1.174e-01
	pTau_transformed	-0.019	0.006	-2.992	2.947e-03	8.350e-03
	Sex	-0.015	0.005	-3.306	1.035e-03	4.399e-03
	APOE4 Status	0.001	0.005	0.117	9.069e-01	9.927e-01
	Time b/w LP and MRI	-0.000	0.001	-0.115	9.084e-01	9.968e-01
superior temporal	Intercept	1.062	0.107	9.935	6.717e-21	3.263e-20
	Age	0.006	0.003	1.898	5.849e-02	1.808e-01
	Age^2	-0.000	0.000	-2.676	7.771e-03	2.642e-02
	pTau_transformed	-0.015	0.005	-2.771	5.851e-03	1.243e-02

ROI	Predictor	Estimate	Std. Error	T-Statistic	pUncorrected	pFDR
	Sex	-0.009	0.004	-2.145	3.255e-02	6.148e-02
	APOE4 Status	-0.000	0.004	-0.068	9.459e-01	9.927e-01
	Time b/w LP and MRI	-0.000	0.001	-0.084	9.330e-01	9.968e-01
supramarginal	Intercept	1.099	0.120	9.135	3.508e-18	4.970e-18
	Age	0.006	0.004	1.577	1.156e-01	1.973e-01
	Age^2	-0.000	0.000	-2.333	2.017e-02	3.609e-02
	pTau_transformed	-0.018	0.006	-3.013	2.759e-03	8.350e-03
	Sex	-0.013	0.005	-2.775	5.783e-03	1.639e-02
	APOE4 Status	0.001	0.005	0.262	7.938e-01	9.927e-01
	Time b/w LP and MRI	-0.000	0.001	-0.017	9.864e-01	9.968e-01
temporal pole	Intercept	0.833	0.115	7.228	2.568e-12	2.646e-12
	Age	0.009	0.003	2.701	7.203e-03	7.428e-02
	Age^2	-0.000	0.000	-3.432	6.629e-04	6.854e-03
	pTau_transformed	-0.009	0.006	-1.567	1.180e-01	1.254e-01
	Sex	-0.006	0.004	-1.426	1.547e-01	1.814e-01
	APOE4 Status	-0.002	0.004	-0.448	6.542e-01	9.927e-01
	Time b/w LP and MRI	-0.001	0.001	-0.832	4.058e-01	9.968e-01
transverse temporal	Intercept	1.056	0.111	9.501	2.087e-19	4.435e-19
	Age	0.007	0.003	1.966	5.002e-02	1.808e-01
	Age^2	-0.000	0.000	-2.388	1.740e-02	3.287e-02
	pTau_transformed	-0.018	0.006	-3.150	1.757e-03	8.350e-03
	Sex	-0.008	0.004	-2.003	4.587e-02	8.208e-02
	APOE4 Status	-0.003	0.004	-0.755	4.505e-01	9.927e-01
	Time b/w LP and MRI	0.000	0.001	0.609	5.429e-01	9.968e-01

Table C5: Estimated outputs of each linear regression model assessing the effects of CSF $pTau_{181}$ on cortical-adjacent WM R1. Covariates in each model included age, sex, APOE4 status, and time between lumbar puncture and MRI. Abbreviations: pTau_transformed, CSF tau phosphorylated at threonine 181 (log-transformed); LP, lumbar puncture; MRI, magnetic

resonance imaging; pUncorrected, *p*-value uncorrected for multiple comparisons; pFDR, Benjamini-Hochberg FDR-corrected *p*-value.

Table C6: Outputs of linear regression models assessing effects of CSF neurogranin on cortical GM R1

ROI	Predictor	Estimate	Std. Error	T-Statistic	pUncorrected	pFDR
bankssts	Intercept	0.752	0.018	42.494	5.100e-149	1.239e-148
	Age	-0.000	0.000	-0.713	4.764e-01	7.265e-01
	Neurogranin_transformed	-0.006	0.003	-2.158	3.151e-02	7.142e-02
	Sex	0.003	0.002	1.237	2.167e-01	9.656e-01
	APOE4 Status	0.002	0.002	0.982	3.267e-01	9.850e-01
	Time b/w LP and MRI	0.001	0.000	1.972	4.936e-02	6.713e-02
caudal anterior cingulate	Intercept	0.703	0.028	25.390	1.711e-84	1.818e-84
	Age	0.000	0.000	1.851	6.492e-02	2.453e-01
	Neurogranin_transformed	-0.005	0.004	-1.167	2.438e-01	3.316e-01
	Sex	-0.005	0.003	-1.627	1.045e-01	9.656e-01
	APOE4 Status	0.001	0.003	0.245	8.064e-01	9.850e-01
	Time b/w LP and MRI	0.001	0.001	1.543	1.237e-01	1.502e-01
caudal middle frontal	Intercept	0.750	0.017	43.046	7.850e-151	2.224e-150
	Age	-0.000	0.000	-0.621	5.353e-01	7.265e-01
	Neurogranin_transformed	-0.005	0.003	-1.826	6.859e-02	1.296e-01
	Sex	0.001	0.002	0.396	6.921e-01	9.656e-01
	APOE4 Status	0.002	0.002	0.861	3.897e-01	9.850e-01
	Time b/w LP and MRI	0.001	0.000	2.297	2.213e-02	3.762e-02
cuneus	Intercept	0.795	0.023	35.276	7.601e-124	9.940e-124
	Age	-0.000	0.000	-1.404	1.611e-01	4.979e-01
	Neurogranin_transformed	-0.008	0.003	-2.426	1.570e-02	5.307e-02
	Sex	-0.004	0.003	-1.374	1.703e-01	9.656e-01
	APOE4 Status	-0.002	0.003	-0.764	4.455e-01	9.850e-01
	Time b/w LP and MRI	0.002	0.001	3.007	2.807e-03	1.466e-02
entorhinal	Intercept	0.847	0.043	19.568	5.077e-60	5.077e-60
	Age	-0.000	0.000	-1.147	2.520e-01	5.529e-01
	Neurogranin_transformed	-0.006	0.006	-0.944	3.457e-01	4.353e-01
	Sex	0.003	0.005	0.479	6.323e-01	9.656e-01

ROI	Predictor	Estimate	Std. Error	T-Statistic	pUncorrected	pFDR
	APOE4 Status	0.003	0.005	0.614	5.397e-01	9.850e-01
	Time b/w LP and MRI	0.001	0.001	0.985	3.250e-01	3.348e-01
frontal pole	Intercept	0.724	0.019	38.072	6.348e-134	8.993e-134
	Age	-0.000	0.000	-0.451	6.523e-01	7.492e-01
	Neurogranin_transformed	-0.007	0.003	-2.393	1.717e-02	5.307e-02
	Sex	-0.003	0.002	-1.255	2.103e-01	9.656e-01
	APOE4 Status	0.001	0.002	0.604	5.461e-01	9.850e-01
	Time b/w LP and MRI	0.001	0.000	3.480	5.575e-04	1.106e-02
fusiform	Intercept	0.698	0.015	45.639	3.729e-159	1.811e-158
	Age	0.000	0.000	0.654	5.135e-01	7.265e-01
	Neurogranin_transformed	-0.002	0.002	-0.899	3.692e-01	4.483e-01
	Sex	0.001	0.002	0.657	5.118e-01	9.656e-01
	APOE4 Status	-0.000	0.002	-0.236	8.132e-01	9.850e-01
	Time b/w LP and MRI	0.001	0.000	2.083	3.792e-02	5.606e-02
inferior parietal	Intercept	0.765	0.019	41.135	1.740e-144	3.698e-144
	Age	-0.000	0.000	-0.656	5.120e-01	7.265e-01
	Neurogranin_transformed	-0.009	0.003	-3.066	2.320e-03	3.890e-02
	Sex	-0.000	0.002	-0.185	8.533e-01	9.656e-01
	APOE4 Status	0.002	0.002	1.087	2.778e-01	9.850e-01
	Time b/w LP and MRI	0.001	0.000	2.808	5.240e-03	1.980e-02
inferior temporal	Intercept	0.682	0.015	44.498	1.559e-155	5.890e-155
	Age	0.000	0.000	1.196	2.326e-01	5.529e-01
	Neurogranin_transformed	-0.002	0.002	-0.991	3.224e-01	4.216e-01
	Sex	0.001	0.002	0.319	7.502e-01	9.656e-01
	APOE4 Status	-0.000	0.002	-0.094	9.254e-01	9.850e-01
	Time b/w LP and MRI	0.001	0.000	2.344	1.960e-02	3.702e-02
insula	Intercept	0.676	0.015	45.682	2.722e-159	1.542e-158
	Age	0.001	0.000	4.650	4.543e-06	1.147e-04
	Neurogranin_transformed	-0.003	0.002	-1.531	1.267e-01	1.958e-01
	Sex	0.001	0.002	0.480	6.312e-01	9.656e-01
	APOE4 Status	-0.000	0.002	-0.130	8.965e-01	9.850e-01

ROI	Predictor	Estimate	Std. Error	T-Statistic	pUncorrected	pFDR
	Time b/w LP and MRI	0.001	0.000	2.311	2.134e-02	3.762e-02
isthmus cingulate	Intercept	0.765	0.023	32.863	1.504e-114	1.705e-114
	Age	0.000	0.000	0.588	5.569e-01	7.265e-01
	Neurogranin_transformed	-0.007	0.003	-1.929	5.441e-02	1.088e-01
	Sex	0.000	0.003	0.044	9.652e-01	9.656e-01
	APOE4 Status	0.001	0.003	0.262	7.937e-01	9.850e-01
	Time b/w LP and MRI	0.001	0.001	1.508	1.323e-01	1.551e-01
lateral occipital	Intercept	0.762	0.020	38.587	9.806e-136	1.450e-135
	Age	0.000	0.000	0.778	4.372e-01	7.265e-01
	Neurogranin_transformed	-0.009	0.003	-2.896	3.996e-03	3.890e-02
	Sex	-0.002	0.002	-0.710	4.782e-01	9.656e-01
	APOE4 Status	0.000	0.002	0.012	9.902e-01	9.902e-01
	Time b/w LP and MRI	0.001	0.000	2.840	4.747e-03	1.980e-02
lateral orbitofrontal	Intercept	0.697	0.017	42.222	4.037e-148	9.151e-148
	Age	-0.000	0.000	-0.063	9.501e-01	9.501e-01
	Neurogranin_transformed	-0.002	0.002	-0.766	4.440e-01	5.032e-01
	Sex	-0.003	0.002	-1.349	1.780e-01	9.656e-01
	APOE4 Status	-0.002	0.002	-0.899	3.690e-01	9.850e-01
	Time b/w LP and MRI	0.001	0.000	2.737	6.474e-03	2.201e-02
lingual	Intercept	0.760	0.020	38.791	1.896e-136	2.930e-136
	Age	-0.000	0.000	-0.104	9.173e-01	9.451e-01
	Neurogranin_transformed	-0.007	0.003	-2.437	1.523e-02	5.307e-02
	Sex	0.000	0.002	0.137	8.911e-01	9.656e-01
	APOE4 Status	0.000	0.002	0.107	9.145e-01	9.850e-01
	Time b/w LP and MRI	0.001	0.000	2.419	1.602e-02	3.404e-02
medial orbitofrontal	Intercept	0.652	0.015	42.718	1.475e-149	3.858e-149
	Age	0.000	0.000	1.902	5.786e-02	2.453e-01
	Neurogranin_transformed	-0.000	0.002	-0.150	8.811e-01	8.811e-01
	Sex	-0.003	0.002	-1.351	1.774e-01	9.656e-01
	APOE4 Status	-0.001	0.002	-0.685	4.936e-01	9.850e-01
	Time b/w LP and MRI	0.001	0.000	2.473	1.380e-02	3.351e-02

ROI	Predictor	Estimate	Std. Error	T-Statistic	pUncorrected	pFDR
middle temporal	Intercept	0.699	0.014	49.380	1.308e-170	4.447e-169
	Age	0.000	0.000	1.323	1.866e-01	5.287e-01
	Neurogranin_transformed	-0.004	0.002	-1.679	9.397e-02	1.521e-01
	Sex	0.000	0.002	0.253	8.003e-01	9.656e-01
	APOE4 Status	0.000	0.002	0.172	8.636e-01	9.850e-01
	Time b/w LP and MRI	0.001	0.000	2.994	2.923e-03	1.466e-02
paracentral	Intercept	0.771	0.019	39.601	4.398e-139	7.121e-139
	Age	-0.000	0.000	-0.439	6.611e-01	7.492e-01
	Neurogranin_transformed	-0.002	0.003	-0.720	4.722e-01	5.179e-01
	Sex	0.002	0.002	0.832	4.062e-01	9.656e-01
	APOE4 Status	-0.000	0.002	-0.067	9.465e-01	9.850e-01
	Time b/w LP and MRI	0.000	0.000	0.676	4.991e-01	4.991e-01
parahippocampal	Intercept	0.669	0.019	34.633	1.807e-121	2.275e-121
	Age	0.000	0.000	3.094	2.113e-03	1.796e-02
	Neurogranin_transformed	-0.001	0.003	-0.505	6.136e-01	6.322e-01
	Sex	0.001	0.002	0.500	6.171e-01	9.656e-01
	APOE4 Status	-0.002	0.002	-0.798	4.256e-01	9.850e-01
	Time b/w LP and MRI	0.001	0.000	1.763	7.870e-02	9.910e-02
pars opercularis	Intercept	0.728	0.016	46.553	5.166e-162	5.076e-161
	Age	0.000	0.000	1.406	1.604e-01	4.979e-01
	Neurogranin_transformed	-0.005	0.002	-1.933	5.396e-02	1.088e-01
	Sex	-0.001	0.002	-0.290	7.723e-01	9.656e-01
	APOE4 Status	0.000	0.002	0.177	8.594e-01	9.850e-01
	Time b/w LP and MRI	0.001	0.000	2.246	2.529e-02	4.095e-02
pars orbitalis	Intercept	0.734	0.017	44.018	5.423e-154	1.844e-153
	Age	0.000	0.000	0.720	4.720e-01	7.265e-01
	Neurogranin_transformed	-0.007	0.002	-2.698	7.279e-03	4.950e-02
	Sex	-0.001	0.002	-0.638	5.236e-01	9.656e-01
	APOE4 Status	-0.000	0.002	-0.178	8.585e-01	9.850e-01
	Time b/w LP and MRI	0.001	0.000	3.123	1.922e-03	1.466e-02
pars triangularis	Intercept	0.739	0.016	46.533	5.972e-162	5.076e-161

ROI	Predictor	Estimate	Std. Error	T-Statistic	pUncorrected	pFDR
	Age	0.000	0.000	0.558	5.769e-01	7.265e-01
	Neurogranin_transformed	-0.006	0.002	-2.402	1.677e-02	5.307e-02
	Sex	-0.002	0.002	-0.799	4.251e-01	9.656e-01
	APOE4 Status	0.000	0.002	0.167	8.676e-01	9.850e-01
	Time b/w LP and MRI	0.001	0.000	3.256	1.226e-03	1.389e-02
pericalcarine	Intercept	0.778	0.024	32.260	1.681e-112	1.844e-112
	Age	0.000	0.000	0.446	6.559e-01	7.492e-01
	Neurogranin_transformed	-0.008	0.004	-2.233	2.608e-02	6.334e-02
	Sex	-0.004	0.003	-1.490	1.371e-01	9.656e-01
	APOE4 Status	-0.000	0.003	-0.146	8.838e-01	9.850e-01
	Time b/w LP and MRI	0.001	0.001	2.607	9.491e-03	2.689e-02
postcentral	Intercept	0.763	0.019	40.759	3.236e-143	6.472e-143
	Age	0.000	0.000	1.128	2.602e-01	5.529e-01
	Neurogranin_transformed	-0.005	0.003	-1.781	7.573e-02	1.355e-01
	Sex	0.001	0.002	0.553	5.809e-01	9.656e-01
	APOE4 Status	0.000	0.002	0.055	9.560e-01	9.850e-01
	Time b/w LP and MRI	0.001	0.000	1.938	5.329e-02	6.969e-02
posterior cingulate	Intercept	0.763	0.034	22.724	6.187e-73	6.374e-73
	Age	0.000	0.000	1.925	5.498e-02	2.453e-01
	Neurogranin_transformed	-0.009	0.005	-1.749	8.109e-02	1.379e-01
	Sex	0.000	0.004	0.072	9.426e-01	9.656e-01
	APOE4 Status	0.001	0.004	0.305	7.607e-01	9.850e-01
	Time b/w LP and MRI	0.001	0.001	0.992	3.216e-01	3.348e-01
precentral	Intercept	0.786	0.020	39.838	4.505e-140	7.658e-140
	Age	-0.000	0.000	-0.143	8.862e-01	9.416e-01
	Neurogranin_transformed	-0.004	0.003	-1.354	1.765e-01	2.609e-01
	Sex	0.002	0.002	0.931	3.524e-01	9.656e-01
	APOE4 Status	0.001	0.002	0.413	6.797e-01	9.850e-01
	Time b/w LP and MRI	0.001	0.000	2.012	4.486e-02	6.355e-02
precuneus	Intercept	0.765	0.019	40.614	1.005e-142	1.898e-142
	Age	-0.000	0.000	-1.089	2.770e-01	5.540e-01

ROI	Predictor	Estimate	Std. Error	T-Statistic	pUncorrected	pFDR
	Neurogranin_transformed	-0.007	0.003	-2.470	1.394e-02	5.307e-02
	Sex	0.000	0.002	0.204	8.381e-01	9.656e-01
	APOE4 Status	0.000	0.002	0.203	8.393e-01	9.850e-01
	Time b/w LP and MRI	0.001	0.000	2.669	7.929e-03	2.451e-02
rostral anterior cingulate	Intercept	0.629	0.019	33.951	8.689e-119	1.055e-118
	Age	0.000	0.000	3.322	9.769e-04	1.107e-02
	Neurogranin_transformed	0.002	0.003	0.627	5.307e-01	5.639e-01
	Sex	-0.000	0.002	-0.073	9.420e-01	9.656e-01
	APOE4 Status	0.001	0.002	0.646	5.190e-01	9.850e-01
	Time b/w LP and MRI	0.001	0.000	1.200	2.307e-01	2.615e-01
rostral middle frontal	Intercept	0.740	0.017	43.574	1.482e-152	4.581e-152
	Age	-0.000	0.000	-1.246	2.136e-01	5.529e-01
	Neurogranin_transformed	-0.006	0.003	-2.267	2.394e-02	6.261e-02
	Sex	-0.002	0.002	-1.022	3.075e-01	9.656e-01
	APOE4 Status	0.002	0.002	0.982	3.269e-01	9.850e-01
	Time b/w LP and MRI	0.001	0.000	3.437	6.504e-04	1.106e-02
superior frontal	Intercept	0.726	0.016	45.870	1.163e-159	7.908e-159
	Age	-0.000	0.000	-0.798	4.255e-01	7.265e-01
	Neurogranin_transformed	-0.003	0.002	-1.218	2.239e-01	3.172e-01
	Sex	0.001	0.002	0.377	7.062e-01	9.656e-01
	APOE4 Status	0.001	0.002	0.448	6.544e-01	9.850e-01
	Time b/w LP and MRI	0.001	0.000	2.126	3.412e-02	5.273e-02
superior parietal	Intercept	0.771	0.019	40.117	4.950e-141	8.858e-141
	Age	-0.000	0.000	-0.841	4.010e-01	7.265e-01
	Neurogranin_transformed	-0.007	0.003	-2.402	1.678e-02	5.307e-02
	Sex	-0.000	0.002	-0.121	9.037e-01	9.656e-01
	APOE4 Status	0.001	0.002	0.420	6.746e-01	9.850e-01
	Time b/w LP and MRI	0.001	0.000	2.440	1.515e-02	3.404e-02
superior temporal	Intercept	0.739	0.015	47.696	1.566e-165	2.662e-164
	Age	0.000	0.000	2.442	1.505e-02	8.528e-02
	Neurogranin_transformed	-0.007	0.002	-2.914	3.771e-03	3.890e-02

ROI	Predictor	Estimate	Std. Error	T-Statistic	pUncorrected	pFDR
	Sex	0.001	0.002	0.293	7.693e-01	9.656e-01
	APOE4 Status	-0.000	0.002	-0.224	8.227e-01	9.850e-01
	Time b/w LP and MRI	0.001	0.000	2.473	1.380e-02	3.351e-02
supramarginal	Intercept	0.751	0.017	45.373	2.563e-158	1.089e-157
	Age	0.000	0.000	0.273	7.846e-01	8.605e-01
	Neurogranin_transformed	-0.007	0.002	-2.852	4.577e-03	3.890e-02
	Sex	-0.001	0.002	-0.259	7.954e-01	9.656e-01
	APOE4 Status	0.001	0.002	0.598	5.501e-01	9.850e-01
	Time b/w LP and MRI	0.001	0.000	2.367	1.840e-02	3.680e-02
temporal pole	Intercept	0.656	0.020	33.547	2.106e-117	2.469e-117
	Age	0.001	0.000	4.563	6.748e-06	1.147e-04
	Neurogranin_transformed	-0.002	0.003	-0.845	3.984e-01	4.671e-01
	Sex	0.002	0.002	0.699	4.849e-01	9.656e-01
	APOE4 Status	-0.002	0.002	-0.923	3.566e-01	9.850e-01
	Time b/w LP and MRI	0.001	0.000	1.161	2.465e-01	2.704e-01
transverse temporal	Intercept	0.809	0.022	36.979	4.913e-130	6.682e-130
	Age	0.000	0.000	2.754	6.156e-03	4.186e-02
	Neurogranin_transformed	-0.008	0.003	-2.330	2.029e-02	5.749e-02
	Sex	0.000	0.003	0.043	9.656e-01	9.656e-01
	APOE4 Status	-0.002	0.003	-0.764	4.450e-01	9.850e-01
	Time b/w LP and MRI	0.001	0.000	2.984	3.018e-03	1.466e-02

Table C6: Estimated outputs of each linear regression model assessing the effects of CSF neurogranin on cortical GM R1. Covariates in each model included age, sex, APOE4 status, and time between lumbar puncture and MRI. Abbreviations: neurogranin_transformed, CSF neurogranin (log-transformed); LP, lumbar puncture; MRI, magnetic resonance imaging; pUncorrected, *p*-value uncorrected for multiple comparisons; pFDR, Benjamini-Hochberg FDR-corrected *p*-value.

Table C7: Outputs of linear regression models assessing effects of CSF neurogranin on cortical-adjacent WM R1

ROI	Predictor	Estimate	Std. Error	T-Statistic	pUncorrected	pFDR
bankssts	Intercept	1.206	0.123	9.817	1.723e-20	4.606e-20
	Age	0.005	0.003	1.546	1.229e-01	2.671e-01
	Age^2	-0.000	0.000	-2.258	2.447e-02	4.626e-02
	Neurogranin_transformed	-0.020	0.005	-3.656	2.914e-04	2.477e-03
	Sex	-0.010	0.004	-2.192	2.897e-02	6.997e-02
	APOE4 Status	0.001	0.004	0.132	8.948e-01	9.907e-01
	Time b/w LP and MRI	-0.000	0.001	-0.155	8.771e-01	9.473e-01
caudal anterior cingulate	Intercept	1.111	0.116	9.611	8.918e-20	1.516e-19
	Age	0.008	0.003	2.523	1.203e-02	1.023e-01
	Age^2	-0.000	0.000	-3.426	6.772e-04	8.687e-03
	Neurogranin_transformed	-0.012	0.005	-2.274	2.352e-02	2.962e-02
	Sex	-0.016	0.004	-3.758	1.971e-04	1.675e-03
	APOE4 Status	0.006	0.004	1.502	1.339e-01	9.907e-01
	Time b/w LP and MRI	-0.000	0.001	-0.180	8.574e-01	9.473e-01
caudal middle frontal	Intercept	1.286	0.127	10.165	1.050e-21	4.462e-21
	Age	0.002	0.004	0.533	5.943e-01	6.735e-01
	Age^2	-0.000	0.000	-1.355	1.763e-01	2.067e-01
	Neurogranin_transformed	-0.018	0.006	-3.217	1.403e-03	4.576e-03
	Sex	-0.003	0.005	-0.666	5.057e-01	5.210e-01
	APOE4 Status	-0.001	0.004	-0.141	8.883e-01	9.907e-01
	Time b/w LP and MRI	0.001	0.001	0.797	4.261e-01	9.473e-01
cuneus	Intercept	1.200	0.121	9.956	5.665e-21	1.926e-20
	Age	0.001	0.003	0.304	7.610e-01	8.086e-01
	Age^2	-0.000	0.000	-0.819	4.132e-01	4.132e-01
	Neurogranin_transformed	-0.014	0.005	-2.589	9.985e-03	1.559e-02
	Sex	-0.022	0.004	-5.052	6.713e-07	2.282e-05
	APOE4 Status	-0.002	0.004	-0.447	6.549e-01	9.907e-01
	Time b/w LP and MRI	0.000	0.001	0.431	6.667e-01	9.473e-01

ROI	Predictor	Estimate	Std. Error	T-Statistic	pUncorrected	pFDR
entorhinal	Intercept	0.678	0.128	5.297	1.963e-07	1.963e-07
	Age	0.015	0.004	4.104	4.942e-05	1.680e-03
	Age^2	-0.000	0.000	-4.996	8.804e-07	2.993e-05
	Neurogranin_transformed	-0.005	0.006	-0.881	3.788e-01	3.788e-01
	Sex	-0.009	0.005	-1.865	6.296e-02	1.168e-01
	APOE4 Status	-0.001	0.005	-0.280	7.797e-01	9.907e-01
	Time b/w LP and MRI	-0.000	0.001	-0.280	7.793e-01	9.473e-01
frontal pole	Intercept	1.099	0.125	8.807	4.153e-17	5.043e-17
	Age	0.005	0.004	1.458	1.456e-01	2.671e-01
	Age^2	-0.000	0.000	-2.279	2.322e-02	4.626e-02
	Neurogranin_transformed	-0.021	0.006	-3.860	1.326e-04	2.254e-03
	Sex	0.001	0.005	0.121	9.041e-01	9.041e-01
	APOE4 Status	-0.002	0.004	-0.561	5.751e-01	9.907e-01
	Time b/w LP and MRI	0.000	0.001	0.343	7.316e-01	9.473e-01
fusiform	Intercept	1.124	0.116	9.688	4.803e-20	9.606e-20
	Age	0.006	0.003	1.956	5.122e-02	2.488e-01
	Age^2	-0.000	0.000	-2.897	3.978e-03	1.932e-02
	Neurogranin_transformed	-0.016	0.005	-3.159	1.707e-03	4.576e-03
	Sex	-0.007	0.004	-1.559	1.198e-01	1.697e-01
	APOE4 Status	-0.001	0.004	-0.142	8.873e-01	9.907e-01
	Time b/w LP and MRI	-0.000	0.001	-0.543	5.873e-01	9.473e-01
inferior parietal	Intercept	1.201	0.127	9.455	2.993e-19	4.240e-19
	Age	0.005	0.004	1.344	1.797e-01	2.671e-01
	Age^2	-0.000	0.000	-2.109	3.555e-02	5.494e-02
	Neurogranin_transformed	-0.021	0.006	-3.747	2.057e-04	2.331e-03
	Sex	-0.016	0.005	-3.572	3.987e-04	2.259e-03
	APOE4 Status	0.001	0.004	0.211	8.326e-01	9.907e-01
	Time b/w LP and MRI	0.000	0.001	0.335	7.377e-01	9.473e-01
inferior temporal	Intercept	1.134	0.108	10.452	9.975e-23	5.653e-22
	Age	0.005	0.003	1.768	7.779e-02	2.511e-01
	Age^2	-0.000	0.000	-2.721	6.793e-03	2.887e-02

ROI	Predictor	Estimate	Std. Error	T-Statistic	pUncorrected	pFDR
	Neurogranin_transformed	-0.015	0.005	-3.131	1.875e-03	4.576e-03
	Sex	-0.009	0.004	-2.166	3.087e-02	6.997e-02
	APOE4 Status	0.001	0.004	0.191	8.486e-01	9.907e-01
	Time b/w LP and MRI	-0.001	0.001	-0.713	4.764e-01	9.473e-01
insula	Intercept	1.068	0.111	9.601	9.531e-20	1.543e-19
	Age	0.005	0.003	1.491	1.367e-01	2.671e-01
	Age^2	-0.000	0.000	-2.127	3.408e-02	5.494e-02
	Neurogranin_transformed	-0.008	0.005	-1.615	1.071e-01	1.138e-01
	Sex	-0.008	0.004	-2.103	3.612e-02	7.224e-02
	APOE4 Status	0.001	0.004	0.183	8.546e-01	9.907e-01
	Time b/w LP and MRI	0.000	0.001	0.079	9.371e-01	9.473e-01
isthmus cingulate	Intercept	1.145	0.133	8.584	2.154e-16	2.441e-16
	Age	0.007	0.004	1.858	6.396e-02	2.511e-01
	Age^2	-0.000	0.000	-2.446	1.490e-02	4.222e-02
	Neurogranin_transformed	-0.013	0.006	-2.208	2.785e-02	3.382e-02
	Sex	-0.016	0.005	-3.272	1.163e-03	5.649e-03
	APOE4 Status	-0.001	0.005	-0.118	9.063e-01	9.907e-01
	Time b/w LP and MRI	-0.000	0.001	-0.153	8.785e-01	9.473e-01
lateral occipital	Intercept	1.255	0.112	11.244	1.275e-25	2.168e-24
	Age	0.002	0.003	0.739	4.606e-01	5.593e-01
	Age^2	-0.000	0.000	-1.372	1.710e-01	2.067e-01
	Neurogranin_transformed	-0.024	0.005	-4.806	2.191e-06	7.449e-05
	Sex	-0.019	0.004	-4.566	6.666e-06	1.133e-04
	APOE4 Status	-0.002	0.004	-0.451	6.522e-01	9.907e-01
	Time b/w LP and MRI	0.000	0.001	0.288	7.737e-01	9.473e-01
lateral orbitofrontal	Intercept	1.075	0.121	8.855	2.909e-17	3.663e-17
	Age	0.007	0.003	2.159	3.147e-02	2.016e-01
	Age^2	-0.000	0.000	-3.160	1.703e-03	1.158e-02
	Neurogranin_transformed	-0.014	0.005	-2.549	1.119e-02	1.654e-02
	Sex	-0.004	0.004	-1.005	3.157e-01	3.578e-01
	APOE4 Status	0.001	0.004	0.210	8.334e-01	9.907e-01

ROI	Predictor	Estimate	Std. Error	T-Statistic	pUncorrected	pFDR
	Time b/w LP and MRI	0.000	0.001	0.376	7.072e-01	9.473e-01
lingual	Intercept	1.147	0.119	9.622	8.080e-20	1.446e-19
	Age	0.003	0.003	0.967	3.342e-01	4.545e-01
	Age^2	-0.000	0.000	-1.595	1.115e-01	1.516e-01
	Neurogranin_transformed	-0.014	0.005	-2.585	1.009e-02	1.559e-02
	Sex	-0.016	0.004	-3.694	2.517e-04	1.712e-03
	APOE4 Status	-0.003	0.004	-0.817	4.142e-01	9.907e-01
	Time b/w LP and MRI	0.000	0.001	0.271	7.869e-01	9.473e-01
medial orbitofrontal	Intercept	1.095	0.122	8.978	1.154e-17	1.509e-17
	Age	0.005	0.003	1.524	1.282e-01	2.671e-01
	Age^2	-0.000	0.000	-2.503	1.273e-02	3.935e-02
	Neurogranin_transformed	-0.011	0.005	-2.049	4.113e-02	4.822e-02
	Sex	-0.007	0.004	-1.682	9.328e-02	1.510e-01
	APOE4 Status	-0.001	0.004	-0.159	8.736e-01	9.907e-01
	Time b/w LP and MRI	0.000	0.001	0.411	6.810e-01	9.473e-01
middle temporal	Intercept	1.195	0.112	10.648	1.971e-23	2.234e-22
	Age	0.004	0.003	1.352	1.772e-01	2.671e-01
	Age^2	-0.000	0.000	-2.307	2.158e-02	4.626e-02
	Neurogranin_transformed	-0.017	0.005	-3.386	7.808e-04	4.501e-03
	Sex	-0.011	0.004	-2.744	6.349e-03	2.159e-02
	APOE4 Status	-0.001	0.004	-0.168	8.669e-01	9.907e-01
	Time b/w LP and MRI	-0.000	0.001	-0.066	9.473e-01	9.473e-01
paracentral	Intercept	1.262	0.128	9.826	1.603e-20	4.606e-20
	Age	0.002	0.004	0.468	6.401e-01	7.020e-01
	Age^2	-0.000	0.000	-1.193	2.334e-01	2.560e-01
	Neurogranin_transformed	-0.013	0.006	-2.286	2.279e-02	2.962e-02
	Sex	-0.006	0.005	-1.238	2.166e-01	2.616e-01
	APOE4 Status	-0.001	0.005	-0.160	8.731e-01	9.907e-01
	Time b/w LP and MRI	-0.000	0.001	-0.221	8.252e-01	9.473e-01
parahippocampal	Intercept	0.973	0.132	7.356	1.113e-12	1.183e-12
	Age	0.010	0.004	2.593	9.883e-03	1.023e-01

ROI	Predictor	Estimate	Std. Error	T-Statistic	pUncorrected	pFDR
	Age^2	-0.000	0.000	-3.309	1.022e-03	8.687e-03
	Neurogranin_transformed	-0.011	0.006	-1.795	7.345e-02	8.324e-02
	Sex	-0.014	0.005	-2.898	3.968e-03	1.499e-02
	APOE4 Status	-0.004	0.005	-0.944	3.456e-01	9.907e-01
	Time b/w LP and MRI	-0.001	0.001	-0.913	3.619e-01	9.473e-01
pars opercularis	Intercept	1.193	0.122	9.802	1.939e-20	4.709e-20
	Age	0.005	0.003	1.357	1.757e-01	2.671e-01
	Age^2	-0.000	0.000	-2.163	3.114e-02	5.294e-02
	Neurogranin_transformed	-0.017	0.005	-3.124	1.914e-03	4.576e-03
	Sex	-0.007	0.004	-1.492	1.365e-01	1.856e-01
	APOE4 Status	0.001	0.004	0.130	8.966e-01	9.907e-01
	Time b/w LP and MRI	0.000	0.001	0.314	7.540e-01	9.473e-01
pars orbitalis	Intercept	1.161	0.116	10.044	2.788e-21	1.053e-20
	Age	0.004	0.003	1.143	2.535e-01	3.591e-01
	Age^2	-0.000	0.000	-2.041	4.191e-02	5.937e-02
	Neurogranin_transformed	-0.016	0.005	-3.018	2.709e-03	5.757e-03
	Sex	-0.004	0.004	-0.945	3.454e-01	3.670e-01
	APOE4 Status	-0.002	0.004	-0.370	7.112e-01	9.907e-01
	Time b/w LP and MRI	0.000	0.001	0.198	8.431e-01	9.473e-01
pars triangularis	Intercept	1.148	0.120	9.539	1.548e-19	2.392e-19
	Age	0.006	0.003	1.697	9.050e-02	2.564e-01
	Age^2	-0.000	0.000	-2.631	8.859e-03	3.347e-02
	Neurogranin_transformed	-0.015	0.005	-2.819	5.059e-03	9.556e-03
	Sex	-0.004	0.004	-0.946	3.449e-01	3.670e-01
	APOE4 Status	0.000	0.004	0.060	9.521e-01	9.907e-01
	Time b/w LP and MRI	0.000	0.001	0.284	7.768e-01	9.473e-01
pericalcarine	Intercept	1.061	0.132	8.009	1.322e-14	1.450e-14
	Age	0.003	0.004	0.783	4.339e-01	5.464e-01
	Age^2	-0.000	0.000	-1.232	2.187e-01	2.479e-01
	Neurogranin_transformed	-0.006	0.006	-1.024	3.065e-01	3.158e-01
	Sex	-0.019	0.005	-3.874	1.256e-04	1.423e-03

ROI	Predictor	Estimate	Std. Error	T-Statistic	pUncorrected	pFDR
	APOE4 Status	-0.004	0.005	-0.810	4.183e-01	9.907e-01
	Time b/w LP and MRI	0.001	0.001	0.794	4.277e-01	9.473e-01
postcentral	Intercept	1.253	0.119	10.544	4.660e-23	3.169e-22
	Age	0.001	0.003	0.273	7.851e-01	8.089e-01
	Age^2	-0.000	0.000	-0.955	3.403e-01	3.506e-01
	Neurogranin_transformed	-0.013	0.005	-2.517	1.223e-02	1.733e-02
	Sex	-0.007	0.004	-1.593	1.120e-01	1.697e-01
	APOE4 Status	-0.000	0.004	-0.118	9.064e-01	9.907e-01
	Time b/w LP and MRI	0.000	0.001	0.197	8.443e-01	9.473e-01
posterior cingulate	Intercept	1.216	0.130	9.347	6.915e-19	9.404e-19
	Age	0.005	0.004	1.373	1.705e-01	2.671e-01
	Age^2	-0.000	0.000	-2.086	3.766e-02	5.567e-02
	Neurogranin_transformed	-0.015	0.006	-2.596	9.793e-03	1.559e-02
	Sex	-0.011	0.005	-2.391	1.725e-02	4.512e-02
	APOE4 Status	-0.001	0.005	-0.133	8.940e-01	9.907e-01
	Time b/w LP and MRI	-0.000	0.001	-0.420	6.751e-01	9.473e-01
precentral	Intercept	1.296	0.123	10.553	4.344e-23	3.169e-22
	Age	0.001	0.003	0.221	8.252e-01	8.252e-01
	Age^2	-0.000	0.000	-0.965	3.349e-01	3.506e-01
	Neurogranin_transformed	-0.015	0.005	-2.718	6.859e-03	1.227e-02
	Sex	-0.005	0.004	-1.220	2.231e-01	2.616e-01
	APOE4 Status	-0.001	0.004	-0.240	8.102e-01	9.907e-01
	Time b/w LP and MRI	0.000	0.001	0.521	6.027e-01	9.473e-01
precuneus	Intercept	1.172	0.133	8.796	4.506e-17	5.283e-17
	Age	0.006	0.004	1.503	1.335e-01	2.671e-01
	Age^2	-0.000	0.000	-2.314	2.116e-02	4.626e-02
	Neurogranin_transformed	-0.018	0.006	-2.996	2.909e-03	5.818e-03
	Sex	-0.013	0.005	-2.642	8.561e-03	2.646e-02
	APOE4 Status	-0.001	0.005	-0.138	8.903e-01	9.907e-01
	Time b/w LP and MRI	-0.000	0.001	-0.112	9.105e-01	9.473e-01
rostral anterior cingulate	Intercept	1.108	0.114	9.679	5.209e-20	9.839e-20

ROI	Predictor	Estimate	Std. Error	T-Statistic	pUncorrected	pFDR
	Age	0.007	0.003	2.109	3.558e-02	2.016e-01
	Age^2	-0.000	0.000	-2.927	3.627e-03	1.932e-02
	Neurogranin_transformed	-0.012	0.005	-2.392	1.723e-02	2.343e-02
	Sex	-0.006	0.004	-1.364	1.732e-01	2.265e-01
	APOE4 Status	0.004	0.004	0.870	3.848e-01	9.907e-01
	Time b/w LP and MRI	0.000	0.001	0.152	8.795e-01	9.473e-01
rostral middle frontal	Intercept	1.264	0.129	9.814	1.761e-20	4.606e-20
	Age	0.003	0.004	0.686	4.934e-01	5.785e-01
	Age^2	-0.000	0.000	-1.553	1.213e-01	1.527e-01
	Neurogranin_transformed	-0.018	0.006	-3.127	1.900e-03	4.576e-03
	Sex	-0.007	0.005	-1.580	1.150e-01	1.697e-01
	APOE4 Status	-0.000	0.005	-0.043	9.656e-01	9.907e-01
	Time b/w LP and MRI	0.001	0.001	0.808	4.198e-01	9.473e-01
superior frontal	Intercept	1.185	0.105	11.284	9.215e-26	2.168e-24
	Age	0.004	0.003	1.341	1.807e-01	2.671e-01
	Age^2	-0.000	0.000	-2.392	1.722e-02	4.504e-02
	Neurogranin_transformed	-0.016	0.005	-3.339	9.224e-04	4.501e-03
	Sex	-0.008	0.004	-2.106	3.588e-02	7.224e-02
	APOE4 Status	0.002	0.004	0.671	5.025e-01	9.907e-01
	Time b/w LP and MRI	0.000	0.001	0.224	8.228e-01	9.473e-01
superior parietal	Intercept	1.243	0.128	9.741	3.151e-20	6.696e-20
	Age	0.003	0.004	0.813	4.167e-01	5.449e-01
	Age^2	-0.000	0.000	-1.570	1.173e-01	1.527e-01
	Neurogranin_transformed	-0.018	0.006	-3.204	1.464e-03	4.576e-03
	Sex	-0.014	0.005	-3.012	2.764e-03	1.175e-02
	APOE4 Status	-0.001	0.005	-0.137	8.909e-01	9.907e-01
	Time b/w LP and MRI	0.000	0.001	0.075	9.399e-01	9.473e-01
superior temporal	Intercept	1.140	0.112	10.196	8.145e-22	3.956e-21
	Age	0.006	0.003	1.748	8.123e-02	2.511e-01
	Age^2	-0.000	0.000	-2.556	1.096e-02	3.726e-02
	Neurogranin_transformed	-0.015	0.005	-3.108	2.019e-03	4.576e-03

ROI	Predictor	Estimate	Std. Error	T-Statistic	pUncorrected	pFDR
	Sex	-0.008	0.004	-1.849	6.526e-02	1.168e-01
	APOE4 Status	-0.001	0.004	-0.298	7.661e-01	9.907e-01
	Time b/w LP and MRI	0.000	0.001	0.096	9.234e-01	9.473e-01
supramarginal	Intercept	1.191	0.126	9.462	2.833e-19	4.188e-19
	Age	0.005	0.004	1.417	1.573e-01	2.671e-01
	Age^2	-0.000	0.000	-2.206	2.795e-02	5.002e-02
	Neurogranin_transformed	-0.018	0.006	-3.300	1.057e-03	4.501e-03
	Sex	-0.011	0.005	-2.468	1.402e-02	3.972e-02
	APOE4 Status	0.000	0.004	0.012	9.907e-01	9.907e-01
	Time b/w LP and MRI	0.000	0.001	0.170	8.652e-01	9.473e-01
temporal pole	Intercept	0.876	0.121	7.265	2.027e-12	2.088e-12
	Age	0.009	0.003	2.620	9.122e-03	1.023e-01
	Age^2	-0.000	0.000	-3.368	8.328e-04	8.687e-03
	Neurogranin_transformed	-0.009	0.005	-1.659	9.784e-02	1.073e-01
	Sex	-0.006	0.004	-1.266	2.064e-01	2.599e-01
	APOE4 Status	-0.003	0.004	-0.596	5.515e-01	9.907e-01
	Time b/w LP and MRI	-0.001	0.001	-0.727	4.679e-01	9.473e-01
transverse temporal	Intercept	1.140	0.116	9.791	2.114e-20	4.792e-20
	Age	0.006	0.003	1.798	7.295e-02	2.511e-01
	Age^2	-0.000	0.000	-2.258	2.449e-02	4.626e-02
	Neurogranin_transformed	-0.017	0.005	-3.299	1.059e-03	4.501e-03
	Sex	-0.007	0.004	-1.708	8.848e-02	1.504e-01
	APOE4 Status	-0.004	0.004	-1.036	3.010e-01	9.907e-01
	Time b/w LP and MRI	0.001	0.001	0.800	4.241e-01	9.473e-01

Table C7: Estimated outputs of each linear regression model assessing the effects of CSF neurogranin on cortical-adjacent WM R1. Covariates in each model included age, sex, APOE4 status, and time between lumbar puncture and MRI. Abbreviations: neurogranin_transformed, CSF neurogranin (log-transformed); LP, lumbar puncture; MRI, magnetic resonance imaging;

pUncorrected, *p*-value uncorrected for multiple comparisons; pFDR, Benjamini-Hochberg FDR-corrected *p*-value.

Table C8: Outputs of linear regression models assessing effects of CSF NfL on cortical GM R1

ROI	Predictor	Estimate	Std. Error	T-Statistic	pUncorrected	pFDR
bankssts	Intercept	0.724	0.012	61.888	9.672e-205	2.192e-204
	Age	-0.000	0.000	-0.600	5.486e-01	8.110e-01
	NfL_transformed	-0.002	0.003	-0.731	4.651e-01	9.112e-01
	Sex	0.002	0.002	0.750	4.537e-01	8.570e-01
	APOE4 Status	0.002	0.002	0.765	4.449e-01	9.984e-01
	Time b/w LP and MRI	0.001	0.000	1.879	6.095e-02	7.970e-02
caudal anterior cingulate	Intercept	0.680	0.018	37.733	6.618e-132	7.032e-132
	Age	0.000	0.000	1.586	1.135e-01	4.824e-01
	NfL_transformed	-0.002	0.004	-0.413	6.797e-01	9.112e-01
	Sex	-0.006	0.003	-1.823	6.908e-02	7.829e-01
	APOE4 Status	0.000	0.003	0.146	8.837e-01	9.984e-01
	Time b/w LP and MRI	0.001	0.001	1.462	1.446e-01	1.695e-01
caudal middle frontal	Intercept	0.719	0.012	62.450	3.860e-206	1.010e-205
	Age	-0.000	0.000	-1.188	2.355e-01	6.846e-01
	NfL_transformed	0.002	0.003	0.578	5.635e-01	9.112e-01
	Sex	0.001	0.002	0.332	7.399e-01	9.150e-01
	APOE4 Status	0.001	0.002	0.691	4.900e-01	9.984e-01
	Time b/w LP and MRI	0.001	0.000	2.383	1.764e-02	3.332e-02
cuneus	Intercept	0.762	0.015	51.024	1.907e-175	2.401e-175
	Age	-0.000	0.000	-0.816	4.150e-01	7.426e-01
	NfL_transformed	-0.005	0.004	-1.491	1.369e-01	6.137e-01
	Sex	-0.006	0.003	-1.992	4.706e-02	7.829e-01
	APOE4 Status	-0.003	0.003	-0.990	3.227e-01	9.984e-01
	Time b/w LP and MRI	0.001	0.001	2.808	5.232e-03	2.224e-02
entorhinal	Intercept	0.772	0.028	27.283	1.019e-92	1.019e-92
	Age	-0.001	0.000	-2.385	1.756e-02	1.990e-01
	NfL_transformed	0.015	0.007	2.195	2.878e-02	4.893e-01
	Sex	0.005	0.005	0.971	3.323e-01	8.570e-01
	APOE4 Status	0.003	0.005	0.526	5.993e-01	9.984e-01
	Time b/w LP and MRI	0.001	0.001	1.288	1.987e-01	2.111e-01

ROI	Predictor	Estimate	Std. Error	T-Statistic	pUncorrected	pFDR
frontal pole	Intercept	0.682	0.013	54.132	2.761e-184	3.911e-184
	Age	-0.000	0.000	-1.009	3.138e-01	6.864e-01
	NfL_transformed	0.001	0.003	0.344	7.313e-01	9.112e-01
	Sex	-0.003	0.002	-1.386	1.666e-01	8.570e-01
	APOE4 Status	0.001	0.002	0.368	7.134e-01	9.984e-01
	Time b/w LP and MRI	0.002	0.000	3.522	4.790e-04	9.027e-03
fusiform	Intercept	0.683	0.010	67.841	4.468e-219	5.064e-218
	Age	0.000	0.000	0.083	9.338e-01	9.682e-01
	NfL_transformed	0.001	0.002	0.542	5.880e-01	9.112e-01
	Sex	0.001	0.002	0.687	4.924e-01	8.760e-01
	APOE4 Status	-0.001	0.002	-0.329	7.425e-01	9.984e-01
	Time b/w LP and MRI	0.001	0.000	2.159	3.142e-02	4.451e-02
inferior parietal	Intercept	0.726	0.012	58.790	7.920e-197	1.496e-196
	Age	-0.000	0.000	-0.383	7.021e-01	8.545e-01
	NfL_transformed	-0.004	0.003	-1.338	1.817e-01	6.178e-01
	Sex	-0.002	0.002	-0.890	3.739e-01	8.570e-01
	APOE4 Status	0.002	0.002	0.800	4.244e-01	9.984e-01
	Time b/w LP and MRI	0.001	0.000	2.639	8.657e-03	2.848e-02
inferior temporal	Intercept	0.665	0.010	65.915	1.479e-214	6.286e-214
	Age	0.000	0.000	0.490	6.244e-01	8.416e-01
	NfL_transformed	0.002	0.002	0.617	5.378e-01	9.112e-01
	Sex	0.001	0.002	0.373	7.094e-01	9.150e-01
	APOE4 Status	-0.000	0.002	-0.193	8.473e-01	9.984e-01
	Time b/w LP and MRI	0.001	0.000	2.416	1.617e-02	3.332e-02
insula	Intercept	0.651	0.010	66.726	1.795e-216	8.719e-216
	Age	0.000	0.000	3.105	2.042e-03	5.768e-02
	NfL_transformed	0.002	0.002	0.976	3.299e-01	9.112e-01
	Sex	0.001	0.002	0.560	5.759e-01	9.140e-01
	APOE4 Status	-0.001	0.002	-0.286	7.750e-01	9.984e-01
	Time b/w LP and MRI	0.001	0.000	2.471	1.389e-02	3.332e-02
isthmus cingulate	Intercept	0.733	0.015	48.084	3.026e-166	3.429e-166

ROI	Predictor	Estimate	Std. Error	T-Statistic	pUncorrected	pFDR
	Age	0.000	0.000	0.496	6.199e-01	8.416e-01
	NfL_transformed	-0.002	0.004	-0.647	5.183e-01	9.112e-01
	Sex	-0.001	0.003	-0.358	7.202e-01	9.150e-01
	APOE4 Status	0.000	0.003	0.074	9.412e-01	9.984e-01
	Time b/w LP and MRI	0.001	0.001	1.395	1.637e-01	1.855e-01
lateral occipital	Intercept	0.727	0.013	55.408	8.408e-188	1.243e-187
	Age	0.000	0.000	1.116	2.652e-01	6.846e-01
	NfL_transformed	-0.006	0.003	-1.792	7.386e-02	5.495e-01
	Sex	-0.004	0.003	-1.499	1.347e-01	8.570e-01
	APOE4 Status	-0.001	0.002	-0.259	7.961e-01	9.984e-01
	Time b/w LP and MRI	0.001	0.000	2.601	9.646e-03	2.848e-02
lateral orbitofrontal	Intercept	0.676	0.011	62.327	7.795e-206	1.893e-205
	Age	-0.000	0.000	-1.091	2.760e-01	6.846e-01
	NfL_transformed	0.004	0.003	1.585	1.139e-01	6.137e-01
	Sex	-0.002	0.002	-0.962	3.367e-01	8.570e-01
	APOE4 Status	-0.002	0.002	-0.965	3.352e-01	9.984e-01
	Time b/w LP and MRI	0.001	0.000	2.947	3.396e-03	1.649e-02
lingual	Intercept	0.723	0.013	55.606	2.430e-188	3.755e-188
	Age	-0.000	0.000	-0.257	7.972e-01	9.035e-01
	NfL_transformed	-0.002	0.003	-0.534	5.933e-01	9.112e-01
	Sex	-0.001	0.002	-0.279	7.804e-01	9.150e-01
	APOE4 Status	-0.000	0.002	-0.131	8.957e-01	9.984e-01
	Time b/w LP and MRI	0.001	0.000	2.389	1.735e-02	3.332e-02
medial orbitofrontal	Intercept	0.639	0.010	64.052	9.574e-210	3.255e-209
	Age	0.000	0.000	0.610	5.425e-01	8.110e-01
	NfL_transformed	0.004	0.002	1.751	8.081e-02	5.495e-01
	Sex	-0.002	0.002	-0.849	3.962e-01	8.570e-01
	APOE4 Status	-0.001	0.002	-0.701	4.837e-01	9.984e-01
	Time b/w LP and MRI	0.001	0.000	2.716	6.897e-03	2.606e-02
middle temporal	Intercept	0.679	0.009	72.631	7.343e-230	2.497e-228
	Age	0.000	0.000	0.836	4.039e-01	7.426e-01

ROI	Predictor	Estimate	Std. Error	T-Statistic	pUncorrected	pFDR
	NfL_transformed	-0.000	0.002	-0.045	9.644e-01	9.644e-01
	Sex	0.000	0.002	0.037	9.703e-01	9.703e-01
	APOE4 Status	0.000	0.002	0.008	9.939e-01	9.984e-01
	Time b/w LP and MRI	0.001	0.000	2.977	3.087e-03	1.649e-02
paracentral	Intercept	0.761	0.013	59.507	2.204e-198	4.408e-198
	Age	-0.000	0.000	-0.365	7.151e-01	8.545e-01
	NfL_transformed	-0.001	0.003	-0.248	8.040e-01	9.112e-01
	Sex	0.002	0.002	0.651	5.153e-01	8.760e-01
	APOE4 Status	-0.000	0.002	-0.140	8.888e-01	9.984e-01
	Time b/w LP and MRI	0.000	0.000	0.648	5.175e-01	5.175e-01
parahippocampal	Intercept	0.639	0.013	50.782	9.646e-175	1.171e-174
	Age	0.000	0.000	1.078	2.819e-01	6.846e-01
	NfL_transformed	0.008	0.003	2.668	7.945e-03	2.701e-01
	Sex	0.003	0.002	1.165	2.446e-01	8.570e-01
	APOE4 Status	-0.002	0.002	-0.869	3.856e-01	9.984e-01
	Time b/w LP and MRI	0.001	0.000	2.171	3.055e-02	4.451e-02
pars opercularis	Intercept	0.700	0.010	67.713	8.899e-219	7.564e-218
	Age	0.000	0.000	0.629	5.298e-01	8.110e-01
	NfL_transformed	0.001	0.003	0.364	7.163e-01	9.112e-01
	Sex	-0.001	0.002	-0.404	6.863e-01	9.150e-01
	APOE4 Status	-0.000	0.002	-0.002	9.984e-01	9.984e-01
	Time b/w LP and MRI	0.001	0.000	2.300	2.199e-02	3.738e-02
pars orbitalis	Intercept	0.693	0.011	62.662	1.146e-206	3.474e-206
	Age	-0.000	0.000	-0.040	9.682e-01	9.682e-01
	NfL_transformed	0.001	0.003	0.259	7.959e-01	9.112e-01
	Sex	-0.002	0.002	-0.859	3.910e-01	8.570e-01
	APOE4 Status	-0.001	0.002	-0.421	6.739e-01	9.984e-01
	Time b/w LP and MRI	0.001	0.000	3.171	1.639e-03	1.393e-02
pars triangularis	Intercept	0.704	0.011	66.946	5.457e-217	3.092e-216
	Age	-0.000	0.000	-0.124	9.011e-01	9.682e-01
	NfL_transformed	0.001	0.003	0.266	7.905e-01	9.112e-01

ROI	Predictor	Estimate	Std. Error	T-Statistic	pUncorrected	pFDR
	Sex	-0.002	0.002	-0.979	3.281e-01	8.570e-01
	APOE4 Status	-0.000	0.002	-0.054	9.567e-01	9.984e-01
	Time b/w LP and MRI	0.001	0.000	3.288	1.099e-03	1.246e-02
pericalcarine	Intercept	0.744	0.016	46.538	5.755e-162	6.312e-162
	Age	0.000	0.000	0.604	5.459e-01	8.110e-01
	NfL_transformed	-0.005	0.004	-1.178	2.393e-01	7.397e-01
	Sex	-0.006	0.003	-2.003	4.590e-02	7.829e-01
	APOE4 Status	-0.001	0.003	-0.336	7.372e-01	9.984e-01
	Time b/w LP and MRI	0.001	0.001	2.481	1.351e-02	3.332e-02
postcentral	Intercept	0.739	0.012	59.842	1.499e-199	3.185e-199
	Age	0.000	0.000	0.990	3.230e-01	6.864e-01
	NfL_transformed	-0.002	0.003	-0.647	5.178e-01	9.112e-01
	Sex	0.000	0.002	0.150	8.810e-01	9.150e-01
	APOE4 Status	-0.000	0.002	-0.110	9.127e-01	9.984e-01
	Time b/w LP and MRI	0.001	0.000	1.850	6.509e-02	8.197e-02
posterior cingulate	Intercept	0.714	0.022	32.371	1.549e-111	1.596e-111
	Age	0.000	0.000	1.373	1.706e-01	6.445e-01
	NfL_transformed	-0.001	0.005	-0.101	9.196e-01	9.623e-01
	Sex	-0.001	0.004	-0.174	8.620e-01	9.150e-01
	APOE4 Status	0.001	0.004	0.139	8.893e-01	9.984e-01
	Time b/w LP and MRI	0.001	0.001	0.949	3.430e-01	3.534e-01
precentral	Intercept	0.761	0.013	58.557	3.212e-196	5.460e-196
	Age	-0.000	0.000	-0.463	6.436e-01	8.416e-01
	NfL_transformed	0.001	0.003	0.165	8.692e-01	9.533e-01
	Sex	0.002	0.002	0.790	4.299e-01	8.570e-01
	APOE4 Status	0.001	0.002	0.291	7.711e-01	9.984e-01
	Time b/w LP and MRI	0.001	0.000	2.031	4.289e-02	5.833e-02
precuneus	Intercept	0.731	0.012	58.636	1.997e-196	3.574e-196
	Age	-0.000	0.000	-0.929	3.532e-01	7.064e-01
	NfL_transformed	-0.002	0.003	-0.825	4.100e-01	9.112e-01
	Sex	-0.001	0.002	-0.314	7.539e-01	9.150e-01

ROI	Predictor	Estimate	Std. Error	T-Statistic	pUncorrected	pFDR
	APOE4 Status	-0.000	0.002	-0.028	9.774e-01	9.984e-01
	Time b/w LP and MRI	0.001	0.000	2.587	1.005e-02	2.848e-02
rostral anterior cingulate	Intercept	0.624	0.012	51.559	9.727e-177	1.272e-176
	Age	0.000	0.000	1.876	6.136e-02	4.507e-01
	NfL_transformed	0.006	0.003	1.924	5.513e-02	5.495e-01
	Sex	0.001	0.002	0.537	5.914e-01	9.140e-01
	APOE4 Status	0.002	0.002	0.723	4.699e-01	9.984e-01
	Time b/w LP and MRI	0.001	0.000	1.466	1.435e-01	1.695e-01
rostral middle frontal	Intercept	0.704	0.011	62.650	1.226e-206	3.474e-206
	Age	-0.000	0.000	-1.685	9.279e-02	4.507e-01
	NfL_transformed	0.001	0.003	0.379	7.051e-01	9.112e-01
	Sex	-0.002	0.002	-1.151	2.504e-01	8.570e-01
	APOE4 Status	0.002	0.002	0.771	4.414e-01	9.984e-01
	Time b/w LP and MRI	0.001	0.000	3.493	5.310e-04	9.027e-03
superior frontal	Intercept	0.705	0.010	67.801	1.246e-218	8.473e-218
	Age	-0.000	0.000	-1.259	2.087e-01	6.846e-01
	NfL_transformed	0.002	0.003	0.641	5.218e-01	9.112e-01
	Sex	0.001	0.002	0.394	6.936e-01	9.150e-01
	APOE4 Status	0.001	0.002	0.336	7.371e-01	9.984e-01
	Time b/w LP and MRI	0.001	0.000	2.217	2.717e-02	4.199e-02
superior parietal	Intercept	0.743	0.013	58.463	5.685e-196	9.204e-196
	Age	-0.000	0.000	-0.347	7.288e-01	8.545e-01
	NfL_transformed	-0.005	0.003	-1.462	1.444e-01	6.137e-01
	Sex	-0.002	0.002	-0.787	4.319e-01	8.570e-01
	APOE4 Status	0.000	0.002	0.204	8.385e-01	9.984e-01
	Time b/w LP and MRI	0.001	0.000	2.258	2.451e-02	3.968e-02
superior temporal	Intercept	0.702	0.010	68.179	7.403e-220	1.259e-218
	Age	0.000	0.000	1.694	9.097e-02	4.507e-01
	NfL_transformed	-0.001	0.002	-0.331	7.411e-01	9.112e-01
	Sex	-0.000	0.002	-0.141	8.881e-01	9.150e-01
	APOE4 Status	-0.001	0.002	-0.506	6.131e-01	9.984e-01

ROI	Predictor	Estimate	Std. Error	T-Statistic	pUncorrected	pFDR
	Time b/w LP and MRI	0.001	0.000	2.432	1.544e-02	3.332e-02
supramarginal	Intercept	0.715	0.011	65.035	1.871e-212	7.068e-212
	Age	0.000	0.000	0.060	9.525e-01	9.682e-01
	NfL_transformed	-0.002	0.003	-0.647	5.178e-01	9.112e-01
	Sex	-0.002	0.002	-0.751	4.530e-01	8.570e-01
	APOE4 Status	0.001	0.002	0.332	7.398e-01	9.984e-01
	Time b/w LP and MRI	0.001	0.000	2.305	2.168e-02	3.738e-02
temporal pole	Intercept	0.631	0.013	49.146	6.537e-170	7.664e-170
	Age	0.001	0.000	2.948	3.393e-03	5.768e-02
	NfL_transformed	0.004	0.003	1.388	1.659e-01	6.178e-01
	Sex	0.002	0.002	0.991	3.222e-01	8.570e-01
	APOE4 Status	-0.002	0.002	-1.041	2.986e-01	9.984e-01
	Time b/w LP and MRI	0.001	0.000	1.371	1.710e-01	1.875e-01
transverse temporal	Intercept	0.765	0.014	52.773	1.809e-180	2.460e-180
	Age	0.000	0.000	1.839	6.668e-02	4.507e-01
	NfL_transformed	0.000	0.004	0.083	9.340e-01	9.623e-01
	Sex	-0.001	0.003	-0.206	8.370e-01	9.150e-01
	APOE4 Status	-0.003	0.003	-0.981	3.274e-01	9.984e-01
	Time b/w LP and MRI	0.002	0.001	2.996	2.910e-03	1.649e-02

Table C8: Estimated outputs of each linear regression model assessing the effects of CSF NfL on cortical GM R1. Covariates in each model included age, sex, APOE4 status, and time between lumbar puncture and MRI. Abbreviations: NfL_transformed, CSF neurofilament light chain protein (log-transformed); LP, lumbar puncture; MRI, magnetic resonance imaging; pUncorrected, *p*-value uncorrected for multiple comparisons; pFDR, Benjamini-Hochberg FDR-corrected *p*-value.

Table C9: Outputs of linear regression models assessing effects of CSF NfL on cortical-adjacent WM R1

ROI	Predictor	Estimate	Std. Error	T-Statistic	pUncorrected	pFDR
bankssts	Intercept	1.095	0.118	9.260	1.349e-18	2.184e-18
	Age	0.007	0.004	1.886	6.002e-02	1.570e-01
	Age^2	-0.000	0.000	-2.534	1.166e-02	2.308e-02
	NfL_transformed	-0.015	0.006	-2.476	1.372e-02	1.022e-01
	Sex	-0.015	0.005	-3.241	1.291e-03	3.376e-03
	APOE4 Status	-0.001	0.004	-0.213	8.312e-01	9.593e-01
	Time b/w LP and MRI	-0.000	0.001	-0.458	6.470e-01	9.947e-01
caudal anterior cingulate	Intercept	1.036	0.111	9.348	6.917e-19	1.470e-18
	Age	0.009	0.003	2.688	7.500e-03	6.375e-02
	Age^2	-0.000	0.000	-3.590	3.723e-04	5.091e-03
	NfL_transformed	-0.005	0.006	-0.873	3.830e-01	4.069e-01
	Sex	-0.018	0.004	-4.142	4.212e-05	2.864e-04
	APOE4 Status	0.005	0.004	1.297	1.952e-01	9.585e-01
	Time b/w LP and MRI	-0.000	0.001	-0.270	7.876e-01	9.947e-01
caudal middle frontal	Intercept	1.186	0.121	9.776	2.396e-20	1.015e-19
	Age	0.003	0.004	0.867	3.862e-01	4.528e-01
	Age^2	-0.000	0.000	-1.620	1.061e-01	1.244e-01
	NfL_transformed	-0.014	0.006	-2.372	1.817e-02	1.022e-01
	Sex	-0.008	0.005	-1.680	9.385e-02	9.972e-02
	APOE4 Status	-0.002	0.004	-0.456	6.485e-01	9.585e-01
	Time b/w LP and MRI	0.000	0.001	0.454	6.499e-01	9.947e-01
cuneus	Intercept	1.116	0.116	9.642	6.878e-20	1.949e-19
	Age	0.002	0.003	0.522	6.020e-01	6.244e-01
	Age^2	-0.000	0.000	-1.016	3.104e-01	3.104e-01
	NfL_transformed	-0.007	0.006	-1.268	2.055e-01	2.462e-01
	Sex	-0.025	0.005	-5.529	5.880e-08	9.996e-07
	APOE4 Status	-0.003	0.004	-0.691	4.902e-01	9.585e-01
	Time b/w LP and MRI	0.000	0.001	0.293	7.698e-01	9.947e-01

ROI	Predictor	Estimate	Std. Error	T-Statistic	pUncorrected	pFDR
entorhinal	Intercept	0.659	0.122	5.400	1.158e-07	1.158e-07
	Age	0.015	0.004	4.230	2.914e-05	9.908e-04
	Age^2	-0.000	0.000	-5.092	5.518e-07	1.876e-05
	NfL_transformed	-0.007	0.006	-1.217	2.245e-01	2.462e-01
	Sex	-0.011	0.005	-2.257	2.459e-02	3.389e-02
	APOE4 Status	-0.002	0.005	-0.374	7.085e-01	9.585e-01
	Time b/w LP and MRI	-0.000	0.001	-0.441	6.593e-01	9.947e-01
frontal pole	Intercept	0.978	0.120	8.126	5.832e-15	6.610e-15
	Age	0.007	0.004	1.808	7.132e-02	1.590e-01
	Age^2	-0.000	0.000	-2.563	1.074e-02	2.308e-02
	NfL_transformed	-0.015	0.006	-2.518	1.221e-02	1.022e-01
	Sex	-0.005	0.005	-1.058	2.905e-01	2.905e-01
	APOE4 Status	-0.004	0.004	-0.923	3.564e-01	9.585e-01
	Time b/w LP and MRI	0.000	0.001	0.010	9.919e-01	9.947e-01
fusiform	Intercept	1.033	0.112	9.262	1.329e-18	2.184e-18
	Age	0.007	0.003	2.244	2.540e-02	1.234e-01
	Age^2	-0.000	0.000	-3.134	1.851e-03	9.836e-03
	NfL_transformed	-0.012	0.006	-2.097	3.664e-02	1.022e-01
	Sex	-0.011	0.004	-2.467	1.406e-02	2.304e-02
	APOE4 Status	-0.002	0.004	-0.454	6.504e-01	9.585e-01
	Time b/w LP and MRI	-0.001	0.001	-0.796	4.265e-01	9.947e-01
inferior parietal	Intercept	1.082	0.122	8.843	3.180e-17	4.325e-17
	Age	0.006	0.004	1.681	9.365e-02	1.590e-01
	Age^2	-0.000	0.000	-2.384	1.759e-02	2.848e-02
	NfL_transformed	-0.015	0.006	-2.415	1.620e-02	1.022e-01
	Sex	-0.022	0.005	-4.540	7.505e-06	8.506e-05
	APOE4 Status	-0.001	0.005	-0.158	8.747e-01	9.593e-01
	Time b/w LP and MRI	0.000	0.001	0.021	9.833e-01	9.947e-01
inferior temporal	Intercept	1.047	0.104	10.039	2.917e-21	1.653e-20
	Age	0.006	0.003	2.043	4.169e-02	1.404e-01
	Age^2	-0.000	0.000	-2.952	3.342e-03	1.420e-02

ROI	Predictor	Estimate	Std. Error	T-Statistic	pUncorrected	pFDR
	NfL_transformed	-0.010	0.005	-1.925	5.497e-02	1.051e-01
	Sex	-0.012	0.004	-3.015	2.741e-03	6.213e-03
	APOE4 Status	-0.000	0.004	-0.109	9.130e-01	9.701e-01
	Time b/w LP and MRI	-0.001	0.001	-0.927	3.547e-01	9.947e-01
insula	Intercept	1.030	0.106	9.705	4.208e-20	1.431e-19
	Age	0.005	0.003	1.686	9.250e-02	1.590e-01
	Age^2	-0.000	0.000	-2.268	2.387e-02	3.382e-02
	NfL_transformed	-0.009	0.005	-1.687	9.237e-02	1.341e-01
	Sex	-0.011	0.004	-2.729	6.638e-03	1.328e-02
	APOE4 Status	0.000	0.004	0.030	9.760e-01	9.760e-01
	Time b/w LP and MRI	-0.000	0.001	-0.152	8.789e-01	9.947e-01
isthmus cingulate	Intercept	1.077	0.128	8.440	6.144e-16	7.461e-16
	Age	0.008	0.004	2.101	3.624e-02	1.369e-01
	Age^2	-0.000	0.000	-2.636	8.714e-03	2.308e-02
	NfL_transformed	-0.012	0.006	-1.873	6.184e-02	1.051e-01
	Sex	-0.020	0.005	-3.967	8.663e-05	4.909e-04
	APOE4 Status	-0.002	0.005	-0.337	7.360e-01	9.585e-01
	Time b/w LP and MRI	-0.000	0.001	-0.403	6.874e-01	9.947e-01
lateral occipital	Intercept	1.119	0.108	10.333	2.654e-22	2.478e-21
	Age	0.004	0.003	1.172	2.419e-01	3.163e-01
	Age^2	-0.000	0.000	-1.725	8.528e-02	1.036e-01
	NfL_transformed	-0.016	0.005	-3.006	2.818e-03	9.581e-02
	Sex	-0.024	0.004	-5.761	1.690e-08	5.746e-07
	APOE4 Status	-0.004	0.004	-0.899	3.693e-01	9.585e-01
	Time b/w LP and MRI	-0.000	0.001	-0.085	9.324e-01	9.947e-01
lateral orbitofrontal	Intercept	1.000	0.116	8.590	2.062e-16	2.597e-16
	Age	0.008	0.003	2.408	1.650e-02	1.122e-01
	Age^2	-0.000	0.000	-3.360	8.552e-04	5.815e-03
	NfL_transformed	-0.011	0.006	-1.875	6.159e-02	1.051e-01
	Sex	-0.008	0.005	-1.809	7.122e-02	8.127e-02
	APOE4 Status	-0.000	0.004	-0.039	9.690e-01	9.760e-01

ROI	Predictor	Estimate	Std. Error	T-Statistic	pUncorrected	pFDR
	Time b/w LP and MRI	0.000	0.001	0.109	9.135e-01	9.947e-01
lingual	Intercept	1.064	0.114	9.291	1.062e-18	1.900e-18
	Age	0.004	0.003	1.176	2.403e-01	3.163e-01
	Age^2	-0.000	0.000	-1.787	7.476e-02	9.414e-02
	NfL_transformed	-0.007	0.006	-1.226	2.209e-01	2.462e-01
	Sex	-0.019	0.004	-4.210	3.168e-05	2.693e-04
	APOE4 Status	-0.004	0.004	-1.055	2.919e-01	9.585e-01
	Time b/w LP and MRI	0.000	0.001	0.126	8.999e-01	9.947e-01
medial orbitofrontal	Intercept	1.032	0.117	8.833	3.418e-17	4.470e-17
	Age	0.006	0.003	1.712	8.773e-02	1.590e-01
	Age^2	-0.000	0.000	-2.661	8.120e-03	2.308e-02
	NfL_transformed	-0.008	0.006	-1.327	1.854e-01	2.361e-01
	Sex	-0.010	0.005	-2.251	2.492e-02	3.389e-02
	APOE4 Status	-0.001	0.004	-0.339	7.350e-01	9.585e-01
	Time b/w LP and MRI	0.000	0.001	0.237	8.126e-01	9.947e-01
middle temporal	Intercept	1.098	0.108	10.164	1.056e-21	7.181e-21
	Age	0.005	0.003	1.649	9.998e-02	1.590e-01
	Age^2	-0.000	0.000	-2.554	1.102e-02	2.308e-02
	NfL_transformed	-0.011	0.005	-2.070	3.909e-02	1.022e-01
	Sex	-0.015	0.004	-3.629	3.218e-04	1.216e-03
	APOE4 Status	-0.002	0.004	-0.497	6.198e-01	9.585e-01
	Time b/w LP and MRI	-0.000	0.001	-0.327	7.438e-01	9.947e-01
paracentral	Intercept	1.197	0.123	9.770	2.503e-20	1.015e-19
	Age	0.003	0.004	0.727	4.677e-01	5.130e-01
	Age^2	-0.000	0.000	-1.385	1.668e-01	1.890e-01
	NfL_transformed	-0.013	0.006	-2.124	3.431e-02	1.022e-01
	Sex	-0.010	0.005	-2.064	3.963e-02	5.182e-02
	APOE4 Status	-0.002	0.005	-0.379	7.050e-01	9.585e-01
	Time b/w LP and MRI	-0.000	0.001	-0.471	6.381e-01	9.947e-01
parahippocampal	Intercept	0.915	0.127	7.227	2.584e-12	2.745e-12
	Age	0.010	0.004	2.773	5.827e-03	6.375e-02

ROI	Predictor	Estimate	Std. Error	T-Statistic	pUncorrected	pFDR
	Age^2	-0.000	0.000	-3.460	5.989e-04	5.091e-03
	NfL_transformed	-0.008	0.006	-1.320	1.875e-01	2.361e-01
	Sex	-0.017	0.005	-3.384	7.849e-04	2.424e-03
	APOE4 Status	-0.005	0.005	-1.123	2.620e-01	9.585e-01
	Time b/w LP and MRI	-0.001	0.001	-1.078	2.818e-01	9.947e-01
pars opercularis	Intercept	1.100	0.117	9.421	3.877e-19	9.486e-19
	Age	0.006	0.003	1.669	9.590e-02	1.590e-01
	Age^2	-0.000	0.000	-2.411	1.638e-02	2.785e-02
	NfL_transformed	-0.013	0.006	-2.305	2.166e-02	1.022e-01
	Sex	-0.011	0.005	-2.462	1.423e-02	2.304e-02
	APOE4 Status	-0.001	0.004	-0.190	8.493e-01	9.593e-01
	Time b/w LP and MRI	-0.000	0.001	-0.021	9.835e-01	9.947e-01
pars orbitalis	Intercept	1.072	0.111	9.652	6.396e-20	1.949e-19
	Age	0.005	0.003	1.425	1.549e-01	2.194e-01
	Age^2	-0.000	0.000	-2.274	2.348e-02	3.382e-02
	NfL_transformed	-0.011	0.006	-1.923	5.526e-02	1.051e-01
	Sex	-0.008	0.004	-1.806	7.171e-02	8.127e-02
	APOE4 Status	-0.003	0.004	-0.660	5.095e-01	9.585e-01
	Time b/w LP and MRI	-0.000	0.001	-0.062	9.508e-01	9.947e-01
pars triangularis	Intercept	1.061	0.116	9.178	2.532e-18	3.913e-18
	Age	0.007	0.003	1.952	5.165e-02	1.463e-01
	Age^2	-0.000	0.000	-2.845	4.672e-03	1.765e-02
	NfL_transformed	-0.010	0.006	-1.747	8.136e-02	1.257e-01
	Sex	-0.008	0.005	-1.741	8.242e-02	9.040e-02
	APOE4 Status	-0.001	0.004	-0.214	8.303e-01	9.593e-01
	Time b/w LP and MRI	0.000	0.001	0.037	9.708e-01	9.947e-01
pericalcarine	Intercept	1.016	0.127	8.023	1.203e-14	1.319e-14
	Age	0.003	0.004	0.828	4.082e-01	4.626e-01
	Age^2	-0.000	0.000	-1.304	1.932e-01	2.119e-01
	NfL_transformed	0.001	0.006	0.102	9.187e-01	9.187e-01
	Sex	-0.019	0.005	-3.846	1.398e-04	5.941e-04

ROI	Predictor	Estimate	Std. Error	T-Statistic	pUncorrected	pFDR
	APOE4 Status	-0.004	0.005	-0.907	3.650e-01	9.585e-01
	Time b/w LP and MRI	0.001	0.001	0.820	4.129e-01	9.947e-01
postcentral	Intercept	1.178	0.114	10.353	2.257e-22	2.478e-21
	Age	0.002	0.003	0.515	6.072e-01	6.244e-01
	Age^2	-0.000	0.000	-1.153	2.496e-01	2.572e-01
	NfL_transformed	-0.009	0.006	-1.675	9.469e-02	1.341e-01
	Sex	-0.010	0.004	-2.301	2.191e-02	3.239e-02
	APOE4 Status	-0.001	0.004	-0.354	7.237e-01	9.585e-01
	Time b/w LP and MRI	-0.000	0.001	-0.007	9.947e-01	9.947e-01
posterior cingulate	Intercept	1.135	0.125	9.112	4.203e-18	6.213e-18
	Age	0.006	0.004	1.635	1.029e-01	1.590e-01
	Age^2	-0.000	0.000	-2.294	2.232e-02	3.382e-02
	NfL_transformed	-0.012	0.006	-1.965	5.006e-02	1.051e-01
	Sex	-0.016	0.005	-3.176	1.608e-03	3.905e-03
	APOE4 Status	-0.002	0.005	-0.381	7.037e-01	9.585e-01
	Time b/w LP and MRI	-0.001	0.001	-0.662	5.083e-01	9.947e-01
precentral	Intercept	1.215	0.118	10.322	2.915e-22	2.478e-21
	Age	0.002	0.004	0.490	6.244e-01	6.244e-01
	Age^2	-0.000	0.000	-1.181	2.382e-01	2.531e-01
	NfL_transformed	-0.011	0.006	-1.918	5.577e-02	1.051e-01
	Sex	-0.009	0.005	-2.029	4.318e-02	5.437e-02
	APOE4 Status	-0.002	0.004	-0.499	6.183e-01	9.585e-01
	Time b/w LP and MRI	0.000	0.001	0.278	7.811e-01	9.947e-01
precuneus	Intercept	1.076	0.128	8.423	6.962e-16	8.162e-16
	Age	0.007	0.004	1.795	7.339e-02	1.590e-01
	Age^2	-0.000	0.000	-2.547	1.124e-02	2.308e-02
	NfL_transformed	-0.014	0.006	-2.206	2.794e-02	1.022e-01
	Sex	-0.018	0.005	-3.525	4.737e-04	1.611e-03
	APOE4 Status	-0.002	0.005	-0.431	6.664e-01	9.585e-01
	Time b/w LP and MRI	-0.000	0.001	-0.389	6.976e-01	9.947e-01
rostral anterior cingulate	Intercept	1.035	0.110	9.422	3.906e-19	9.486e-19

ROI	Predictor	Estimate	Std. Error	T-Statistic	pUncorrected	pFDR
	Age	0.008	0.003	2.309	2.148e-02	1.217e-01
	Age^2	-0.000	0.000	-3.107	2.025e-03	9.836e-03
	NfL_transformed	-0.007	0.005	-1.254	2.106e-01	2.462e-01
	Sex	-0.008	0.004	-1.960	5.069e-02	6.155e-02
	APOE4 Status	0.003	0.004	0.651	5.154e-01	9.585e-01
	Time b/w LP and MRI	0.000	0.001	0.009	9.926e-01	9.947e-01
rostral middle frontal	Intercept	1.161	0.124	9.379	5.400e-19	1.224e-18
	Age	0.004	0.004	0.991	3.222e-01	3.912e-01
	Age^2	-0.000	0.000	-1.805	7.187e-02	9.398e-02
	NfL_transformed	-0.012	0.006	-2.011	4.502e-02	1.051e-01
	Sex	-0.012	0.005	-2.445	1.492e-02	2.306e-02
	APOE4 Status	-0.002	0.005	-0.358	7.202e-01	9.585e-01
	Time b/w LP and MRI	0.000	0.001	0.491	6.235e-01	9.947e-01
superior frontal	Intercept	1.088	0.101	10.743	9.035e-24	3.072e-22
	Age	0.005	0.003	1.602	1.100e-01	1.626e-01
	Age^2	-0.000	0.000	-2.630	8.874e-03	2.308e-02
	NfL_transformed	-0.007	0.005	-1.468	1.430e-01	1.945e-01
	Sex	-0.011	0.004	-2.824	4.988e-03	1.060e-02
	APOE4 Status	0.001	0.004	0.360	7.191e-01	9.585e-01
	Time b/w LP and MRI	0.000	0.001	0.052	9.583e-01	9.947e-01
superior parietal	Intercept	1.142	0.123	9.315	8.853e-19	1.672e-18
	Age	0.004	0.004	1.114	2.658e-01	3.347e-01
	Age^2	-0.000	0.000	-1.815	7.030e-02	9.398e-02
	NfL_transformed	-0.013	0.006	-2.144	3.265e-02	1.022e-01
	Sex	-0.019	0.005	-3.865	1.300e-04	5.941e-04
	APOE4 Status	-0.002	0.005	-0.451	6.523e-01	9.585e-01
	Time b/w LP and MRI	-0.000	0.001	-0.188	8.513e-01	9.947e-01
superior temporal	Intercept	1.050	0.108	9.761	2.688e-20	1.015e-19
	Age	0.006	0.003	2.007	4.543e-02	1.404e-01
	Age^2	-0.000	0.000	-2.779	5.716e-03	1.943e-02
	NfL_transformed	-0.009	0.005	-1.759	7.931e-02	1.257e-01

ROI	Predictor	Estimate	Std. Error	T-Statistic	pUncorrected	pFDR
	Sex	-0.011	0.004	-2.642	8.574e-03	1.534e-02
	APOE4 Status	-0.002	0.004	-0.586	5.579e-01	9.585e-01
	Time b/w LP and MRI	-0.000	0.001	-0.121	9.038e-01	9.947e-01
supramarginal	Intercept	1.087	0.121	8.975	1.180e-17	1.672e-17
	Age	0.006	0.004	1.716	8.687e-02	1.590e-01
	Age^2	-0.000	0.000	-2.454	1.456e-02	2.605e-02
	NfL_transformed	-0.013	0.006	-2.113	3.523e-02	1.022e-01
	Sex	-0.016	0.005	-3.360	8.554e-04	2.424e-03
	APOE4 Status	-0.001	0.004	-0.304	7.612e-01	9.585e-01
	Time b/w LP and MRI	-0.000	0.001	-0.094	9.254e-01	9.947e-01
temporal pole	Intercept	0.813	0.116	7.038	8.738e-12	9.003e-12
	Age	0.009	0.003	2.701	7.219e-03	6.375e-02
	Age^2	-0.000	0.000	-3.479	5.588e-04	5.091e-03
	NfL_transformed	-0.001	0.006	-0.110	9.129e-01	9.187e-01
	Sex	-0.007	0.005	-1.443	1.498e-01	1.543e-01
	APOE4 Status	-0.003	0.004	-0.762	4.464e-01	9.585e-01
	Time b/w LP and MRI	-0.001	0.001	-0.707	4.802e-01	9.947e-01
transverse temporal	Intercept	1.044	0.112	9.322	8.391e-19	1.672e-18
	Age	0.007	0.003	2.110	3.550e-02	1.369e-01
	Age^2	-0.000	0.000	-2.517	1.222e-02	2.308e-02
	NfL_transformed	-0.012	0.006	-2.193	2.888e-02	1.022e-01
	Sex	-0.012	0.004	-2.646	8.476e-03	1.534e-02
	APOE4 Status	-0.006	0.004	-1.361	1.743e-01	9.585e-01
	Time b/w LP and MRI	0.000	0.001	0.512	6.093e-01	9.947e-01

Table C9: Estimated outputs of each linear regression model assessing the effects of CSF NfL on cortical-adjacent WM R1. Covariates in each model included age, sex, APOE4 status, and time between lumbar puncture and MRI. Abbreviations: NfL_transformed, CSF neurofilament light chain protein (log-transformed); LP, lumbar puncture; MRI, magnetic resonance imaging;

pUncorrected, *p*-value uncorrected for multiple comparisons; pFDR, Benjamini-Hochberg FDR-corrected *p*-value.

Table C10: Outputs of linear regression models assessing effects of CSF tTau on cortical GM R1

ROI	Predictor	Estimate	Std. Error	T-Statistic	pUncorrected	pFDR
bankssts	Intercept	0.746	0.016	47.950	2.634e-166	6.397e-166
	Age	-0.000	0.000	-0.366	7.142e-01	8.484e-01
	tTau_transformed	-0.007	0.003	-2.163	3.114e-02	7.058e-02
	Sex	0.002	0.002	1.030	3.038e-01	9.878e-01
	APOE4 Status	0.002	0.002	1.119	2.640e-01	9.912e-01
	Time b/w LP and MRI	0.001	0.000	1.843	6.609e-02	8.807e-02
caudal anterior cingulate	Intercept	0.704	0.024	28.999	3.562e-99	3.785e-99
	Age	0.000	0.000	2.044	4.159e-02	2.020e-01
	tTau_transformed	-0.007	0.005	-1.451	1.476e-01	2.281e-01
	Sex	-0.006	0.003	-1.782	7.559e-02	9.316e-01
	APOE4 Status	0.001	0.003	0.371	7.111e-01	9.912e-01
	Time b/w LP and MRI	0.001	0.001	1.481	1.395e-01	1.694e-01
caudal middle frontal	Intercept	0.746	0.015	48.609	2.662e-168	7.542e-168
	Age	-0.000	0.000	-0.354	7.236e-01	8.484e-01
	tTau_transformed	-0.005	0.003	-1.798	7.287e-02	1.304e-01
	Sex	0.000	0.002	0.191	8.488e-01	9.878e-01
	APOE4 Status	0.002	0.002	0.955	3.402e-01	9.912e-01
	Time b/w LP and MRI	0.001	0.000	2.206	2.794e-02	4.967e-02
cuneus	Intercept	0.789	0.020	39.835	4.604e-140	6.021e-140
	Age	-0.000	0.000	-0.963	3.359e-01	6.534e-01
	tTau_transformed	-0.010	0.004	-2.544	1.134e-02	5.474e-02
	Sex	-0.004	0.003	-1.632	1.035e-01	9.316e-01
	APOE4 Status	-0.002	0.003	-0.566	5.715e-01	9.912e-01
	Time b/w LP and MRI	0.001	0.001	2.858	4.484e-03	2.247e-02
entorhinal	Intercept	0.824	0.038	21.650	5.424e-69	5.424e-69
	Age	-0.000	0.000	-1.138	2.559e-01	5.800e-01
	tTau_transformed	-0.003	0.007	-0.428	6.686e-01	7.333e-01
	Sex	0.002	0.005	0.379	7.046e-01	9.878e-01
	APOE4 Status	0.003	0.005	0.586	5.585e-01	9.912e-01
	Time b/w LP and MRI	0.001	0.001	0.961	3.369e-01	3.580e-01

ROI	Predictor	Estimate	Std. Error	T-Statistic	pUncorrected	pFDR
frontal pole	Intercept	0.717	0.017	42.846	3.550e-150	5.029e-150
	Age	-0.000	0.000	-0.105	9.167e-01	9.449e-01
	tTau_transformed	-0.008	0.003	-2.360	1.878e-02	5.805e-02
	Sex	-0.004	0.002	-1.524	1.282e-01	9.316e-01
	APOE4 Status	0.002	0.002	0.750	4.539e-01	9.912e-01
	Time b/w LP and MRI	0.001	0.000	3.340	9.173e-04	1.693e-02
fusiform	Intercept	0.694	0.013	51.619	3.603e-177	1.750e-176
	Age	0.000	0.000	0.667	5.053e-01	7.045e-01
	tTau_transformed	-0.002	0.003	-0.715	4.750e-01	6.043e-01
	Sex	0.001	0.002	0.550	5.828e-01	9.878e-01
	APOE4 Status	-0.000	0.002	-0.191	8.489e-01	9.912e-01
	Time b/w LP and MRI	0.001	0.000	2.057	4.038e-02	5.969e-02
inferior parietal	Intercept	0.760	0.016	46.478	8.826e-162	1.876e-161
	Age	-0.000	0.000	-0.104	9.171e-01	9.449e-01
	tTau_transformed	-0.011	0.003	-3.275	1.149e-03	3.108e-02
	Sex	-0.001	0.002	-0.498	6.190e-01	9.878e-01
	APOE4 Status	0.003	0.002	1.322	1.869e-01	9.912e-01
	Time b/w LP and MRI	0.001	0.000	2.616	9.238e-03	3.141e-02
inferior temporal	Intercept	0.677	0.013	50.201	4.872e-173	1.841e-172
	Age	0.000	0.000	1.164	2.452e-01	5.800e-01
	tTau_transformed	-0.002	0.003	-0.707	4.799e-01	6.043e-01
	Sex	0.000	0.002	0.199	8.424e-01	9.878e-01
	APOE4 Status	-0.000	0.002	-0.079	9.369e-01	9.912e-01
	Time b/w LP and MRI	0.001	0.000	2.311	2.136e-02	4.566e-02
insula	Intercept	0.673	0.013	51.659	2.761e-177	1.565e-176
	Age	0.001	0.000	4.656	4.412e-06	1.500e-04
	tTau_transformed	-0.004	0.003	-1.507	1.326e-01	2.147e-01
	Sex	0.001	0.002	0.305	7.603e-01	9.878e-01
	APOE4 Status	-0.000	0.002	-0.027	9.786e-01	9.912e-01
	Time b/w LP and MRI	0.001	0.000	2.241	2.558e-02	4.832e-02
isthmus cingulate	Intercept	0.763	0.020	37.283	8.358e-131	9.472e-131

ROI	Predictor	Estimate	Std. Error	T-Statistic	pUncorrected	pFDR
	Age	0.000	0.000	0.944	3.459e-01	6.534e-01
	tTau_transformed	-0.009	0.004	-2.183	2.960e-02	7.058e-02
	Sex	-0.000	0.003	-0.151	8.799e-01	9.878e-01
	APOE4 Status	0.001	0.003	0.421	6.738e-01	9.912e-01
	Time b/w LP and MRI	0.001	0.001	1.369	1.716e-01	2.012e-01
lateral occipital	Intercept	0.756	0.017	43.551	1.761e-152	2.603e-152
	Age	0.000	0.000	1.181	2.384e-01	5.800e-01
	tTau_transformed	-0.010	0.003	-3.014	2.742e-03	3.108e-02
	Sex	-0.002	0.002	-1.019	3.087e-01	9.878e-01
	APOE4 Status	0.001	0.002	0.249	8.033e-01	9.912e-01
	Time b/w LP and MRI	0.001	0.000	2.671	7.878e-03	2.976e-02
lateral orbitofrontal	Intercept	0.687	0.015	47.261	3.359e-164	7.614e-164
	Age	-0.000	0.000	-0.199	8.421e-01	9.236e-01
	tTau_transformed	-0.000	0.003	-0.048	9.620e-01	9.620e-01
	Sex	-0.003	0.002	-1.448	1.483e-01	9.316e-01
	APOE4 Status	-0.002	0.002	-0.954	3.404e-01	9.912e-01
	Time b/w LP and MRI	0.001	0.000	2.727	6.681e-03	2.839e-02
lingual	Intercept	0.752	0.017	43.710	5.384e-153	8.321e-153
	Age	0.000	0.000	0.223	8.239e-01	9.236e-01
	tTau_transformed	-0.008	0.003	-2.409	1.646e-02	5.596e-02
	Sex	-0.000	0.002	-0.113	9.104e-01	9.878e-01
	APOE4 Status	0.001	0.002	0.286	7.748e-01	9.912e-01
	Time b/w LP and MRI	0.001	0.000	2.285	2.283e-02	4.566e-02
medial orbitofrontal	Intercept	0.652	0.013	48.589	5.302e-168	1.387e-167
	Age	0.000	0.000	1.860	6.367e-02	2.405e-01
	tTau_transformed	-0.001	0.003	-0.236	8.139e-01	8.648e-01
	Sex	-0.003	0.002	-1.393	1.644e-01	9.316e-01
	APOE4 Status	-0.001	0.002	-0.655	5.127e-01	9.912e-01
	Time b/w LP and MRI	0.001	0.000	2.463	1.420e-02	3.714e-02
middle temporal	Intercept	0.695	0.012	55.797	7.347e-189	2.498e-187
	Age	0.000	0.000	1.450	1.479e-01	4.571e-01

ROI	Predictor	Estimate	Std. Error	T-Statistic	pUncorrected	pFDR
	tTau_transformed	-0.004	0.002	-1.584	1.140e-01	1.938e-01
	Sex	0.000	0.002	0.062	9.509e-01	9.878e-01
	APOE4 Status	0.000	0.002	0.270	7.876e-01	9.912e-01
	Time b/w LP and MRI	0.001	0.000	2.915	3.759e-03	2.247e-02
paracentral	Intercept	0.767	0.017	44.734	4.455e-156	7.213e-156
	Age	-0.000	0.000	-0.391	6.957e-01	8.484e-01
	tTau_transformed	-0.002	0.003	-0.550	5.824e-01	7.072e-01
	Sex	0.002	0.002	0.746	4.560e-01	9.878e-01
	APOE4 Status	-0.000	0.002	-0.042	9.664e-01	9.912e-01
	Time b/w LP and MRI	0.000	0.000	0.662	5.086e-01	5.086e-01
parahippocampal	Intercept	0.663	0.017	39.015	3.140e-137	3.954e-137
	Age	0.000	0.000	2.837	4.790e-03	3.257e-02
	tTau_transformed	-0.000	0.003	-0.112	9.109e-01	9.385e-01
	Sex	0.001	0.002	0.432	6.663e-01	9.878e-01
	APOE4 Status	-0.002	0.002	-0.817	4.142e-01	9.912e-01
	Time b/w LP and MRI	0.001	0.000	1.784	7.522e-02	9.472e-02
pars opercularis	Intercept	0.725	0.014	52.653	3.981e-180	4.512e-179
	Age	0.000	0.000	1.639	1.021e-01	3.471e-01
	tTau_transformed	-0.005	0.003	-1.977	4.872e-02	9.744e-02
	Sex	-0.001	0.002	-0.512	6.086e-01	9.878e-01
	APOE4 Status	0.001	0.002	0.303	7.618e-01	9.912e-01
	Time b/w LP and MRI	0.001	0.000	2.139	3.303e-02	5.348e-02
pars orbitalis	Intercept	0.726	0.015	49.491	6.122e-171	2.081e-170
	Age	0.000	0.000	1.036	3.006e-01	6.388e-01
	tTau_transformed	-0.008	0.003	-2.603	9.592e-03	5.474e-02
	Sex	-0.002	0.002	-0.944	3.460e-01	9.878e-01
	APOE4 Status	-0.000	0.002	-0.016	9.869e-01	9.912e-01
	Time b/w LP and MRI	0.001	0.000	2.972	3.138e-03	2.247e-02
pars triangularis	Intercept	0.732	0.014	52.409	1.965e-179	1.670e-178
	Age	0.000	0.000	0.854	3.935e-01	6.690e-01
	tTau_transformed	-0.006	0.003	-2.319	2.089e-02	5.919e-02

ROI	Predictor	Estimate	Std. Error	T-Statistic	pUncorrected	pFDR
	Sex	-0.002	0.002	-1.075	2.831e-01	9.878e-01
	APOE4 Status	0.001	0.002	0.304	7.610e-01	9.912e-01
	Time b/w LP and MRI	0.001	0.000	3.124	1.914e-03	2.169e-02
pericalcarine	Intercept	0.769	0.021	36.224	2.598e-127	2.849e-127
	Age	0.000	0.000	0.680	4.969e-01	7.045e-01
	tTau_transformed	-0.009	0.004	-2.108	3.568e-02	7.582e-02
	Sex	-0.005	0.003	-1.744	8.195e-02	9.316e-01
	APOE4 Status	0.000	0.003	0.011	9.912e-01	9.912e-01
	Time b/w LP and MRI	0.001	0.001	2.504	1.267e-02	3.590e-02
postcentral	Intercept	0.759	0.016	46.148	9.452e-161	1.890e-160
	Age	0.000	0.000	1.383	1.674e-01	4.743e-01
	tTau_transformed	-0.006	0.003	-1.901	5.806e-02	1.097e-01
	Sex	0.001	0.002	0.364	7.163e-01	9.878e-01
	APOE4 Status	0.000	0.002	0.180	8.569e-01	9.912e-01
	Time b/w LP and MRI	0.001	0.000	1.834	6.735e-02	8.807e-02
posterior cingulate	Intercept	0.740	0.030	25.002	1.999e-82	2.060e-82
	Age	0.001	0.000	1.868	6.255e-02	2.405e-01
	tTau_transformed	-0.007	0.006	-1.150	2.507e-01	3.552e-01
	Sex	-0.001	0.004	-0.150	8.811e-01	9.878e-01
	APOE4 Status	0.001	0.004	0.304	7.612e-01	9.912e-01
	Time b/w LP and MRI	0.001	0.001	0.940	3.479e-01	3.584e-01
precentral	Intercept	0.782	0.017	45.038	2.966e-157	5.042e-157
	Age	0.000	0.000	0.048	9.615e-01	9.615e-01
	tTau_transformed	-0.005	0.003	-1.326	1.855e-01	2.742e-01
	Sex	0.002	0.002	0.785	4.329e-01	9.878e-01
	APOE4 Status	0.001	0.002	0.484	6.283e-01	9.912e-01
	Time b/w LP and MRI	0.001	0.000	1.942	5.283e-02	7.484e-02
precuneus	Intercept	0.758	0.017	45.779	1.355e-159	2.559e-159
	Age	-0.000	0.000	-0.672	5.023e-01	7.045e-01
	tTau_transformed	-0.008	0.003	-2.499	1.288e-02	5.474e-02
	Sex	-0.000	0.002	-0.044	9.647e-01	9.878e-01

ROI	Predictor	Estimate	Std. Error	T-Statistic	pUncorrected	pFDR
	APOE4 Status	0.001	0.002	0.375	7.077e-01	9.912e-01
	Time b/w LP and MRI	0.001	0.000	2.523	1.203e-02	3.590e-02
rostral anterior cingulate	Intercept	0.633	0.016	38.803	2.553e-136	3.100e-136
	Age	0.000	0.000	3.120	1.945e-03	2.204e-02
	tTau_transformed	0.001	0.003	0.450	6.529e-01	7.333e-01
	Sex	-0.000	0.002	-0.038	9.696e-01	9.878e-01
	APOE4 Status	0.001	0.002	0.629	5.297e-01	9.912e-01
	Time b/w LP and MRI	0.001	0.000	1.243	2.145e-01	2.431e-01
rostral middle frontal	Intercept	0.733	0.015	49.074	1.069e-169	3.304e-169
	Age	-0.000	0.000	-0.904	3.663e-01	6.555e-01
	tTau_transformed	-0.006	0.003	-2.184	2.953e-02	7.058e-02
	Sex	-0.003	0.002	-1.285	1.994e-01	9.685e-01
	APOE4 Status	0.002	0.002	1.104	2.704e-01	9.912e-01
	Time b/w LP and MRI	0.001	0.000	3.317	9.956e-04	1.693e-02
superior frontal	Intercept	0.722	0.014	51.794	2.047e-177	1.392e-176
	Age	-0.000	0.000	-0.647	5.180e-01	7.045e-01
	tTau_transformed	-0.003	0.003	-1.087	2.778e-01	3.778e-01
	Sex	0.000	0.002	0.234	8.148e-01	9.878e-01
	APOE4 Status	0.001	0.002	0.499	6.180e-01	9.912e-01
	Time b/w LP and MRI	0.001	0.000	2.074	3.869e-02	5.969e-02
superior parietal	Intercept	0.767	0.017	45.385	2.360e-158	4.223e-158
	Age	-0.000	0.000	-0.403	6.869e-01	8.484e-01
	tTau_transformed	-0.009	0.003	-2.574	1.043e-02	5.474e-02
	Sex	-0.001	0.002	-0.370	7.115e-01	9.878e-01
	APOE4 Status	0.001	0.002	0.610	5.424e-01	9.912e-01
	Time b/w LP and MRI	0.001	0.000	2.296	2.219e-02	4.566e-02
superior temporal	Intercept	0.731	0.014	53.541	1.235e-182	2.100e-181
	Age	0.000	0.000	2.701	7.208e-03	4.085e-02
	tTau_transformed	-0.007	0.003	-2.754	6.152e-03	5.229e-02
	Sex	-0.000	0.002	-0.015	9.878e-01	9.878e-01
	APOE4 Status	-0.000	0.002	-0.063	9.502e-01	9.912e-01

ROI	Predictor	Estimate	Std. Error	T-Statistic	pUncorrected	pFDR
	Time b/w LP and MRI	0.001	0.000	2.315	2.111e-02	4.566e-02
supramarginal	Intercept	0.746	0.015	51.270	3.679e-176	1.564e-175
	Age	0.000	0.000	0.739	4.603e-01	7.045e-01
	tTau_transformed	-0.009	0.003	-3.015	2.733e-03	3.108e-02
	Sex	-0.001	0.002	-0.553	5.808e-01	9.878e-01
	APOE4 Status	0.002	0.002	0.807	4.200e-01	9.912e-01
	Time b/w LP and MRI	0.001	0.000	2.189	2.922e-02	4.967e-02
temporal pole	Intercept	0.649	0.017	37.688	1.450e-132	1.700e-132
	Age	0.001	0.000	4.327	1.922e-05	3.267e-04
	tTau_transformed	-0.002	0.003	-0.478	6.332e-01	7.333e-01
	Sex	0.001	0.002	0.613	5.401e-01	9.878e-01
	APOE4 Status	-0.002	0.002	-0.930	3.532e-01	9.912e-01
	Time b/w LP and MRI	0.001	0.000	1.141	2.547e-01	2.793e-01
transverse temporal	Intercept	0.803	0.019	41.740	1.628e-146	2.214e-146
	Age	0.001	0.000	3.014	2.745e-03	2.333e-02
	tTau_transformed	-0.009	0.004	-2.418	1.607e-02	5.596e-02
	Sex	-0.001	0.003	-0.202	8.403e-01	9.878e-01
	APOE4 Status	-0.002	0.003	-0.601	5.483e-01	9.912e-01
	Time b/w LP and MRI	0.001	0.000	2.848	4.627e-03	2.247e-02

Table C10: Estimated outputs of each linear regression model assessing the effects of CSF tTau on cortical GM R1. Covariates in each model included age, sex, APOE4 status, and time between lumbar puncture and MRI. Abbreviations: tTau_transformed, CSF total Tau (log-transformed); LP, lumbar puncture; MRI, magnetic resonance imaging; pUncorrected, *p*-value uncorrected for multiple comparisons; pFDR, Benjamini-Hochberg FDR-corrected *p*-value.

Table C11: Outputs of linear regression models assessing effects of CSF tTau on cortical-adjacent WM R1

ROI	Predictor	Estimate	Std. Error	T-Statistic	pUncorrected	pFDR
bankssts	Intercept	1.169	0.120	9.716	3.859e-20	7.718e-20
	Age	0.006	0.003	1.715	8.710e-02	2.009e-01
	Age^2	-0.000	0.000	-2.387	1.745e-02	3.377e-02
	tTau_transformed	-0.022	0.006	-3.551	4.299e-04	3.654e-03
	Sex	-0.012	0.004	-2.614	9.296e-03	2.258e-02
	APOE4 Status	0.001	0.004	0.330	7.416e-01	9.995e-01
	Time b/w LP and MRI	-0.000	0.001	-0.322	7.479e-01	9.947e-01
caudal anterior cingulate	Intercept	1.085	0.113	9.569	1.239e-19	2.106e-19
	Age	0.009	0.003	2.631	8.844e-03	7.517e-02
	Age^2	-0.000	0.000	-3.514	4.933e-04	6.894e-03
	tTau_transformed	-0.012	0.006	-2.057	4.037e-02	4.902e-02
	Sex	-0.017	0.004	-4.036	6.542e-05	4.103e-04
	APOE4 Status	0.007	0.004	1.595	1.115e-01	9.995e-01
	Time b/w LP and MRI	-0.000	0.001	-0.285	7.762e-01	9.947e-01
caudal middle frontal	Intercept	1.251	0.124	10.090	1.922e-21	8.198e-21
	Age	0.002	0.004	0.684	4.942e-01	5.601e-01
	Age^2	-0.000	0.000	-1.472	1.419e-01	1.664e-01
	tTau_transformed	-0.020	0.007	-3.068	2.301e-03	5.884e-03
	Sex	-0.005	0.005	-1.026	3.056e-01	3.149e-01
	APOE4 Status	0.000	0.005	0.018	9.858e-01	9.995e-01
	Time b/w LP and MRI	0.001	0.001	0.650	5.161e-01	9.947e-01
cuneus	Intercept	1.162	0.118	9.813	1.782e-20	5.508e-20
	Age	0.001	0.003	0.428	6.692e-01	7.110e-01
	Age^2	-0.000	0.000	-0.924	3.558e-01	3.558e-01
	tTau_transformed	-0.013	0.006	-2.095	3.682e-02	4.637e-02
	Sex	-0.023	0.004	-5.368	1.368e-07	4.651e-06
	APOE4 Status	-0.002	0.004	-0.357	7.212e-01	9.995e-01
	Time b/w LP and MRI	0.000	0.001	0.336	7.372e-01	9.947e-01

ROI	Predictor	Estimate	Std. Error	T-Statistic	pUncorrected	pFDR
entorhinal	Intercept	0.680	0.125	5.424	1.018e-07	1.018e-07
	Age	0.015	0.004	4.147	4.132e-05	1.405e-03
	Age^2	-0.000	0.000	-5.023	7.725e-07	2.627e-05
	tTau_transformed	-0.008	0.007	-1.186	2.364e-01	2.436e-01
	Sex	-0.009	0.005	-1.977	4.870e-02	8.191e-02
	APOE4 Status	-0.001	0.005	-0.174	8.616e-01	9.995e-01
	Time b/w LP and MRI	-0.000	0.001	-0.348	7.281e-01	9.947e-01
frontal pole	Intercept	1.069	0.122	8.769	5.504e-17	6.683e-17
	Age	0.006	0.004	1.641	1.015e-01	2.009e-01
	Age^2	-0.000	0.000	-2.412	1.633e-02	3.377e-02
	tTau_transformed	-0.026	0.006	-4.080	5.446e-05	9.258e-04
	Sex	-0.001	0.004	-0.325	7.455e-01	7.455e-01
	APOE4 Status	-0.001	0.004	-0.298	7.662e-01	9.995e-01
	Time b/w LP and MRI	0.000	0.001	0.137	8.910e-01	9.947e-01
fusiform	Intercept	1.097	0.114	9.646	6.673e-20	1.194e-19
	Age	0.007	0.003	2.101	3.630e-02	1.763e-01
	Age^2	-0.000	0.000	-3.006	2.816e-03	1.371e-02
	tTau_transformed	-0.019	0.006	-3.140	1.817e-03	5.884e-03
	Sex	-0.008	0.004	-1.921	5.541e-02	8.191e-02
	APOE4 Status	0.000	0.004	0.046	9.637e-01	9.995e-01
	Time b/w LP and MRI	-0.001	0.001	-0.711	4.776e-01	9.947e-01
inferior parietal	Intercept	1.164	0.124	9.350	6.734e-19	9.955e-19
	Age	0.005	0.004	1.511	1.315e-01	2.009e-01
	Age^2	-0.000	0.000	-2.234	2.602e-02	4.213e-02
	tTau_transformed	-0.024	0.007	-3.660	2.867e-04	3.249e-03
	Sex	-0.018	0.005	-4.014	7.140e-05	4.103e-04
	APOE4 Status	0.002	0.005	0.411	6.810e-01	9.995e-01
	Time b/w LP and MRI	0.000	0.001	0.152	8.791e-01	9.947e-01
inferior temporal	Intercept	1.107	0.106	10.422	1.284e-22	7.276e-22
	Age	0.006	0.003	1.913	5.642e-02	1.846e-01
	Age^2	-0.000	0.000	-2.831	4.882e-03	2.075e-02

ROI	Predictor	Estimate	Std. Error	T-Statistic	pUncorrected	pFDR
	tTau_transformed	-0.017	0.006	-3.099	2.083e-03	5.884e-03
	Sex	-0.010	0.004	-2.532	1.173e-02	2.659e-02
	APOE4 Status	0.001	0.004	0.374	7.084e-01	9.995e-01
	Time b/w LP and MRI	-0.001	0.001	-0.875	3.821e-01	9.947e-01
insula	Intercept	1.060	0.109	9.741	3.151e-20	6.923e-20
	Age	0.005	0.003	1.569	1.176e-01	2.009e-01
	Age^2	-0.000	0.000	-2.180	2.986e-02	4.419e-02
	tTau_transformed	-0.010	0.006	-1.823	6.900e-02	7.568e-02
	Sex	-0.009	0.004	-2.304	2.173e-02	4.346e-02
	APOE4 Status	0.001	0.004	0.307	7.594e-01	9.995e-01
	Time b/w LP and MRI	-0.000	0.001	-0.007	9.947e-01	9.947e-01
isthmus cingulate	Intercept	1.116	0.131	8.536	3.075e-16	3.485e-16
	Age	0.007	0.004	1.960	5.075e-02	1.846e-01
	Age^2	-0.000	0.000	-2.528	1.185e-02	3.193e-02
	tTau_transformed	-0.014	0.007	-1.982	4.813e-02	5.643e-02
	Sex	-0.017	0.005	-3.545	4.398e-04	2.136e-03
	APOE4 Status	-0.000	0.005	-0.025	9.804e-01	9.995e-01
	Time b/w LP and MRI	-0.000	0.001	-0.242	8.086e-01	9.947e-01
lateral occipital	Intercept	1.212	0.109	11.084	5.012e-25	8.520e-24
	Age	0.003	0.003	0.957	3.391e-01	4.270e-01
	Age^2	-0.000	0.000	-1.533	1.260e-01	1.530e-01
	tTau_transformed	-0.027	0.006	-4.716	3.351e-06	1.139e-04
	Sex	-0.021	0.004	-5.132	4.520e-07	7.684e-06
	APOE4 Status	-0.001	0.004	-0.167	8.676e-01	9.995e-01
	Time b/w LP and MRI	0.000	0.001	0.049	9.613e-01	9.947e-01
lateral orbitofrontal	Intercept	1.053	0.119	8.852	2.965e-17	3.734e-17
	Age	0.008	0.003	2.280	2.315e-02	1.516e-01
	Age^2	-0.000	0.000	-3.251	1.249e-03	8.493e-03
	tTau_transformed	-0.016	0.006	-2.574	1.042e-02	1.687e-02
	Sex	-0.006	0.004	-1.300	1.944e-01	2.171e-01
	APOE4 Status	0.002	0.004	0.363	7.166e-01	9.995e-01

ROI	Predictor	Estimate	Std. Error	T-Statistic	pUncorrected	pFDR
	Time b/w LP and MRI	0.000	0.001	0.236	8.139e-01	9.947e-01
lingual	Intercept	1.117	0.117	9.555	1.364e-19	2.208e-19
	Age	0.004	0.003	1.087	2.778e-01	3.778e-01
	Age^2	-0.000	0.000	-1.691	9.168e-02	1.213e-01
	tTau_transformed	-0.014	0.006	-2.351	1.924e-02	2.844e-02
	Sex	-0.017	0.004	-4.011	7.240e-05	4.103e-04
	APOE4 Status	-0.003	0.004	-0.686	4.933e-01	9.995e-01
	Time b/w LP and MRI	0.000	0.001	0.158	8.748e-01	9.947e-01
medial orbitofrontal	Intercept	1.078	0.119	9.025	8.085e-18	1.057e-17
	Age	0.006	0.003	1.621	1.057e-01	2.009e-01
	Age^2	-0.000	0.000	-2.575	1.038e-02	3.193e-02
	tTau_transformed	-0.013	0.006	-2.104	3.601e-02	4.637e-02
	Sex	-0.008	0.004	-1.933	5.393e-02	8.191e-02
	APOE4 Status	-0.000	0.004	-0.026	9.790e-01	9.995e-01
	Time b/w LP and MRI	0.000	0.001	0.307	7.589e-01	9.947e-01
middle temporal	Intercept	1.164	0.110	10.583	3.379e-23	3.830e-22
	Age	0.005	0.003	1.504	1.333e-01	2.009e-01
	Age^2	-0.000	0.000	-2.422	1.587e-02	3.377e-02
	tTau_transformed	-0.019	0.006	-3.278	1.138e-03	5.884e-03
	Sex	-0.013	0.004	-3.147	1.777e-03	6.531e-03
	APOE4 Status	0.000	0.004	0.013	9.898e-01	9.995e-01
	Time b/w LP and MRI	-0.000	0.001	-0.240	8.108e-01	9.947e-01
paracentral	Intercept	1.241	0.126	9.869	1.144e-20	3.890e-20
	Age	0.002	0.004	0.572	5.675e-01	6.224e-01
	Age^2	-0.000	0.000	-1.271	2.046e-01	2.244e-01
	tTau_transformed	-0.015	0.007	-2.308	2.150e-02	3.046e-02
	Sex	-0.007	0.005	-1.507	1.327e-01	1.611e-01
	APOE4 Status	-0.000	0.005	-0.022	9.823e-01	9.995e-01
	Time b/w LP and MRI	-0.000	0.001	-0.323	7.470e-01	9.947e-01
parahippocampal	Intercept	0.956	0.130	7.381	9.476e-13	1.007e-12
	Age	0.010	0.004	2.680	7.678e-03	7.517e-02

ROI	Predictor	Estimate	Std. Error	T-Statistic	pUncorrected	pFDR
	Age^2	-0.000	0.000	-3.375	8.111e-04	6.894e-03
	tTau_transformed	-0.012	0.007	-1.828	6.824e-02	7.568e-02
	Sex	-0.015	0.005	-3.123	1.921e-03	6.531e-03
	APOE4 Status	-0.004	0.005	-0.824	4.102e-01	9.995e-01
	Time b/w LP and MRI	-0.001	0.001	-1.009	3.135e-01	9.947e-01
pars opercularis	Intercept	1.163	0.119	9.762	2.671e-20	6.487e-20
	Age	0.005	0.003	1.505	1.332e-01	2.009e-01
	Age^2	-0.000	0.000	-2.275	2.344e-02	3.985e-02
	tTau_transformed	-0.019	0.006	-3.100	2.072e-03	5.884e-03
	Sex	-0.008	0.004	-1.856	6.419e-02	8.730e-02
	APOE4 Status	0.001	0.004	0.299	7.650e-01	9.995e-01
	Time b/w LP and MRI	0.000	0.001	0.147	8.833e-01	9.947e-01
pars orbitalis	Intercept	1.136	0.113	10.040	2.892e-21	1.093e-20
	Age	0.004	0.003	1.289	1.980e-01	2.805e-01
	Age^2	-0.000	0.000	-2.150	3.218e-02	4.559e-02
	tTau_transformed	-0.018	0.006	-3.085	2.178e-03	5.884e-03
	Sex	-0.005	0.004	-1.288	1.986e-01	2.171e-01
	APOE4 Status	-0.001	0.004	-0.177	8.596e-01	9.995e-01
	Time b/w LP and MRI	0.000	0.001	0.034	9.731e-01	9.947e-01
pars triangularis	Intercept	1.119	0.118	9.486	2.339e-19	3.615e-19
	Age	0.006	0.003	1.831	6.782e-02	1.922e-01
	Age^2	-0.000	0.000	-2.735	6.514e-03	2.461e-02
	tTau_transformed	-0.017	0.006	-2.701	7.216e-03	1.291e-02
	Sex	-0.006	0.004	-1.271	2.043e-01	2.171e-01
	APOE4 Status	0.001	0.004	0.203	8.393e-01	9.995e-01
	Time b/w LP and MRI	0.000	0.001	0.145	8.845e-01	9.947e-01
pericalcarine	Intercept	1.038	0.130	7.993	1.483e-14	1.627e-14
	Age	0.003	0.004	0.832	4.057e-01	4.756e-01
	Age^2	-0.000	0.000	-1.281	2.010e-01	2.244e-01
	tTau_transformed	-0.004	0.007	-0.632	5.279e-01	5.279e-01
	Sex	-0.019	0.005	-4.022	6.909e-05	4.103e-04

ROI	Predictor	Estimate	Std. Error	T-Statistic	pUncorrected	pFDR
	APOE4 Status	-0.004	0.005	-0.798	4.253e-01	9.995e-01
	Time b/w LP and MRI	0.001	0.001	0.767	4.434e-01	9.947e-01
postcentral	Intercept	1.222	0.116	10.486	7.535e-23	5.124e-22
	Age	0.001	0.003	0.388	6.979e-01	7.190e-01
	Age^2	-0.000	0.000	-1.048	2.951e-01	3.040e-01
	tTau_transformed	-0.014	0.006	-2.218	2.715e-02	3.692e-02
	Sex	-0.008	0.004	-1.886	6.006e-02	8.509e-02
	APOE4 Status	-0.000	0.004	-0.014	9.891e-01	9.995e-01
	Time b/w LP and MRI	0.000	0.001	0.100	9.201e-01	9.947e-01
posterior cingulate	Intercept	1.187	0.127	9.317	8.725e-19	1.187e-18
	Age	0.006	0.004	1.494	1.359e-01	2.009e-01
	Age^2	-0.000	0.000	-2.179	2.989e-02	4.419e-02
	tTau_transformed	-0.017	0.007	-2.488	1.327e-02	2.051e-02
	Sex	-0.013	0.005	-2.699	7.245e-03	1.895e-02
	APOE4 Status	0.000	0.005	0.001	9.995e-01	9.995e-01
	Time b/w LP and MRI	-0.000	0.001	-0.532	5.953e-01	9.947e-01
precentral	Intercept	1.268	0.120	10.533	5.133e-23	4.363e-22
	Age	0.001	0.003	0.344	7.307e-01	7.307e-01
	Age^2	-0.000	0.000	-1.060	2.897e-01	3.040e-01
	tTau_transformed	-0.016	0.006	-2.587	1.004e-02	1.687e-02
	Sex	-0.007	0.004	-1.533	1.260e-01	1.587e-01
	APOE4 Status	-0.000	0.004	-0.101	9.193e-01	9.995e-01
	Time b/w LP and MRI	0.000	0.001	0.406	6.848e-01	9.947e-01
precuneus	Intercept	1.140	0.131	8.730	7.389e-17	8.663e-17
	Age	0.006	0.004	1.639	1.019e-01	2.009e-01
	Age^2	-0.000	0.000	-2.418	1.605e-02	3.377e-02
	tTau_transformed	-0.020	0.007	-2.899	3.949e-03	8.392e-03
	Sex	-0.014	0.005	-2.998	2.892e-03	8.939e-03
	APOE4 Status	0.000	0.005	0.022	9.824e-01	9.995e-01
	Time b/w LP and MRI	-0.000	0.001	-0.252	8.011e-01	9.947e-01
rostral anterior cingulate	Intercept	1.096	0.112	9.797	2.051e-20	5.811e-20

ROI	Predictor	Estimate	Std. Error	T-Statistic	pUncorrected	pFDR
	Age	0.007	0.003	2.223	2.675e-02	1.516e-01
	Age^2	-0.000	0.000	-3.005	2.822e-03	1.371e-02
	tTau_transformed	-0.016	0.006	-2.710	7.030e-03	1.291e-02
	Sex	-0.007	0.004	-1.637	1.023e-01	1.338e-01
	APOE4 Status	0.004	0.004	1.061	2.896e-01	9.995e-01
	Time b/w LP and MRI	0.000	0.001	0.007	9.941e-01	9.947e-01
rostral middle frontal	Intercept	1.233	0.126	9.778	2.358e-20	6.167e-20
	Age	0.003	0.004	0.836	4.036e-01	4.756e-01
	Age^2	-0.000	0.000	-1.667	9.635e-02	1.213e-01
	tTau_transformed	-0.021	0.007	-3.117	1.959e-03	5.884e-03
	Sex	-0.009	0.005	-1.945	5.252e-02	8.191e-02
	APOE4 Status	0.001	0.005	0.128	8.980e-01	9.995e-01
	Time b/w LP and MRI	0.001	0.001	0.645	5.191e-01	9.947e-01
superior frontal	Intercept	1.148	0.103	11.125	3.578e-25	8.520e-24
	Age	0.004	0.003	1.497	1.352e-01	2.009e-01
	Age^2	-0.000	0.000	-2.518	1.221e-02	3.193e-02
	tTau_transformed	-0.016	0.005	-2.929	3.599e-03	8.158e-03
	Sex	-0.009	0.004	-2.484	1.342e-02	2.852e-02
	APOE4 Status	0.003	0.004	0.803	4.223e-01	9.995e-01
	Time b/w LP and MRI	0.000	0.001	0.072	9.427e-01	9.947e-01
superior parietal	Intercept	1.209	0.125	9.662	5.908e-20	1.116e-19
	Age	0.003	0.004	0.958	3.384e-01	4.270e-01
	Age^2	-0.000	0.000	-1.681	9.364e-02	1.213e-01
	tTau_transformed	-0.020	0.007	-3.064	2.333e-03	5.884e-03
	Sex	-0.016	0.005	-3.385	7.839e-04	3.332e-03
	APOE4 Status	0.000	0.005	0.031	9.755e-01	9.995e-01
	Time b/w LP and MRI	-0.000	0.001	-0.074	9.410e-01	9.947e-01
superior temporal	Intercept	1.107	0.110	10.090	1.929e-21	8.198e-21
	Age	0.006	0.003	1.888	5.972e-02	1.846e-01
	Age^2	-0.000	0.000	-2.667	7.974e-03	2.711e-02
	tTau_transformed	-0.016	0.006	-2.835	4.825e-03	9.650e-03

ROI	Predictor	Estimate	Std. Error	T-Statistic	pUncorrected	pFDR
	Sex	-0.009	0.004	-2.213	2.744e-02	5.183e-02
	APOE4 Status	-0.001	0.004	-0.152	8.792e-01	9.995e-01
	Time b/w LP and MRI	-0.000	0.001	-0.044	9.649e-01	9.947e-01
supramarginal	Intercept	1.153	0.123	9.335	7.575e-19	1.073e-18
	Age	0.006	0.004	1.567	1.179e-01	2.009e-01
	Age^2	-0.000	0.000	-2.324	2.065e-02	3.695e-02
	tTau_transformed	-0.020	0.006	-3.053	2.423e-03	5.884e-03
	Sex	-0.013	0.005	-2.854	4.546e-03	1.288e-02
	APOE4 Status	0.001	0.004	0.166	8.682e-01	9.995e-01
	Time b/w LP and MRI	0.000	0.001	0.028	9.779e-01	9.947e-01
temporal pole	Intercept	0.857	0.118	7.248	2.258e-12	2.326e-12
	Age	0.009	0.003	2.696	7.311e-03	7.517e-02
	Age^2	-0.000	0.000	-3.429	6.688e-04	6.894e-03
	tTau_transformed	-0.009	0.006	-1.508	1.325e-01	1.408e-01
	Sex	-0.006	0.004	-1.461	1.449e-01	1.699e-01
	APOE4 Status	-0.002	0.004	-0.509	6.108e-01	9.995e-01
	Time b/w LP and MRI	-0.001	0.001	-0.806	4.207e-01	9.947e-01
transverse temporal	Intercept	1.110	0.114	9.737	3.258e-20	6.923e-20
	Age	0.006	0.003	1.957	5.111e-02	1.846e-01
	Age^2	-0.000	0.000	-2.378	1.788e-02	3.377e-02
	tTau_transformed	-0.020	0.006	-3.270	1.171e-03	5.884e-03
	Sex	-0.009	0.004	-2.083	3.788e-02	6.779e-02
	APOE4 Status	-0.004	0.004	-0.845	3.984e-01	9.995e-01
	Time b/w LP and MRI	0.001	0.001	0.649	5.165e-01	9.947e-01

Table C11: Estimated outputs of each linear regression model assessing the effects of CSF tTau on cortical-adjacent WM R1. Covariates in each model included age, sex, APOE4 status, and time between lumbar puncture and MRI. Abbreviations: tTau_transformed, CSF total Tau (log-transformed); LP, lumbar puncture; MRI, magnetic resonance imaging; pUncorrected, *p*-value uncorrected for multiple comparisons; pFDR, Benjamini-Hochberg FDR-corrected *p*-value.